UNIVERSITÀ DEGLI STUDI DI TRIESTE

XXX CICLO DEL DOTTORATO DI RICERCA IN CHIMICA

Funded by the European Union's Horizon 2020 research and innovation programme under the
Marie Sklodowska-Curie grant agreement No. 642014

p-Coumaroylquinic Acids in Coffee Manufacturing: Sensing Systems and Profiling

Settore scientifico-disciplinare: **CHIM/06**

Ph.D. STUDENT
ANGGY LUSANNA GUTIÉRREZ ORTIZ

Ph.D. PROGRAM DIRECTOR
PROF. BARBARA MILANI

THESIS SUPERVISOR
PROF. CRISTINA FORZATO

THESIS CO-SUPERVISOR
PROF. FEDERICO BERTI

ANNO ACCADEMICO 2016/2017

UNIVERSITÀ DEGLI STUDI DI TRIESTE

XXX CICLO DEL DOTTORATO DI RICERCA IN CHIMICA

Funded by the European Union's Horizon 2020 research and innovation programme under the
Marie Sklodowska-Curie grant agreement No. 642014

p-Coumaroylquinic Acids in Coffee Manufacturing: Sensing Systems and Profiling

Settore scientifico-disciplinare: **CHIM/06**

Ph.D. STUDENT
ANGGY LUSANNA GUTIÉRREZ ORTIZ

Ph.D. PROGRAM DIRECTOR
PROF. BARBARA MILANI

THESIS SUPERVISOR
PROF. CRISTINA FORZATO

THESIS CO-SUPERVISOR
PROF. FEDERICO BERTI

ANNO ACCADEMICO 2016/2017

To my Grandmother

“Little science takes you away from God

but more of it takes you to Him”[1]

[1] Louis Pasteur

Table of Contents

List of Figures

List of Tables

Schemes

List of abbreviations

1-*p*CoQA	1-*p*-coumaroylquinic acid
3,4-diCQA	3,4-dicaffeoylquinic acid
3,5-diCQA	3,5-dicaffeoylquinic acid
3-CQA	3-caffeoylquinic acid
3-CQL	3-caffeoylquinide or 3-caffeoylquinic-1, 5-lactone
3-FQA	3-feruloylquinic acid
3-*p*CoQA	3-*p*-coumaroylquinic acid
4,5-diCQA	4,5-dicaffeoylquinic acid
4-CQA	4-caffeoylquinic acid
4-CQL	4-caffeoylquinic-1, 5-lactone
4-FQA	4-feruloylquinic acid
4-*p*CoQA	4-*p*-coumaroylquinic
4-VPy	4-vinylpyridine
5-CQA	5-caffeoylquinic acid
5-FQA	5-feruloylquinic acid
5-*p*CoQA	5-*p*-coumaroylquinic
AAF	acrylamidofluorescein
AIBN	azobisisobutyronitrile
AM	acrylamide
BPA	bisphenol A
CA	caffeic acid
CAF	caffeine
cAMP	5',3'-cyclic adenosine monophosphate
CCC	pH-gradient counter current chromatography
CD_3OD	Deuterated methanol
$CDCl_3$	Deuterated chloroform
CGAs	chlorogenic acids
CL	chemiluminescent
CQAs	caffeoylquinic acids
DAP	1,3-Diaminopropane
diCQAs	dicaffeoylquinic acids
DIPEA	N,N-Diisopropylethylamine
DMAP	4-Dimethylaminopyridine
dmb	dry matter bases
DMF	Dimethylformamide
DMSO	Dimethyl sulfoxide
DMSO-d_6	Deuterated Dimethyl sulfoxide
DVB	divinylbenzene
EDANS	5-((2-Aminoethyl) amino)naphthalene-1-sulfonic acid
EGDMA	dimethacrylate
EtOAc	Ethyl acetate
EtOH	Ethanol
FA	ferulic acid
FITC	Fluorescein Isothiocyanate
FLP	fluorophore-linker-polymerizable unit

FLRLP	fluorophore-linker-receptor-linker-polymerizable unit
fMIPs	Fluorescent Molecularly Imprinted Polymers
fNIPs	Fluorescent non-imprinted polymers
FOs	Fiber Optic Sensing
FQAs	feruloylquinic acids
FT-IR	Infrared spectroscopy
GA	glutaraldehyde
GC	gas chromatography
H-5CQA	hydrogenated 5-caffeoylquinic acid
HEMA	2-hydroxyethylmethacrylate
HPLC y	high performance liquid chromatography
HSA	human serum albumin
ICP-MS	inductively coupled plasma-mass spectrometer
ITC	internal electron transfer transitions
LC-MS	Liquid Chromatography Mass Spectroscopy
MAA	methacrylic acid
MAE	microwave-assisted extraction
MBA	MBA N,N'-methylenebisacrylamide
MeOH	methanol
MIP	molecularly imprinted polymers
MIP-HF-SPME	hollow fiber solid phase microextraction
MIT	molecular imprinting technology
MISPE	molecularly imprinting solid-phase extraction
MS	mass spectrometry
NBD	nitrobenzoxadiazole
NIPAM	N-Isopropylacrylamide
NMR	nuclear magnetic resonance spectroscopy
OTC	oxytetracycline
PBS	Phosphate buffered saline
*p*CoA	*p*-Coumaric acid
*p*CoQAs	*p*-coumaroylquinic acids
PET	photoinduced electron transfer
PQ	Paraquat
QA	quinic acid
RC	regenerated cellulose
SA	sinapic acid
SAW	surface-acoustic wave
SERS	surface Enhanced Raman Spectroscopy
SPE	solid phase extraction
SPR	surface plasmon resonance
TBTU	**Tetraethylammonium tetrafluoroborate**
TC	tetracycline
TLC	Thin layer chromatography
UV-Vis	ultraviolet-visible spectroscopy
UHPLC-DAD	ultra-high-performance liquid chromatography–diode array detector
WL	weight loss

University of Trieste

PhD School in Organic Chemistry (Cicle XXX)

_p_-Coumaroylquinic Acids in Coffee Manufacturing: Sensing Systems and Profiling
PhD Thesis

PhD student: Anggy Lusanna Gutierrez Ortiz

Supervisor: Prof. Cristina Forzato

Co-supervisor: Prof. Federico Berti

Abstract

This research is part of a PhD industrial program that belongs to the IPCOS (Imprinted Polymers as Coffee Sensors) network, which arises from the interest in searching new methodologies for the recognition of some bioactive compounds present in coffee by designing sensing systems based on molecularly imprinted polymers.

In recent years, the coffee industry has experienced an enormous growth due to the constant increase in demand from consumers who ask for top quality products which are also able to provide nutritional benefits on health. This tendency stimulated the industry to improve the quality control processes in order to obtain a final product with a better taste and a higher nutritional value. It is well known that some chemical compounds present in coffee can provide some positive health benefits. Nowadays, coffee represents one of the most commercialized food products in the world, the second one after olive oil, strongly affecting the world economy. In the literature, there is a wide variety of reports on the chemical composition of volatile and non-volatile fractions of coffee, and within the latter, chlorogenic acids (CGAs) have recently been the subject of a large number of investigations. CGAs are esters of (-)-quinic acid with different *trans*-cinnamic acids (such as caffeic, ferulic and *p*-coumaric acid) and they are secondary metabolites belonging to the family of polyphenols which are involved in the defense mechanisms of plants against external agents. CGAs are well known for their antioxidant activities providing positive health effects. Although their concentrations may vary from one source to another, green coffee beans are particularly rich of CGAs, especially of caffeoylquinic acids (CQAs). As a matter of fact, CGAs play an important role in coffee quality, since their concentration after the roasting process determines the bitterness and acidity of the final beverage and since the flavor of the final product determines its commercial value, CGAs are an important indicator of the coffee quality. Therefore, the development of a reliable, rapid and simple method with good sensitivity and selectivity for CGAs analysis is of great interest to the coffee industry. Moreover, in the last years, due to the potential health benefits, pharmaceutical and nutritional industries have been focused their attention to the CGAs content in green coffee.

All studies reported in literature about the concentration of CGAs in coffee are mainly focused on the quantification of caffeoylquinic acids (CQAs), di-caffeoylquinic acids (di-CQAs) and feruloylquinic acids (FQAs) while minor CGAs such as *p*-coumaroylquinic acids (*p*CoQAs) are the less studied. Since analytical standards of *p*CoQAs are not commercially available their identification is difficult by simple HPLC methods. In this project, all four isomers of *p*-coumaroylquinic acid were synthesized by a condensation reaction between a suitable protected quinic acid and the acyl chloride obtained from *p*-coumaric acid. All isomers have been fully characterized by means of NMR spectroscopy and circular dichroism in order to set up a record of reference data. Acyl migration was observed in the synthesis of 3-*O*-*p*-coumaroylquinic acid and 4-*O*-*p*-coumaroylquinic acid, and for this reason calculations to determine the most stable conformations of all isomers have also been performed to explain the acyl migration observed during the synthesis procedure.

Since according to the literature walnut leaves are particularly rich on *p*CoQAs, the non-commercially available isomers of *p*CoQAs were used to qualitatively identify them in aqueous extracts of walnut leaves in order to improve and optimize a UHPLC method already used at Illycaffè. Both hydroxycinnamic and other classes of chlorogenic acids present in *Juglans regia* L. were fully identified and quantified. In particular, in addition to caffeic, ferulic, *p*-coumaric and sinapic acids, *cis* and *trans* mono-caffeoylquinic, di-caffeoylquinic, mono-feruloylquinic acids and *cis* and *trans* mono-*p*-coumaroylquinic acid isomers were detected and quantified by UHPLC and the seasonal variations of these secondary metabolites were investigated.

Moreover, considering that the determination of CGAs in wild coffee species might provide useful data to establish a taxonomic classification based on the chemical patterns that could contribute to open new worldwide trade markets as well as being useful for the pharmaceutical industry, we report the identification and quantification of main CGAs by UHPLC present in *C. arabica* and *C. canephora* from different geographical origins and seven wild species of the Eucoffea section: *C. liberica, C. arabusta, C. eugenioides, C. sessiliflora, C. congensis, C. pseudozanguebarie, C. racemosa* and *C. brevipes,* highlighting the concentrations of *p*CoQAs.

The interest towards the molecular imprinting technology (MIT) has increased in the last years because this technique offers the possibility of mimicking biological systems (substrates and receptors) by creating a highly crosslinked polymer with remarkable recognition properties for a specific compound. In general, molecularly imprinted polymers (MIPs) offer some characteristics such as high-selectivity, easy preparation, chemical and thermal stability, and low cost. Herein, (MIPs) were prepared as possible recognition elements for 5-*O*-caffeoylquinic acid (5-CQA). Polymers were prepared by the non- covalent approach, evaluating the interactions, mostly hydrogen bonding, between the monomers and the target molecule (5-CQA). Syntheses of all MIPs were carried out by high dilution radical polymerization using different functional monomers. All polymers have been characterized by ^{1}H-NMR, UV-Vis spectroscopy and Dynamic Laser Light Scattering. The polymers binding capability and selectivity were investigated by rebinding tests using an UHPLC method for the quantification of the captured analyte. In order to set up the bases for the development of an optical

sensor based on fluorescent properties two different approaches were followed: in the first one, fluorescent molecularly imprinted polymers (fMIP) were prepared using a well-known naphtalimide derivative as the fluorescent functional monomer and 4-vinylpiridine as co-monomer, while in the second one, the analyte was derivatized with the fluorescent group 5-[(2-Aminoethyl) amino] naphthalene-1-sulfonyl (EDANS) or fluorescein Isothiocyanate (FITC) and a MIP was prepared using a histidine derivative as the functional monomer. In the latter case a competition for the binding sites in the polymer that allows the displacement of the analyte in the matrix polymer has been observed. Interactions of fMIPs with the analyte showed a quenching of the fluorescence intensity in water:DMSO medium in a range of concentration of the analyte between 78 µM and 80mM.

Publications:

Gutiérrez Ortiz, A. L.; Berti, F.; Navarini, L., Monteiro, A., Resmini, M., Forzato, C.; Synthesis of *p*-coumaroylquinic acids and analysis of their interconversion; *Tetrahedron: Asymmetry*, (2017); 28: 419-427.

Gutiérrez Ortiz, A. L.; Berti, F.; Navarini, L.; Crisafulli, P.; Colomban, S. Forzato, C. Aqueous Extracts of Walnut (Juglans regia L.) leaves: quantitative analyses of hydroxycinnamic and chlorogenic acids; *J. Chrom. Science*; (2018)

Chapter 1

INTRODUCTION

1.1 Chemistry of Coffee

1.1.1 Coffee

Coffee represents the most commercialized food product[1], about 1.4 billion cups of coffee are consumed every day worldwide[2], making coffee the most consumed beverage in the world[3]. The known data for world coffee trade started in 1700 with about 10 000 tons per year [4] and since then it has shown a constant increase, in fact, according to the international coffee organization (ICOS), world coffee exports amounted to 10.62 million bags in December 2017, compared with 10.54 million in December 2016[2]. Among the leading coffee consuming countries were the Netherlands and Finland, consuming 260.4 and 184.9 liters per capita respectively[2]. Coffee market has a great influence in the global economy, providing an income for more than 20 million families around the world every year which makes coffee a very interesting field of study for different scientific disciplines[5,6]. The term coffee refers not only to the roasted beans used for beverage preparation but also to the plant, which comprises seeds and fruits. The stages involved in coffee beans transformation to the final beverage are different, such as ripening, harvesting, drying, roasting, grinding, storage and brewing [7] and they all contribute to the quality of the final beverage. As all plant organisms, the coffee plant produces an immeasurable amount of chemical compounds resulting in a very complex system. Several hundreds of substances have been identified in green coffee beans and their composition is influenced by several factors such as genetic aspects and coffee species, degree of maturation, environmental conditions, geographical position, agricultural practices and all these factors determine the organoleptic characteristics of the brew[8].

There are several legends about the origin of coffee. The word 'coffee' is probably derived from the former Kingdom of Kaffa (today part of Ethiopia) so, it seems the first coffee beans came from Ethiopia, where the coffee fruit and beans were chewed and found to be stimulating, then plantations spread to neighboring areas as Yemen, Arabia and Egypt and in the 1500's the first infusion preparation practices using the roasted coffee beans started[4,9]. Coffee spread in Europe in the 1600s when the Turks defeated in Vienna abandoned sacks containing coffee beans. Then, the Austrians discovered that the powder of these beans could be used to prepare an aromatic beverage. However, in Italy, the coffee had its appearance approximately in the year 1570 before the success in Vienna, thanks to the botanical doctor Prospero Alpino who introduced some sacks from the East into the country. Nowadays, the coffee cultivation areas are quite extensive and the coffee crops can be found in the tropical regions of the planet.[9]

From a botanical point of view, coffee plant belongs to genus *Coffea* of the Rubiaceae family, in which more than 500 genera and more than 8000 species are included[10,11]. Although more than 100 species belonging to the genus *Coffea* have been identified, only a reduced number of species are commercially important.

Coffea arabica, (also known as Arabica) which grows well on hilly, well-watered and drained slopes, today, is the most important strain in the world and accounts for approximately 70% of the coffee global market while, *Coffea canephora*, always known in the trade market as Robusta, accounts for approximately 30% and is mainly produced in Vietnam (**Figure 1.1.1**). Robusta beans are widely perceived to be inferior in flavor and aroma than Arabica. The third commercial species is *Coffea liberica*, which is the most important coffee species grown in Malaysia and it accounts for approximately 1% of the world's coffee production. Other wild coffee species are known and they locally grow in their respective areas of origin.[8,12,13]

The chemical composition of one species is different from the others and its study is not only important to improve the quality of the beverage but also because of the pharmacological effects. As a matter of fact, the increase in coffee consumption in the last years is due to greater knowledge and control of the different steps of the process to bring the harvested coffee fruits to consumers as a beverage, improving the ability to produce not only good quality coffee but also to show coffee as a functional food product.

Figure 1.1.1 Arabica and Robusta roasted coffee beans

1.1.2 Wild Coffee Species

Coffee has been classified into taxonomic groups according to their geographical origin, interspecific phylogenetic relationships and also on the basis of biochemical traits. Although coffee is cultivated in all intertropical zone of the planet, the distribution of coffee wild species is mainly focused in a limited area from West Africa to Madagascar and some islands in the Indian Ocean[14]. The sub-genus *Coffea* is normally divided in two sections, the first one is the *Eucoffea* section, to which the two main species *C. arabica* and *C. canephora* belong while the second section is the *Mascarocoffea* in which are included more than 50 species from Indian Ocean area that have been sub-divided in different categories according to the botanical criteria[15,16]. Some authors have divided the *Eucoffea* section into two sub-sections according to the geographical distribution of trees: those found in West and Central Africa belong to the *Eucoffea* sub-section, while trees originated from East and South-East Africa belong to the *Mozambicoffea* sub-section. Other studies have allowed the classification on the basis of the biochemical traits. For instance, some diterpenes

such as cafestol and kahweol can be used as parameters for taxonomic classifications as well as caffeine, lipids and chlorogenic acids content [17,18], since their concentrations are not only important for the development and growth of plants but also influence the organoleptic properties and quality of the seeds. However, until now, it has only been determined the chemical composition of some species and only the concentration of chlorogenic acids of approximately 20 wild *c*offee species has been reported.

1.1.3 Composition of Coffee

From a chemical point of view, coffee is composed of two main fractions: a volatile fraction, responsible for the aroma of coffee[19] and a non-volatile fraction, formed of water and dry matter. The dry matter of coffee beans consists basically of minerals and organic substances such as carbohydrates, lipids, proteins, alkaloids, carboxylic and phenolic acids which are precursors of the compounds contributing to the aroma [8,20,21]. As mentioned above, the different species, as well as climate, agricultural practices, maturity, fermentation, drying, storage, roasting and the method of preparation of the beverage,[22,23] influence the chemical composition and quality of taste, acidity, body, bitterness, sweetness and aroma of a cup of coffee [4,24]. Several studies have shown the correlation between the chemical composition of different classes of substances with the quality of the brew[25]. A simplified version of the coffee composition is shown in table 1.1.1[8] , as can be observed, in general, green coffee beans of the *Coffea arabica* contain a higher amount of lipids and sucrose than *Coffea canephora*, which has a higher content of polysaccharides, caffeine and chlorogenic acids. However, the chemical composition is very different after roasting, which is a very important step carried out at high temperatures (between 170-230 °C for 10-15 min approximately) and high pressure[26]. Roasted coffee beans contain several of the chemical compounds found in green coffee although in different concentrations and in addition, hundreds of other substances that are formed through several reactions such as caramelization, degradation of carbohydrates and the Maillard reaction are present, which are responsible of the sensory and organoleptic qualities that are appreciated in the brew.[27,28]

Table 1.1.1 Average composition of green coffee (% dry matter)[8]

Constituent	*Arabica*	*Robusta*
Caffeine and traces purines	1.2	2.2
Trigonelline	1.0	0.7
Total amino acids	10.3	10.3
free amino acids	0.5	0.8
Carbohydrates (by difference)	58.9	60.8
Aliphatic acids	1.7	1,6
Chlorogenic acids	6.5	10

Lipids	16.0	10
Glycosides	0.2	traces
Minerals	4.2	4.4
potassium	1.7	1.8

1.1.4 Non Volatile Fraction

Water. The water content in the beans influences all the processes of the coffee production, germination, growth, fermentation, drying, storage, transportation and roasting. Parchment Coffee must be dried to a moisture to have a water content between 10% and 12%, in order to maintain its chemical and microbiological stability during storage, to prevent bean damage and to obtain good sensory characteristics in coffee roasting.[29]

Alkaloids. Coffee contains several alkaloids that contribute to the bitter taste of coffee. The main ones are caffeine and trigonelline. Other alkaloids are present in lower concentrations such as paraxanthine, theobromine and theophylline. Robusta coffee contains more caffeine (2.1%) than Arabica (1.3%). On the other hand, trigonelline is found in greater quantity in Arabica (0.6% to 1.3%) than in Robusta (0.3% to 0.9%). The contents of paraxanthine, theobromine and theophylline are greater in Robusta than in Arabica. Mainly the caffeine in green beans is found to form a 1: 1 complex with potassium chlorogenate and the caffeine content remains stable during roasting so, due to its solubility in water, is extracted almost entirely during the preparation of the beverage. On the other hand, depending upon the roasting conditions, 85% of trigonelline is transformed into pyridines, pyrroles, nicotinic acid and other nitrogen compounds.[8,30]

Carbohydrates. The main polysaccharides in green coffee are mannan or galactomannan (mannose and galactose polymers), which constitute 50% of the polysaccharides of the beans, while arabinogalactan (galactose and arabinose polymer) 30%, cellulose (glucose polymer) 15% and pectic substances 5%. Mature, healthy coffee beans contain more sucrose than immature and defective grains. The main difference in the composition of carbohydrates between coffee species is a higher content of sucrose in *Coffea arabica* (6% to 9%) than *Coffea canephora* (3% to 7%)[4,31]. After roasting, between 15% and 20% of the polysaccharides contained in the coffee beans are degraded, sucrose decomposes completely and caramelization produces pigments that give a caramel color and a bitter taste to the drink, as well as formic, acetic, glycolic, lactic and other aromatic compounds such as furans. More than 99% of the reducing sugars react with the amino acids in the well known Maillard reaction or glycation and in this way the melanoidins are formed, which contribute to the brown pigment of the coffee beans and also give a characteristic flavor to the beverage. In addition, these reactions produce the pyrroles, thiophenes, oxazoles, thiazoles and pyrazines responsible for the aroma of roasted coffee.[32,33]

Lipids. The total lipid content in green coffee is between 7-17% and the lipid fraction is mostly concentrated in the beans as coffee oil is present as a waxy layer leading to the formation of flavors and fat-soluble vitamins that contribute to the texture of the beverage[8]. The lipid content is different in the two main species since *Coffea arabica* contains a higher lipid amount (15%) than *Coffea canephora* (10%). There are more free fatty acids in stored grains than in fresh beans and triglycerides reach approximately 75% of coffee lipids. The unsaponifiable matter constitutes about 20% of the total lipid content. Diterpenes and diterpene esters (mainly with palmitic acid) constitute about 15% of the total lipid content but their content depends on the coffee species since kahweol esters are present in *Coffea arabica*, esters of cafestol are present in both species while 16-*O*-methylcafestol is found only in *Coffea canephora.* This latter compound, due to its stability during roasting, is used as a marker to identify possible contents of Robusta coffee in blends. Sterols are also present in the unsaponifiable matter up to 2.2% of the coffee lipids in both species[34,35]. During roasting, lipids composition changes, some fatty acids increase, unsaponifiable lipids decrease and some lipids are oxidized to form aldehydes and other volatile compounds.[36]

Proteins and amino acids. The free amino acids represent about 5% of the dry matter in green coffee and can vary from one species to the other. The total content of free amino acids is higher in mature beans than in immature ones and it is generally higher in Robusta than in Arabica. Anyway, it is possible to find some amino acids in less quantity in the mature coffee bean as it has been reported in the literature for the concentrations of tryptophan, threonine, glycine, tyrosine, serine, alanine lysine and arginine, which decrease with a higher degree of maturation[8]. Amino acids are present as proteins and the total protein content in green coffee is between 10-13% in quite all coffee species and they are made up of 50% of albumins (soluble in water) and 50% of insoluble globulins. In coffee beans stored at high temperatures there is a higher content of free amino acids. The enzymes contained in coffee beans can catalyze the degradation of carbohydrates, lipids, proteins and chlorogenic acids of the same bean[37] and this degradation, as well as a decrease of the protein content, in the roasted coffee bean depends on the degree of roasting. The amino acids react and generate aroma compounds of roasted coffee, as for example in the reaction of Strecker they are transformed into aldehydes, CO_2 and ammonia while in the Maillard reaction they react with the reducing sugars and produce the melanoidins and various volatile nitrogen and sulfur compounds. [38]

Carboxylic Acids. As in most plants, some aliphatic acids, such as citric, acetic and malic acid are also found in the coffee, followed by phosphoric acid and other 35 different acids that, after chlorogenic acids, are the most abundant acids in coffee. The total content in green coffee is similar in both Arabica and Robusta except for quinic acid, the aliphatic part of chlorogenic acids, that is found in higher concentrations in Arabica[8]. The perceived acidity in the final beverage is a product of the residual concentrations of these acids and depends on the degree of roasting. The main acids of roasted coffee are: chlorogenic, quinic, citric, acetic, malic, formic, phosphoric, glycolic and lactic acid and additionally other 36 different acids have also been found [39].

Some of these acids come from green coffee and others are produced during roasting from carbohydrates, sucrose, citric, malic and phosphoric acids, trigonelline and lipids. Also in the volatile fraction of roasted coffee are present more than 20 acids such as propanoic, butanoic, pentanoic, heptanoic acid and other fatty acids[40].

In recent years, great attention has been paid to the concentration of chlorogenic acids and their degradation products in green and roasted coffee, since they are an indicator of the quality of coffee (they are responsible for the bitterness and astride of the beverage) but they also have possible health benefits. For this reason, chlorogenic acids will be described with more details in the next section.

1.1.5 Volatile Fraction: Aroma of Coffee.

About 300 volatile compounds have been found in green coffee [37]; the majority corresponds to pyridines, furans, amines, aldehydes, ketones, alcohols, acids and various sulfur compounds. Some of them allow to differentiate between one species and another as is the case of 2-Methylisoborneol [4], which apparently is one of the main responsible for the characteristic aroma of Robusta coffee. There is no a single compound responsible for the characteristic odor of roasted coffee, but its aroma is the result of the formation of various volatile compounds during roasting. About 850 volatile compounds are found in the aroma of coffee, which are not found in green beans, mainly furans, pyrazines, ketones, pyrroles, phenols, hydrocarbons, acids, aldehydes, esters, alcohols and thiophenes, thiazoles and oxazoles [41]. These are precursors of different kinds of aroma such as caramel, toasted, almond, citrus, fruit, cooked, but also unpleasant aroma such as earth, smoked and fetid and others [42,43]. Thanks to analytical methods used for its determination , such as gas chromatography (GC), with a sniffing port as the detector (GC-O) and mass spectrometry (GC–MS)[44,45,46] It has been possible to identify 20 key compounds for the formation of the characteristic aroma of roasted coffee, among these, the most outstanding is 2-furfurylthiol (FFT) [47] , which is generated by reactions of cysteine with arabinose that is released from the polysaccharides in coffee and shows a particular smell of roasted sulfur [4]. The olfactory sensations are ephemeral and they are not easy to describe and to classify since there is not a scale of the smell, like the one of the sounds or the one of the color. Each person has different sensitivity for odors and tastes, and the thresholds of smell and taste of each substance are different. The intensity of odors can be mild, weak or strong. In addition, odors can be described as irritating or intolerable[48]. In a kilogram of roasted coffee, it can be found approximately 500 mg of volatile substances. However, the volatile profile in the cup will be different depending of the extraction method[49]. About half the amount of volatile compounds generated during coffee roasting is lost during the milling, storage and preparation of the beverage extract. The most important constituents of coffee flavor are the ones with the highest “signal-to-concentration” ratio, which mean the ones that can be easily detected at a certain

concentration. Some of the most important volatile compounds found in roasted coffee are shown in **Figure 1.1.2.**

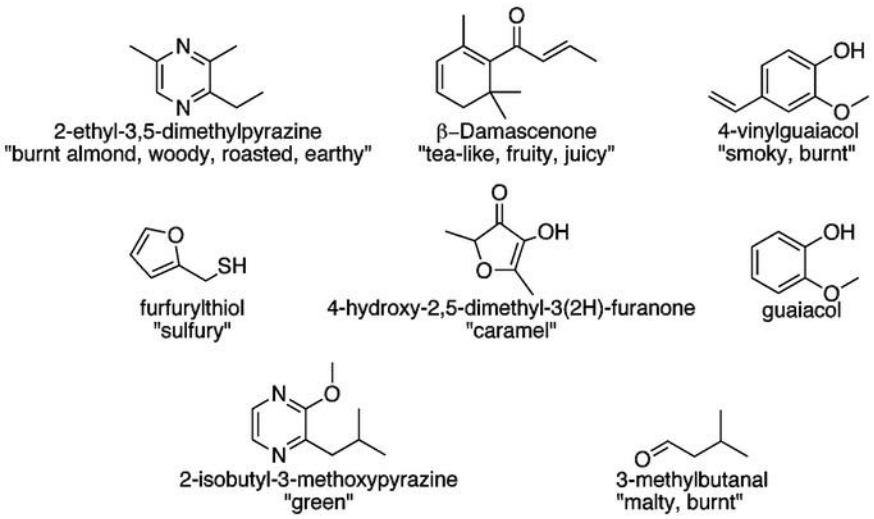

Figure 1.1.2. Molecular structure of some volatile compounds present in coffee.

1.1.6 Chlorogenic Acids.

Chlorogenic acids (CGAs) belong to the phenolic compounds present in plants,[50,51] which are secondary metabolites involved in defense mechanisms against environmental stress of plants.[52 53] Although CGAs are present in many vegetables[54] and fruits like potatoes, pears, apples, berries,[55] green coffee beans are particularly rich of these compounds,[56,51] being in fact, the main source of CGAs in the human diet.[5] Moreover, CGAs are considered as an indicator of the quality in coffee, affecting the flavor and the nutritional value of the final product,[55,25] since, as mentioned above, the final content of CGAs and their corresponding lactones formed after roasting process are responsible for the acidity, bitterness and astringency of the beverage.[56,57] Moreover, a high content of CGA after roasting with no oxidation products would be a positive aspect for coffee quality related to health benefits. In the last years, some health benefits have also been associated with CGAs and several reports have claimed that CGAs contribute to the prevention of cardiovascular diseases and types 2 diabetes.[55,58,59,60] CGAs are esters formed between quinic acid and *trans*-cinnamic acids (such as caffeic, ferulic and *p*-coumaric acid);[61] (**Figure 1.1.3**) therefore, depending on the type of the cinnamic acid and the esterified hydroxyl group of the cyclohexane ring of the quinic acid, a great variety of CGAs can be formed not only as monoesters but also as di- and triesters (table 1.1.6).[62] Esters at position C-1 of the quinic acid core have been not detected in green coffee beans but they are present in the plant kingdom although to a much minor extent. For example, cynarin is present in artichoke (*Cynara* species) and in *Echinacea* species which is a 1,3-dicaffeoylquinic acid. The total content of CGAs in coffee depends on the coffee species (*Coffee Arabica* 4-8% and *Coffee canephora* 7-14% of the dry matter basis),[50,63] but also on

the degree of roasting, the agriculture practices as well as the soil composition.[52] The most abundant CGA is 5-caffeoylquinic acid (also called chlorogenic acid), but a total number of 76 CGAs have been recognized in the last years. Moreover, it is important to note that the numbering system of these compounds is not always coherent in literature since many authors adopted the IUPAC numbering while others used the non-IUPAC numbering. This fact can create confusion in the identification of the different regioisomers and it is thus important to specify the numbering system adopted as well as to show the correct stereochemistry of all isomers. The IUPAC numbering for the quinic acid moiety, which was introduced in 1976[64], defines C-5 the carbon atom with the OH group in *cis* configuration with the COOH group as indicated in **Figure 1.1.3**

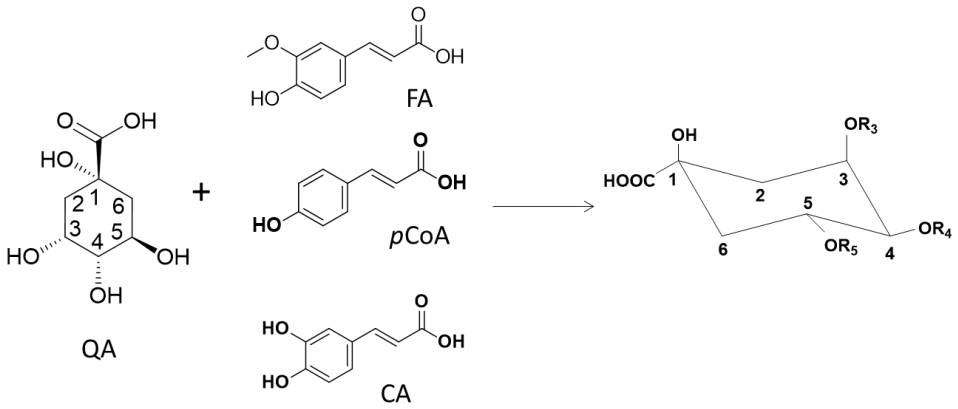

Figure 1.1.3 Formation of Chlorogenic acids between D-(-)-quinic acid (QA) and caffeic acid (CA), ferulic acid (FA), p-coumaric (*p*CoQA) [62,64].

Table 1.1.2 Main classes of CGAs found in coffee.

Class of CGAs	Name	R_3	R_4	R_5
Caffeoylquinicacids (CQAs)	3- caffeoylquinic acid (3-CQA)	CA	H	H
	4- caffeoylquinic acid (3-CQA)	H	CA	H
	5- caffeoylquinic acid (3-CQA)	H	H	CA
***p*-Coumaroylquinic acids (pCoQAs)**	*3-p*-Coumaroylquinic acid (3-*p*CoQA)	*p*-Co	H	H
	4-p-Coumaroylquinic acid (4-*p*CoQA)	H	*p*-Co	H
	5-p-Coumaroylquinic acid(5-*p*CoQA)	H	H	*p*-Co
Feruloylquinic acids (FQAs)	3-feruloylquinic acids (3-FQA)	FA	H	H
	4-feruloylquinic acids (4-FQA)	H	FA	H
	5-feruloylquinic acids (5-FQA)	H	H	FA
	3,4-dicaffeoylquinic acid (3,4-diCQA)	CA	CA	H

di-Caffeoylquinic acids (diCQA)	3,5-dicaffeoylquinic acid (3,5-diCQA)	CA	H	CA
	4,5-dicaffeoylquinic acid (4,5-diCQA)	H	CA	CA

1.1.7 Biosynthesis of CGAs

CGAs are biosynthesized in the perisperm and mostly accumulated in the beans, but they are also present in the leaves and in coffee pulp[65,66]. Different routes of synthesis have been proposed for the formation of the CGAs in plants[67]:

1) The transesterification of caffeoyl-CoA and quinic acid through the activity of hydroxycinnamoyl-CoA: quinate hydroxycinnamoyl transferase (HQT)

2) The hydroxylation of *p*coumaroyl quinate to CGA.

3) The hydroxylation of *p*-cumaroyl-shikimate to caffeoyl shikimic acid, which is then converted to caffeoyl-CoA, a substrate of hydroxycinnamoyl-CoA: shikimate hydroxycinnamoyl transferase HCT.

Studies have reported that CGAs and shikimate esters are synthesized by phenylpropanoid pathway (**Figure 1.1.4)**[67,68] that gives rise to diverse classes of CGAs, where the CQAs are the majority group. Several enzymes that participate in the biosynthesis process have been identified, however, the mechanisms are complex and until now they are not entirely clarified. At the beginning of the phenylpropanoid pathway, the deamination of phenylalanine in cinnamate is carried out through the enzyme phenylalanine ammonia lyase (PAL). The levels of phenylalanine ammonia lyase respond to several regulatory signals and it has been reported that it is the major factor that affects the levels of CGA in transgenic systems. Four enzymes are needed to complete two hydroxylations in the aromatic ring and a conjugation of the hydroxycinnamate and quinate moieties: cinnamate-4-hydroxylase (C4H), 4-coumaroyl-CoA ligase (4CL), cumaroyl-CoA: quinate hydroxycinnamoyltransferase (HQT) and coumarate / coumaroylquinate-3-hydroxylase (C3H).[69,70]

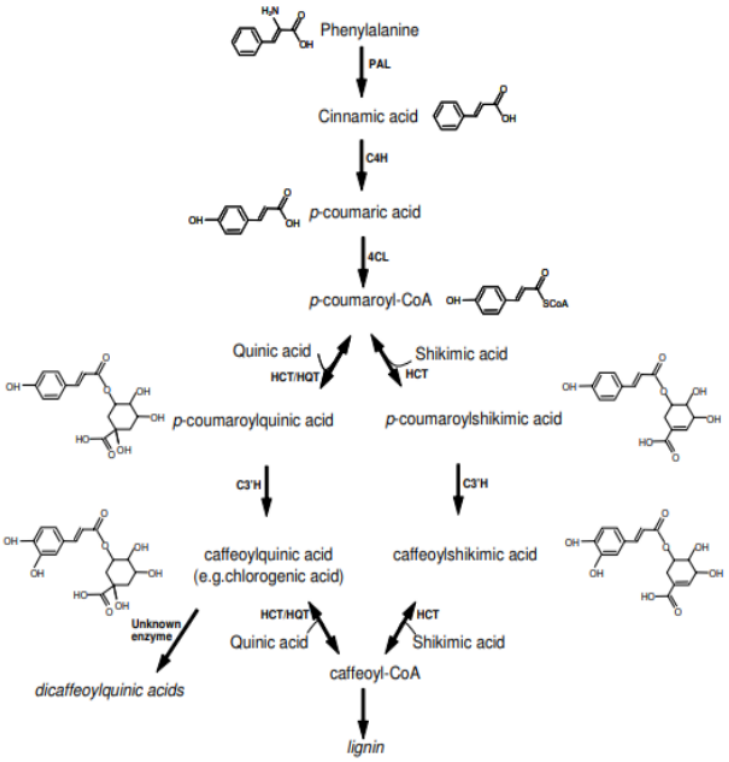

Figure 1.1.4. A simplified diagram of enzymes and major products in the synthesis of chlorogenic acid in plants. The product names appear between the arrows. Enzymes involved in this pathway are: PAL, phenylalanine ammonia lyase; C4H, cinnamate 4-hydroxylase; 4CL, 4-hydroxycinnamoyl-CoA ligase; HCT, hydroxycinnamoyl-CoA shikimate/quinate hydroxycinnamoyl transferase; HQT, hydroxycinnamoyl CoA quinate hydroxycinnamoyl transferase; C3'H, *p*-coumaroyl ester 3'-hydroxylase. [67]

1.1.8 Interactions of CGAs with Caffeine

In 1907 it was demonstrated that the potassium chlorogenate crystallizes with caffeine forming a non-covalent 1: 1 complex which has only been detected in aqueous media[71,72,73]. However, the nature of the attractive forces and the possible physiological significance of the complex have not yet been fully clarified. It has been noticed that in the presence of an excess of caffeine, the characteristic peak of the UV absorption of an aqueous solution of chlorogenic acid shift to higher wavelengths[71]. According to the literature, the stability of the complex is influenced by the benzene ring, the conjugated double bond and the phenolic groups. The fact that methylation of the phenolic hydroxyl and elimination of the carboxyl group in model complexes does not lead to a decrease in the strength of the complex shows that hydrogen bonding is not the driving force in the complex formation but it is probably due to the Π-Π stacking[72,73]. Some studies have reported that chlorogenate potassium decreases toxicity and reduces the diuretic effect of caffeine in rabbits and inhibits the action of caffeine in the muscle of frogs[71]. Therefore, this type of complexation can be carried out by plants as a strategy to control the compartmentalization of caffeine in tissues and to avoid any possible

self-toxicity since the main function of caffeine in plants is to protect them against attacks of predators thanks to its toxic effect on insects and some animals.[74,75]

1.1.9 Determination and Identification of CGAs.

The experimental procedure for determining CGAs in coffee beans is rather complex since it comprises extraction, separation and purification processes. Their identification and quantification is usually done by HPLC coupled with mass spectrometry (LC-MS).[52,56,58,63,76,,77,78,79,80] The fragmentation patterns of different classes of CGAs have been already established in the literature by using LC-MS, allowing the identification of specific isomers according to their corresponding base ions. According to published reports the most efficient method for the structurally identification and characterization of CGAs and their acyl-quinic acids derivatives is by LC–ion trap-MS^n, using fragment-targeted MS^n, leading to their identification without the need of isolation[76,77,81]. But, this type of instrumentation requires great care to ensure that an adequate energy collision is used to produce the characteristic fragmentations of each region-isomer, achieving its total and reliable identification. However, when the MS is not available, identification by HPLC through the assignment of specific retention times can result a little complicated due to the lack of authentic standards, which must be synthesized, since 5-CQA is the only CGA commercially available and it is often used as a universal standard. [82]

Other analytical methods employed for the identification and analysis of CGAs include infrared spectroscopy (FT-IR), nuclear magnetic resonance spectroscopy (NMR), ultraviolet spectroscopy (UV-Vis), difference spectra spectrophotometry and gas chromatography[83,84]. In recent years, technological advances have allowed the determination of CGAs by chemiluminescent (CL), a method detecting CGAs by flow injection based on the CL reaction of acidic potassium permanganate with CGAs in the presence of formaldehyde as an enhancer[85]. Some biomimetic sensors based on tetra nuclear copper complex have also been developed miming the active size of the catechol oxidase making possible to determine CGAs by square voltammetry[86]. Moreover, other techniques, like microwave-assisted extraction (MAE), pH-gradient counter current chromatography (CCC) are being used for the extraction and separation of CGAs from flowers of *Lonicera* japonica Thunb[83]. In recent years, attention have been paid to the determination of CGAs by molecularly imprinted polymers (MIP) which offer the possibility of specific molecular recognition. MIPs as a possible method for the recognition of CGAs will be described in detail in the next sections.

1.1.10 Changes During Roasting

The residual amount of CGAs after roasting contribute to the flavor and aroma of the brew[87,88,89]. CGAs are thermally unstable and degrade almost completely during roasting through a series of chemical reactions (F**igure 1.1.5**) giving rise to a wide range of volatile phenolic compounds [90,91,92]. They can undergo hydrolysis reactions releasing hydroxycinnamic acids or forming compounds of low molecular weights, dehydration and formation of an intramolecular bond to produce their corresponding quinolactones (CGLs) which contribute to the bitterness of the final brew and which have also shown some biological effects[50,93,94,95]. CGAs can also undergo isomerization and epimerization reactions and can even participate in the formation of polymeric compounds responsible of the pigment of roasted beans like melanoidins[96,97]. Depending on the type of the blend, the type and degree of roasting and the analytical method[98], the residual content of chlorogenic acids in roasted coffee can vary between 0.5 to 7%[83]. However, it should be noted that the concentration of chlorogenic acids in roasted coffee is higher than in other food sources of CGAs[93]. It has been reported that during the first minutes of roasting, the isomerization reactions take place causing a decrease of the isomers in position 5 and an increase of the isomers in positions 3 and 4 of the quinic acid ring[50]. The formation of the lactones occurs approximately after 6-7% of the weight loss[50] and the 1,5 quinides are the major lactones formed during roasting and as it is expected, those derived from the CQAs are the main ones (**Figure 1.1.6**). The main lactone is 3-caffeoylquinide or 3-caffeoylquinic-1, 5-lactone (3-CQL), that can reach maximum levels of 230 and 254mg (%dmb), in Arabica and Robusta coffee, respectively. The second main lactone is 4-caffeoylquinic-1, 5-lactone (4-CQL), with average contents of 116 and 139 mg% in Arabica and Robusta [50]. Other lactones from FQA, diCQA and *p*CoQA have been also identified in roasted coffee although in significantly lower concentrations[99,97,100].

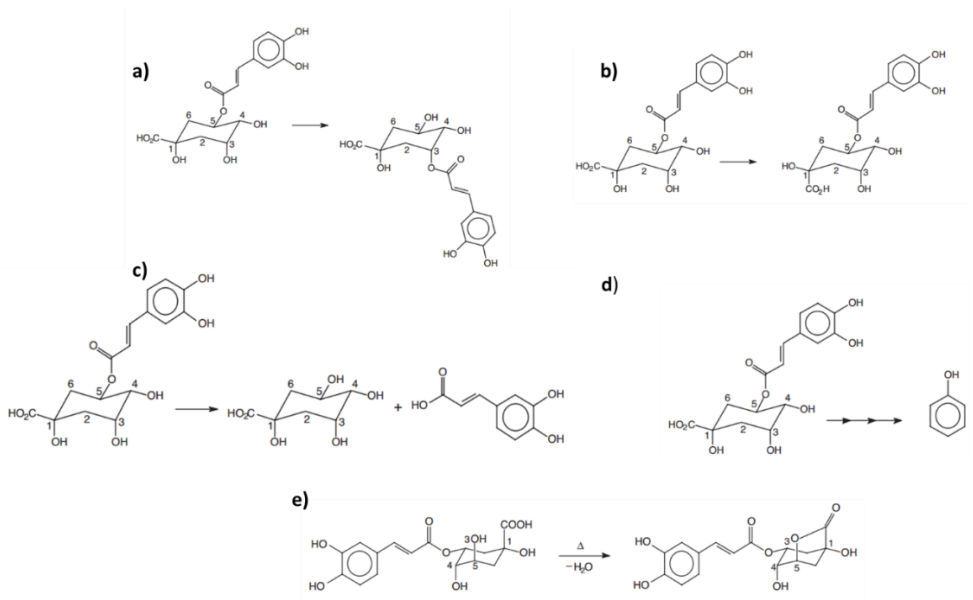

Figure 1.1.5. Changes of CGAs during roasting: **a)** Positional Isomerization, **b)** Epimerization **c)** Hydrolysis **d)** Degradation into low molecular weight compounds and **e)** Lactonization

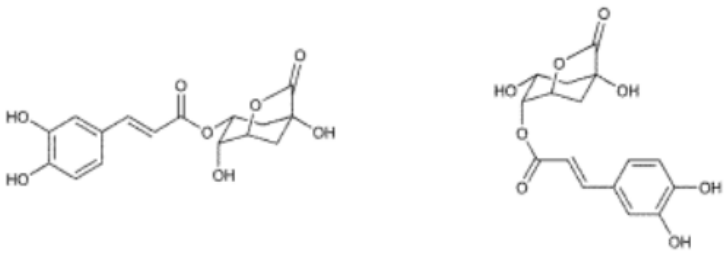

3-CQL **4-CQL**

Figure 1.1.6. Molecular structure of main CQLs.

1.1.11 Chemical Synthesis of CGAs

Since Panizzi et al.[101,102] reported the first synthesis of the CGAs, several authors have carried out the synthesis of different isomers of CQA (Sefkow et al.)[103,104] and FQA (Dokli et al.).[105] The synthesis of *p*CoQAs was performed for the first time by Haslam et al. who obtained all isomers of *O*-*p*-coumaroylquinic acids using acyl migration as a synthetic method and also by condensation of *O*-acetyl *p*-coumaroyl chloride with 1-*O*-ethoxycarbonyl quinide, but the final yields were very low (6%).[106,107] It must be noted that a different nomenclature was used at that time deriving from a different numbering system of the substituents at the cyclohexane ring. To avoid confusion in identifying the different isomers we have to remind that in the present work the IUPAC numbering system is adopted[64] (the OH group being on the same side of the carboxylic group is the position 5 of the cyclohexane ring). In the same way, Chao-Mie Ma et al.[108] carried out the synthesis of 5-*O*-*p*-coumaroylquinic acid by condensation between quinic acid, bisacetonide and *p*-acetylcoumaroylchloride, in order to evaluate its potential antifungal activity. Even though it seems that all methods described in the literature involved the esterification reaction between an acyl chloride and a derivative of the quinic acid prepared in order to protect in a selective way the hydroxyl groups of the cyclohexane ring, there is still a lack of information about the route of synthesis and spectroscopy data of the others groups of CGAs, like the isomers of *p*-coumaroylquinic acids, which are less abundant in coffee and for this reason are the less studied.

1.1.12 Metabolism of CGAs

Taking into account that the concentrations of the CGAs in the coffee beverage are higher than those of their corresponding CGLs, because the latter are less soluble in water and they can vary according to the type of roasting, extraction method, commercial blend[109,110], it has been reported that a cup of 200 mL of Arabica coffee contains between 70 and 200 mg of CGA, while a cup of Robusta coffee contains between 70 and 350 mg. These concentrations can vary upon the roasting degree and the extraction method. Coffee abstainers

may ingest less than 100 mg of CGA per day while coffee drinkers can consume around one gram of CGA per day [55,62,111,112] and this amount of CGA, when consumed regularly, seems to be sufficient to produce therapeutic effects. The benefits that CGAs can bring to health have been widely reported in the literature[25,55,113,114,115] and were mentioned above, however, to exhibit their antioxidant properties, CGAs must be able to penetrate gastrointestinal barriers and enter into the blood system. Some "in vivo" studies to evaluate the absorption and effects of these compounds have been reported in the literature and various hypotheses about the absorption process of these compounds have been proposed[116,117,118]. The amount of CGAs or hydroxycinnamic acids available to act as an antioxidant in vivo will depend on the absorption in the digestive tract[119,120]. Some reports indicate that most of the ingested CGAs can be metabolized and their metabolites are found in the plasma[121,122]. Studies conducted in rats indicate that the CGA can be absorbed and found as intact forms (100-170 µg/l) in plasma.[123] On the other hand, studies in the human metabolism show that the non-absorbed CGAS reach the colon where they are hydrolyzed by the microflora into their corresponding hydroxycinnamic acids and quinic acid. Then, absorption and additional metabolism are carried out in the liver and kidney[114] (**Figure 1.1.7**) forming benzoic acid which is conjugated with glycine to form hippuric acid. This mechanism would significantly decrease the antioxidant activity of the CGAs since the hippuric acid does not show antioxidant activity.[55,119] CQAs have been detected in plasma even 4 hours after the ingestion, while intact 5-CQA have been found in urine after drinking coffee; however, absorption and metabolism mechanisms are different depending upon the group of CGAs. [55,117,124]

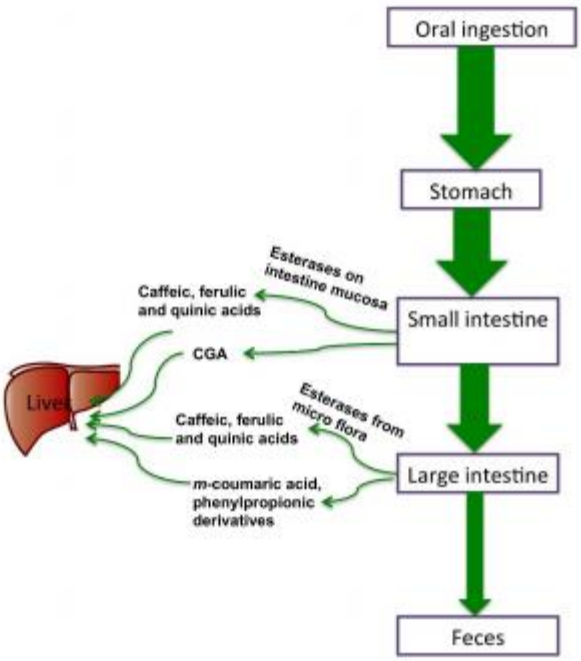

Figure 1.1.7. Simplified representation of CGAs Absorption [114]

[1] Farah, A. Coffee constituents in Coffee: emerging health effects and disease prevention. Edited by Chu YF, Iowa, Wiley-Blackwell, **2012**, ISBN 978-0-470-95878-0, chapter 2, 22–57.
[2] International Coffee Organization website: www.ico.org
[3] Nieber, K. The Impact of Coffee on Health. *Planta Med*., **2017**, 83(16): 1256-1263.
[4] Oestreich-Janzen, Chemistry of Coffee in Comprehensive Natural Products II: Chemistry & Biology, Ed by L. M and Liu H-W. CAFEA GmbH, Hamburg, Germany, **2010**, ISBN 978-0-08-045381-1, chapter 3, 1085-1113.
[5] Petracco, M. Our everyday cup of coffee: the chemistry behind its magic. *J. Chem. Edu*., **2005**, 82, 1161-1167.
[6] BrigittaPatay, E.; Bencsik, T.;Papp, N.; Phytochemical overview and medicinal importance of *Coffea* species from the past until now. *Asian Pac. J. Trop. Med*., **2016**, 9, 1127-1135.
[7] Tucker, C. M., Coffee Culture: Local Experiences Global Connexions. 2nd ed., edited by Routledge, **2011**, New York, ISBN 978-1-138-93302-6.
[8] Illy A. The experience of coffee consumption; in Espresso coffee. The science of quality, 2nd ed., edited by Illy A., Viani R., Elsevier Academic Press, London (UK), **2005**, ISBN: 978-0-1237-0371-2.
[9] Smith R.F. A history of coffee; in Coffee: botany, biochemistry, and production of beans and beverage, edited by Clifford M.N., Willson K. C., The AVI Publishing Company, Inc., Westport (CN), **1985**, ISBN: 978 -1-4615-66595, chapter 1, 1-12.
[10] Davis, A. P.; Govaert, R.; Bridson, D. M.; Stoffelen, P. An annotated taxonomic conspectus of the genus Coffea (Rubiaceae). *Botan. J. Linn. Soc*., **2006**, 152, 465–51.
[11] Vieira, H. D. Coffee: The Plant and its Cultivation in Plant Parasitic Nematodes of Coffee. Edited by Souza. R.M. Springer, **2008**, ISBN 978-1-4020-8719-6, chapter 1, 3-19.
[12] Mirian T. S.; Amaral da Silva, E. A.; de Castro, R. D.; Dussert, S.; Walters, C.; Derek Bewley, J. and Hilhorst, H. W. M Coffee seed physiology. *Braz. J. Plant Physiol*. **2006**, 18 (1), 149-163.
[13] Ismail, I.; Anuar, M. S. and Shamsudin, R. Physical Properties of Liberica Coffee (*Coffea liberica*) Berries and Beans. *J. Sci. & Technol*., **2014**, 22, 6 –79.
[14] Chevalier, A. Les caféiers duglobe. III: Systématique des caféiers et faux caféiers. Maladies et insectes nuisibles. Encycl. Biol. P. Lechavalier, **1947**, Paris, 112-122.
[15] Bridson, DM.; Verdcourt, B. Flora of tropical East Africa-Rubiaceae (Part 2), Polhill RM. Ed.,1988, ISBN: 9061913373, 333 pp.
[16] Anthony F.; Noirot, M.; Clifford M.N. Biochemical diversity in the genus Coffea L.: chlorogenic acids, caffeine, and mozambioside contents. *Genet Resour Crop Evol*.,1993, 40,61–70.
[17] J. J. Rakotomalala. Diversité biochimique des caféiers: Analyse des acides hydroxycinnamiques, bases puriques et diterpènes glycosidiques. Particularités des caféiers sauvages de la région malgache (Mascarocoffea Chev.), **1993**, Travaux et Documents3Microédités. ORSTOM.Paris.
[18] C. Campa, J. J. Rakotomalala, A. de Kochko, H. serge. Chlorogenic acids: diversity in green beans of wild coffee species. *Adv. Plant Physiol.*, **2008**, 10, 421-437.
[19] Feldman J. R., Ryder W. S., Kung J. T. Importance of non-volatile compounds to the flavor of coffee. *J. Agric. Food Chem*., **1969**, 17, 733-73.
[20] Clifford M. N. Chemical and physical aspects of green coffee and coffee products, in Coffee: botany, biochemistry, and production of beans and beverage, edited by Clifford M.N., Willson K.C, The AVI Publishing Company, Inc., Westport (CN), **1985,** ISBN: 978-1-4615-6659-5, chapter 13, 305-374.
[21] Kölling-Speer I., Speer K. Raw coffee composition; in Espresso coffee. The science of quality, 2nd ed., edited by Illy A., Viani R., **2005**, Elsevier Academic Press, London (UK), ISBN: 978-0-1237-0371-2, chapter 3, 148-166.
[22] Budryn G.; Nebesny E.; Podsędek A.; Żyżelewicz D.; Materska, M.; Janowski S.; Janda B. Effect of different extraction methods on the recovery of chlorogenic acids, caffeine and Maillard reacton products in coffee beans. *Eur. Food Res. Technol.*, **2009**, 228, 913-922.
[23] Delaroza, F.; Rakocevic, M.; Malta, G.B.; Sanchez, P.M.; Bruns, R. E.; Scarminio, L.S. Factorial design effects of plant density, pattern and light availability on the caffeine, chlorogenic acids, lipids, reducing sugars and ash contents of *Coffea arabica* L. beans and leaves. *Anal. Methods,* **2017,** 9, 3612-3618.
[24] Sunarharum, W.; Williams, D. J; Smyth, H. E. Complexity of coffee flavor: A compositional and sensory perpespective. *Food Res. Int.,* **2014**, 62, 315-325.

[25] Farah, A.; Monteiro, M. C.; Calado, V, Franca, A. S.; Trugo, L. C. Correlation between cup quality and chemical attributes of Brazilian coffe. *Food Chem.*, **2006**, 98, 373–380.
[26] Yeretzian C., Jordan A., Badoud R., Lindinger W. From the green bean to the cup of coffee: investigating coffee roasting by on-line monitoring of volatiles. *Eur. Food Res. Tech*., **2002**, 214, 92-104.
[27] Van Boekel M. A. J. S. Formation of flavour compounds in the Maillard reaction. *Biotech. Advan*., **2006**, 24, 230–233.
[28] Barter R. A short introduction to the theory and practice of profile roasting. Tea and Coffee Trade Journal, **2004**, 68, 34-37.
[29] Baggenstoss, J.; Perren, R.; Escher, F. Water content of roasted coffee: impact on grinding behaviour, extraction, and aroma retention. *Eur. Food Res. Technol.*, **2008**, 227(5), 1357–1365.
[30] Macrae, R. Nitrogenous Components in Coffee. Vol. 1. Chemistry. Edited by CLarke, R. J. and Macrae, R. England. Elsevier Applied Science Publisher, **1985,** ISBN: 978-94-009-4948-5, Chapter 3, 115-149.
[31] L. C. Trugo. Carbohydrates in Coffee. Vol. 1. Chemistry. Edited by CLarke, R. J. and Macrae, R. England. Elsevier Applied Science Publisher, **1985,** ISBN**:** 978-94-009-4948-5 Chapter 3, 83-113.
[32] Bradbury, A. G. W. Carbohydrates in Coffee recent developments. Edited by Clarke, R. J.; Viltzthum, O. G. Blackwell Science, **2001**, ISBN 0632-055553-7. Chapter 1, 1-15.
[33] Murkovic, M.; Derler, K. Analysis of amino acids and carbohydrates in green coffee. *J. Biochem. Biophys. Meth.*, **2006**, 69, 25-32.
[34] Ratnayake, W. M. N., Hollywood, R., O'Gradyc, E., Stavric B. Lipid content and composition of coffee brews prepared by different methods. *Food Chem. Tox*., **1993**, 31, 263–269.
[35] Speer, K.; Kolling S. I.; The lipid fraction of the coffee bean. *Brazilian Journal of Plant Physiology,* **2006**, 18, 201-216.
[36] Folstar, P. Lipids in in Coffee. Vol. 1. Chemistry. Edited by Clarke, R. J. and Macrae, R. England. Elsevier Applied Science Publisher, **1985,** ISBN**:** 978-94-009-4948-5. Chapter 6, 203-217.
[37] Flament, I.; The volatile compounds identified in green coffee beans in Coffee flavor chemistry, Wiley & Sons, Chichester, **2001**, ISBN: 0-471-72038-0, chapter 2, 11-33.
[38] Schenker, S., Heinemann, C., Huber, M., Pompizzi, R., Perren, R., Escher, R. Impact of roasting conditions on the formation of aroma compounds in coffee beans. *J. Food Sci*., **2002**, 67, 60–66.
[39] Jham, G. N.; Fernandes, S. A.; Garcia, C. F.; da Silva A. A.; Comparison of GC and HPLC for the Quantification of Organic Acids in Coffee. *Phytochem. Anal.*, **2002**, 13, 99–104.
[40] Woodman, J. S. Carboxylic Acids in Coffee. Vol. 1. Chemistry. Edited by Clarke, R.J. and Macrae, R. England. Elsevier Applied Science Publisher, **1985,** ISBN**:** 978-94-009-4948-5 **-**. Chapter 8, 266-287.
[41] Blank, I., Sen, A., Grosch, W. Potent odorants of the roasted powder and brew of Arabica coffee. Z. *Lebensm. Unters. Forsch*., **1992**, 195, 239–245.
[42] Czerny, M., Grosch, W. Potent Odorants of raw Arabica coffee. Their changes during roasting. *J. Agric. Food Chem*., **2000**, 48, 868–872.
[43] Yang, N.; Liu, Ch.; Liu, X.; Kreuzfeldt Degn, T.; Munchow, M.; Fisk, I. Determination of volatile marker compounds of common coffee roast defects. *Food Chem.*, **2016**, 211, 206–214.
[44] Akiyama, M., Murakami, K., Hirano, Y., Ikeda, M., Iwatsuki, K., Wada, A., Tokuno, K., Onishi, M., Iwabuchi, H. Characterization of headspace aroma compounds of freshly brewed arabica coffees and studies on a characteristic aroma compound of Ethiopian coffee. *J. Food Sci*., **2008**, 73, 335-34.
[45] Chin, S. T., Eyres, G. T., Marriott, P. J. Identification of potent odorants in wine and brewed coffee using gas chromatography. Olfactometry and comprehensive two-dimensional gas chromatography. *J. Chromat*. A, **2011**, 1218, 7487-7498.
[46] López-Galilea, I., Fournier, N., Cid, C., Guichard, E. Changes in headspace volatile concentrations of coffee brews caused by the roasting process and the brewing procedure. *J. Agric. Food Chem*., **2006**, 54, 8560-8566.
[47] Mayer, F., Czerny, M., Grosch, W. Sensory study on the character impact aroma compounds of a coffee beverage. *Eur. Food Res. Technol*., **2000**, 211, 272–276.
[48] Semmelroch, P.; Grosch, W. Studies on Character Impact Odorants of Coffee Brews. *Agric. Food Chem.*,.**1996**,.*44*, 537–543.

[49] Gloess, A. N., Schönbächler, B., Klopprogge, B., D'Ambrosio, L., Chatelain, K., Bongartz, A., Strittmatter, A., Rast, M., Yeretzian, C. Comparison of nine common coffee extraction methods: instrumental and sensory analysis. *Eur. Food Res. Techno*l., **2013**, 236, 607-627.

[50] Farah, A.; De Paulis, T.; Moreira, D.; Trugo L.; Martin, P. Effect of Roasting on the Formation of Chlorogenic Acid Lactones in Coffee. *J. Agric. Food Chem.,* **2005**, *53*, 1505-1513.

[51] Sinisi, V.; Boronova, K.; Colomban, S.; Navarini, L.; Berti, F.; Forzato, C. Synthesis of Mono-, Di-, and Tri-3,4-dimethoxycinnamoyl-1,5-γ-quinides. *Eur. J. Org. Chem.,* **2014**, 1321-1326.

[52] Monteiro, M.; Farah, A. Chlorogenic acids in Brazilian Coffea arabica cultivars from various consecutive crops. *Food Chem*., **2012**, *134*, 611-614.

[53] Jaganath, I. B.; Croizer, A. Dietary Flavonoids and Phenolic Compounds in Plant phenolics and Human Health. Edited by Fraga, C. New Jersey. Wesley, **2010,** ISBN 978-0-470-28721-7, chapter 1, 1-39.

[54] Clifford, M.; Knight, S.; Surucu, B.; Kuhnert, N. Characterization by LC-MSn of Four New Classes of Chlorogenic Acids in Green Coffee Beans: Dimethoxycinnamoylquinic Acids, Diferuloylquinic Acids, Caffeoyl-dimethoxycinnamoylquinic Acids, and Feruloyl-dimethoxycinnamoylquinic Acids *J. Agric. Food Chem.,* **2006**, *54*, 1957-1969.

[55] Olthof, M.; Hollman, P.; Katan, M. Chlorogenic acid and caffeic acid are absorbed in humans. *J. Nutrition,* **2001**, *131*(1), 66-71.

[56] Perrone, D.; Farah, A.; Donangelo, C.; De Paulis, T.; Martin, P Comprehensive analysis of major and minor chlorogenic acids and lactones in economically relevant Brazilian coffee cultivars. *Food Chem*., **2008**, *106*, 859-867.

[57] Frank, O.; Zehentbauer, G.; Hofmann, T. Bioresponse-guided decomposition of roast coffee beverage and identification of key bitter taste compounds. *Food Res. Technol*., **2006**, *222*, 492-508.

[58] Farah, A.; Monteiro, M.; Donangelo, C.; Lafay, S. Chlorogenic acids from green coffee extract are highly bioavailable in humans. *J. Nutrition,* **2008**, 138, 2309-2315.

[59] Mills, C.; Concha, M.; Mottram, D.; Gibson, G.; Spencer, J.P.E. The effect of processing on chlorogenic acid content of commercially available coffee. *J. Food Chem*., **2013**, 141, 3335-3340.

[60] Ludwig, I.; Sanchez, L.; Caemmerer, B.; Kroh, L. Extraction of coffee antioxidants: Impact of brewing time and method *Food Res. Int*., **2012**, *48*(1), 57-64.

[61] Clifford, M.; Knight, S.; Surucu, B.; Kuhnert, N. Characterization by LC-MSn of Four New Classes of Chlorogenic Acids in Green Coffee Beans: Dimethoxycinnamoylquinic Acids, Diferuloylquinic Acids, Caffeoyl-dimethoxycinnamoylquinic Acids, and Feruloyl-dimethoxycinnamoylquinic Acids *J. Agric. Food Chem*., **2006**, 54, 1957-1969.

[62] Clifford, M.; Chlorogenic acids and other cinnamates nature, occurrence, dietary burden, absorption and metabolism *J. Sci. Food Agric.,* **2000**, *80*, 1033-1043.

[63] Ky, C.; Noirot, M.; Hamon, S. Comparison of Five Purification Methods for Chlorogenic Acids in Green Coffee Beans (Coffea sp.) *J. Agric. Food Chem*. **1997**, *45*, 786-790.

[64] IUPAC Commission on the Nomenclature of Organic Chemistry (CNOC) and IUPAC-IUB Commission on Biochemical Nomenclature (CBN), *Biochem. J.*, **1976**, 153, 23–31.

[65] Joët, T.; Laffargue, A.; Salmona, J.; Doulbeau, S.; Descroix, F.; Bertrand, B.; de Kochko, A.; Dussert, S. Metabolic pathways in tropical dicotyledonous albuminous seeds: *Coffea arabica* as a case study. *New Phytol*., **2009**, 182, 146–162.

[66] Eira, M. T. S.; da Silva, A.; de Castro, R.; Dussert, S.; Walters, C.; Bewley, D.; Hilhorst, H. Coffee seed physiology, *Braz. J. Plant Physiol.*,**2006**, 18, 149-163.

[67] Comino, C.; Hehn, A.; Moglia, A.; Menin, B.; Bourgaud, F.; Lanteri, S.; Portis, E. The isolation and mapping of a novel hydroxycinnamoyltransferase in the globe artichoke chlorogenic acid pathway. *BMC Plant Biology,* **2009**, 9,1-13.

[68] Koshira, Y.; Jackson, M. C.; Katahira, R.; Wang, M. L.; Nagai, C.; Ashihara, H. Biosynthesis of chlorogenic acids in growing and ripening fruits of *Coffea arabica* and *Coffea canephora* plants. *Z. Naturforsch*., **2007**, 62, 731-742.

[69] Lallemand, L.; Zubieta, C.; Lee, S. G.; Wang, Y.; Acajjaoui, S.; Timmins, J.; McSweeney, S.;. Jez, J.; McCarthy, J.; McCarthy, A. A Structural Basis for the Biosynthesis of the Major Chlorogenic Acids Found in Coffee, *Plant Physiol,* **2012**, 160, 249-260.

[70] da Costa e Silva, O.; Klein, L.; Schmelzer, E.; Trezzini, G.F.; Hahlbrock, K. BPF-1, a pathogen-induced DNA-binding protein involved in the plant defense response. *Plant J*., **1993**, 4, 125-35.
[71] Sondheimer, E.; Covitz, F.; Marquisee, M. J. Association of naturally occurring compounds; the chlorogenic acid caffeine complex. *Arch. Biophys. Biochem*., **1961**, 93, 63-71.
[72] D'Amelio, N.; Fontanive, L.; Uggeri, F.; Suggi-Liverani, F.; Navarini, L. NMR reinvestigation of the caffeine chlorogenate complex in aqueous solution and in coffee brews. *Food Bioph*., **2009**, 4, 321-330.
[73] Horman, I.; Viani, R. The nature and complexation of the caffeine-chlorogenate complex of coffee. *J. Food Sci*., **1972**, 37, 925-927.
[74] Nathanson, J. A. Caffeine and related methylxanthines: possible naturally occuring pesticides. *Science*, **1984**, 226, 184-187.
[75] Ashihara, H.; Sano, H.; Crozier, A. Caffeine and related purine alkaloids: biosynthesis, catabolism, function and genetic engineering. *Phytochem*., **2008**, 69, 841-85.
[76] Clifford, M. N. Some Notes on the Chlorogenic Acids. 3. LC and LC–MS Version 3. Technical Report, **2017**.
[77] Clifford, M. N.; Jaganath, I. B.; Ludwig, I. A. Crozie, A. Chlorogenic acids and the acyl-quinic acids: discovery, biosynthesis, bioavailability and bioactivity. *Nat. Prod. Rep*. **2017**, 34, 1391-1421.
[78] Moeenfard, M.; Rocha, L.; Alves, A. Quantification of Caffeoylquinic Acids in Coffee Brews by HPLC-DAD. *J. Anal. Methods Chem*., **2014,** ID 965353, 10 pp.
[79] Salman, H. A.; Ramasamy, S.; Mahmood, B. S. Detection of caffeic and chlorogenic acids from methanolic extract of *Annona squamosa* bark by LC-ESI-MS/MS. *J. Intercult. Ethnopharmacol.*, **2018**, 7, 76–81.
[80] Craig, A. P.; Fields, C.; Liang, N.; Kitts, D.; Erickson, A. Performance review of a fast HPLC-UV method for the quantification of chlorogenic acids in green coffee bean extracts. *Talanta*, **2016**, 154, 481-485.
[81] Clifford, M.N.; Johnston, K. L.; Knight, S.; Kuhnert, N. Hierarchical scheme for LC-MSn identification acids. *J. Agric. Food Chem.,* **2003**, 51, 290-2911.
[82] Clifford, M. N.; Madala, N. E. Surrogate Standards: A Cost-Effective Strategy for Identification of Phytochemicals. *J. Agric. Food Chem.,***2017**, 65, 3589–3590.
[83] Upadhyay, R.; Mohan Rao, L. J. An outlook on chlorogenic acids-occurrence, chemistry, technology, and biological activities. Crit. Rev. *Food Sci. Nutr*., **2013**, 53, 968-984.
[84] Navarra, G.; Moschetti, M.; Guarrasi, V.; Mangione, M. R.; Militello, V.; Leone,M. Simultaneous Determination of Caffeine and Chlorogenic Acids in Green Coffee by UV/Vis Spectroscopy. *J. Chem.*, **2017**, ID 6435086, 8 pp.
[85] Wang, X.; Wang, J.; Yang, N. Chemiluminescent determination of chlorogenic acids in fruits. *Food Chem*. **2007**, 102, 422-426.
[86] Vieira, I. C.; Micke, G. A.; Neves, A.; Peralta, R. A.; Santhiago, M. de Carvalho, M. L. Determination of chlorogenic acid in coffee using a biomimetic sensor based on a new tetranuclear copper (II) complex. *Talanta*, **2008**, 77, 394–399.
[87] Trugo, L. C. and Macrae, R. A study of the effect of roasting on the chlorogenic acid composition of coffee using HPLC.*Food Chem*. **1984**, 15,219–227.
[88] Kucera, l.; Papoušek, R.; Kurka, O.; Barták, P.; Bednár, P. Study of composition of espresso coffee prepared from various roast degrees of *Coffea arabica* L. coffee bean. *Food Chem.*, **2016**, 199, 727–735.
[89] Montavon, P.; Duruz, E.; Rumo, G.; Pratz, G. Evolution of green coffee protein profiles with maturation and relationship to coffee cup quality. *J. Agric. Food Chem*., **2003**, 51:1328–2334.
[90] Leloup, V.; Louvrier, A.; Liardon R. Degradation mechanisms of chlorogenic acids during roasting. In Proceedings 16thInt. Sci. Coll. Coffee (Kyoto), **1995**, 192-198.
[91] Moon, J. K.; Yoo, H. S.; Shibamoto T. Role of roasting conditions in the level of chlorogenic acid content in coffee beans: correlation with coffee acidity. *J. Sci. Food Agric*., **2009**, 57, 5365-5369.
[92] Blumberg, F.; Frank, O.; Hofmann T. Quantitative studies on the influence of the bean roasting parameters and hot water percolation on the concentrations of bitter compounds in coffee brew. *J. Agric. Food Chem*., **2010**, 58, 3720–372.
[93] Farah, A.; Monteiro, R. C.; Calado, V.; Franca, A.; Trugo, L. C. Correlation between cup quality and chemical attributes of Brazilian coffee. *Food Chem*., **2006**, 98, 373-380.
[94] Clifford, M. N. Chlorogenic acids and other cinnamates: nature, occurrence, dietary burden, absorption, and metabolism. *J. Sci. Food Agric*., **2000**, 80, 1033-1043.

[95] Schrader, K.; Kiehne, A.; Engelhardt, U. H.; Maier, H. G. Determination of chlorogenic acids with lactones in roasted coffee. *J. Sci. Food Agric*., **1996**, 71, 392-398.
[96] Steinhart, H.; Luger, A. An analytical distinction between untrated and steam-treated roasted coffee. In Proceedings 17th Int. Sci. Coll. Coffee (Nairobi), **1997**, 155-160.
[97] Scholz, B. M.; Maier, H. G. Isomers of quinic acid and quinide in roasted coffee. *Lebensm. Unters. Forsch*., **1990**, 190, 132-134.
[98] Jeon, J. S.; Kim, H. T.; Jeong, I. H.; Hong, S. R., Oh, M. S.; Park, K.; Shim, J. H.; El-Aty, A. M. A. Determination of chlorogenic acids and caffeine in homemade brewed coffee prepared under various conditions. *J. Chromatogr. B*, **2017**, 1064, 115-123.
[99] Flores-Parra, A.; Gutierrez-Avella, D. M.; Contreras, R.; Khuong-Huu, F.^{13}C and ^{1}H NMR investigations of quinic acid derivatives: Complete spectral assignment and elucidation of preferred conformations. *Magn. Res. Chem*.**, 1989**, 27, 544–555.
[100] Scholz-Bottcher, B. M.; Ludges, E.; Maier, H. G. New stereoisomers of quinic acid and their lactones. *Liebigs Annalen der Chemie*, **1991**, 10, 1029–103.
[101] Panizzi, L.; Scarpati, M.; Oriente, G. *Gazz. Chim. Ital.,* **1956**, 86, 913-922.
[102] Panizzi, L.; Scarpati, M.; Oriente, G. Sintesi dell'acido clorogenico, *Experientia,* **1955**, *11*, 383-384.
[103] Sefkow, M.; Kelling, A.; Schilde, U. First Efficient Syntheses of 1-, 4-, and 5-Caffeoylquinic Acid. *Eur. J. Org. Chem.* **2001**, 2735-2742.
[104] Sefkow, M. First Efficient Synthesis of Chlorogenic Acid *Eur. J. Org. Chem*. **2001**, 1137-1141.
[105] Dokli, I.; Navarini, L.; Hamerŝak, Z. Syntheses of 3-, 4-, and 5-*O*-feruloylquinic acids *Tetrahedron: Asymmetry*, **2013**, *24*, 785-790.
[106] Haslam, E.; Haworth, R.; Makinson, G. Synthesis of 3-*O*-p-Coumaroylquinic Acid *J. Chem. Soc.* **1961**, 5153-5156.
[107]Haslam, E.; G.; G.; J. Synthesis and Properties of Some Hydroxycinnamoyl Esters of Quinic Acid. *J. Chem. Soc*., **1964**, 2137-2146.
[108] Ma, C.; Kully, M.; Khan, J.; Hattori, M.; Daneshtalab, M. Synthesis of chlorogenic acid derivatives with promising antifungal activity. *Bioorg. Med. Chem*. **2007**, *15*, 6830-6833.
[109] Gloess, A. N.; Schönbächler, B.; Klopprogge, B.; D'Ambrosio, L., Chatelain, K.; Bongartz, A.; Strittmatter, A.; Rast, M.; Yeretzian, C. Comparison of nine common coffee extraction methods: instrumental and sensory analysis. *Eur. Food Res. Technol.*, **2013**, 236, 607-627.
[110] Ludwig, I. A.; Mena, P.; Calani, L.; Cid, C.; Del Rio, D.; Leand, M.; Crozier, A. Variations in caffeine and chlorogenic acid contents of coffees: what are we drinking? *Food Funct*., **2014**, 5, 1718-1726.
[111] Farah, A.; Donangelo, C. M.; Phenolic compounds in coffee. *Braz. J. Plant Physiol*., **2006**, 18, 23-36.
[112] Lafay, S.; Gil-Izquierdo, A.; Bioavailability of phenolic acids. *Phytochem. Rev.* **2008**, 7, 301–311.
[113] Zhao, Y.; Wang, J.; Ballevre, O.; Luo, H.; Zhang, W. Antihypertensive effects and mechanisms of chlorogenic acids. *Hypertension Research*, **2011**, 1–5.
[114] Liang, N; Kitts, D. Role of Chlorogenic Acids in Controlling Oxidative and Inflammatory Stress Conditions. *Nutrients,* **2016**, 8, 1-20.
[115]Kajikawa, M.; Maruhashi, T.; Hidaka, T.; Nakano, Y.; Kurisu, S.; Matsumoto, T.; Iwamoto, Y.; Kishimoto, S.; Matsui, S.; Aibara, Y.; Yusoff, F. M.; Kihara, Y.; Chayama, K.; Goto, C.; Noma, K.; Nakashima, A.; Watanabe, T.; Tone, H.; Hibi, M.; Osaki, N.; Katsuragi, Y.; Higashi, Y. Coffee with a high content of chlorogenic acids and low content of hydroxyhydroquinone improves postprandial endothelial dysfunction in patients with borderline and stage 1 hypertension. *Eur. J. Nutr*., **2018**, doi.org/10.1007/s00394-018-1611-7.
[116] Nardini, M.; Cirillo, E.; Natella, F.; Scaccini, C. Absorption of phenolic acids in humans after coffee consumption. *J. Agric. Food Chem*., **2002**, 50, 5735-5741.
[117] Monteiro, M.; Farah, A.; Perrone, D.; Trugo L. C.; Donangelo, C. Chlorogenic acid compounds from coffee are differentially absorbed and metabolized in humans. *J. Nutr*., **2007**, 137, 2196-2201.
[118] Farah, A.; Monteiro, M.; Donangelo, C.; M.; Lafay, S. Chlorogenic acids from green coffee extract are highly bioavailable in humans. *J. Nutr*., **2008**, 138, 2309-2315.
[119] Gonthier, M. P.; Verny, M. A.; Besson, C.; Rémésy, C.; Scalbert, A. Chlorogenic acid bioavailability largely depends on its metabolism by the gut microflora in rats. *J. Nutr*., **2003**, 133, 1853–1859.

[120] Manach, C.; Scalbert, A.; Morand, C.; Rémésy, C.; Jimènez, L. Polyphenols: food sources and bioavailability. *Am. J. Clin. Nutr.,* **2004**, 79, 727–47.

[121] Renouf, M.; Guy, P. A.; Marmet, C.; Fraerinf, A. L.; Longet, K.; Moulin, J.; Enslen, M.; Barron, D.; Dionisi, F.; Cavin, C.; Williamson, G.; Steiling , H. Measurement of caffeic and ferulic acid equivalents in plasma after coffee consumption: small intestine and colon are key sites for coffee metabolism. Mol. *Nutr. Food Res.,* **2010**, 54, 760-766.

[122] Nagy, K.; Redeuil, K.; Williamson, G.; Rezzi, S.; Dionisi, F.; Longet, K.; Destaillats, F.; Renouf, F. First identification of dimethoxycinnamic acids in human plasma after coffee intake by liquid chromatography-mass spectrometry. *J. Chromatogr. A*., **2011**, 1218, 491-497.

[123] Lafay, S.; Gil-Izquierdo, A.; Manach, C.; Morand, C.; Besson, C.; Scalbert, A. Chlorogenic acid is absorbed in its intact form in the stomach of rats. *J. Nutr*. **2006**, 136, 1192–1197.

[124] Andreasen, M. F.; Kroon, P. A.; Williamson, G.; Garcia-Conesa M. T. Esterase activity able to hydrolyze dietary antioxidant hydroxycinnamates is distributed along the intestine of mammals. *J. Agric. Food Chem*., **2001**, 49, 5679-568.

1.2 Molecular Imprinting Technology (MIT)

1.2.1 Molecular Imprinted Polymers (MIPs)

Molecularly imprinted polymers are synthetic materials able to specifically and selectively recognize a target compound. These macromolecules have been inspired by natural systems such as: antibodies, hormones and enzymes which are perfect receptors for a specific target. MIPs consist on the formation of a complex between a target molecule, that acts as a template, and one or more functional monomers, in which are present acryoyl or vinyl groups that allow polymerization and are chosen based on their ability of interacting with the functional groups of the template[1]. The synthesis is carried out in the presence of a cross-linking agent and a radical initiator in a suitable porogenic solvent leading to the formation of a rigid three dimensional network around the template (analyte). After polymerization, the template is removed from the matrix, creating specific recognition sites that are complementary in shape, size and chemical functionality to the target, conferring to the polymer a kind of permanent memory that will allow it to selectively recognize the analyte from mixtures of similar compounds[2]. On the contrary of natural receptors, the resulting MIPs have proven to be robust and stable to drastic changes of pH, temperature and solvents. Moreover, molecular imprinting technology is a low cost technique of easy preparation and it represents an interesting option in various fields of chemistry and biology such as development of sensors, artificial antibodies and chromatography stationary phases. Recently, the most advanced application is the incorporation of MIPs as adsorbents for solid-phase extraction (MISPE) that is already accepted in several analytical laboratories, allowing the commercialization of some MIPs.[3,1,4] In literature, two different strategies have been reported to prepare MIPs, which are based on covalent or non-covalent interactions (**Figure 1.2.1**).

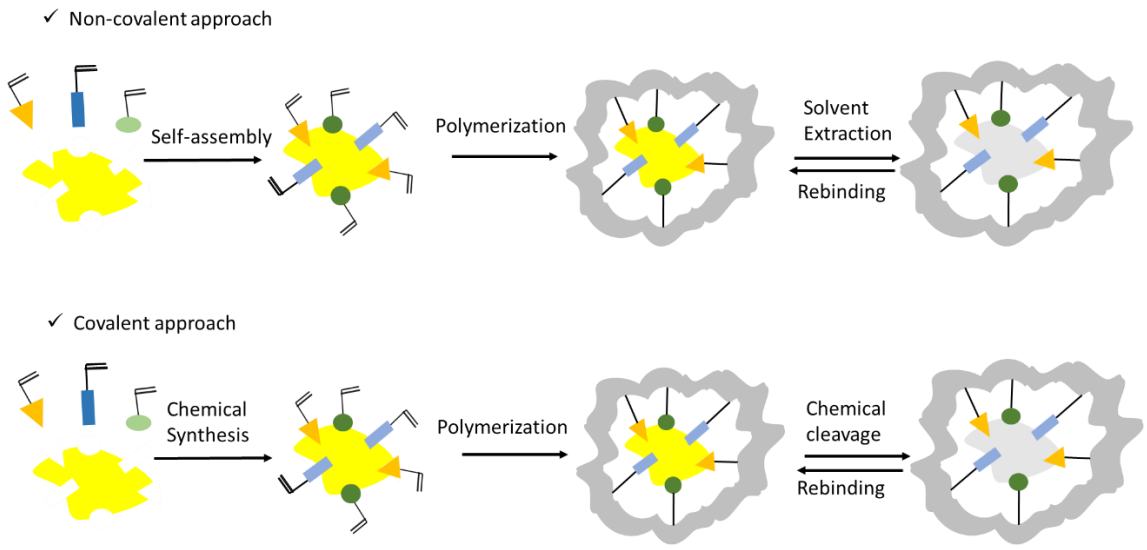

Figure 1.2.1. Schematic representation of non-covalent and covalent molecular imprinting approaches.

The covalent approach, introduced by Wulff et. al, involves the formation of covalent bonds between the template and the monomer before polymerization through a chemical reaction, so, after polymerization cleavage of the corresponding bond is necessary to remove the template from the polymer. This latter approach offers the possibility of obtaining more homogenous polymers, minimizing the number of non-specific sites[5], however, the main disadvantage is the difficulty of creating a reversible covalent bond that can be cleaved under mild conditions. This strategy is so restricted to only a few types of templates. The most common functional groups used for creating covalent bonds are aldehyde, boronic acid, diols and amines.[6,7,8.]

The non-covalent approach is so far, the most common strategy for preparing MIPs. It was proposed for the first time by Mosbach and Arshady and is based on the formation of relatively weak non-covalent interactions (e.g. hydrogen bonding, ionic interactions, Van der Waals forces) between the template and the monomer[9], thus, in this case, functional monomers have a particular orientation to the template before polymerization. Unlike the first strategy mentioned above, this type of approach allows the design of polymers for a wide range of templates capable of interacting with a large variety of commercial monomers. At the end of the polymerization process, the template is removed by washing the polymer with aqueous solutions of acids or bases.[2] Furthermore, the non-covalent methodology is simpler than the covalent one and higher affinity binding sites are obtained. Non-covalent polymers interactions are ruled by an equilibrium process during the pre-polymerization, therefore, a high amount of the monomer is often used to displace the equilibrium towards the formation of the complex, which can lead to the formation of non-selective binding sites. Moreover, in order to increase the binding capacity and selectivity, multiple functional monomers can be incorporated into the polymer. However, characterization of the biding sites during and after polymerization is still not complete. Another limitation is the need of several points of interactions, since molecules with a single interacting group will lead to polymers with lower recognition properties. [3,10]

1.2.2 Composition of MIPs

Although the synthesis of different types of MIPs have already been reported in the literature, their synthesis comprises a very complex chemical process with different variables that can be changed. Efficient polymers must be rigid enough in order to maintain the structure of the cavity after the removal of the template but at the same time must be flexible to allow the equilibrium between the release and capture of the template. To achieve these optimal properties, it is necessary to carry out a careful optimization of all polymer components. Such as: nature and concentration of the template, type of functional monomer (s), crosslinker, initiator and solvent, which determine the morphology and recognition properties of the MIPs[11]. The template is the essential component of the polymer, since the functional groups of the monomer(s) will be organized around it. From the free radical polymerization point of view, the analyte should be inert and does not participate in the polymerization process and must be stable under polymerization conditions[3]. The choice of the functional monomers is extremely important since they will create specific binding interactions

with the template. To successfully achieve the imprinting process, the functional groups of the analyte must be complementary to those of the monomer. In the case of covalent polymers, functional monomer(s) and template are bound in a stoichiometric way, but for non-covalent polymers, the optimization of ratio template/monomer is carried out by preparing different polymers with different formulations. Most of the imprinting polymers are based on polystyrene or polyacrylamide, due to their large availability in commerce.[12] The crosslinker is necessary to chemically link two or more linear polymers chains, but it influences the selectivity of the polymer and it will contribute to determine the morphology of the matrix (gel, macroporous or microgel powder) which directly affects the performance of the MIP.[13] The crosslinker will also stabilize the imprinted binding site and it will confer mechanical stability to the polymer. Generally, the crosslinker is used in higher concentrations with respect to the other components because it has been demonstrated that a high concentration of crosslinker enables the microcavities to maintain the three dimensional network after the removal of the template.[3] Initiators are used at lower levels with respect to the total number of moles of polymerisable double bonds and they are used as the radical source in free radical polymerization. A common initiator used in the preparation of a great number of MIPs is the azobisisobutyronitrile (AIBN). On the other hand, the nature of the solvent determines the strength of the binding interactions and can also influence the morphology of the polymer. The solvent is quite often call "porogen", since it is involved in the creation of the pores in macroporous polymers.[3] Three main conditions must be satisfied by the choice of the porogenic solvent, first, all components should be soluble, second the solvent should be able to produce large pores to ensure the performance of the MIP and finally the porogenic solvents should be relatively low polar to reduce the interferences during the formation of the template-monomer complex.[2]

1.2.3 MIPs Preparation

Nowadays, free radical polymerization is the most common synthetic method used for the preparation of MIPs. This method has shown a wide variety of industrial applications for the large-scale production of various types of plastics. Its greatest advantage is the possibility of carrying out the synthesis under relatively mild reaction conditions, such as relatively low temperatures and atmospheric pressure, so that a large number of monomers can be used. In addition, this method shows a considerable tolerance to impurities in the system, such as the presence of water. [11] Nevertheless, the presence of atmospheric oxygen can retard radical polymerization so it is recommended to remove oxygen from the solutions before polymerization.[3] The free radical polymerization comprises three steps as can be observed in **scheme 1.2.1**: initiation, propagation and termination.[14] The initiation leads to the polymerization of thousands of monomer molecules where free radicals are produced by homolytic dissociation of the initiator. Free radicals can be generated in different ways, including thermal decomposition or high-energy radiation. Two reactions commonly used to produce radicals for polymerization are the thermal or photochemical decomposition of

benzoyl peroxide or azobisisobutysonitrile (AIBN). When the species already originated by the thermal or photochemical decomposition of the initiator find the double bond of the vinyl monomer, they are added to the Π-bond and regeneration of another radical takes place. The chain radical is formed by adding successive monomers. Ideally, this propagation could continue until the monomer (s) is consumed, however, the polymerization ends due to the strong tendency of the radicals to react in pairs to form a covalent bond of paired electrons, which generates a radical loss of activity. This tendency is compensated in the radical polymerization by the small concentration of radical species compared to the monomers. The bimolecular reaction between the two radicals can take place in two ways: combination/coupling or disproportionation. In the combination mechanism a single macromolecule is formed by a covalent bond between two radical chains, while, during disproportionation, two polymer molecules are formed, one saturated and one unsaturated as a result of the transfer of a beta hydrogen from one radical center to another.[14] Once the propagation ends, either linear or cross-linked polymers can be formed depending upon the properties of the functional monomers used.

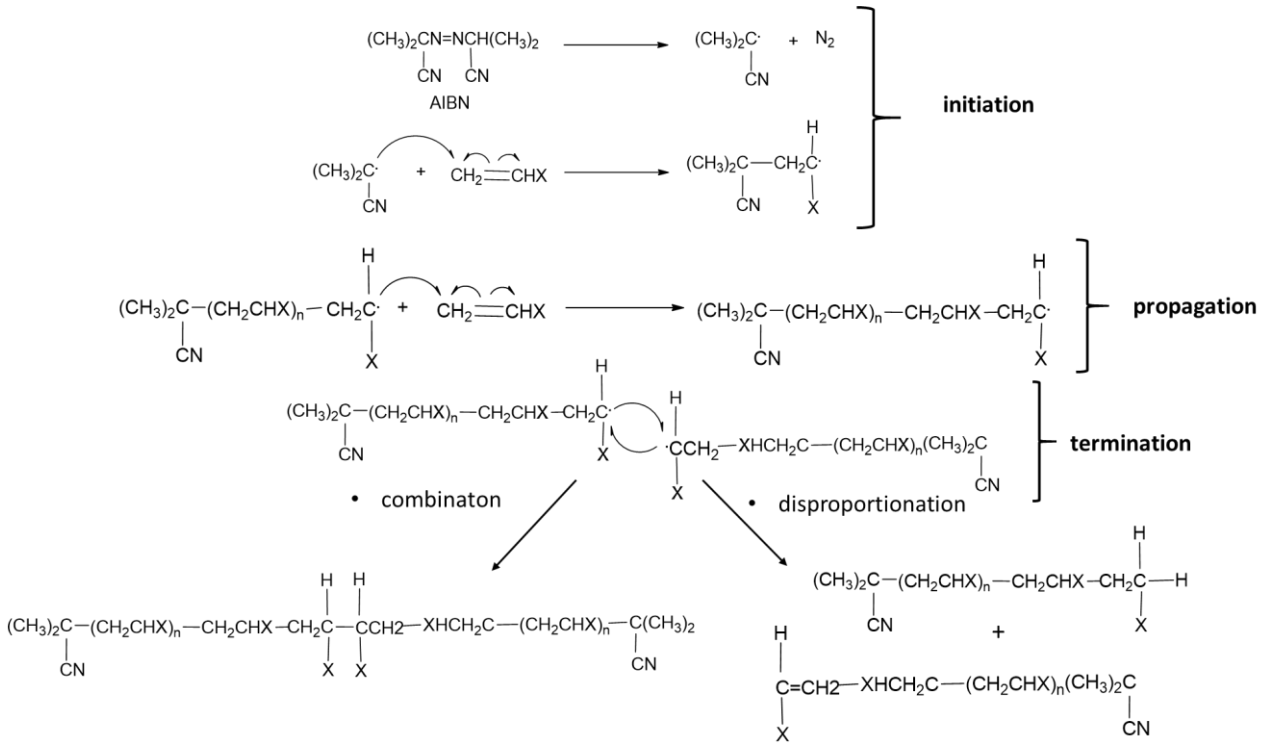

Scheme 1.2.1 Radical polymerization.

1.2.4 Configuration of Monomer Units.

The configuration of a polymer refers to the order of different monomeric units along the polymeric chain. The mechanism involved in the polymerization process will lead to the formation of the thermodynamically favored product. Therefore, the structural arrangements of monomer units in the polymer will be influenced

by the type of substituents (R) on the double bond of the monomer. As can be observed in Equation 1.2.1, addition of the radical could take place in two different ways.[15].

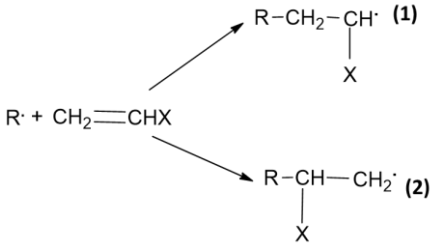

Equation 1.2.1. Addition of radicals in Vinyl Polymer Chains

Two types of arrangements are possible during the addition of monomers (Equation 1.2.2). *The head-to-tail* or 1,3-placement of monomer units happens when the successive addition of monomer molecules to the propagating radical occurs in the same manner leading to a final polymer product in which the substituents are on alternate carbon atoms. Instead, if the addition in the polymer chain propagation is alternately by reactions 1 and 2, as described above, the final polymer will have a structure with a 1,2-placement or *head-to-head* (H-H) arrangement of substituents at one or more places in the final polymer chain. In the equations shown above, the product of the most stable reaction 1 will have a *head-to-tail* arrangement because its stabilization is favored by resonance effect and steric factors. Moreover, if a regular *head-to-tail* placement is obtained, the configuration will be regioselective and it is called *isogeric*, while if the final polymer contains alternated regions of both placements it is known as *syndioregic* and finally, when random arrangements are present the final polymer configuration, is called *aergic.* The possibility of obtaining a regular *head-to-head* placement is remote, and it appears that only an occasional monomer unit enters the chain in reverse manner to provide an isolated *head-to-head* unit.[14,15]

Head to Tail **placement**

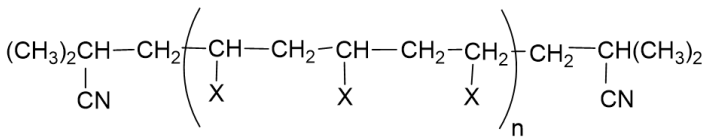

Head to Head **placement**

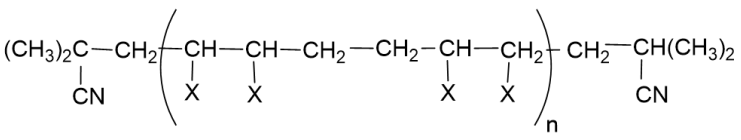

Equation 1.2.2. Configuration of Monomer Units in Vinyl Polymer Chains

1.2.5 Cross-linked Polymers

As mentioned above linear or crosslinked polymers (**Figure 1.2.2**) can be formed depending upon the structures of the functional monomers used. Those functional monomers containing one polymerisable vinyl group are known as mono-functional monomers and they will lead to the formation of linear polymers. While functional monomers with two or more polymerisable groups often used as crosslinkers can produced crosslinked or non-linear polymers. In crosslinked polymers the branches of the polymeric backbone are covalently linked to other polymer chains creating a polymeric network. This type of polymerization between mono-functional and multi-functional monomers is called copolymerization. Non-linear polymers can be prepared by free radical polymerization as linear polymers and they are usually classified in branched macromolecules, microgels and macroscopic networks.[3] Crosslinked polymers have shown a great number of industrial applications. Particularly in molecular imprinting technology, macroscopic polymers networks are the most studied and synthesized materials due to their rigidity which confers mechanical stability to the imprinted site. A very important parameter to be considered during copolymerization, that will define the properties and structure of the non-linear polymer, is the cross-linked ratio, that is the percentage of crosslinker with respect to the total number of monomer moles and the volume of the porogenic solvent.[2,11] Nowadays, thanks to several studies published in the literature, it is possible to make some generalizations and predict the physical nature of the final polymer. Polymerizations carried out at low or high ratio of crosslinkers and with low volumes of solvents do not allow the phase separation of the polymer and the final product is a lightly solvated gel-type polymer, which generally have very low specific surface areas and when the crosslinker ratio is very low they have poor mechanical properties. If the polymerization occurs at relatively higher crosslinker ratios and in the presence of higher volumes of solvents, macroporous polymers are obtained, since in this case the polymer will be able to phase separate from the medium and can precipitate from the polymerization mixture. These type of polymers are characterized by their higher specific surfaces areas and mechanical stability showing permanently porous structures even in the dry state and allowing the access to the pores also with thermodynamically non-compatible solvents[3,13,16.] On the other hand, at even more diluted conditions, thus higher volumes of solvents, the polymer particles usually in micro or nano scale remain in a non-aggregated state and polymers can be obtained as a powder. The final products are known as microgels powders and they have shown higher surface and an easy accessibility to the binding sites. Although the features of macroporous polymers make them very attractive to the preparation of MIPs[17], in the recent year, great attention has been paid to microgel powders and their applications in molecular imprinting technology such as the controlled drug delivery, artificial enzymes in catalysis and as recognition elements for biosensors.[18,19,20,21]

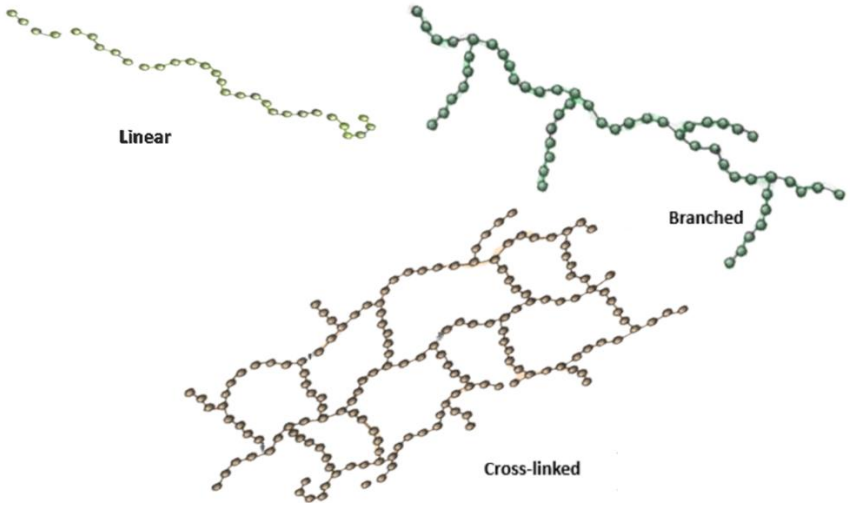

Figure 1.2.2. Polymers structures

1.2.6 Sensors based on Molecularly Imprinted Polymers.

By definition, a chemical sensor is "*a self-contained device that is capable of providing real-time analytical information about a test sample*"[22] and this information can be qualitative or quantitative. The essential part of a sensor is the receptor whose function is to bind the analyte with high affinity and selectivity. Then, a transducer transforms the binding process into a measurable output signal (**Figure 1.2.3**), so, the recognition and transduction function are integrated in the same device[23]. The first chemical sensor was the glass electrode for pH determination[22], however, in latest years, due to the need to automatize industrial processes, there has been a notable increase in the development of chemistry sensors and their applications.

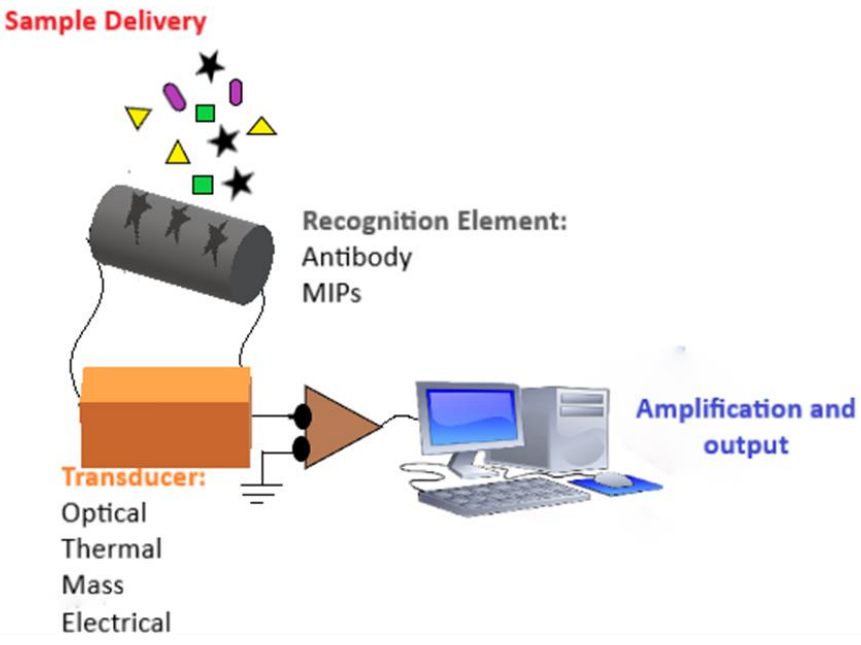

Figure 1.2.3. General Structure of a Sensor

Biosensors are chemical sensors where the recognition is based on biochemical or biological elements. The receptor can be composed of distinct molecular units called recognition receptors or alternatively, it can be a material that includes in its composition recognition sites.[24,2526] Therefore, MIPs can be considered as biomimetic receptors since these materials can show specificities and affinities perfectly comparable with the natural ones and their advantages, such as chemical and physical stability, make them compatible with several detection conditions and confer relatively long life times. MIPs are a very interesting and versatile alternative as receptor or recognitions elements for sensing. In a sensor based on MIPs, as a result of the interaction between the template and the receptor (MIP) one or more physical or chemical properties of the polymer vary and these variations should be directly proportional to the concentration of the template.[272829] In order to allow the interpretation of this variation MIPs can be combined with several transducers such as electrochemical, calorimetric, piezoelectric, and optical transducers.

The use of MIPs as receptors is greatly depending upon the immobilization methods, which can help to preserve the stability and life time. Different immobilization techniques have been reported in the literature such as physical entrapment, adsorption, covalent binding and cross-linking. The selection of the method is influenced by the nature of the MIP as well as the type of transducer and operating conditions of the sensor. The most common methods are those where a bond is formed between the functional group of the receptor and a reactive group of the support. Furthermore, integration of MIPs in sensors can be carried out *in situ* by using a photochemical or thermal initiator to promote polymerization. This approach offers the possibility of controlling modifications of inert electrode surfaces with thin films of specific polymers.[27,30]

The first prototype of a sensor based on MIP was a capacitance sensor consisting of a field -effect capacitor. The MIP membrane was imprinted with phenylalanine and its binding to the polymer resulted in a change of the capacitance that only allowed the qualitative identification of the template[31]. Subsequently, other types of sensors, that are not based on any specific property of the analyte, have been recently developed by the combination of MIPs with a piezoelectric transducer to create acoustic sensors[27]. A good example is the Quartz crystal microbalance devices (QCM), which are mass-sensitive acoustic sensors where the oscillation frequency changes according to mass changes at the transducer surface upon the analyte binding to the polymer. QCM are easy to prepare and low cost devices. Following this approach, a sensor for detecting glucose was set up.[32] The polymer, made of poly(o-phenylenediamine), was electrosynthesized at the surface sensor area in the presence of the template. Then, the resulting thin polymer layer was able to selectively detect the analyte over other compounds. Other QCM sensors were prepared by electropolymerization of o-phenylenediamine on a QCM surface for detecting sorbitol.[33] The sensor showed high selectivity for the analyte over a concentration range of 1-15mM compared with glucose, mannitol and fructose. QCM have been also applied for detecting cells and viruses. A QCM MIP sensor able to specifically bind yeast cells was developed and could be used at concentrations between $1x10^4$ and $1x10^9$ cell per mL under flow conditions[34].

Others sensors able to measure the mass accumulation on the surface are those with optical transducers using the surface Plasmon resonance (SPR). The sensitivity of SPR sensors for small target molecules can be increased by including gold nanoparticles in the MIP layer. Following this approach, a SPR sensing device for detecting dopamine [35] and theophylline [36] has been created and analyte concentrations down to the nanomolar and micromolar range respectively were detected.

Conductometric transducers have been also used for designing MIPs sensors[37], offering the possibility to improve the detection limit. Conductometric devices measure the conductivity changes of a selective layer in contact between two electrodes separated by membrane of an imprinted polymer. An example of this sensor type is the one based on atrazine imprinted acrylic polymer membrane allowing the quantification of the herbicide atrazine. The flexibility and stability of this device was controlled by optimizing the type of crosslinker and its molar ratio together with the optimization of the volume of porogenic solvent in the mixture. The sensor showed a detection limit of 5 nmol· L^{-1}, which seems to be dependent on the ability of the polymer to change its conformation upon the analyte binding. Moreover, rapid measurement times, around 6-10min, and high selectivity for the analyte over other related triazine herbicides were observed[38].

In recent years, with the advances in technology, there has been a growing interest in the development and design of nanosensors, that is, in the miniaturization of the devices. An excellent alternative that allows to detect and quantify the analyte with this approach is the Surface Enhanced Raman Spectroscopy (SERS). This technique was employed for developing MIP-nanosensors for propranolol and bisphenol A in which low sensitivity and reproducibility were improved by combining the MIP with noble metal nanocomposites. As a result, a single particle nanosensor Au-MIP with a signal amplification was obtained able to detect the desired analytes with a detection limit of 10^{-7}mol·L^{-1} and 0.52µmol·L^{-1} respectively.[39,40,41]

Hitherto, a great variety of sensors based on MIPs have been created due to the advances in the optical fiber technology. The most common fields are the detection of contaminants in water, food, drug delivery, analytical sensing of bioactive molecules and metals detection[42,43,44,,4546,47]. Furthermore, when the target molecule or the receptor (MIPs) exhibit a special property such as UV-Vis absorption, bio and chemo-luminescence, reflectance, electrochemical activity or fluorescence that can be modified by the binding process, these can be exploited for the creation of MIP-sensors. Of all the possible transductions mechanisms, optical fluorescence is particularly interesting because of its great sensitivity and spatial resolution.

1.2.7 Fiber optic Sensing (FOs)

The FO sensors are based on a standard optical fiber that is composed of a very thin glass that guides the light through itself[48]. Although initially these type of sensors were applied in the field of medicine[49], this type

of technology has had a massive increase in recent years due to its use in the field of telecommunications, which has allowed to explore a wide variety of applications. **(Figure 1.2.4**).

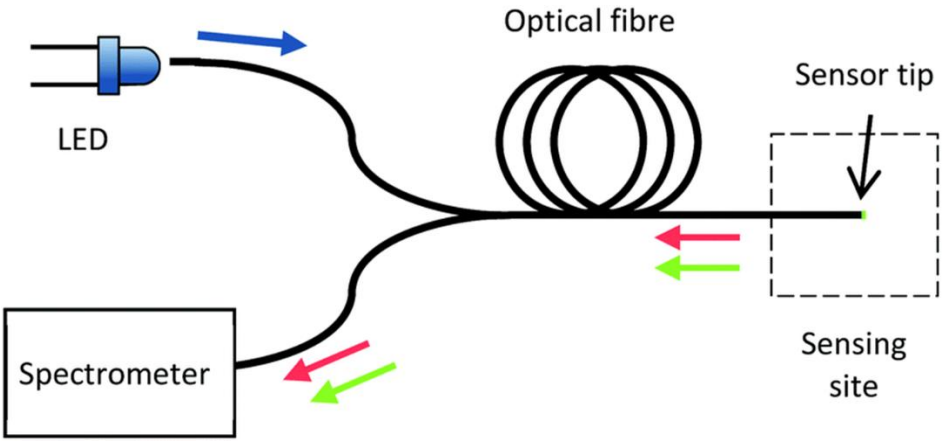

Figure 1.2.4 Diagram of the optical layout of the sensor [50]

As observed in **Figure 1.2.5** an optical fiber has three main components: the coating to protect the fiber from environmental effects, the cladding, which is used as a reflection layer and the core. To keep the light wave inside of the core, the central optical refractive index n_1 must be maintained higher than the cladding index n_2. In general, FO sensors are designed to detect physical (such as vibration, strain, temperature, acceleration, pressure) or chemical parameters (pH value, identification, concentration). The source in a FO sensor can be a LED, diode or a laser, while the medium is the optical fiber. The transducer plays the main roles in optical-sensing mechanism by converting the measured physical quantity to a light energy. The optical fiber allows the connection between the transducer with the detector and the processing devices are used to display the effect of the measurement to the original light source. Different processing devices are used depending on their applications, but the most common are spectrum analyzers and oscilloscopes.[48,51]

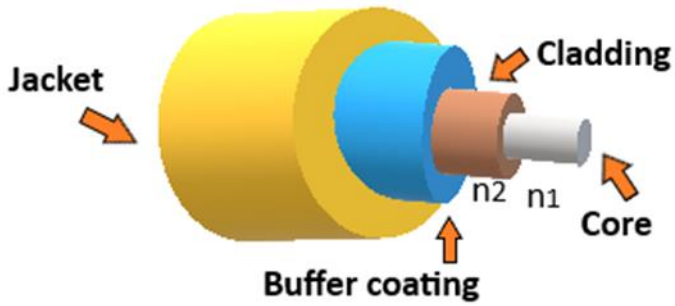

Figure 1.2.5. Scheme of a Fiber Optic (FO)

FO sensors are basically classified into two categories according to the design mechanism: intrinsic and extrinsic sensing. Thus, if the transducer is placed outside the fiber, the system will be extrinsic, which mean that the sensor system depends only on the transducer part located outside the FO cable to convert the parameter of interest into a measurable electrical signal. In extrinsic sensors, the optical fiber is used only to transmit the light to a sensing part where the signal leaves the fiber and is modulated by the transducer. Then, the modulated light turns back to the fiber to reach the detector. The modulation can be performed by changing the intensity, phase, frequency, spectral content or polarization of the original light coming to the transducer. This type of system offers the possibility of reaching inaccessible environments like electrical transformers. On the other hand, in intrinsic systems the light never goes out during the sensing mechanism because the transducer is placed inside the fiber. In these sensors there is a sensing region within the fiber to modulate the light. The modulation is carried out by optimizing the intensity, phase difference, resonance frequency or spectral interference. Intrinsic sensors are difficult to design but they offer a series of advantages over the extrinsic ones like the possibility of providing sensing over very long distances, durability to hard environmental conditions and the capability of high-sensitivity measurements. [52,53]

It is worth noting that extrinsic or intrinsic sensors do not measure the quantity of analyte in a direct way, these systems measure the effect of the analyte concentration on some optical wave parameters. Indeed, two main categories of FO sensors can be found in literature[48]. The first one depends on the type of modulation technique used. The information impressed in the propagating light wave can change the intensity of light, phase, frequency, wavelength or polymerization. While in the second category FO sensors are grouped by examining the type of spectroscopy used to analyze the target molecule. Spectroscopy is generally used to measure the changes of the fluorescence, absorption or reflection light caused by the modulation as sensing progresses.[54]

In the last years, chemical FO sensors were mainly used for detecting specific pollutants in water, air and soil[55,56] but nowadays thanks to its several advantages such as low cost, limited loss of light over long distances and the possibility of miniaturization and integration. FO sensors have been designed for other implementations like detecting a particular compound or material in mixtures making possible their use for a great range of criminal, medical and engineering purposes.

Fluorescent spectroscopy offers a high sensitivity in comparison to other spectroscopic techniques allowing the detection of particular compounds and analytes in low concentrations. This spectroscopy technique does not consume analytes and no reference is needed. The technical requirements are relatively simple since light can travel without physical wave-guide. Recently, a great range of fluorescence-based FOs have been developed with applications in biochemistry, biotechnology, analytical chemistry and photochemistry[57,58,59]. In a fluorescent FO sensor, the fluorescence source influenced by the target molecule can change some properties of upcoming light resulting in a light wave with different characteristics, thus a measurement

device able to detect the differences will give the material concentration. Depending on the purpose of the sensor, the fluorescence changes can be in its intensity, color, lifetime or even the polarization of the emission[48,60]. A great variety of fluorescence-based FOs exists nowadays, but there are two types commonly used in chemical sensing. The simplest one is known as "end-tip" sensor in which the light crosses with the probe fluorescent material after traveling to end. At this point the fluorescent affected signal reflects back in the same fiber to the demodulator. In these devices the pulsed light can both work on digital domain or can be continuous. Measurement of the fluorescence is possible thanks to a spectrofluorometer placed after the demodulator. The design of an "end-tip" sensor is a complex process since the fluorescent material is placed within a transparent matrix to allow the access of the analyte which will also permit interfering fluorescence which can disturb the receptor element and can negatively affect the performance of the system. The second type is the "etched" or "waveguide binding" configuration where evanescent properties of the fiber are used. In these systems the electric field formed during total internal reflection in the refraction environment can be absorbed by fluorophores around the interface. Etched regions filled with fluorescent material inside the fiber are created and these can be used to generate time division multiplexing for several measurements[48,61,62]. Several fluorescence sensors have been developed using MIPs coating as recognition elements either by employing "end-tip" or "etched" mechanisms. An outstanding example is a MIP fluorescence sensor designed to detect cocaine, based on an "end-tip" system[63]. Others MIPs fluorescence sensors have been able to detect mycotoxin, citrinin, Bisphenol A (BPA)[64], basic red9 dye[65], Z-L-Phe and others[66,48] (**Figure 1.2.6**).

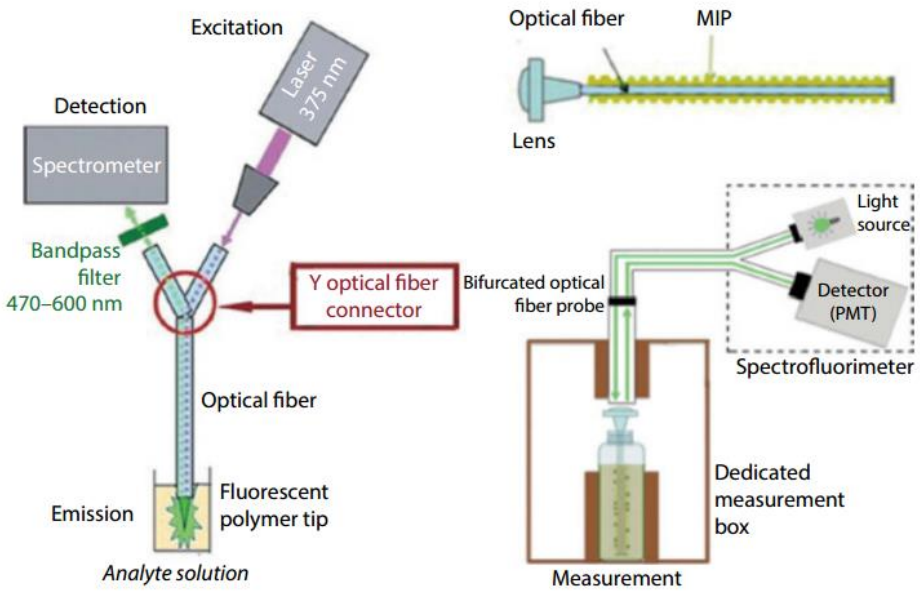

Figure1.2.6 Experimental setup of MIPs-based FO sensors to a) Z-L-Phe and b) red9 dye.[48]

1.2.8 Fluorescent Molecularly Imprinted Polymers (fMIPs)

As described above, in FO sensors the transducer converts the incoming signal into an electrical or optical signal that is transmitted and interpreted by the measurement device at the end. In fluorescence-based FO sensors with MIPs the binding process generate and spread fluorescence to the surroundings. By exciting the transducer this fluorescence sensor is able to change the properties of the transmitted light. Integration of fMIPs to the sensing system can be done either by attaching them to the fiber with an intermediate polymer or by coupling fMIPs to a fiber with a magnetic separator.[48]

Fluorescence sensors based on molecularly imprinted polymers can be developed taking advantage of the fluorescent properties of some of its components, either monomers present inside the polymer or template. Since not all analytes are fluorescents, fluorescent dyes are usually integrated into a MIP matrix to afford fMIPs. These dyes are placed in the binding sites of the polymers and can be sensitive to the local environment.[67,68,69] When the analyte binding occurs the fluorescent properties changes of the polymer can be measured, usually fluorescence quenching, shift or even fluorescence enhancement happen (**Figure 1.2.7**). Fluorescence enhancement is the most promising because it is more specific and is the least likely to give false positives.[56] Shifts in the emission band of the dye are noticed due to the differences in dipolar interactions between solvent molecules that are filling the empty pockets and target molecules with the embedded fluorophore. Furthermore, other factors such as hydrogen-bonding or electrostatic interactions can affect the emission spectra. A complication of using fMIPs as recognition elements is that traces of the template could remain entrapped in the polymer causing a decrease in the sensitivity. [70]

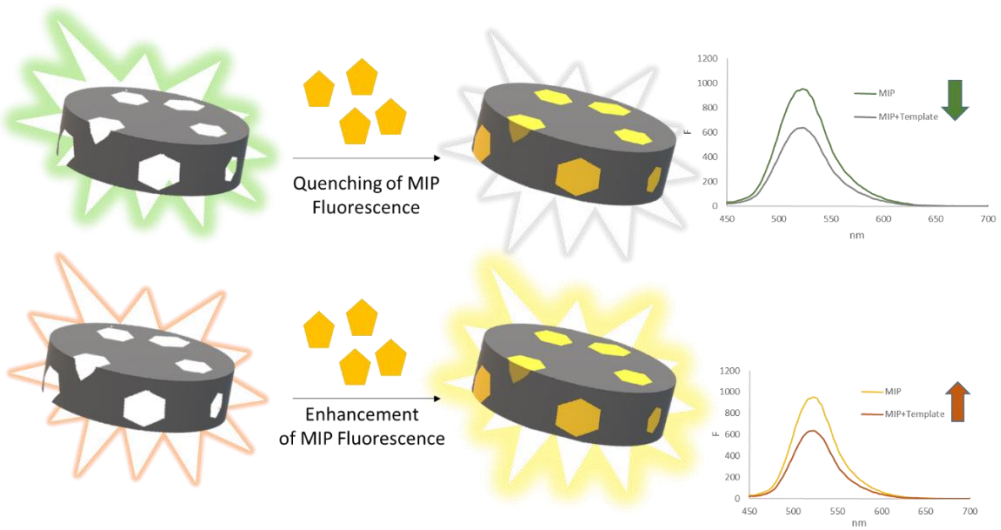

Figure 1.2.7 Representation of quenching and enhancement of MIP fluorescence by binding of the template.

To achieve polymerization allyl- or acrylamido- groups are incorporated into the fluorophores without affecting their fluorescence, transforming them in suitable fluorescent monomers for polymerization. Currently a variety of fluorescent monomers have been used for the synthesis of fMIPs and the most common

are fluorescein, dansyl or nitrobenzoxadiazole (NBD).[70] For example, λ-cyhalothrin (LC), which is a pesticide found in food, was detected by integrating allylfluorescein into MIP microspheres made of acrylamide (AM) as the monomer and ethylene glycol dimethacrylate (EGDMA) as the crosslinker. In the presence of the target molecule, a fluorescence quenching of 20% was observed originated by the ability of the analyte to promote the electron transfer. The limit of detection was < 0.1nM. Additionally, to improve selectivity and sensitivity, fMIP layer was directly synthesized onto the core shell of Fe_3O_4/SiO_2 particles and the system was tested in a real honey sample spiked with the analyte achieving a good recovery.[71] Another example mentioned before, of employing fluorescein as a functional monomer, is its integration as acrylamidofluorescein (AAF) with EGDMA and acrylamide to polymerize a thin MIP film onto an optical fiber to detect cocaine. The binding process led to an enhancement of the fluorescence due to the ability of the template to deprotonate the functional monomer.[63]

The simultaneous integration of both fluorescence functional monomer and template into a single cavity make them to interact as close as possible, however, these interactions will occur in random distribution, so, a strategy to promote more specific interactions is the use of hydrogen bond-donating or accepting fluorophores.[70] A fluorophore that has shown a fluorescence enhancement after the formation of two hydrogen bonds with the template cyclobarbital is the 2-acrylomidoquinoline. The fluorescence enhancement is generated by the hydrogen bonds formed between amino and carboxylic groups of both the analyte and the quinolone moiety. The fMIP was prepared by using EGDMA as crosslinker and a 3-fold enhancement of the fluorescence intensity was observed in the presence of the template, while the non-imprinted polymer (fNIP) does not show the same sensitivity.[72] Other fluorophores are capable of forming hydrogen bonds causing a decrease of the fluorescence signal, as in the case of the modified aminorhodanine. Benzylidine-3-acrylamidorhodanine was used as the functional monomer to detect (Z)-N'-cyclododecylidenepicolino-hydrazonamide. The binding of the template causes a 2-fold decrease of the fluorescence intensity.[73] Nevertheless, the drawback of this type of systems, based on hydrogen bonds, is their application in aqueous solutions because in this environment there is a strong competition with water. For this reason, other recognition mechanisms have been designed, promoting the detection in aqueous solutions. For instance, 3',5'-cyclic adenosine monophosphate (cAMP) was detected through electrostatic interactions with *trans*-4-[*p*-(*N,N*-dimethylamino)styryl]-*N*-vinylbenzyl-pyridiumchloride used as the monomer and 2-hydroxyethylmethacrylate (HEMA) as the co-monomer to interact with the aromatic base unit of the template through Π-stacking and hydrogen bonding. A fluorescence quenching of 20% was observed in the presence of the analyte between 0.1-10μM. The system showed a good selectivity in the presence of other molecules structurally similar to the analyte.[74] Charge-transfer complexes created by electrostatic interactions have also allowed the detection of the herbicides DQ and paraquat (PQ), fMIP was prepared by modification of the fluorescent dye disodium 6,8-dihydroxypyrene-1,3-disulfonate with methacrylamide unit for polymerization using HEMA as the crosslinker and methacrylic acid (MAA) as the co-

monomer. The binding process led to a fluorescence quenching and the detection limits were 162 and 281 nM, respectively[75] .

As mentioned in previous sections, due to the non-covalent interactions between the template and the functional monomer, the dissociated species and the complex will always be in equilibrium during polymerization, so, a strategy to avoid this is to introduce species capable to form a reversible covalent bond with the target molecule, allowing the cavities formed in the polymer to be reusable. Since there are not so many species capable of achieving this, a possible option is to use boronic esters that allow covalent bonding with the analyte. An outstanding example, where this approach has been employed, is in the detection of (D)-fructose using an antracene-boronic acid with methacrylate as the functional monomer. The binding interactions result in a fluorescence enhancement proportional to the concentration of the analyte bound allowing the quantification of the analyte between 1mM a 100mM.[76]

The potential of fMIPs as recognition elements in sensors has allowed its application in the detection of toxic metal ions in aqueous solutions[77]. In this case, the imprinting can be carried out by using functional monomers able to coordinate the metal ion of interest. A suitable example is the detection of Pb^{2+} with a fMIP made of 9-vinylcarbazole as the co-monomer and Pb^{II}(MAA) as the template. When lead ions are captured in a concentration range between micro and millimolars a decrease in fluorescence was observed. 9-vinylcarbazole have been also used as a functional monomer to detect Hg^{2+} ions by copolymerization with 4-vinylpyridine (4-Vpy). The sensor works in a concentration range between $5 \cdot 10^{-7}$ and $1 \cdot 10^{-4}$M but this system showed some drawbacks such as the influence of the membrane thickness on the response time and the selectivity through other metal ions[78]. Improvements in selectivity were achieved in the design of a sensor based on fMIPs for detecting copper by forming a complex between $Cu^{2+}$and the fluorescence monomer 4-[-2-(4'-methyl-2,2'-bipyridin-4-yl)vinyl] phenyl methacrylate with HEMA and 3-(acryoloyloxy)-2-hydroxypropyl methacrylate. Rebinding of the metal ion leads to a significant fluorescence quenching and the system turned out to have a reusability of 50 cycles and a detection limit of 0.04 µM.[79]

A different approach to improve the performance of fMIPs is the integration of additional subunits into the fluorescent monomer, affording fluorescent probe monomers. Thus, instead of having the classical arrangement of fluorophore-linker-polymerizable unit (FLP), the fluorescent probe will consist of at least four subunits: fluorophore-linker-receptor-linker-polymerizable unit (FLRLP). For instance, following this approach, an imprinted polymer to recognize human serum albumin (HSA) was prepared using dansylmethacrylate functionalized with ethylenediamine as the monomer and AM and *N,N*'-methylenebisacrylamide (MBA) as the crosslinkers. In this system, the combination of a rigid hydrogen bondable site in the pyrrolidine moiety and a fluorescent unit (dansyl moiety) leads to a fMIP with protein recognition cavities that show selective detection toward the target protein with an increase in fluorescence. The corresponding fNIP did not show any significant change.[80]

So far, systems in which fluorescent functional monomers are incorporated into the polymeric matrix producing a change in the emission intensity or emission wavelength after the recognition of the template have been described. The main advantage of this approach is to use the polymer as a sensor itself since one of its intrinsic properties is used as the transducing system. However, in cases where neither the polymer nor the analyte are fluorescent, a strategy to develop fluorescent sensors is to design competitive or displacement assays, which can be carried out by synthesizing a fluorescent analogue of the analyte that can compete for the binding sites in the polymer with the real analyte of interest, providing that the MIP is still able to bind the target molecule. For instance, by designing a competitive or displacement sensor a fluorescent tracer was used to carry out a competitive flow-through assay for detecting chloramphenicol[81]. Here, the competition between the analyte and 2-amino-1-(4-nitrophenyl)-1,3-propanediol, a fluorescent molecule structurally similar to the target allowed the detection of the analyte in a range between 25µM and 310µM. In other systems, penicillin-type β-lactam antibiotics in human urine was detected by an automated molecularly imprinted sorbent assay carried out with a bulk polymer made of ethyleneglicol dimethacrylate as the crosslinker, methacrylamide as the co-monomer and *N*-[3,5-bis-(trifluoromethyl) phenyl]-*N*'-(4-vinylphenyl) urea as the functional monomer. The polymer was imprinted with penicillin G procaine salt and the concentration of the analyte was determined measuring the emission signal of the fluorescent competitor pyrenemethylacetamido penicillanic acid (PAAP) displaced by the target molecule from the polymer binding sites. The sensor showed a detection limit of $1.97 \cdot 10^{-7}$M.[82] With the same approach (**Figure 1.2.8**) it was possible the detection of the stress marker cortisol. Oriented, homogeneous cavities with two binding sites for cortisol were fabricated using a cortisol motif as the template molecule which was immobilized on a β-cyclodextrin (β-CD)-grafted gold-coated sensor chip, followed by copolymerization of 2-methacryloyloxyethyl phosphorylcholine as the hydrophilic comonomer. Detection of cortisol was demonstrated by a competitive binding assay using a fluorescent competitor. The analyte was detected with a detection limit of 4.8 pM. In addition, detection of cortisol in saliva samples was demonstrated as a feasibility study.[83]

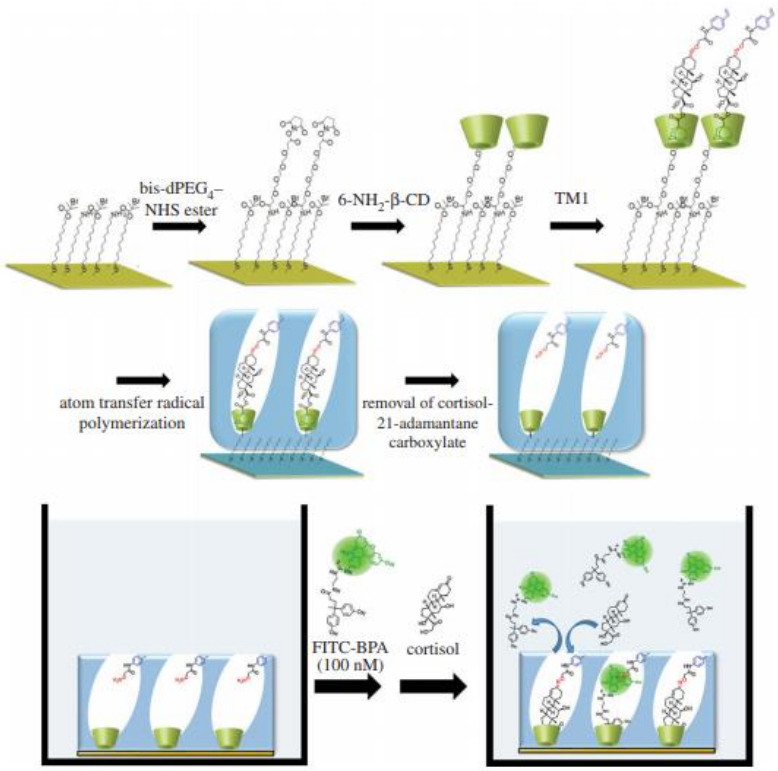

Figure 1.2.8 Preparation of the cortisol-MIP thin layer containing oriented cavities with dual binding sites within the imprinted cavity and schematic of the competitive binding assay using FITC-BPA as the fluorescent competitor.[83]

Displacement methods based on the competition between the free analyte and modified dye have allowed the design of colored optical sensors to detect analytes that do not possess a color itself[84]. For instance, a colorimetric sensor array based on dye displacement composed of seven MIPs was able to detect seven different aromatic amines[85]. The MIPs were made of MAA and EDGMA and saturated with benzofurazan, which is a small molecule with shape and similar functionalities to the target molecules. The use of dye conferred to the polymer a strong yellow color and with the addition of the analyte, the dye was displaced and significant decrease in the intensity of the polymer color was noticed.

On the other hand, there is also the possibility of finding systems where the target molecule possesses its own fluorescence or color and this property can be exploited for the design of fMIPs-sensor. A selective and sensitive system based on MIP to monitor the carbaryl pesticide in water by measuring its fluorescence emission was developed with a detection limit of 0.27µg/mL.[86] Another example is the quantification of β-estradiol using MIPs, which take advantage of both the intrinsic fluorescence of the analyte and the fluorescence led by a fluorescent dye that could bind to the polymer in a competitive mode.[87] To summarize, fMIPs have been widely used for optical sensing since the binding process can be monitored including fluorescent monomers into the polymer or by directly measuring a fluorescent analyte and in cases where

neither the template or the monomer are not fluorescent competitive assay with a fluorescent analog as a probe can be designed to allow the detection of the real analyte.

1.2.9 Applications of Molecularly imprinted polymers (MIPs) in Food.

In the latest years, the agricultural sector and the production of food at the industrial level has increased significantly worldwide and food safety has to be monitored during production, transportation, storage and consumption. Therefore, novel technologies have been developed to guarantee quality and safety. Currently, consumers are more aware of the effect of the components of food on human health, which has led to the creation of new regulations that must be obligatorily respected by the food industry to ensure hygiene and safety. Selective, precise and accurate methods for determining food components and contaminants both in raw or processed food are necessary and these should be developed with the aim of reducing analysis time, effort spent on sample preparation and being more environmentally friendly.[88] Food is a very complex matrix, mainly formed by proteins, lipids, carbohydrates, vitamins, minerals and fibers which make difficult the separation and the quantification of the target molecule. As a result, extensive and complicated techniques for sample extraction and preparation must be performed before the analytical analyses both for removing unwanted matrix constituents or for concentrating the analytes which are present at low concentrations or traces.[89] Usually, purification methods involve several steps and are based on organic solvent extractions, but they are time consuming, not always specific and require high amount of sample and organic solvents. The most preferred instrumental techniques for the detection and quantification of the target molecules are: high performance liquid chromatography (HPLC), gas chromatography (GC) coupling with mass spectrometry (MS) and inductively coupled plasma-mass spectrometer (ICP-MS). Most recently, imprinted polymers have become a useful technology with a wide range of applications in food manufacturing, processing and analysis of quality control and safety.[90] MIPs have been successfully applied as sensors for detecting hazardous contaminants or specific molecules in food, as well as for the removal of undesirable components from food matrices and in food microbiology. Among the applications of MIPs in food chemistry, the most widely used is solid phase extraction (SPE), for which several MIPs have been already commercialized.[91,92] As can be observed in **Figure 1.2.9** in molecularly imprinted solid phase extraction (MISPE) the sample source is passed through a selective MIP able to specifically retain one or a small group of compounds. After washing, the bulk matrix of the extract is eliminated, and the MIP is eluted to recover the target molecule (s) which is so purified and in a concentrated form. Thus, MISPE allows to clean up and pre-concentrate samples that can be quantified by using another analytical technique such as HPLC.

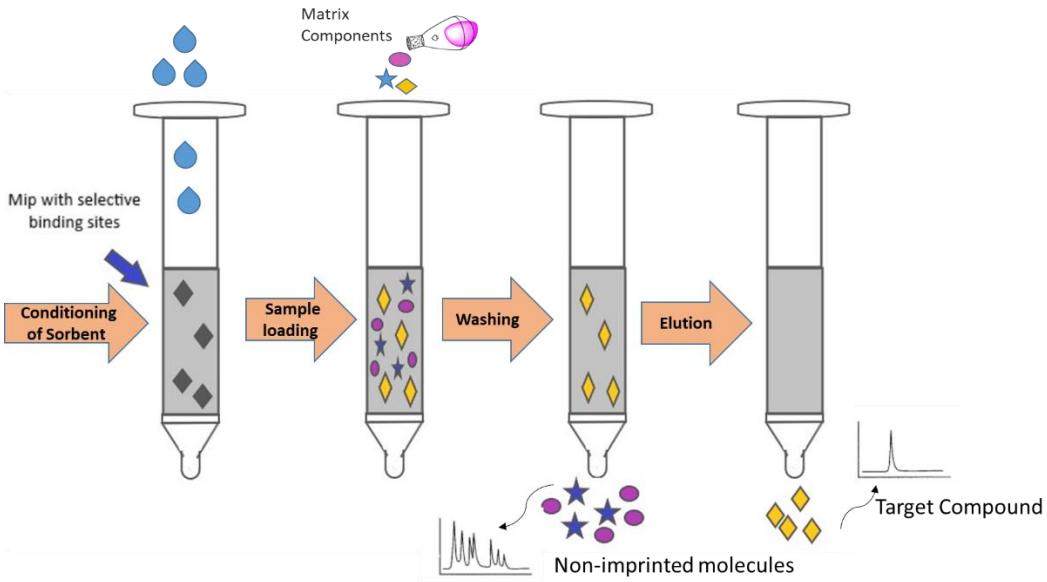

Figure 1.2.9 Sample concentration and purification by molecular imprinting SPE.

In food industry great attention have been focused on the detection of contaminants or anti-microbial drugs that could be potentially harmful to the human being. Later on, there has been a huge interest in the design of MIPs capable of detecting the drugs that act within humans, but some efforts have also been invested in the study of drugs in animals. Of special interest in this area are antibiotics since their use for the treatment of animals used for human consumption cover half of the antibiotic world production[93]. MIPs to detect a series of macrolide antibiotics such as erythtomycin A, oleandomycin and tylosin were tested and the polymers showed efficient selectivity towards their respective templates.[94] Detection of chloramphenicol, a bacteriostatic antibiotic banned by government regulations in food, was carried out by MIPs prepared through aqueous suspension polymerization. The MIPs were packed into SPE cartridges to detect the target antibiotic in milk and shrimp samples with recoveries of above 80%.[95] Other MIPs have been packed into SPE tubes to selective target tetracycline (TC) and oxytetracycline (OTC). The antibiotics removed from pig-kidney tissue were cleaning up by MISPE and analyzed by HPLC.[96] Another MIP to detect a class of tetracycline was also synthesized to remove the antibiotics from water.[97] Steroids have been also chosen as templates for MIPs production, for instance cortisol could be separated from structurally related steroids with HPLC using a polymer imprinted with the target molecule. An imprinting factor of 9.71 was determined compared with the non-imprinted polymer.[98]

MIPs have been also employed for detecting food additives, which are used to improve food character such as taste, color, texture and food longevity. However, some industrial dyes are genotoxic or carcinogenic agents and they are illegally used. For instance, Sudan I is the most used industrial dye and is also illegally added to foodstuffs and cosmetics for color increment.[89,90] Sudan I was detected by a MIP prepared through

bulk polymerization using MAA and 4-vinylpyridene as the functional monomer. The MIP packed in SPE cartridges allowed the determination of concentration of 10 ppm of the analyte in spiked red chili powder for HPLC detection by using MISPE.[99] Another system based on MIP-thin-layer chromatography (TLC)-SERS biosensor to detect Sudan I at level traces in ground paprika was developed. A gold solution was used to increase the Raman signals of the analyte and the enhancement factor was approximately of $4 \cdot 10^4$. In this study the pretreatment of food samples was simplified by TLC progress and the detection limit was 1ppm[100]. Several natural sweeteners such as glucose, galactose, fructose and mannose have been used as target molecules for imprinting approaches. In these studies, MIPs have shown a high regio- and enantioselectivity allowing their use in binding assays as well as sensor development.[101,102]

The biggest problem in the food industry is the presence of contaminants such as foodborne pathogens and microbial toxins. MIPs, in conjugation with other methods, have become very efficient recognition elements for food contaminants. Probably, the most important contaminant, in terms of toxicity and diffusion, are mycotoxins.[89] In this sense, an analytical method to detect ochratoxin A (OTA) in red wines was developed based on a two dimensional solid phase extraction (SPE) clean up protocol on C18-silica and one MIP. An OTA-mimic template was used in presence of a sterically hindered tertiary amine and highly hydrophobic *tert*- butyl group as functional monomers. Spiked samples provided a recovery above 90% and the detection limit was of 0.01 ng/mL. The system showed reusability after five cycles but a similar performance was observed in control experiments with the corresponding NIP.[103] In the same way, some semi-covalent MIPs have been designed to recognize pesticide residues. There are two types of pesticide detected on food samples, widely known as triazine and urea-based herbicides. A polymer prepared with MAA as the functional monomer was used to detect fenuron, a phenylurea herbicide in plant samples. By MISPE was also possible to recover 95-115% of spiked herbicide in potato, carrots, wheat and barley using HPLC-UV. This method allowed the determination of fenuron at concentrations below of the maximum levels recommended by the legislation.[104] Atrazine have been detected by a potentiometric sensor based on a molecularly imprinted membrane. A good potentiometric response has been afforded giving a detection limit of $2 \cdot 10^{-5}$ M. The sensor could be used for more than two months without any significant change and the response time was less than 10 second.[105] Other types of fluorescence sensors using the molecularly imprinted technology were created for detecting atrazine. Polymer synthesis consisted of radical polymerization of diethylaminoethyl methacrylate or methacrylic acid as functional monomers and ethylene glycol dimethacrylate as the crosslinker. After grinding of the polymer block and splitting off the template molecules a suspension of the polymer was used for the herbicide-specific sensor system, which consists in the competition between fluorescent-labeled and the unlabeled template for the specific binding sites. Selective detection of triazine was achieved within 4 hours between a concentration range of 0.01-100 mM.[106]

Furthermore, a large number of studies for targeting typical food components have been carried out. Among these, cholesterol has been the major food component detected by MIPs. Self-assembled molecularly imprinted films were used as recognition elements immobilized on gold electrode surfaces. The electrochemical sensor allowed the determination of cholesterol in a range of 15-60μM with response time of 5min.[107] Nicotine and its oxidation products in nicotine chewing gum were detected by packing MIPs in SPE tubes. Without this cleaning system none of target analytes had been determined by using HPLC separation.[108] Another important secondary metabolite that has been successfully analyzed by molecularly imprinted technology is the caffeine (CAF). A bio-mimic bulk acoustic wave (BAW) sensor was fabricated by coating the MIP. The sensor showed high selectivity and a sensitive mass response to the template. The response range of the sensor was between $5 \cdot 10^{-9}$ and $1 \cdot 10^{-4}$M. Recoveries were 96.1–105.6% at pH 8. The system was employed in real samples and proved to be a convenient method with the advantages of high sensitivity, good selectivity and ease of handling.[109] Electrochemical sensors have been also employed for detecting CAF. A sensor was constructed through multiwalled carbon nanotubes and gold nanoparticles that were first modified onto the glassy carbon electrode surface by a potentiostatic deposition method. Subsequently, *o*-aminothiophenol (ATP) was assembled on the surface of the above electrode through Au–S bond before electropolymerization. During the assembly and electropolymerization processes, CAF was embedded into the poly(*o*-aminothiophenol) film through hydrogen bonding interaction between CAF and ATP, forming a MIP electrochemical sensor with a detection limit of $9 \cdot 10^{-11}$M.[110] Other sensors used to detect CAF in aqueous media have been developed, for instance, a divinylbenzene (DVB) crosslinked polymer toward caffeine was prepared and the MIP exhibited high binding affinity and selectivity by the binding competition of caffeine with several dimethylated and chlorinated xanthines and N-methylated uric acids in aqueous media.[111]

1.2.10 Molecularly Imprinted polymers (MIPs) For Chlorogenic Acids (CGAs) recognition

MIPs based in non-covalent interactions have been mostly used in solid phase extraction and sample concentration for the analysis of CGAs. MIP Monolith was successfully applied to the separation and purification of chlorogenic acid from the leaves extract of *E. ulmodies*, resulting in high purity chlorogenic acid. MIP monolithic stationary phase was prepared in chromatographic column by an in situ synthesis method using caffeic acid as the template. The retention behavior of chlorogenic acid, the template and the other impurities molecules co-existed in the *E. ulmodies* leaves extract on the MIP monolith were studied. Another approach was the development of a modified bisphenol A (BPA) molecularly imprinted polymer sorbent used in the hollow fiber solid phase microextraction (MIP-HF-SPME) of chlorogenic acid (CGA). The pre-polymer solution containing the template was introduced into the polypropylene hollow fiber segment for in situ polymerization. The system was used for selective extraction of chlorogenic acid in *Echinacea*

purpurea, a medicinal plant. The obtained SPME device exhibits excellent characteristics such as high porosity and chemical stability with the limit of detection of 0.08 ng/mL.[112]

On the other hand, MIPs have been successfully applied for extraction of CGA in the leaves of *Eucommia ulmodies*.[113,114] In one case, the polymer was prepared by modified precipitation polymerization using methacrylic acid as the functional monomer, divinylbenzene as the crosslinker and methanol or dimethyl sulfoxide as the porogenic-solvent. The prepared MIPs were microspheres with a narrow particle size distribution. Binding experiments and Scatchard analyses revealed that high and low affinity sites were formed on the MIP. The retention and molecular-recognition properties were evaluated using a mixture of water and acetonitrile as the mobile phase in hydrophilic interaction chromatography. In addition, to shape recognition, hydrophilic interactions seem to work for the recognition of CGA. The system showed a specific molecular-recognition ability for CGA, while other related compounds, such as caffeic acid, gallic acid, protocatechuic acid and vanillic acid, could not be recognized. A rapid and accurate approach was established for simultaneous purification of theophylline and CGA in green tea by coupling hybrid molecularly imprinted solid-phase extraction with HPLC. Satisfactory extraction recoveries for theophylline (96.7%) and chlorogenic acid (95.8%) were afforded and the detection limits were 0.01μg/mL for theophylline and 0.05μg/mL for CGA.[115]

In the same way, some other MIP electrochemical sensors have been developed for CGA detection[116,117,118,119,120], for instance, a sensitive molecularly imprinted electrochemical sensor (**Figure 1.2.10**) was constructed by deposition of a molecularly imprinted siloxane (MIS) film, prepared by sol–gel process, onto Au bare electrode surface. Initially, a (3-mercaptopropyl)siloxane layer (MSL) was formed on the Au bare surface, followed by a siloxane layer obtained from the acid-catalyzed hydrolysis/condensation of a solution constituted by tetraethoxysilane (TEOS), phenyltriethoxysilane (PTEOS), 3-(aminopropyl)trimethoxysilane (APTMS) and 5-CQA, as template. The MIS imprinted film was electrochemically characterized using differential pulse voltammetry (DPV). The MIS/Au sensor was tested in a solution of the CGA template and other similar molecules showing excellent selectivity towards CGA when compared with structurally similar molecules. The detection limit was $1.48 \cdot 10^{-7}$ M and the sensor was successfully applied for the determination of CGA in coffee and tea samples.[120]

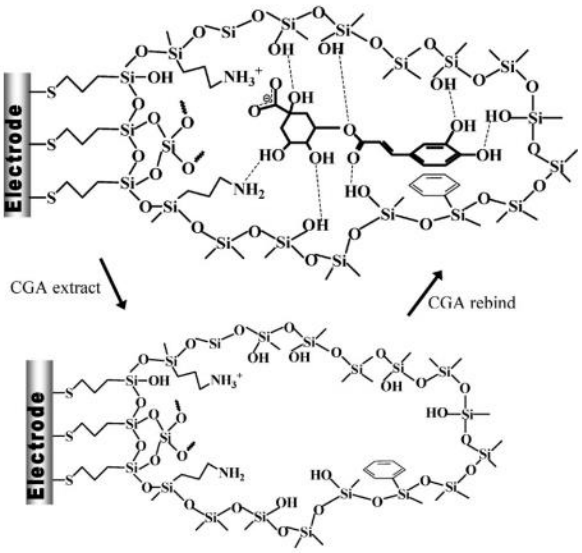

Figure 1.2.10 Schematic representation of the molecularly imprinted siloxane for CGA. [120]

Most recently, a promising technique for the enrichment and determination of chlorogenic acids from herbal medicines was proposed. The system consists in a solid-phase extraction adsorbent based on molecularly imprinted polymers (MIPs), made of 4-vinylpyridine as the functional monomer and hydrogenated 5-CQA as the mimic template. Selective extraction and determination of three isomers of caffeoylquinic acids (CQAs), considered as quality markers for *Lonicera japonica* and *Lianhua qingwen* granules, was successfully achieved. The morphologies and surface groups of the MIPs were assessed by scanning electron microscopy, Brunauer–Emmett–Teller surface area analysis, and Fourier transform infrared spectroscopy. The adsorption isotherms, kinetics, and selectivity of the MIPs were systematically compared with those of non-molecularly imprinted polymers. The MIPs showed high selectivity toward chlorogenic acid, cryptochlorogenic acid, and neochlorogenic acid. A procedure using molecularly imprinted solid-phase extraction coupled with high-performance liquid chromatography was established for their determination. The recoveries of the chlorogenic acids were found from 93.1% to 101.4%. [121]

[1] Vasapollo, G.; Del Sole, R.; Mergola, L.; Lazzoi, M. R.; Scardino, A.; Scorrano, S.; Mele, G. Molecularly imprinted polymers: present and future prospective. *Int. J. Mol. Sci*. **2011**, 12, 5908-5945.

[2] Martin Esteban, A. Recent Molecularly Imprinted Polymer-based Methods for Sample Preparation in Advanced Molecularly Imprinting Materials. Ed by Tiwari, A.; Uzun, L., John Wiley & Sons, **2017**, ISBN 978-1-119-33629-7, chapter 1, 3-21.

[3] Yan, H.; Ho Row, K. Characteristic and Synthetic Approach of Molecularly Imprinted Polymer*. Int. J. Mol. Sci*. **2006**, 7, 155-178.

[4] Davies, M. P.; De Biasi, V.; Perrett, D. Approaches to the rational design of molecularly imprinted polymers. *Anal. Chim. Acta*, **2004**, 504, 7–14.

[5] Wulff, G.; Vesper, W.; Grobe-Insler, R.; Sarhan, A. Enzyme-analogue built polymers. *Makromol. Chem,* **1997**, 178, 2799-2816.

[6] Spivak, D, A. Optimization, evaluation, and characterization of molecularly imprinted polymers. *Adv. Drug Deliv. Rev.,* **2005***,* 57, 1779-1794.

[7] Khasawneh, M. A.; Vallano, P.T.; Remcho, V. Affinity screening by packed capillary high performance liquid chromatography using molecularly imprinted sorbents II. Covalent imprinted polymers. *J. Chromatogr.* A, **2001**, 922, 87-97.
[8] Tang, Y.; Fang, G.; Wang, S. Covalent imprinted polymer for selective and rapid enrichment of ractopamine by a non-covalent approach. *Anal. Bioanal. Chem.*, **2011,** 401, 2275-2282.
[9] Mosbach, K. Molecular imprinting. *Trends Biochem. Sci.*, **1994**, 19, 9-14.
[10] Zang, H.; Ye, L.; Mosbach, K. Non-covalent molecular imprinting with emphasis on its application in separation and drug development. *J. Mol. Recognit.*, **2006**, 19, 248-259.
[11] Cormack, P. A. G.; Elorza Z. A.; Molecularly imprinted polymers: synthesis and characterisation. *J. Chromatogr. B*, **2004**, 804, 173–182.
[12] Haupt, K. Imprinted polymers: the next generation. *Anal. Chem.*, **2003,** 377A-383A.
[13] Sherrington, D. C. Preparation, structure and morphology of polymer supports. *Chem. Commun.*, **1998**, 2275-2286.
[14] Odian, G. Principles of Polimerization. Wiley, IV edition, **2004**, ISBN 0-471-27400-3, chapter 3.
[15] Billmeyer, F. W. Textbook of Polymer Science. Wiley, III edition, **1984**, ISBN 0-471-03196-8, part II.
[16] Sergeyeva, A. Molecularly imprinted polymers as synthetic mimics of biorteceptors. 1. General principles of molecular imprinting. *Biopolym. Cell*, **2004**, 25, 253-265.
[17] Flavin, K.; Resmini, M. Imprinted nanomaterials: a new class of synthetic receptors. *Anal. Bioanal. Chem.*, **2009**, 393, 437-444.
[18] Haginaka, J. Molecularly imprinted polymers as affinity-based separation media for sample preparation *J. Sep. Sci.,* **2009***,* 32, 1548-1565.
[19] Benito-Peña, E.; Martins, S.; Orellana, G.; Moreno-Bondi, M. C. Water-compatible molecularly imprinted polymer for the selective recognition of fluoroquinolone antibiotics in biological samples. *Anal. Bioanal. Chem.*, **2009**, 393, 235-245.
[20] Pasetto, P.; Maddock, S. C.; Resmini, M. Synthesis and characterization of molecularly imprinted catalytic microgels for carbonate hydrolysis. *Anal. Chim. Acta*, **2005**, 542, 66-75.
[21] Mergola, L.; Scorrano, S.; Del Sole, R.; Lazzoi, M. R.; Vasapollo, G. Developments in the synthesis of a water compatible molecularly imprinted polymer as artificial receptor for detection of 3-nitro-L-tyrosine in neurological diseases. *Bios. Bioelectr.*, **2013**, 40, 336-341.
[22] Banica, F. G. Chemical Sensors and Biosensors: Fundamentals and Applications. Wiley, ISBN 978-0-471-89914-32, **2012,** chapter I. 1-19.
[23] Kriz, D.; Ramström, O.; Mosbach, K. Molecularly imprinting: new possibilities for sensor technology. *Anal. Chem. News Feat*., **1997**, 345A-349A.
[24] Turner, A. P. F. Biosensors: sense and sensibility. *Chem. Soc. Rev.*, **2013**, 42, 3184-319.
[25] Holford, T. R. J.; Davis, F.; Higson, S. J. Recent trends in antibody based sensors. *Biosens. Bioelectr.*, **2012**, 34, 12-24.
[26] Choulier, L.; Enander, K. Environmentally sensitive fluorescent sensors based on synthetic peptides. *Sensors*, **2010**, 10, 3126-3144.
[27] Haupt, K.; Belmont, A. S. Molecularly imprinted polymers as recognition elements in sensors in Handbook of Biosensors and Biochips, ed. by Marks, R. S.; Cullen, D. C; Karube, I.; Lowe, C. R.; Weetall, H.; Wiley ISBN 978-0-470-01905-4, **2007**, chapter 14.
[28] Vlatakis, G.; Andersson, L. I.; Müller R., Mosbach K. Drug assay using anti body mimics made by molecular imprinting. *Nature*, **1993**, 361, 645-647.
[29] Holthoff, E. L.; Bright, F. V. Molecularly templated materials in chemical sensing. *Anal. Chim. Acta*, **2007**, 594, 147-161.
[30] Algieri, C.; Drioli, E.; Guzzo, L.; Donato, L. Bio-mimetic sensors based on molecularly imprinted membranes. *Sensors*, **2014**, 14, 13863-13912.
[31] Hedborg, E.; Winquist, F.; Lundstrom, I.; Andersson, L. I.; Mosbach, K. "Some studies of molecularly-imprinted polymer membranes in combination with field-effect devices. *Sens. Act. A*, **1993**, 37-38:796-79.
[32] Malitesta, C.; Losito, I.; Zambonin, P. G. Molecularly imprinted electrosynthesized polymers: new materials for biomimetic sensors. *Anal. Chem.***, 1999**, 71, 1366-137.

[33] Feng, L.; Liu, Yonjun, L.; Tan, Y.; Jiming, H. Biosensor for the determination of sorbitol based on molecularly imprinted electrosynthesized polymers. *Biosens. Bioelentron.*, **2004,** 19, 1513-1519.
[34] Dickert, F. L.; Hayden, O. Bioimprinting of polymers and sol-gel phases. Selective detection of yeasts with imprinted polymers. *Anal. Chem.*, **2002**, 74, 1302-1306.
[35] Matsui, J.; Akamatsu, K.; Hara, N.; Miyoshi, D.; Nawafune, H.; Tamaki, K.; Sugimoto, N. SPR sensor chip for detection of small molecules using molecularly imprinted polymer with embedded gold nanoparticles. *Anal. Chem.*, **2005**, 77, 4282-4285.
[36] Pernites, R. B.; Ponnapati, R. R.; Advincula, R. C. Surface plasmon Resonance (SPR) detection of theophylline via electropolymerized molecularly imprinted polythiophenes. *Macromolecules*, **2010**, 43, 9724-9735.
[37] Dario, K.; Kempe, M.; Mosbach, K. Introduction of molecularly imprinted polymers as recognition elements in conductometric chemical sensors. *Sens. Actuators B*, **1996**, 33, 178-181.
[38] Sergeyeva, T. A.; Piletsky, S. A.; Brovko, A. A.; Slinchenko, E. A.; Sergeeva, L. M.; El'skaya A. V. Selective recognition of atrazine by molecularly imprinted polymer membranes. Development of conductometric sensor for herbicides detection. *Anal. Chim. Acta,* **1999**, 392, 105-111.
[39] Bompart, M.; Gheber, L. A.; De Wilde, Y., Haupt, K. Direct detection of analyte binding to single molecularly imprinted polymer particles by confocal Raman spectroscopy. *Bios. Bioelectr.*, **2009**, 25, 568-571.
[40] Bompart, M.; De Wilde, Y; Haupt, K. Chemical nanosensors based on composite molecularly imprinted polymer particles and Surface- enhanced Raman scattering. *Adv. Mater.*, **2009**, 22, 2343-2348.
[41] Xue, J. Q.; Li, D. W.; Qu L. L.; Long, Y. Surface-imprinted core–shell Au nanoparticles for selective detection of bisphenol A based on surface-enhanced Raman scattering. *Anal. Chim. Acta,* **2013**, *777,* 57-62.
[42] Pellizzoni, E.; Tommasini, M.; Maragon, E.; Rizzolio, F.; Saito, G.; Benedetti, F.; Toffoli, G.; Resmini, M.; Berti, F. Fluorescent molecularly imprinted nanogel for the detection of anticancer drugs in human plasma. *Bios. Bioelectr.,* **2016** ,86, 913-919.
[43] Saini, S. S., Kaur, A. Molecularly imprinted polymers for the detection of food toxins: a minireview. *Adv. Nanopart.*, **2013**, 2, 60-65.
[44] Niessner, R.; Chemical sensor for environmental analysis. *Trac-Trends Anal. Chem.,* **1991***,*10, 310-316.
[45] Krupadam, R. J.; Khan, M. S.; Wate, S. R. Removal of probable human carcinogenic polycyclic aromatic hydrocarbons from contaminated water using molecularly imprinted polymer. *Water Research*, **2010**, 4, 681-688.
[46] Allender, C. J.; Richardson, C., Woodhouse, B.; Heard, C. M.; Brain, K. R. Pharmaceutical applications for molecularly imprinted polymers. *Int. J. Pharm*., **2000**, 195:39-43.
[47] Kriz, O.; Ramstrom, O.; Mosbach, K. Molecularly imprinting-new possibilities for sensor technology. *Anal. Chem.*, **1997**, 69, 824-828.
[48] Yaman, Y. O.; Başaran, N.; Karayagiz, K.; Vatansever, Z.; Yegin, C.; Haluk , Ö. T.; Sari, M. M. Molecularly Imprinted Materials for Fiber-optic Sensor Platforms in Advanced Molecularly Imprinting Materials. Ed by Tiwari, A.; Uzun, L., John Wiley & Sons, 2017, ISBN 978-1-119-33629-7, chapter 6, 217-274.
[49] Mendez, A. Medical applications of fiber-optics: optical fiber sees growthas medical sensors. *Laser Focus World,* **2011** ,47, 91.
[50] Davenport, J. J.; Hickey, M.; Phillips, J. P.; Kyriacoua, P.A. Dual pO2/pCO2 fibre optic sensing film. Analyst, **2017**, 142, 1711-1719.
[51] Grattan, K. T. V.; Sun, T. Fiber optic sensor technology: an overview. *Sens. Actuators, A Phys.* ,**2000**, 82, 40-61.
[52] Ghetia, S.; Ghajjar, R.; Triverdi, P. Classification of fiber optical sensors. *Int. J. Electron. Commun. Comput. Technol*. **2013**, 3, 442-225.
[53] Mescia, L.; Prudenzano, F. Advances on optical fiber sensors. Fibers, **2014**, 2, 1-23.
[54] Lecler, S.; Meyrueis, P. Intrinsic optical fiber sensor, in Fiber optic sensors. Ed by Yasin, M., INTECH Open Access Publisher, **2012**.
[55] Lobnik, A.; Turel, M.; Urek, Š. Optical chemical sensors: Design and applications in Advances in chemical sensors. Ed. by Wang, W. InTech, **2012**, Chapter 1, 1–28.
[56] Ton, X. A.; Acha, V.; Bonomi, P.; Tse Sum Bui, B.; Haupta, K. A disposable evanescent wave fiber optic sensor coated with a molecularly imprinted polymer as a selective fluorescence probe. *Biosens. Bioelectron*., **2015**, 64, 359–366.

[57] Carrasco, S.; Benito-Peña, E.; Walt, D.R.; Moreno-Bondi, M. C. Fiberoptic array using molecularly imprinted microspheres for antibiotic analysis. *Chem. Sci*., **2015**, 6, 3139–3147.
[58] Wang, L.; Zhang, Z. The study of oxidization fluorescence sensor with molecularly imprinted polymer and its application for 6-mercaptopurine (6-MP) determination. *Talanta*, **2008**, 76, 768–771.
[59] Hart, S. J. Dual fiber optic capillary probe for fluorescence detection using molecularly imprinted polymers. *Proc. SPIE*, **2001**, 4201, 112–117.
[60] Gholamzadeh, B.; Nabovati, H. Fiber Optic Sensors. *IJECE*, **2008,** 2, 1107,1117.
[61] Udd, E. Overview of fiber optic sensors in Fiber optic sensors. Ed. by Yin, S.; Ruffin, P. B.; Yu, F. T. S. Taylor and Francis group, **2008**, ISBN 978-1-4200-5365. Chapter 1, 1-32.
[62] Epstein, J. R., Walt, D. R. Fluorescence-based fibre optic arrays: a universal platform for sensing. *Chem. Soc. Rev*., **2003**, 32, 203–214.
[63] Nguyen, T. H.; Hardwick, S.A.; Sun, T., Grattan, K. T. V. Intrinsic fluorescence-based optical fiber sensor for cocaine using a molecularly imprinted polymer as the recognition element. *IEEE Sens. J*., **2012**, 255–260.
[64] Xiong, Y.; Ye, Z.; Xu, J.; Yucheng, L.; Zhang, H. A microvolume molecularly imprinted polymer modified fiber-optic evanescent wave sensor for bisphenol A determination. *Anal. Bioanal. Chem*., **2014***,* 406, 2411–2420.
[65] Foguel, M. V.; Ton, X.A.; Zanoni, M. V. B.; Sotomayor, M. P.; Haupt, K.; Tse Sum Bui, B. A molecularly imprinted polymer-based evanescent wave fiber optic sensor for the detection of basic red 9 dye. *Sens. Actuators B Chem*., **2015**, 218, 222–228.
[66] Ton, X.A.; Tse Sum Bui, B.; Resmini, M., Bonomi, P.; Dika, I.; Soppera, O.; Haupt, K. A versatile fiber-optic fluorescence sensor based on molecularly imprinted microstructures polymerized in situ. *Angew. Chemie Int. Ed*., 52, **2013**, 8317–8321.
[67] Wan, W.; Wagner, S.; Rurack, K. Fluorescent monomers: “bricks” that make a molecularly imprinted polymer “bright”. *Anal. Bioanal. Chem.*, **2016**, 408, 1753-1771.
[68] Moreno-Bondi, M. C.; Navarro-Villoslada, F.; Benito-Peña, E.; Urraca J. L. Molecularly imprinted polymers as selective recognition elements in optical sensing. *Curr. Anal. Chem.*, **2008**, 4,316-340.
[69] Basabe Desmonts, L.; Reinhoudt, D. N.; Crego-Calama, M.; Design of fluorescent materials for chemical sensing. *Chem. Sov. Rev*., **2007**, 36, 993-1017.
[70] Gawlitza, K.; Wan, W.; Wagner, S.; Rurack, K. Fluorescent Molecularly Imprinted Polymers in Advanced Molecularly imprinting Materials. Ed by Tiwari, A.; Uzun, L., John Wiley & Sons, **2017**, ISBN 978-1-119-33629-7, chapter 3, 89-120.
[71] Gao, L.; Li, X.; Zhang, Q.; Dai, J.; Wei, X.; Song, Z.; Yan, Y.; Li, C. Molecularly imprinted polymer microspheres for optical measurement of ultra trace nonfluorescent cyhalothrin in honey. *Food Chem*., **2014**, 156, 1-6.
[72] Kubo, H.; Yoshioka, N.; Takeuchi, T. Fluorescent imprinted polymers prepared with 2-acrylamidoquinoline as a signaling monomer. *Org. Lett*., **2005**, 7, 359-362.
[73] Rathbone, D. L.; Su, D.; Wang, Y.; Billington, D. C.; Molecular recognition by fluorescent imprinted polymers. *Tetrahedron Lett*., **2000**, 41, 123-126.
[74] Turkewitsch, P.; Wandelt, B.; Darling, G. D.; Powell, W. S. Fluorescent functional recognition sites through molecular imprinting. A polymer based fluorescent chemosensor for aqueous cAM. *Anal. Chem*., **1998,** 70, 2025-2030.
[75] Zhenhe, C.; Álvarez-Pérez, M.; Navarro-Villosladaa, F.; Moreno-Bondi, M. C.; Orellana, G. Fluorescent sensing of “quat” herbicides with a multifunctional pyrene-labeled monomer and molecular imprinting. *Sens. Actuators B*, **2014**, 191, 137-142.
[76] Wang, W.; Gao, S.; Wang B. Building fluorescent sensors by template polymerization: the preparation of a fluorescent sensor for D-Fructose. *Org. Lett*, **1999**, 8, 1209-121.
[77] Güney, O.; Cebeci, F. Ç. Molecularly imprinted fluorescent polymers as chemosensors for the detection of mercury ions in aqueous media. *J. Appl. Polym. Sci*., **2010**, 117, 2373–2379.
[78] Güney, O., Yilmaz, Y., Pekcan, O., Metal ion templated chemosensor for metal ions based on fluorescence quenching. *Sens. Actuators B-Chem*., **2002**, 86-89.
[79] Pinheiro, S. C.; Descalzo, A. B.; Raimundo, I. M.; Orellana, G.; Moreno Bondi, M. C.; Fluorescent ion-imprinted polymers for selective Cu(II) optosensing. *Anal. Bioanal. Chem*., **2012**, 3253-3260.

[80] Inoue, Y.; Kuwahara, A.; Ohmori, K.; Sunayama, H.; Ooya, T.; Takeuchi, T. Fluorescent molecularly imprinted polymer thin films for specific protein detection prepared with dansyl ethylenediamine-conjugated O-acryloyl L-hydroxyproline. *Biosens. Bioelectron*., **2013**, 48, 113-119.
[81] Suárez-Rodrìguez, J. L.; Dìaz Garcìa, M. Fluorescent competitive flow -through assay for chloramphenicol using molecularly imprinted polymers. *Biosens. Bioelectr.*, **2001**, 16, 955-961.
[82] Urraca, J. L.; Moreno-Bondi, M. C.; Orellana, G.; Sellergren, B.; Hall, A. J. Molecularly imprinted polymers as antibody mimics in automated on-line fluorescent competitive assays. *Anal. Chem.*, **2007**, 79, 4915-4923.
[83] Suda, N.; Sunayama, H.; Kitayama, Y.; Kamon, Y.; Takeuchi, T. Oriented, molecularly imprinted cavities with dual binding sites for highly sensitive and selective recognition of cortisol. *R. Soc. Open sci.*, **2017**, 4: 170300.
[84] Burgess, I. B.; Loncar, M.; Aizenberg, J. Structural colour in colorimetric sensors and indicator. *J. Mater. Chem.*, **2013**, 1, 6075-6086.
[85] Greene, N.; Shimizu, K. D. Colorimetric molecularly imprinted polymer sensor array using dye displacement. *J. Am. Chem. Soc.*, **2005**, 127:5695-5700.
[86] Sànchez-Barragàn, I.; Karim, K.; Costa Fernàndez, J. M.; Piletsky, S. A.; Sanz Medel, A. A molecularly imprinted polymer for carbaryl determination in water. *Sens. Act. B*, **2007**, 123, 798-804.
[87] Rachkova, A.; McNiven, S.; El'skaya, A.; Yano, K.; Karube, I. Fluorescence detection of β-estradiol using a molecularly imprinted polymer. *Anal. Chim. Acta*, **2000**, 23-29.
[88] Luong, J. H. T.; Bouvrette, P.; Male, K. B. Development and applications of biosensors in food analysis. *Trends Biotechnol*., **1997**, 15, 369-377.
[89] Ulusoy, B. O.; Odabaşi, M.; Aksoy, N. H. Molecular Imprinting Technology for Sensing and Separation in Food Safety in in Advanced Molecularly Imprinting Materials. Ed. by Tiwari, A.; Uzun, L., John Wiley & Sons, **2017**, ISBN 978-1-119-33629-7, Part 2, chapter 9, 353-377.
[90] Lok, C. M.; Son, R. Application of molecularly imprinted polymers in food sample analysis – a perspective. *Food Res. Int.,* **2009**, 16, 127-140.
[91] Mahony, J. O.; Nolan, K.; Smyth, M. R.; Mizaikoff, B. Molecularly imprinted polymers-potential and challenges in analytical chemistry. *Anal. Chim. Acta*, **2005**, 534, 31-39.
[92] Whitcombe, M. J.; Alexander, C.; Vulfson, E. N. Smart polymers for the food industry. *Trends Food Sci. Technol.*, **1997**, 8, 140-145.
[93] Ramstrom, O.; Skudar, K.;Haines, J.; Patel, P.; Bruggemann, O. Food analyses using molecularly imprinted polymers. *J. Agric. Food Chem.*, **2001**, *49*, 2105–2114.
[94] Siemann, M.; Andersson, L. I.; Mosbach, K. Separation and detection of macrolide antibiotics by HPLC using macrolide-imprinted synthetic polymers as stationary phases. *J. Antibiot*., **1997**, 50, 88-91.
[95] Shi, X.; Wu, A.; Zheng, S.; Li, R.; Zhang, D. Molecularly imprinted polymer microspheres for solid-phase extraction of chloramphenicol residues in foods. *J. Chromatogr. B*, **2007**, 850, 24-30.
[96] Caro, E.; Marcé, R. M.; Cormack, P. A. G.; Sherrington, D. C.; Borrull, F. Synthesis and application of an oxytetracycline imprinted polymer for the solid phase extraction of tetracycline antibiotics. *Anal. Chim. Acta*, **2005**, 552, 81-8.
[97] Suedee, R.; Srichana, T.; Chuchome, T.; Kongmark, U. Use of molecularly imprinted polymers from a mixture of tetracycline and its degradation products to produce affinity membranes for the removal of tetracycline from water. *J. Chromatogr. B*, **2004**, 811, 191-200.
[98] Baggiani, C.; Giraudi, G.; Trotta, F.; Giovannoli, C.; Vanni, A. Chromatographic characterization of a molecular imprinted polymer binding cortisol. *Talanta*, **2000**, 51, 71-75.
[99] Puoci, F.; Garreffa, C.; Iemma, F.; Muzzalupo, R.; Spizzirri, U.G.; Picci, N. Molecularly imprinted solid phase extraction for detection of Sudan I in food matrices. *Food Chemistry*, **2005**, 93, 349-353.
[100] Gao, F.; Hu, Y.; Chen, D.; Li-Chan, E.C.; Grant, E., Lu, X. Determination of Sudan I in paprika powder by molecularly imprinted polymers–thin layer chromatography–surface enhanced Raman spectroscopic biosensor. *Talanta*, **2015**, 143, 344-352
[101] Mayes, A. G.; Andersson, L. I.; Mosbach, K. Sugar binding polymers showing high anomeric and epimeric discrimination by non-covalent molecular imprinting. *Anal. Biochem*., **1994**, 222, 483-488.
[102] Wulff, G.; Haarer, J. Enzyme-analogue built polymers. The preparation of defined chiral cavities for the racemic resolution of free sugars. *Makromol. Chem*., **1991**, 192, 1329-1338.

[103] Maier, N. M.; Buttinger, G.; Welhartizki, S.; Gavioli, E.; Lindner, W. Molecularly imprinted polymer-assisted sample clean-up of ochratoxin A from red wine: merits and limitations. *J. Chromatogr. B,* **2004***,* 804, 103-111*.*

[104] Tamayo, F. G.; Casillas, J. L.; Martin-Esteban, A. Highly selective fenuron-imprinted polymer with a homogeneous binding site distribution prepared by precipitation polymerization and its application to the clean-up of fenuron in plant samples. *Anal. Chim. Acta*, **2003**, 482, 165-173.

[105] Agostino, G. D.; Alberti, G.; Biesuz, R.; Pesavento, M. Potentiometric sensor for atrazine based on a molecular imprinted membrane. *Biosensors and Bioelectronics*, **2006**, 22, 145-152.

[106] Piletsky, S. A.; Piletskaya, E. V.; El'skaya ,A. V.; Levi ,R.; Yano, K.; Karube, I. Optical Detection System for Triazine Based on Molecularly-Imprinted Polymers. *Anal. Lett.*, **1997**, 30, 445-455.

[107] Piletsky, S. A.; Piletskaya, E. V.; Sergeyeva, T. A.; Panasyuk, T. L.; Elskaya, A. V. Molecularly imprinted self-assembled films with specificity to cholesterol. *Sens. Actuators*, **1999**, 60, 216-220.

[108] Zander, A.; Findlay, P.; Renner, T.; Sellergren, B.; Swietlow, A. Analysis of nicotine and its oxidation products in nicotine chewing gum by a molecularly imprinted solid-phase extraction. *Anal. Chem.*, **1998**, 70, 3304-3314.

[109] Liang, C.; Peng, H.; Bao, X.; Nie, L.; Yao, S. Study of a molecular imprinting polymer coated BAW bio-mimic sensor and its application to the determination of caffeine in human serum and urine. *Analyst*, **1999**, 124, 1781-1785.

[110] Xianwen, K.; Tingting, L.; Chen, L.; Hong, Z.; Zonglan, X.; Anhong, Z. A novel electrochemical sensor based on molecularly imprinted polymers for caffeine recognition and detection. *J. Solid State Electrochem.***, 2012**, 16, 3207-3213.

[111] Villamena, F. A.; De La Cruz, A. A. Caffeine selectivity of divinylbenzene crosslinked polymers in aqueous media. *J. Appl. Polym. Sci*., **2001**, 82, 195–205.

[112] Golsefidi, M. A.; Es'haghi, Z.; Sarafraz-Yazdi, A. Design, synthesis and evaluation of a molecularly imprinted polymer for hollow fiber–solid phase microextraction of chlorogenic acid in medicinal plants. *J. Chromatogr. A*, **2012**, 1229, 24-29.

[113] Miura, C.; Li, H.; Matsunaga, H.; Haginaka, J. Molecularly imprinted polymer for chlorogenic acid by modified precipitation polymerization and its application to extraction of chlorogenic acid from *Eucommia ulmodies* leaves. *J. Pharm. Biomed. Anal*., **2015**, 114:139-144.

[114] Li, H.; Liu, Y.; Zhang, Z.; Liao,H.; Nie, L.; Yao, S. Separation and purification of chlorogenic acid by molecularly imprinted polymer monolithic stationary phase. *J. Chromatogr. A*, **2005**, 1098, 66–74.

[115] Tang, W.; Li, G.; Ho Row, K.; Zhu, T. Preparation of hybrid molecularly imprinted polymer with double templates for rapid simultaneous purification of theophylline and chlorogenic acid in green tea. *Talanta*, **2016**, 15, 1-8.

[116] Vasilescu, I.; Eremia, S. A. V.; Penu, R.; Albu, C.; Radoi, A.; Litescu, S. C.; Radua, G.L. Disposable dual sensor array for simultaneous determination of chlorogenic acid and caffeine from coffee. *RSC Adv.*, **2015**, 5, 261-268.

[117] Ribeiro, C. M.; Miguel, E. M.; Silva, J. D. S.; da Silva, C. B.; Goulart, M. O. F.; Kubota, L. T.; Gonzaga, F. B.; Santos W. J. R.; Lima P. R. Application of a nanostructured platform and imprinted sol-gel film for determination of chlorogenic acid in food samples. *Talanta*, **2016**, 156-157, 119-125.

[118] Mohammadi, N.; Najafi, M.; Bahrami Adeha, N. Highly defective mesoporous carbon – ionic liquid paste electrode as sensitive voltammetric sensor for determination of chlorogenic acid in herbal extracts. *Sens. Actuators B: Chem*., **2017**, 243, 838-846.

[119] Koirala, K.; Sevilla III, F.B.; Santos, J. H. Biomimetic potentiometric sensor for chlorogenic acid based on electrosynthesized polypyrrole. *Sens. Actuators B: Chem*., **2016**, 391-396.

[120] Rodrigues Santos, W. D. J.; Santhiago, M.; Pagotto Yoshidaa, I. V.; Tatsuo Kubotaa, L. Novel electrochemical sensor for the selective recognition of chlorogenic acid. *Anal. Chim. Acta*, **2011**, 695, 44–50.

[121] Ji, W.; Zhang, M.; Yan, H.; Zhao, H1.; Mu, Y.; Guo, L.; Wang, X. Selective extraction and determination of chlorogenic acids as combined quality markers in herbal medicines using molecularly imprinted polymers based on a mimic template. *Anal. Bioanal. Chem.*, **2017**, 409, 7087-7096.

Chapter 2

AIM OF THE PROJECT

2.1 Aim of the Project

This project is part of IPCOS network, which has received funding from the European Union's Horizon 2020 research and innovation programme under the Marie Sklodowska-Curie grant agreement No. 642014

IPCOS Network has been created to bring innovation to the field of food quality in the coffee industry, by using molecular imprinting technology to study and detect some bioactive compounds present in coffee, which have shown to have an impact on consumers' health. Easy detection and quantification of these bioactive compounds is very important to ensure the highest quality of the final product not only for the flavor and taste point of view but also to guarantee nutritional values. The technological advances of the past two decades have significantly improved coffee quality due to the analytical techniques available such as HPLC, GC, MS; however, these rely on equipment that is expensive, time consuming and requiring specialized operators. There are specific health benefits and risks associated with the concentration of the different active ingredients in food products that influence the quality of the food; Therefore, there is a clear need to develop novel, simple and complementary approaches to detect important food components to ensure the highest quality of the final product

One of the most important indicators of the coffee cup quality is the amounts of chlorogenic acids (CGAs) and of their corresponding lactones (CGLs) present in the coffee beans after roasting. Roasting is a process carried out at high temperatures and high inner pressures and it plays a key role on the final chemical composition of coffee, due to the many reactions that take place in the beans leading to the formation of hundreds of compounds. CGAs confer astringency, bitterness and acidity to the coffee brew and their content in coffee is an important indicator of its quality that is greatly dependent upon the degree of roasting, the type of roaster and method of infusion. Therefore, together with an analytical study of their presence in the coffee matrix it is also important to develop a reliable, rapid, sensitive and simple method for the quantification of these substances.

This research project has been focused in three main objectives:

- Synthesis and characterization of 3-, 4- and 5-*p*-coumaroylquinic acids;
- Study of the concentration profile of CGAs in coffee production;
- Design and development of molecularly imprinted polymers (MIPs) as recognition elements for CGAs.

Since not all CGAs are commercially available, there is a lack of information about the qualitative and quantitative identification of some classes of CGAs in coffee, especially of *p*CoQAs which are the less studied. In order to understand better their role in the quality of coffee and quantify them in coffee matrix, it is necessary to synthesize these compounds to use them as standards. The first part of the project has been carried out at the Department of Chemical and Pharmaceutical Sciences of the University of Trieste (UNITS) were isomers of *p*-coumaroylquinic acids were synthetized following methods described in the literature that

involve the condensation of an acyl chloride with a derivative of quinic acid. All four regioisomers synthetized have been completely characterized, their stability has been determined by computational methods and the acyl migration was studied. Secondly, study of the CGAs concentration in coffee production was carried at the Aromalab at Illycaffè S.p.A. Several qualitative analyses were performed to ensure the development and optimization of a correct protocol already used at the Illycaffè for the identification of these compounds in coffee. However, since coffee is a very complex matrix and *p*CoQAs are present only in low concentrations, in order to facilitate their identification and to improve the analytical analyses, extractions of these phenolic compounds from other sources richer in *p*CoQAs like walnut leaves were performed. Walnut leaves are frequently used in traditional medicine and their aqueous tea infusion has already been demonstrated to possess biological activity. Since the concentration of CGAs determined in walnut leaves was greatly dependent upon the collection time of the samples we decided to carry out a systematic evaluation of the changes of the different chlorogenic acids from the spring until the end of summer in order to investigate the seasonal variations of these secondary metabolites. By the improvement and optimization of the analytical method already used the Illycaffe, a suitable UHPLC analytical method has been development in this project. Subsequently, the same method has been applied to analyze the CGAs profile of samples of *Coffea arabica*, *Coffea canephora* and *Coffea liberica,* which are the most important species from an economical point of view. Several other wild coffee species have also been studied to evaluate differences in the CGAs content between different species, especially the concentration of *p*CoQAs which have not been reported so far.

The last part of the project was focused on the development of recognition systems for chlorogenic acid, based on molecularly imprinted polymers using 5-CQA as the target molecule. Two different approaches have been considered in this project. As a first choice, fluorescent molecularly imprinted polymers, using a fluorescent functional monomer able to interact with 5-CQA, were prepared to develop a switch “on-off” system whose properties can be exploited in an optical sensor. The second approach consisted on the preparation of a molecular imprinted polymer by synthesizing a fluorescent analogue of the analyte that can compete for the binding sites in the polymer or displace the analyte in the matrix polymer. To prepare derivatives of 5-chlorogenic acid (5CQA) two different fluorescent dyes have been chosen: 5-[(2-Aminoethyl) amino] naphthalene-1-sulfonyl (EDANS), which shows an excitation wavelength at 320 nm and emission wavelength at 490nm, and Fluorescein Isothiocyanate (FITC), with excitation and emission wavelength at 490 nm 520 nm respectively. The fluorescent properties and immobilization of MIPs have been carried out at Cobik, a Slovenian center of excellence in optical sensors.

RESULTS AND DISCUSSION

Chapter 3. Synthesis of *p*-Coumaroylquinic Acids (*p*CoQAs)

3.1 Synthesis of *p*-Coumaroylquinic Acids (pCoQAs)

The four commercially unavailable isomers of *p*-coumaroylquinic acid, 1-*p*-coumaroylquinic acid **1a,** 5-*p*-coumaroylquinic acid **2a,** 3-*p*-coumaroylquinic acid **3a,** 4-*p*-coumaroylquinic acid **4a** (**Figure 3.1**) has been synthetized by coupling reactions between the *p*-acetylcoumaroylchloride, and the suitable protected (-)-quinic acid with the desired free hydroxyl group and all the other hydroxyl groups protected in different ways. The syntheses performed were carried out with the route proposed by Sefkow et al.[1,2] and Dokli et al.[3] although with some modifications to improve the yield.

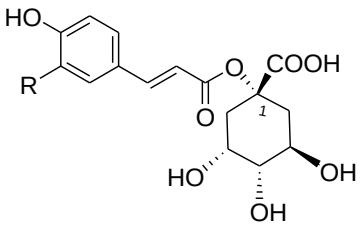

1-*O*-*p*-coumaroylquinic acid **1a** R = H

1-*O*-*caffeo*ylquinic acid **1b** R = OH

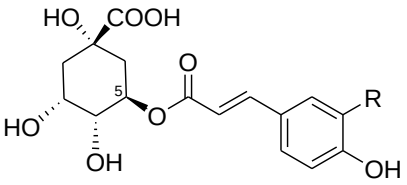

5-*O*-*p*-coumaroylquinic acid **2a** R = H

5-*O*-caffeoylquinic acid **2b** R = OH

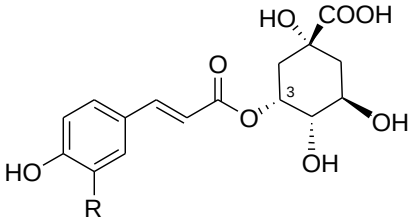

3-*O*-*p*-coumaroylquinic acid **3a** R = H

3-*O*-caffeoylquinic acid **3b** R = OH

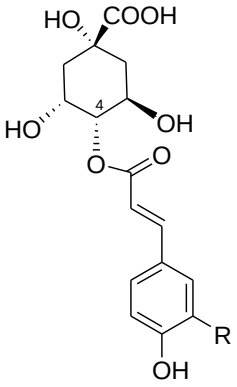

4-*O*-*p*-coumaroylquinic acid **4a** R = H

4-*O*-caffeoylquinic acid **4b** R = OH

Figure 3.1. Chemical structures of the four regioisomers of *p*-Coumaroylquinic Acids (pCoQAs) **1a-4a** and Caffeoylquinic acids (CQAs)**1b-4b**.

p-Acetylcoumaroylchloride was prepared following a known two steps procedure[3,4] (**scheme 3.1**) starting from *p*-coumaric acid. Protection of the hydroxyl group was carried out with acetic anhydride with DMAP in pyridine and subsequently, reaction with oxalyl chloride gave the protected acyl chloride in 95% yield.

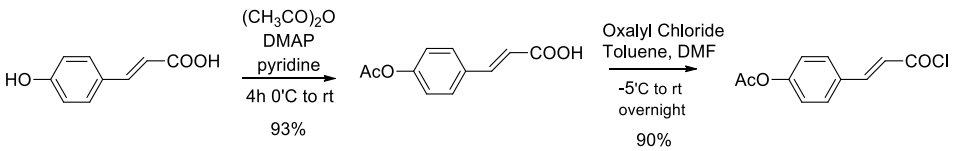

Scheme 3.1. Synthesis of *p*-acetylcoumaroylchloride (*p*AcCoCl).

3.1.1 Synthesis of 1-O-p-coumaroylquinic acid 1 (1-*p*CoQA)

Although in the literature there is no evidence that the regioisomer 1-*O*-caffeoylquinic acid **1b** is present in coffee beans,[5] we decided to perform also the synthesis of 1-*O*-p-coumaroylquinic acid **1a** according to **scheme 3.2**. In fact, the availability of **1a** as a standard can be helpful in confirming the absence of regioisomer at position 1 in coffee beans. To obtain compound **1a**, a protection of the hydroxyl groups at positions 3,4 and 5 was achieved following a literature procedure[3,6] with some modifications. Lactone **5** was synthetized in 72% yield and used without further purification in the following condensation reaction with *p*-acetylcoumaroylchloride, using DMAP and pyridine in dichloromethane at room temperature. The protected ester **6** was obtained in 57% yield after purification by column chromatography. Deprotection reaction of all protecting groups was performed in acidic conditions using HCl (2N)/ THF in a ratio 4:1 under stirring for 11 days giving 1-*O*-p-coumaroylquinic acid **1a** in 85% yield. The formation of the regioisomer **1a** was confirmed by ^{1}H NMR analysis. Comparing the chemical shifts of protons at positions 3,4 and 5 of the quinic core of the final product with protons in the free quinic acid, as can be observed in **Figure 3.2**, there were no significant chemical shifts of protons at positions 3, 4 to indicate they were not involved in the acylation.

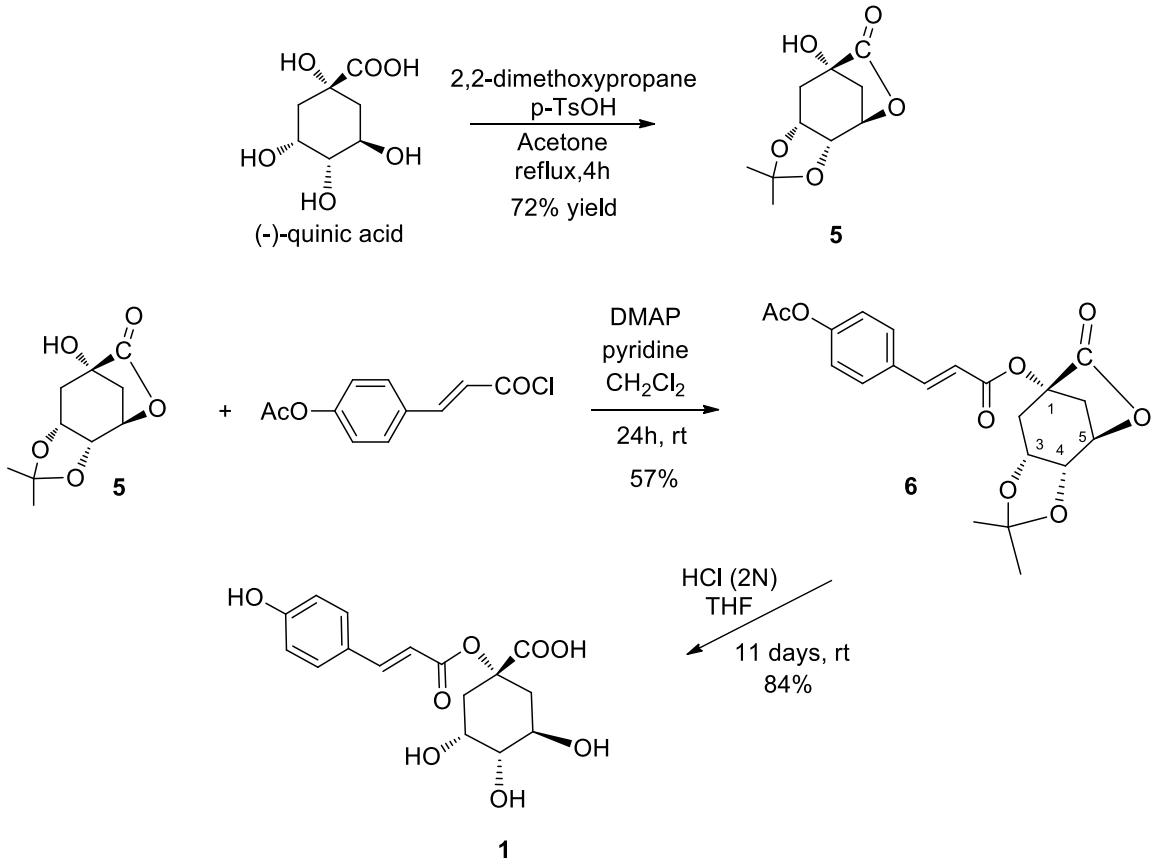

Scheme 3.2. Synthesis of 1-*O*-*p*-coumaroylquinic acid **1a**

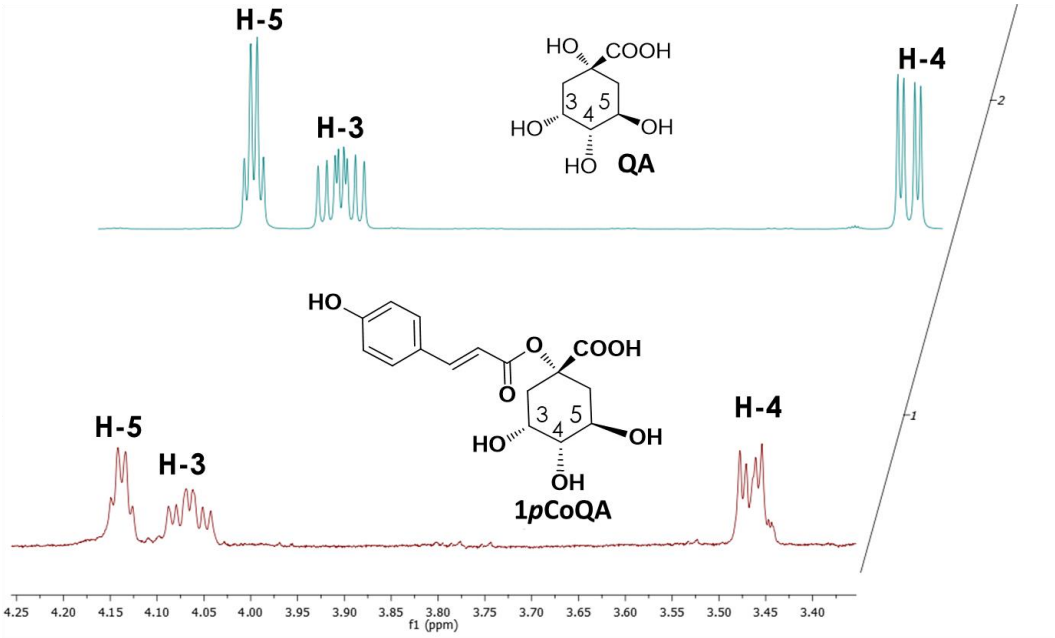

Figure 3.2 Chemical shifts of protons at C-3, C-4 and C-5 in quinic acid (QA) and in 1-*O*-*p*-coumaroylquinic acid **1a** (1-*p*CoQA)

3.1.2 Synthesis of 5-*O*-*p*-coumaroylquinic acid 2a (5-*p*CoQA)

The same lactone **5** was used as the starting building block also for the synthesis of 5-*O*-*p*-coumaroylquinic acid **2a**, following **scheme 3.3**. In this synthesis, lactone ring of compound **5** was opened and protection of the carboxylic group underwent through alcoholysis with EtOH using a literature procedure to afford the ethyl carboxylate **7**[3,7]. ^{1}H NMR of the crude reaction mixture revealed the presence of the ethyl carboxylate derivative **7** although in admixture with lactone **5** in 13:1 ratio respectively. The crude product was used in the following esterification step without purification, as previously described in the synthesis of 1-*p*CoQA, to give compound **8** in 34% yield after purification by column chromatography. Protection of the hydroxyl group was not necessary since Pooter et al.[8] demonstrated that under mild conditions no esterification occurs at axial C-1 hydroxy group of the quinic core. Deprotection reaction was performed in 6 days in presence of HCl (2N)/ THF to obtain 5-*O*-*p*-coumaroylquinic acid **2a** in 77% yield from the protected ester **8**.

To assign the structure of the product obtained, its ^{1}H NMR data were compared to that of the commercial sample of 5-*O*-p-caffeoylquinic acid **2b** which differs only for a hydroxyl group on the aromatic ring. ^{1}H NMR spectra were very similar, except for the aromatic ring protons, showing the same stereochemistry and conformation of the cyclohexane ring. The most stable conformation of compound **2a**, as well as that of **2b**, is the one with the ester group and the carboxylic group in equatorial position, the hydroxyl group at C-4 in equatorial position while the hydroxyl group at C-3 in axial position. The assignment of this conformation was possible analyzing the coupling constants and W_H of the proton signals at C-3, C-4 and C-5 (see table 3.1).

H-5 resonates at 5.34 with a W_H of 23.2 Hz, indicating that H-5 is in axial position while H-3 resonates at 4.16 with a W_H of 10.7 Hz indicating that H-3 is in equatorial position. Both compounds **2a** and **2b** show two quite superimposable spectra for the region of quinic core protons thus demonstrating they have the same conformation.

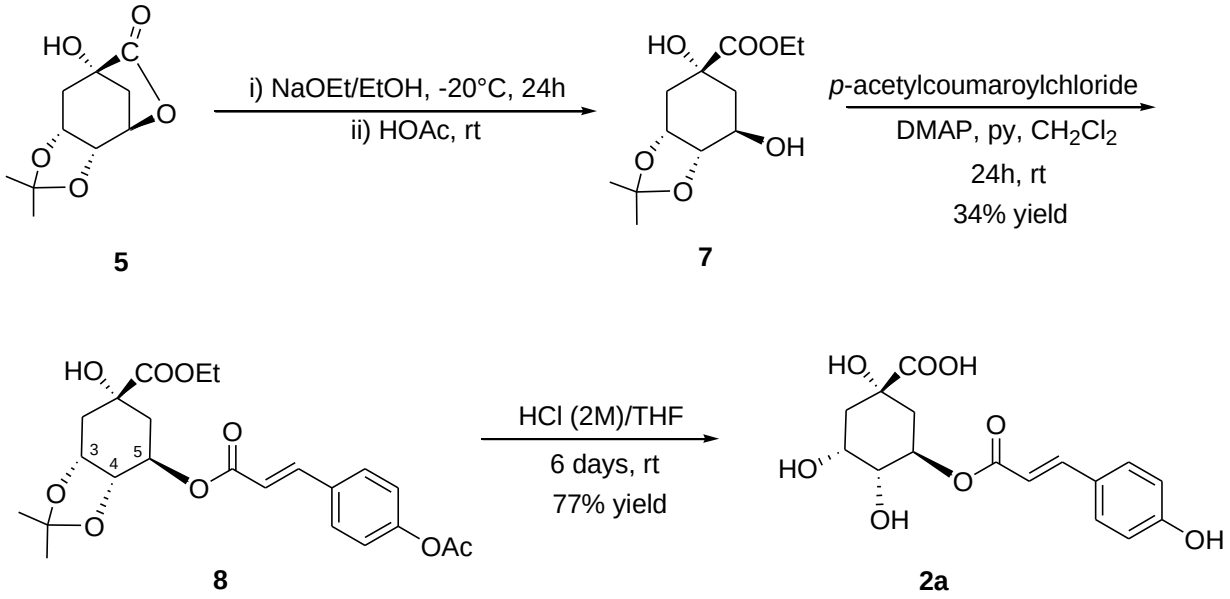

Scheme 3.3. Synthesis of 5-*O*-*p*-coumaroylquinic acid **2a**

Table 3.1 – ^{1}H NMR of *p*CQAs and CQAs in CD_3OD at 500MHz

Compound	Ar protons	Vinyl protons	H-3	H-4	H-5	H-2 H-6
2a	7.47 (d, J 8.5), 6.81 (d, J 8.5)	7.62 (d, J 16.0) , 6.32 (d, J 16.0	4.17 (m, W_H 10.7	3.72 (dd, J_1 3.6, J_2 8.2)	5.34 (dt, J_1 8.9, J_2 4.3, W_H)	2.16-2.25 (2H, m), 2.01-2.11 (2H,m)
2b[9]	7.05 (d, J 2.9), 6.96 (dd, J_1 8.8, J_2 2.9), 6.78 (d, J 8.8)	7.56 (d, J 14.7), 6.26 (d, J 14.7)	4.16 (m, W_H 10.7)	3.72 (dd, J_1 7.0, J_2 3.6)	5.34 (dt, J_1 8.9, J_2 5.3, W_H 23.2)	2.16-2.24 (2H, m), 2.02-2.10 (2H, m)
3a	7.47 (d, J 8.5), 6.81 (d, J 8.5)	7.67 (d, J 15.9), 6.39 (d, J 15.9)	5.39 (m, W_H 13.7)	3.71 (1H, dd, J_1 7.6, J_2 2.7)	4.10 (1H, m, W_H 17.8)	2.10-2.20 (3H, m), 1.93-2.02 (1H, m)
3b[9]	7.04 (d, J 2.4), 6.94 (dd, J_1 8.8, J_2 2.4), 6.78 (d, J 8.8)	7.58 (d, J 16.7), 6.31 (d, J 16.7)	5.35 (m, W_H 11.9)	3.65 (dd, J_1 8.7, J_2 4.3)	4.14 (dt, J_1 8.7, J_2 4.3, W_H 21.7)	2.11-2.22 (3H, m), 1.93-1.99 (1H, m)
4a	7.49 (d, J 8.6), 6.82 (d, J 8.6)	7.73 (d, J 15.9), 6.45 (d, J 15.9)	4.32 (m)	4.81 (dd, $J_1$10.0, J_2 2.8)	4.32 (m)	2.17-2.22 (2H, m), 2.00-2.10 (2H, m)

4b[9]	7.07 (d, J 3.1), 6.96 (dd, J_1 9.4, J_2 3.1), 6.78 (d, J 9.4)	7.64 (d, J 15.6), 6.37 (d, J 15.6)	4.28 (m)	4.80 (dd, J_1 9.6, J_2 3.8)	4.28 (m)	2.16-2.22 (2H, m), 1.98-2.08 (2H, m)

In **Figure 3.3** is reported part of the ^{1}H NMR spectrum of both quinic acid and compound **2a** where it can be clearly observed the downfield shift of proton at C-5 due to the esterification reaction with respect to the same proton in the simple quinic acid.

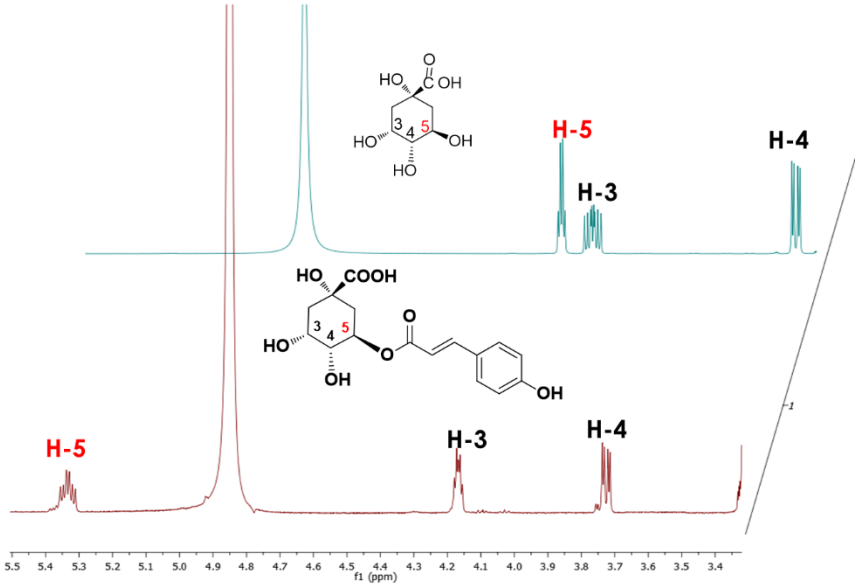

Figure 3.3 Chemical shifts of Quinic acid (QA) and 5-*O*-*p*-coumaroylquinic acid **2a** (5-*p*CoQA)

3.1.3 Synthesis of 3-*O*-*p*-coumaroylquinic acid 3a (3-*p*CoQA)

3-*p*-coumaroylquinic acid **3a** was synthetized following **scheme 3.4**. The carboxylic group of (-)-quinic acid was protected by esterification with MeOH, and successively, the hydroxyl groups at C-4 and C-5 were protected using 2,2,3,3-tetramethoxybutane to obtain the protected methyl quinate **9**[1,3,10,] in 15% yield from (-)-quinic acid. Coupling reaction between *p*-acetylcoumaroylchloride and compound **9** under standard esterification conditions gave the corresponding ester **11** in 20% yield, after purification by column chromatography. Deprotection reaction under acidic conditions by HCl (2N)/ THF (3:1) for 6 days afforded a 4:1 mixture of 3-*O*-*p*-coumaroylquinic acid **3a** and 4-**O**-*p*-coumaroylquinic acid **4a** (62% conversion) as determined by ^{1}H NMR (**Figure 3.4a**). Also in this case, assignment of the structure of the two regioisomers **3a** and **4a** was possible by means of ^{1}H NMR analysis. Compound **4a** could be recognized since a double of doublet at lower field (4.81 ppm) appeared, due to the presence of the acyl group at C-4, together with an overlapped signal of the two protons at C-3 and C-5 at 4.32 ppm. Also in this case the ^{1}H NMR spectrum of **3a** is very similar to the one of 3-*O*-caffeoylquinic acid **3b** (see table 1) to show that they also have the same

conformation. H-5 is in axial position confirmed by the W_H value (17.8 Hz), while H-3 is an equatorial proton due to the lower W_H (13.7 Hz).

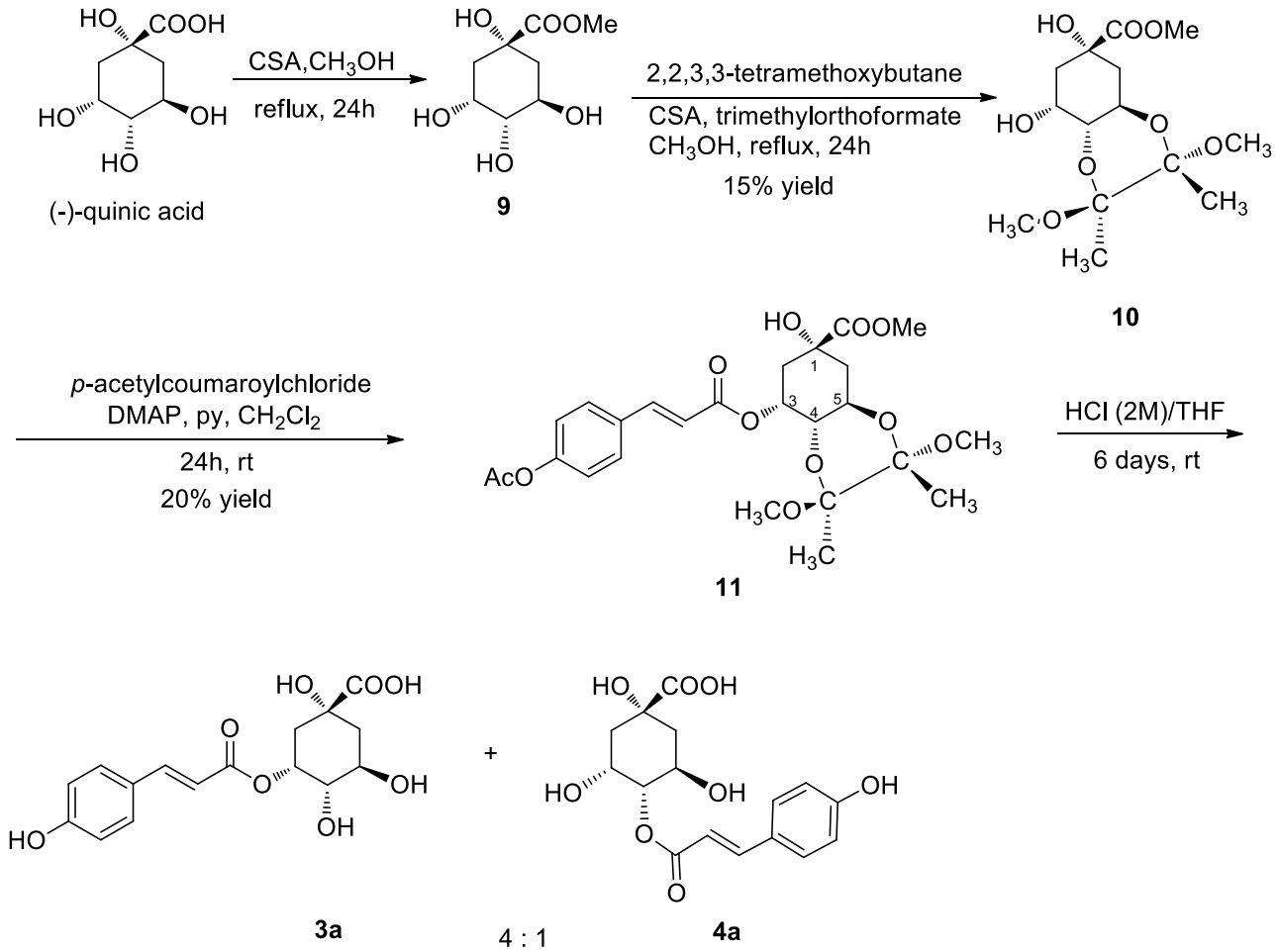

Scheme 3.4. Synthesis of 3-*O*-*p*-coumaroylquinic acid **3a**

Also in this case a downfield shift of proton at C-3 with respect to the free quinic acid can be observed in **Figure 3.4b**.

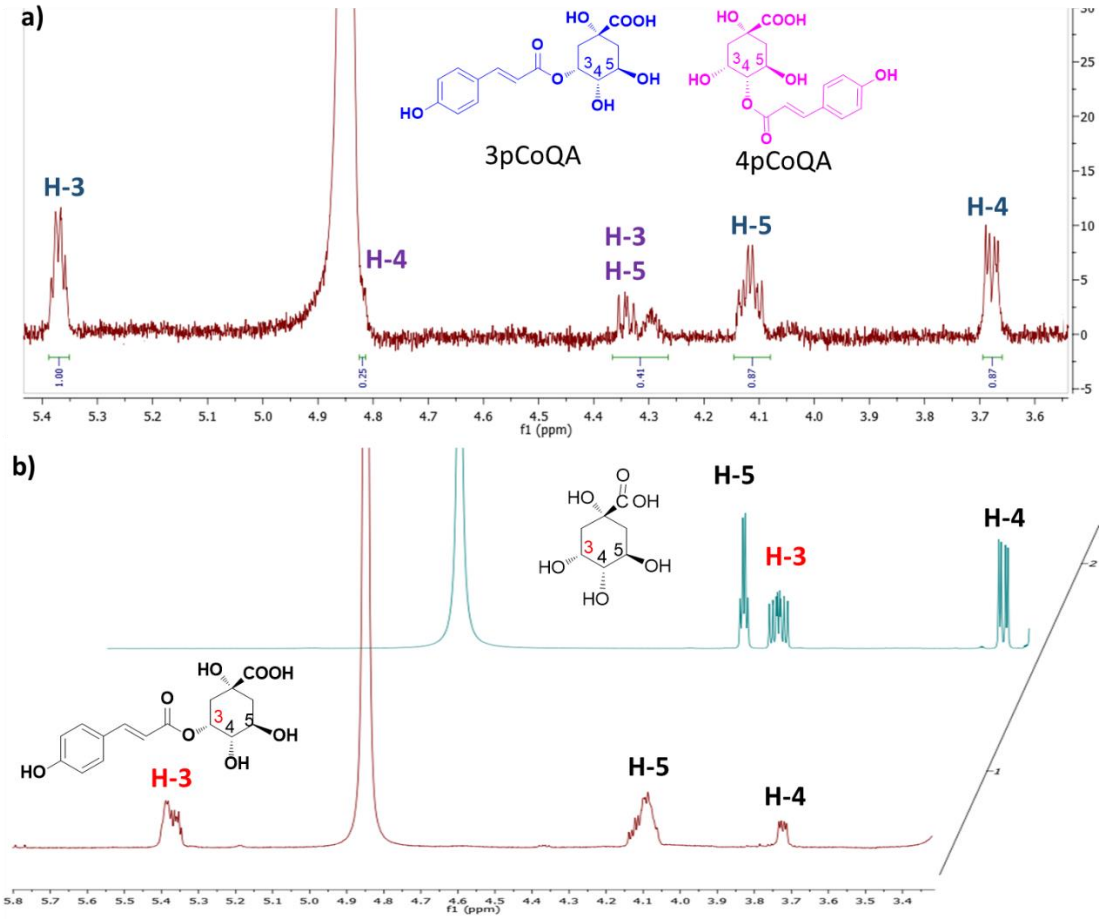

Figure 3.4. a) Mixture of 3-*O*-*p*-coumaroylquinic acid **3a** (3-*p*CoQA) and 4-*O*-*p*-coumaroylquinic acid **4a** (4-*p*CoQA). **b)** Chemical shifts of protons at C-3, C-4 and C-5 for quinic acid (QA) and 3-O-*p*-coumaroylquinic acid **3a** (3-*p*CoQA).

3.1.4 Synthesis of 4-*O*-*p*-coumaroylquinic acid 4a (4-pCoQA)

4-*O*-*p*-coumaroylquinic acid **4a** was obtained after protection at positions 5 and 3 of the quinic acid ring following **scheme 3.5.** 1,5-γ-quinide was synthetized from (-)-quinic acid through intramolecular condensation reaction without any solvent, as described by Wolinsky et al.[11] and the crude product was purified by heating under reflux in ethyl acetate as suggested by Raheem et al[12]. Recrystallizations of the brown sticky residue with EtOH or MeOH as suggested by Wolinsky et al.[11] and other literature procedures[9,13] were not successful since the product was obtained in less than 5% yield. Subsequently, protection with *tert*-butyldimethylsilylchloride (TBSiCl) following a literature procedure[12, 14], gave a mixture of the two monosilylated isomers at positions 3 and 4 of the cyclohexane ring in a 70:30 ratio (3-OTBDMS) : (4-OTBDMS) with the protection at position 3 in major amount, as determined by ^{1}H NMR spectroscopy.[10,11] Different attempts were made in order to separate the two compounds 3-OTBDMS and 4-OTBDMS by flash chromatography but it was not possible to isolate 3-OTBDMS isomer as a pure compound so the mixture of the two was used in the next step. Esterification with *p*-acetylcoumaroylchloride, using pyridine as the

solvent, as suggested by Sefkow et al.[1] and Dokli et al.[3], gave nevertheless the only **15** as a pure compound while no esterification at position 3 was observed as confirmed by ^{1}H NMR analysis of the crude product. Compound **15** was obtained in 20% yield after purification by column chromatography and it was subsequently deprotected under acidic conditions HCl (2N)/ THF (3:1) to give a mixture of isomers **3a** and **4a** in a 1:1 ratio (43% of conversion from the protected ester). Since the starting compound was the only isomer **15**, an acyl migration from C-4 to C-3 of the cyclohexane ring occurred as it was observed by ^{1}H NMR spectroscopy. This kind of rearrangement was already observed by Haslam et al. in 1964[15] when isomers 3-*O*-*p*-coumaroylquinic acid **3a** and 5-*O*-*p*-coumaroylquinic acid **2a** were obtained from 4-*O*-*p*-coumaroylquinic acid **4a** by treatment with sodium hydrogen carbonate. Although in our case deprotection reaction was carried out in acidic conditions it seems that the same acyl migration occurs, probably by formation of the intermediate orthoesters.

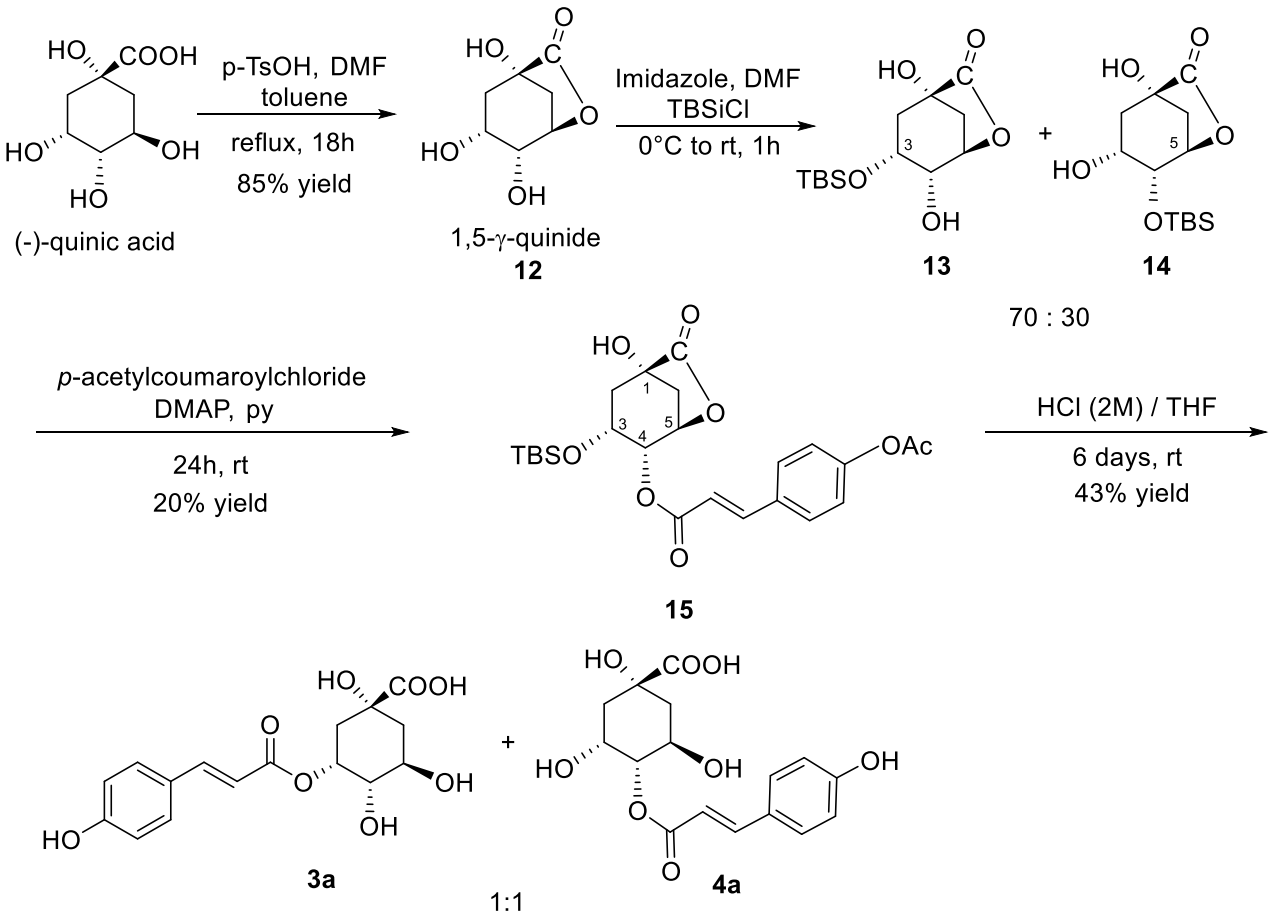

Scheme 3.5 Synthesis of 4-*O*-*p*-coumaroylquinic acid **4a**

In **Figure 3.5a** are reported the ^{1}H NMR spectra of the mixture of isomers 4-*O*-*p*-coumaroylquinic acid **4a** and 3-*O*-*p*-coumaroylquinic acid **3a** and that of quinic acid. Again it can be observed that there is a downfield shift of the proton at C-4 with respect to the free quinic acid. (**Figure 3.5b**)

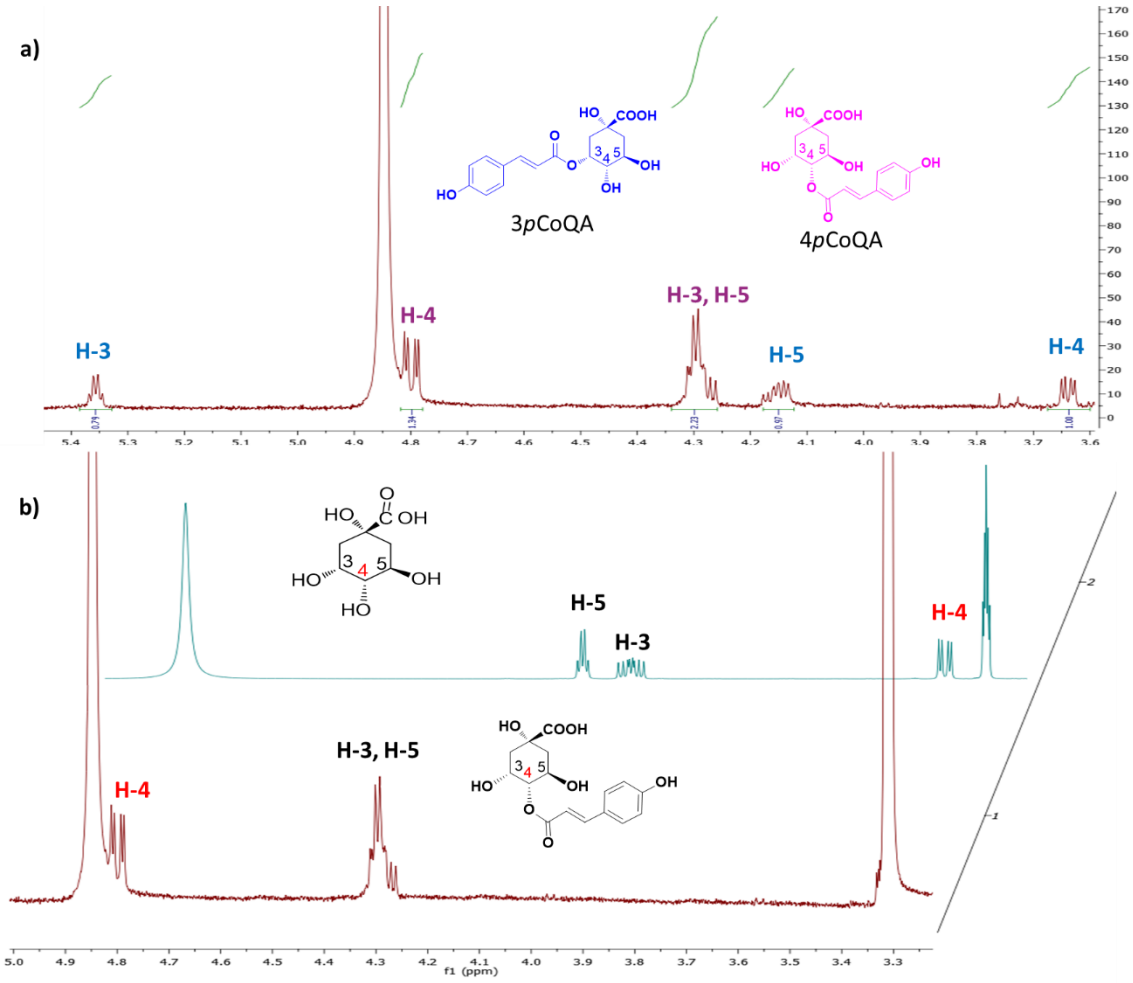

Figure 3.5 a) Mixture of 4-*O*-*p*-coumaroylquinic acid **4a** (4-*p*CoQA) and 3-*O*-*p*-coumaroylquinic acid **3a** (3-*p*CoQA). **b)** Chemical shifts of Quinic acid (QA) and 4-*O*-*p*-coumaroylquinic acid **4a** (4-*p*CoQA).

3.2 Computational study of the acyl migrations

In order to explain the interconversions observed along the syntheses of the esters, we have carried out a computational analysis on the final products and on the main intermediates leading to their formation (**Figure 3.6**).

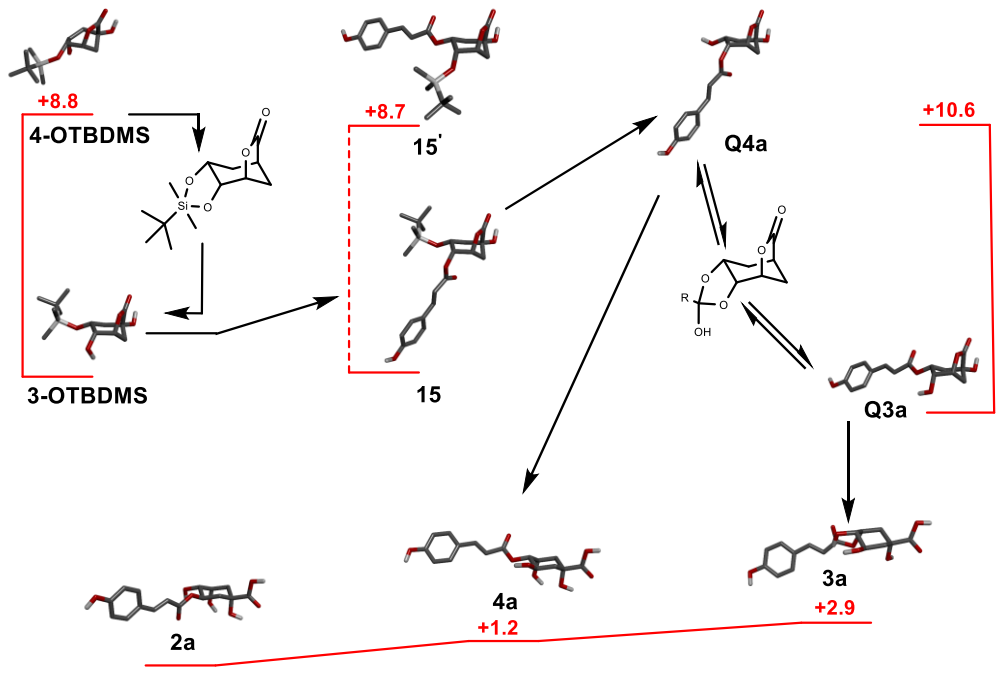

Figure 3.6. Computational analysis of the interconversions between products and between synthetic intermediates. The relative B3lyp-6.31G(d,p) energies are given in Kcal/mol.

The geometries of products and intermediates were optimized first at the HF-6.31G(d) level, and then further refined with a DFT calculation carried out at the B3lyp-6.31G(d,p) level. The final products **2a**, **4a** and **3a** show slight differences in energy, the most stable being the 5-acyloyl derivative **2a**. This explains why its direct synthesis from compounds **7** and **8** is not affected by any isomerization. Esters **4a** and **3a** are only 1.2 and 2.9 Kcal/mol less stable, respectively. The overall conformation of the three compounds is very similar, with the carboxyl group at position 1 always found in an equatorial conformation. As a consequence, ester **3a** is the only product with the coumaroyl group in an axial conformation, as experimentally observed in the NMR spectra. The formation of 20% of **4a** in the synthesis of **3a** from the protected intermediate **9** (Scheme 3.1.3) can therefore be explained by the thermodynamically favored intramolecular acyl transfer from **3a** to **4a**, starting upon deprotection of **9**.

The synthesis of **4a**, as outlined in scheme 3.1.4, involve more complex interconversions. Protection of the starting 1,5-γ-quinide may lead to two different silylated compounds **13** and **14** with the 3-protected derivative as the most abundant in the reaction crude, while compound **15** is the only product deriving from the acylation of such mixture. 3-OTBDMS is actually much more stable that its isomer 4-OTBDMS, by 8.8 Kcal/mol. In quinides, position 4 is axial and for this reason the 4-protected compound is strongly destabilized with the bulky protecting group forcing the quinide to a boat-like conformation. Full equilibration to the most

stable 3-derivative is likely to occur easily, via a pentacoordinate silicon intermediate, and this may explain the fully selective transformation into compound **15**, which, by the way, is even more stable than its isomer **15'** (**Figure 3.6**). In the subsequent step of the synthesis, compound **15** is deprotected and hydrolyzed, and a 1:1 mixture of **4a** and **3a** is obtained. As **15** would lead directly to **4a**, and this compound is more stable than **3a**, the only explanation for the observed result may be found if deprotection occurs before the ring opening reaction of quinides intermediates **Q4a** and **Q3a** (**Figure 3.6**). The relative stability of the two deprotected quinides is reversed with respect to the end products, and **Q3a** is more stable by over 10 Kcal/mol. Interconversion thus happens at the quinide level and not at the product level in this synthetic path, and its outcome is the result of a complex competition between equilibria.

3.3 Circular Dichroism

Circular dichroism spectra of all isomers **1-4a** were registered and a comparison with the one obtained for the commercially available caffeoyl analogues **2b-4b** have been made in order to verify that no significance influence of the substituents on the aromatic ring should be observed.

Moreover, two different solvents were used, methanol and acetonitrile in order to establish if changes can be observed due to hydrogen bonding between the solvent and the compound analyzed.

In **Figure 3.7 a** and **b** the circular dichroism spectra of all compounds in methanol and acetonitrile are reported. The CD spectra of the *p*-coumaroylquinic acids **2a-4a** and that of the corresponding caffeoyl analogs **2b-4b** are very similar indicating that they must have the same absolute configuration of the chiral centers. Furthermore, the same behavior is observed for all compounds in both solvents used (methanol and acetonitrile) as it can be noticed comparing **Figure 3.7a** with **Figure 3.7b.**

Compounds **2a**,**b**-**3a**,**b** present a double Cotton effect, with a positive band in the range 290-340nm and a negative band in the range 200-220nm while compounds **4a** and **4b** have both negative bands. To note that **3a** and **3b** present also a third positive band in the range 220-260nm.

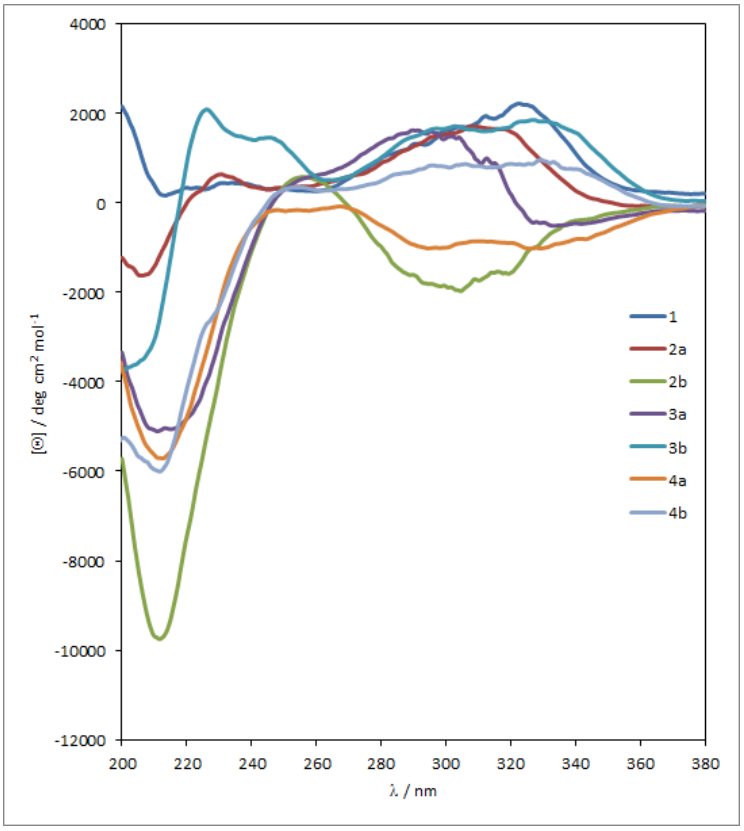

Figure 3.7a – Circular dichroism spectra of compounds **1-4** in MeOH

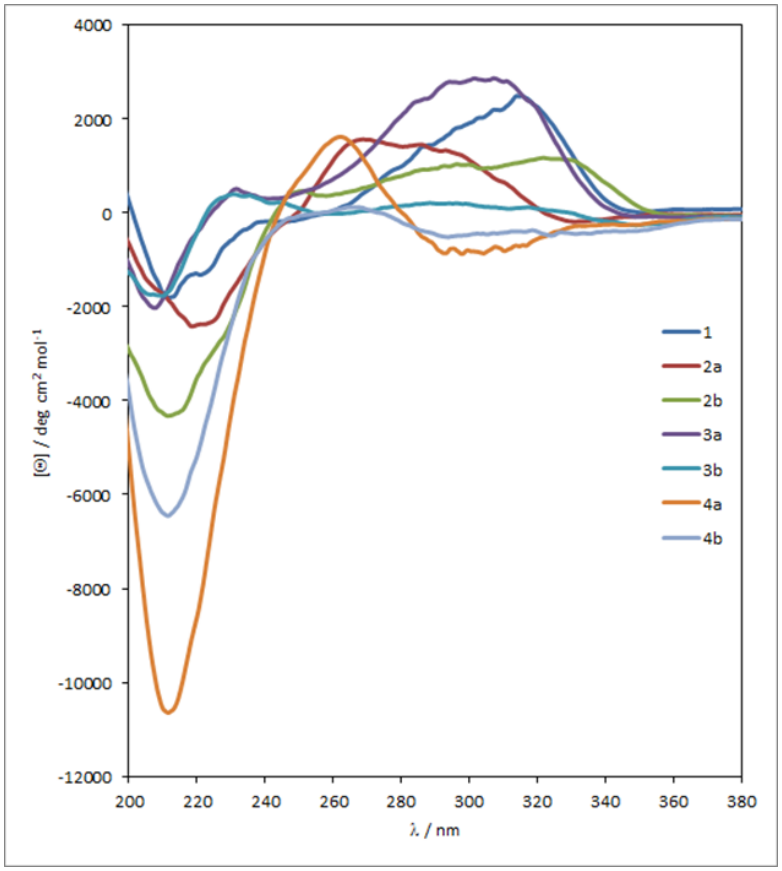

Figure 3.7b - Circular dichroism spectra of compounds **1-4** in MeCN

[1]Sefkow, M.; Kelling, A.; Schilde, U. First Efficient Syntheses of 1-, 4-, and 5-Caffeoylquinic Acid *Eur. J. Org. Chem*, **2001**, 2735-2742.

[2]Sefkow, M. First Efficient Synthesis of Chlorogenic Acid *Eur. J. Org. Chem*. **2001**, 1137-1141.

[3]Dokli, I.; Navarini, L.; Hamerŝak, Z. Syntheses of 3-, 4-, and 5-*O*-feruloylquinic acids, *Tetrahedron: Asymmetry*, **2013**, 24, 785-790.

[4] Criton, M.; Le Mellay-Hamon. Dimeric Cinnamoylamide Derivatives as Inhibitors of Melanogenesis. *V. Biol. Pharm. Bull*., **2011**, 34, 420-425.

[5] Jaiswal, R.; Patras, M.; Eravuchira, P.; Kuhnert, N. Profile and Characterization of the Chlorogenic Acids in Green Robusta Coffee Beans by LC-MSn: Identification of Seven New Classes of Compounds. *J. Agric. Food. Chem*., **2010,** 58, 8722-8737.

[6] Rohloff, J.; Kent, K.; Postich, M.; Becker, M.; Chapman, H.; Kelly, D.; Lew, W.; Louie, M.; McGee, L.; Prisbe, E.; Schultze, L.; Yu, R.; Zhang, L. Practical Total Synthesis of the Anti-Influenza Drug GS-4104 *J. Org. Chem*., **1998**, 63, 4545, 4550.

[7] Federspiel, M.; Fisher, R.; Hennig, M. et al. Industrial Synthesis of the Key Precursor in the Synthesis of the Anti-Influenza Drug Oseltamivir Phosphate (Ro 64-0796/002, GS-4104-02): Ethyl(3R,4S,5S)-4,5-epoxy-3-(1-ethyl-propoxy)-cyclohex-1-ene-1-carboxylate. *Org. Process Res. & Dev*., **1999**, 3, 266-274.

[8] De Pooter, H.; De Brucker, J.; van Sumere, C. F. Synthesis of 3-*O*-coumaryl-, 4-*O*-coumaryl- and 3-*O*-ferulyl-D-(-)-quinic acid. Improved Synthesis of 3-*O*-sinapyl-D-(-)-quinic acid. *Bull. Soc. Chim. Belge*, **1976**, 85, 663-671.

[9] Choi, Y. H.; Kim, H. K.; Linthorst, H. J. M.; Hollander, J. G.; Lefeber, A. W. M.; Erkelens, C.; Nuzillard, J.-M.; Verpoorte, R. NMR metabolomics to revisit the tobacco mosaic virus infection in *Nicotiana tabacum* leaves *J. Nat. Prod*., **2006**, 69 (5), 742-748.

[10] Montchamp, J.; Tian, F.; Hart, M.; Frost, J. Butane 2,3-Bisacetal Protection of Vicinal Diequatorial D. *J. Org. Chem*. **1996**, 61, 3897-3899.

[11] Wolinsky, J.; Novak, R.; Vasileff, R. A Stereospecific Synthesis of (±)-Quinic Acid. *J. Org. Chem*., **1964**, 29, 3596–3598.

[12] Raheem, K.; Botting, N.; Williamson, G.; Barron, D. Total synthesis of 3,5-*O*-dicaffeoylquinic acid and its derivatives. *Tetrahedron Lett*. **2011**, 52, 7175-7177.

[13] Sinisi, V.; Boronova, K.; Colomban, S.; Navarini, L.; Berti, F.; Forzato, C. Synthesis of Mono-, Di-, and Tri-3,4-dimethoxycinnamoyl-1,5-γ-quinides. *Eur. J. Org. Chem*., **2014**, 1321-1326.

[14] Glebocka, A.; Sicinski, R.; Plum, L.; Clagett-Dame, M.; De Luca, H. New 2-Alkylidene 1,25-Dihydroxy-19-norvitamin D3. Analogues of High Intestinal Activity: Synthesis and Biological Evaluation of 2-(3′-Alkoxypropylidene) and 2-(3′-Hydroxypropylidene) Derivatives*. J. Med. Chem*., **2006**, 49, 2009-2020.

[15] Haslam, E.; Makinson, G.; Naumann, G.; Cunningham, J. Synthesis and Properties of Some Hydroxycinnamoyl Esters of Quinic Acid*. J. Chem. Soc*., **1964**, 2137-2146.

RESULTS AND DISCUSSION

Chapter 4. Study of the Concentration profile of CGAs in Walnut (*Juglans regia L.*) leaves

4.1 Chlorogenic acids (CGAs) in Walnut leaves.

Walnut leaves are particularly rich in *p*CoQAs,[1,2,3] for this reason although it was not a subject of study in this project, they were chosen as a potential source to ensure the development of a correct protocol for the later identification of this class of CGAs in coffee to facilitate their identification and to improve the analytical analyses. Walnut leaves are frequently used as traditional remedy and its aqueous tea infusion already demonstrated to possess biological activity,[4,5] however, the concentration of CGAs determined in walnut leaves greatly depends upon the collection time of the samples. In the Aromalab laboratory of Illycaffè, a suitable UHPLC method used for the main CGAs identification was optimized in order to quantify and evaluate seasonal variation of chlorogenic acids derivatives in walnut leaves. It is also known that plants synthesize mainly the *trans*-isomers with respect to the *cis*-isomers of CGAs but the latter have been reported to be formed in tissue or extracts previously exposed to UV light. In this part of the work the presence of *cis* isomers was evaluated thanks to a UV irradiation *ad hoc* experiment on standard solutions of CQAs and *p*CoQAs.[6] Qualitative identification of the *trans*-isomers was performed using synthetized standards of FQAs and *p*CoQAs, not commercially available[7,8] while quantitative analyses are expressed as 5-caffeoylquinic acid equivalents in order to assure reliable results.[9]

Qualitative analyses were carried out using the following standards: caffeic acid (CA) ; *trans* 3-caffeoylquinic acid (*trans* 3-CQA) ; *trans* 4-caffeoylquinic acid (*trans* 4-CQA) ; *trans* 5-caffeoylquinic acid (*trans* 5-CQA) ; *p*-coumaric acid (*p*CoA) ; *trans* 3-*p*-coumaroylquinic acid (*trans* 3-*p*CoQA) **3a** ; *trans* 4-*p*-coumaroylquinic (*trans* 4-pCoQA) **4a**; *trans* 5-*p*-coumaroylquinic (*trans* 5-*p*CoQA) **5a**; ferulic acid (FA) ; *trans* 3-feruloylquinic acid (*trans* 3-FQA) ; 4-feruloylquinic acid (*trans* 4-FQA) ; 5-feruloylquinic acid (*trans* 5-FQA); sinapic acid (SA) ; 3,4-dicaffeoylquinic acid (3,4-diCQA) ; 3,5-dicaffeoylquinic acid (3,5-diCQA) ; 4,5-dicaffeoylquinic acid (4,5-diCQA)(**Figure 4.1**).

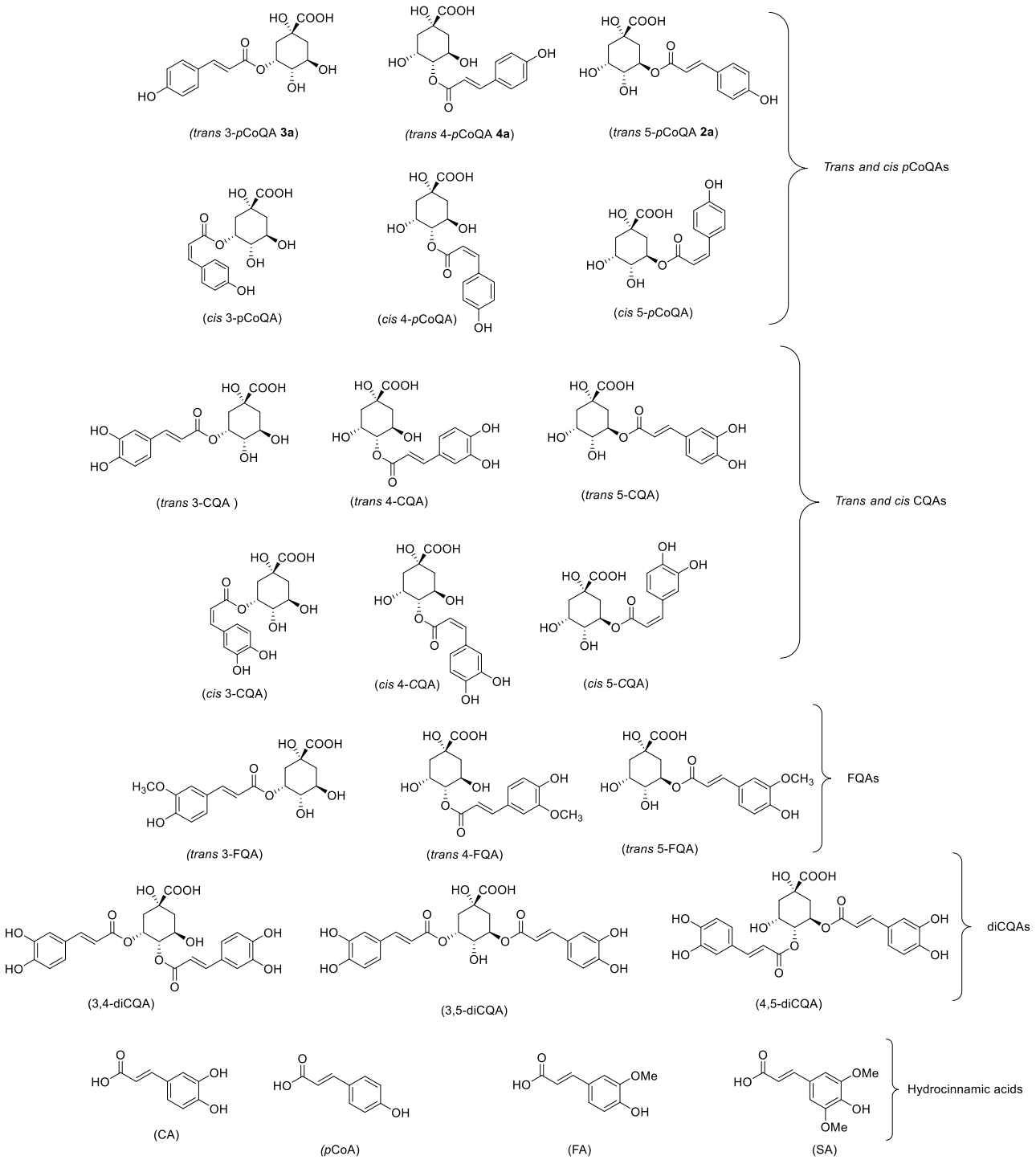

Figure 4.1. Chemical structures of the hydroxycinnamic acid derivatives identified in Walnut leaves. *p*CoQAs: *trans* 3-*p*-coumaroylquinic (*trans* 3-*p*CoQA); *trans* 4-*p*-coumaroylquinic (trans 4-*p*CoQA); *trans* 5-*p*-coumaroylquinic (*trans* 5-*p*CoQA); *cis* 3-*p*-coumaroylquinic (cis 3-*p*CoQA); *cis* 4-*p*-coumaroylquinic (cis 4-pCoQA); *cis* 5-*p*-coumaroylquinic (cis 5-*p*CoQA); CQAs: *trans* 3-caffeoylquinic acid (*trans* 3-CQA), *trans* 4-caffeoylquinic acid (*trans* 4-CQA)); *trans* 5-caffeoylquinic acid (trans 5-CQA);*cis* 3-caffeoylquinic acid (*cis* 3-CQA);; *cis* 4-caffeoylquinic acid (cis 4-CQA); *cis* 5-caffeoylquinic acid (cis 5-CQA); FQAs: *trans* 3-feruloylquinic acid (*trans* 3-FQA; *trans* 4-feruloylquinic acid (*trans* 4-FQA); *trans* 5-feruloylquinic acid (*trans* 5-FQA); diCQAs: 3,4-dicaffeoylquinic acid (3,4-diCQA); 3,5-dicaffeoylquinic acid (3,5-

diCQA), 4,5-dicaffeoylquinic acid (3,5-diCQA); hydrocinnamic acids: caffeic acid (CA); *p*-coumaric acid (*p*CoQA); ferulic acid (FA), sinapic acid (SA).

4.2 Walnut Leaves Characterization

Fresh leaves from different branches were collected from a single *Juglans regia* L. tree, in four different period of growth, from spring to late summer 2016. The dimensions of the leaves were determined and their mean values (on a sample of 15 leaves) are reported in Table 4.1.

Table 4.1 Dimension of Fresh Leaves (cm) at the same growth stage per each month.

		April	***May***	***July***	***September***
Length (cm)	mean	5.27	11.12	15.14	12.61
	St. dev.	1.85	1.20	1.48	3.59
Width (cm)	mean	2.36	5.20	7.35	6.42
	St. dev.	0.79	0.46	0.94	1.73

The percentage of water loss (%WL) are reported in table 4.2 and it was calculated using the following equation:

$$\%WL = 100 - \frac{W_{AF} * 100}{W_{BF}}$$

W_{BF} corresponds to the weight before freeze dried and W_{AF} to the weight after freeze dried.

Table 4.2 Percentages of water loss (%WL)

	April	**May**	**July**	**September**
% WL	71	74	72	67

4.3 Identification and Characterization of isomers *trans*-CGAS

UHPLC analyses were performed at different dilutions in order to have a better identification of all chlorogenic acids. Quantification was performed on peak areas obtained with OpenLab software (Agilent, Germany). Calibration curve of *trans* 5-CQA showed a good response linearity with a coefficient of correlation (r^2) of 0.999. Limit of quantification (LOQ) and limit of detection (LOD) were calculated as 3 times lower concentration of analyte on signal to noise ratio (LOD) or 10 times lowest concentration of analyte on signal to noise ratio (LOQ) resulting 0.88 μg/mL for LOQ and 0.26 μg/mL for LOD.

At the beginning, aqueous diluted samples in a 1:10 ratio were analyzed and three different classes of chlorogenic acids could be unequivocally detected with comparison of authentic samples retention times (**Figure 4.2**). All three isomers *trans* 3-, 4- and 5-CQA and the three *trans* 3-, 4- and 5-*p*CoQA isomers were clearly identified in all collection times while the only *trans* 3-FQA isomer was detected. 3- and 5-CQA as well as 3- and 4-*p*CoQA have already been identified by Pereira et. al[10] while Santos et al. in 2013 identified 4-caffeoylquinic acid.[11]

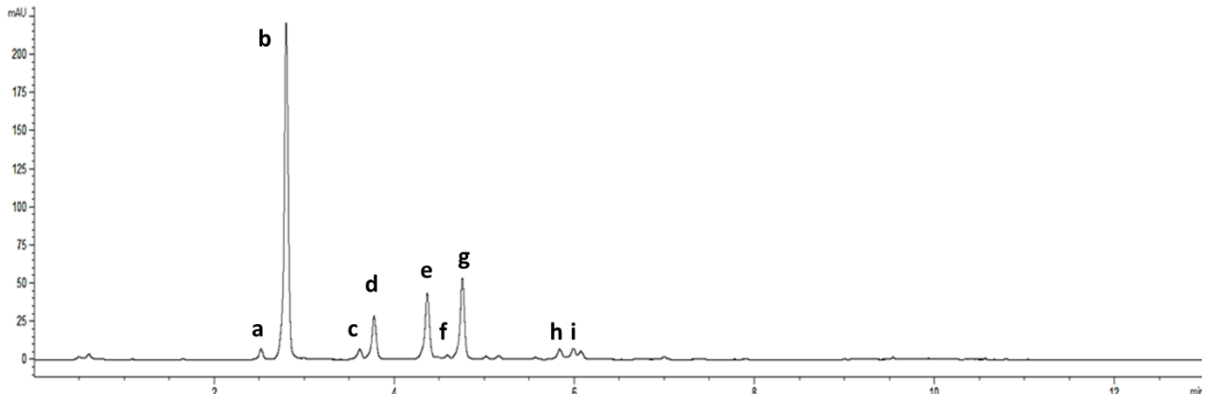

Figure 4.2 UHPLC of 1:10 diluted samples. hydroxycinnamic acid derivatives identified in walnut leaves. Detection at λ= 324nm: *cis* 3-CQA (peak **a**); *trans* 3-CQA (peak **b**); *cis* 3-*p*CoQA (peak **c**); *trans* 3-*p*CoQA (peak **d**), *trans* 5-CQA (peak **e**); *trans* 3-FQA (peak **f**); *trans* 4-CQA (peak **g**); *trans* 5-*p*CoQA (peak **h**); *trans* 4-*p*CoQA (peak **i**)

4.4 Identification and Characterization of isomers *cis*- CGAS

According to the literature, *cis* isomers show the same fragmentation pattern of the corresponding *trans* isomers.[12] The presence of possible *cis* isomers was confirmed by analyses of the specific fragmentation of the UV treated standard solutions: *trans* 3-CQA and *trans* 5-CQA (m/z 353.6) has the same fragmentation pattern[13,14] as well as the corresponding *cis* isomers, giving a base peak at m/z 191.5 while *trans* and *cis* 4-CQA (m/z 353.6) give a base peak at m/z 173.5. Fragmentation of pseudomolecular ion $[M-H]^-$ at m/z 337.1 were found for *p*CoQAs, yielding a base peak at m/z 163 for *trans* and *cis* 3*p*CoQA, 174 m/z for *trans* and *cis* 4*p*CoQA and 191 m/z for *trans* and *cis* 5*p*CoQA (**Figure 4.3**).[15] UHPLC analyses clearly identified *cis* 3-CQA and *cis* 3-*p*CoQA in all collection times for the first time while the presence of *cis* 4- and 5-CQA and *cis* 4- and 5-*p*CoQA was detected via LC-MS/MS method but not fully confirmed via UHPLC, probably due to low concentrations of these regioisomers.

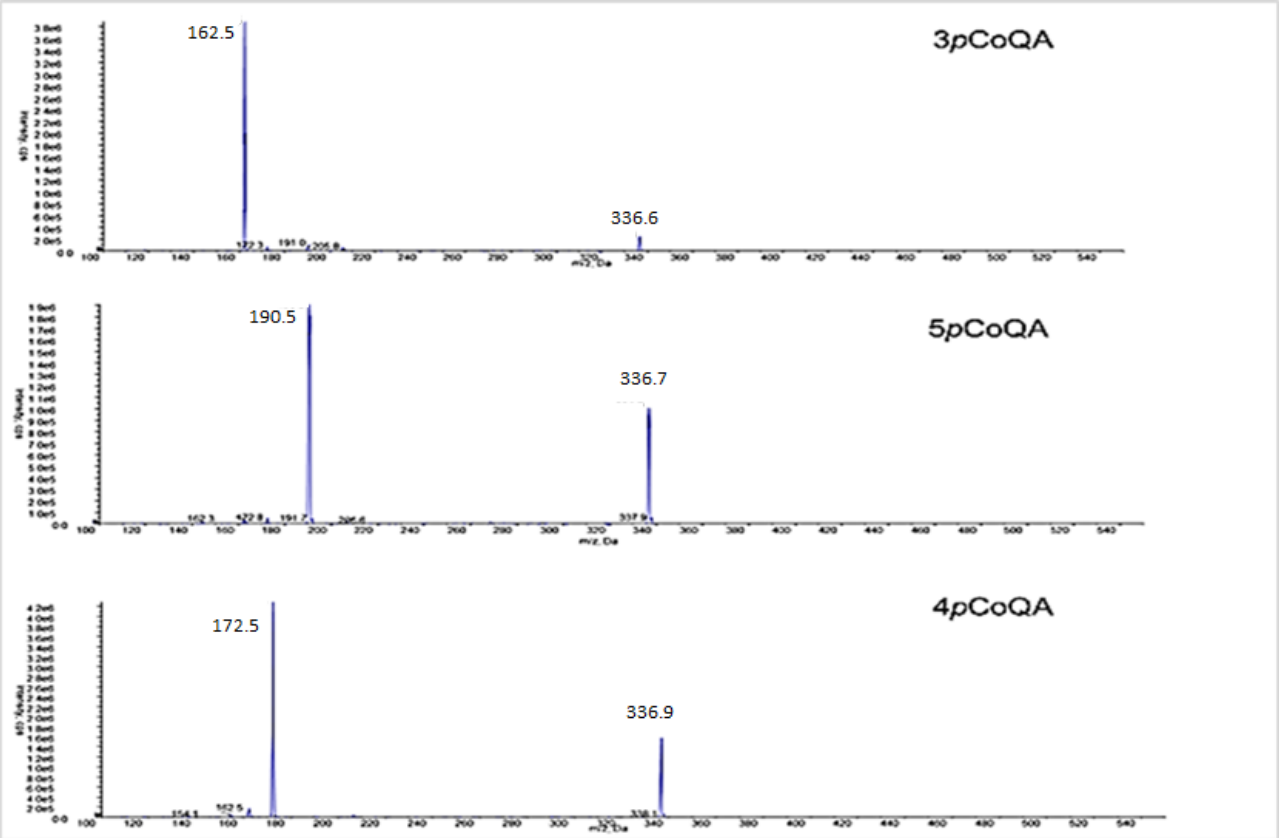

Figure. 4.3. MS^2 spectra for *p*CoQAs

Therefore, in order to confirm the presence of *cis* isomers as well as other class of the CGAs, more concentrated samples were prepared and the analyses were performed on the aqueous extracts both without any dilution and in 1:2 diluted solutions and the results are reported in **Figure 4.4**

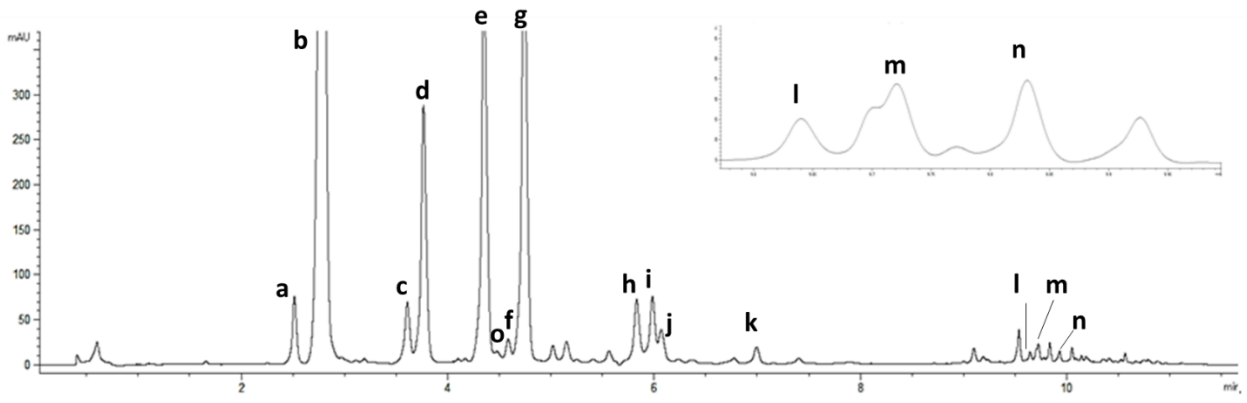

Figure 4.4. UHPLC of hydroxycinnamic acid derivatives identified in walnut leaves. Detection at λ= 324nm. *cis* 3-CQA (peak **a**); *trans* 3-CQA (peak **b**); *cis* 3-*p*CoQA (peak **c**); *trans* 3-*p*CoQA (peak **d**), *trans* 5-CQA (peak **e**); *trans* 3-FQA (peak **f**); *trans* 4-CQA (peak **g**); *trans* 5-*p*CoQA (peak **h**); *trans* 4-*p*CoQA (peak **i**), *pCoQA* (peak **j), FA (**peak **k),** 3,4-diCQA (peak **l**); 3,5-diCQA (peak **m**); 4,5-diCQA (peak **n), CA** (peak **o**).

4.5 Analyses of Seasonal Variations

The concentrations of all identified phenolic compounds, in the different periods, are reported in Table 4.3. All data reported are expressed as mg/g dry weight

Table 4.3. Phenolic compound concentrations of walnut leaves[a] (mg/g dry weight)

Nr.	Comp.	April	May	July	September
1	CA	0.28 (0.00)	0.45 (0.00)	0.38 (0.02)	0.22 (0.00)
***c*-1a**	*cis* 3-CQA	1.27 (0.02)	1.40 (0.13)	1.29 (0.02)	0.63 (0.00)
***t*-1a**	*trans* 3-CQA	35.85 (0.87)	34.02 (1.29)	25.13 (0.46)	12.57 (0.54)
***c*-1b**	*cis* 4-CQA	<LOD	<LOD	<LOD	<LOD
***t*-1b**	*trans* 4-CQA	9.34 (0.01)	5.65 (0.02)	4.40 (0.14)	2.55 (0.01)
***c*-1c**	*cis* 5-CQA	<LOD	<LOD	<LOD	<LOD
***t*-1c**	*trans* 5-CQA	7.98 (0.04)	4.29 (0.10)	2.46 (0.07)	1.56 (0.00)
2	*p*CoA	0.22 (0.00)	0.35 (0.08)	0.19 (0.00)	0.18 (0.00)
***c*-2a**	*cis* 3-*p*CoQA	1.42 (0.00)	2.18 (0.40)	1.22 (0.03)	0.96 (0.00)
***t*-2a**	*trans* 3-*p*CoQA	7.15 (0.01)	8.30 (0.00)	4.24 (0.10)	2.18 (0.01)
***c*-2b**	*cis* 4-*p*CoQA	<LOD	<LOD	<LOD	<LOD
***t*-2b**	*trans* 4-*p*CoQA	1.58 (0.01)	1.27 (0.06)	0.99 (0.02)	0.84 (0.00)
***c*-2c**	*cis* 5-*p*CoQA	<LOD	<LOD	<LOD	<LOD
***t*-2c**	*trans*-5*p*CoQA	1.74 (0.00)	1.19 (0.00)	0.56 (0.01)	0.34 (0.00)
3	FA	0.29 (0.01)	0.33 (0.01)	0.46 (0.02)	0.27
***t*-3a**	*trans* 3-FQA	0.46 (0.00)	0.45 (0.01)	0.26 (0.00)	0.22 (0.00)
***t*-3b**	*trans* 4-FQA	<LOD	<LOD	<LOD	<LOD
***t*-3c**	*trans* 5-FQA	<LOD	<LOD	<LOD	<LOD
4	SA	<LOD	<LOD	<LOD	<LOD
5	3,4-diCQA	0.31 (0.01)	0.20 (0.01)	0.27 (0.01)	0.33 (0.00)
6	3,5-diCQA	0.44 (0.02)	0.18 (0.00)	0.30 (0.01)	0.33 (0.00)
7	4,5-diCQA	0.27 (0.03)	0.18 (0.01)	0.31 (0.03)	0.22 (0.01)
	Total[b]	68.59 (1.02)	60.44 (2.13)	42.47 (0.93)	23.40 (0.59)

[a]Values are expressed as mean (standard deviation) of duplicate analyses. [b]Total: sum of all identified compound.

In the analyses of seasonal variations, in aqueous diluted samples in a 1:10 ratio, we observed that the most concentrated chlorogenic acid is the *trans* 3-CQA with a higher concentration in April (35.85 mg/g, table 4.5).All *trans* isomers at position 3 showed a considerable decrease from July to September; however, both *trans* 3-CQA and *trans* 3-FQA showed a similar behavior with a constant concentration from April to May, while, *trans* 3-*p*-CoQA showed a slight increase of the concentration from April to May (from 7.15 mg/g to 8.30 mg/g).

In general, it was observed that concentrations of *trans* isomers achieved values of half of the initial concentration at the end of Summer. For *cis* isomers a different behavior was observed, since *cis* 3-caffeoylquinic did not show significant variations from April (1.27 mg/g) to July (1.29 mg/g) and then a

decrease of approximately half of the concentration until September, while *cis* 3-*p*CoQA showed the highest concentration in May (2.18 mg/g) to continue with a gradual decrease until September.

As can be observed in **Figure 4.5** The *trans/cis* ratio decreases from April to September which is in accordance with what already observed by Clifford et al. in 2008 [12] and Karaköse in 2015 [16] indicating that during summer a photochemical *trans–cis* isomerization under ultraviolet (UV) irradiation is occurring. Furthermore, it is evident that *trans* 3-*p*CoQA is more easily transformed by UV irradiation in the corresponding *cis* isomer with respect to 3-CQA as observed in 1967 by Kahnt for the corresponding hydroxycinnamic acids. [17]

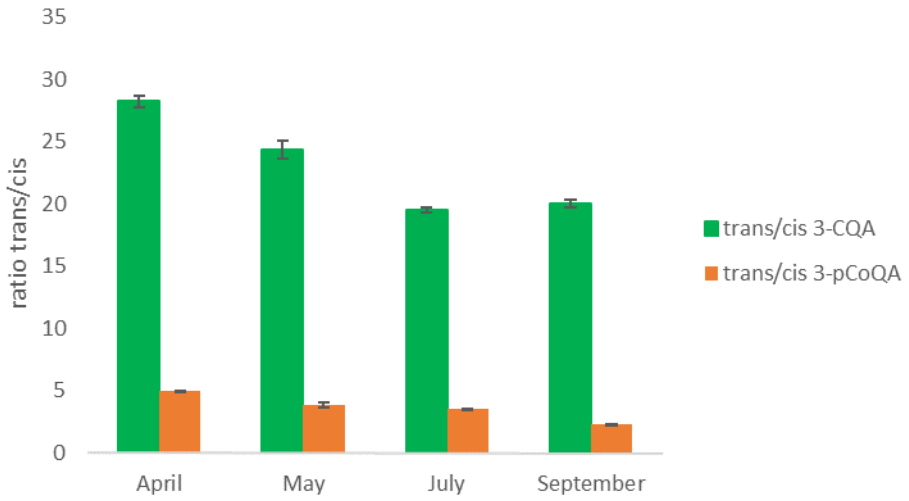

Figure 4.5. *trans/cis* ratios of isomers at position 3**.**

The highest concentration values of isomers at position 5 (*trans* 5-CQA and *trans* 5-*p*CoQA) were found in April (7.98 mg/g and 1.74 mg/g, respectively) and then a gradual decrease was observed until September. *Trans* 4-CQA also showed a constant decrease during summer time (from 9.34 mg/g in April to 2.55 mg/g in September) while *trans* 4-*p*CoQA showed a slight decrease from April (1.58 mg/g) to May (1.27 mg/g) and then it remained quite constant (Table 4.5).

In the aqueous extracts, on 1:2 diluted solutions, minor constituents were found, in these samples three different dicaffeoylquinic acids (3,4-diCQA, 3,5-diCQA and 4,5-diCQA) as well as three hydroxycinnamic acids (CA, *p*CoA and FA) were further identified). *p*CoA was previously identified by Pereira et al.[10] while as far as we know this is the first time that dicaffeoylquinic acids have been detected and quantified in this species and could contribute in the characterization of the phenolic profile of this plant and seasonal variation in the leaf tissue.

A total of fifteen hydroxycinnamic acid derivatives were quantified and their total quantification was ranging between 68.59 mg/g and 23.49 mg/g (**Figure 4.6**). Results from total concentrations of each collection time showed that there are not significant changes during the vegetative growth (between April and May) but after this period it was detected an important decrease in the total concentration, confirming results already reported in the literature where, for most of the chlorogenic acids, variations were studied from April to August and It was also found a decrease of their content during this period. [218]

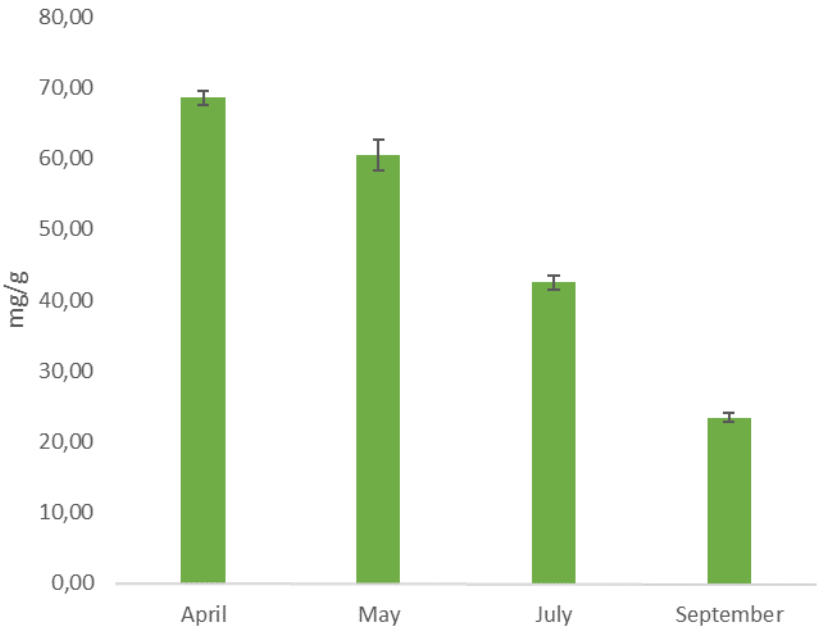

Figure 4.6. Total concentration (mg/g, dry weight) of hydroxycinnamic acid derivatives identified in walnut leaves, between April and September. Error bars are on the top of each column.

Regarding the seasonal analyses, diCQAs were present in all collection times but in significant smaller amount with respect to the simple CGAs. Caffeic acid was present in its highest concentration in May (0.45 mg/g) while *p*CoA and FA had their higher concentrations in May and July respectively (0.35 mg/g and 0.46 mg/g respectively). On the other hand, the lower concentration of diCGAs was observed in May with a total of 0.56 mg/g. Apparently, it seems the concentrations of these hydroxycinnamic acids is lees affected by the seasonal changes.

Caffeoylquinic acids represent the main compounds, with the highest concentration in April (54.43 mg/g) (**Figure 4.7**). In particular, it was found that *trans* 3-CQA was the major compound while *p*-coumaric acid was the minor one for each collection time. It may be noted that, when a consistent comparison is performed, the total amount of quantified phenolic acid derivatives is higher than the one previously reported in the literature due to differences in both extraction and quantification methods.[3,10,15,18] In particular, by comparing the present data (May month) expressed as the sum of 3- and 5-caffeoylquinic acids with those

reported by Pereira et al. 2007 [10] (sampling 31st May; average of 6 different cultivars), an increase of about 47% can be calculated. However, by comparing the sum of 3- and 4-*p*-coumaroylquinic acids with data reported in the same work, the increase is still evident but remarkably lower (about 4.5%). The variation in phenolic acid derivatives content in walnut leaves could be partially due also to the natural climatic differences that occur over the years (22) and to a defense response to stressful environment. [19]

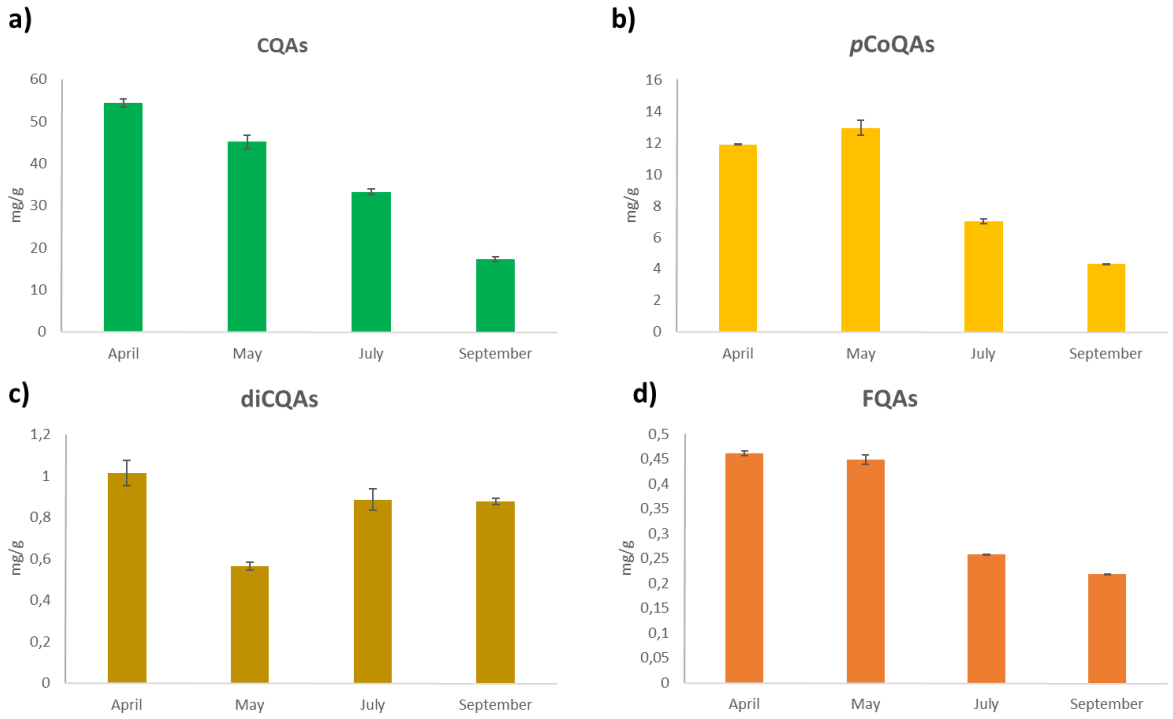

Figure 4.7. Concentrations of the different chlorogenic acids (mg/g, dry weight) identified in walnut leaves between April and September i.e. caffeoylquinic acids (CQAs), *p*-coumaroylquinic acids (*p*CoQAs), dicaffeoylquinic acids (diCQAs) and feruloylquinic acid (FQAs). Error bars are on the top of each column.

On the other hand, in **Figure 4.8** the relative percentage of the different hydroxycinnamic acid derivatives with respect to the sum of the all hydroxycinnamic acid derivatives quantified is reported; it can be noticed that CQAs represent around 77% with higher concentration in April and July and *p*CoQAs around 18% with a higher peak in May, while diCQAs and cinnamic acids showed the highest percentages in September (3.74% and 2.87% respectively).

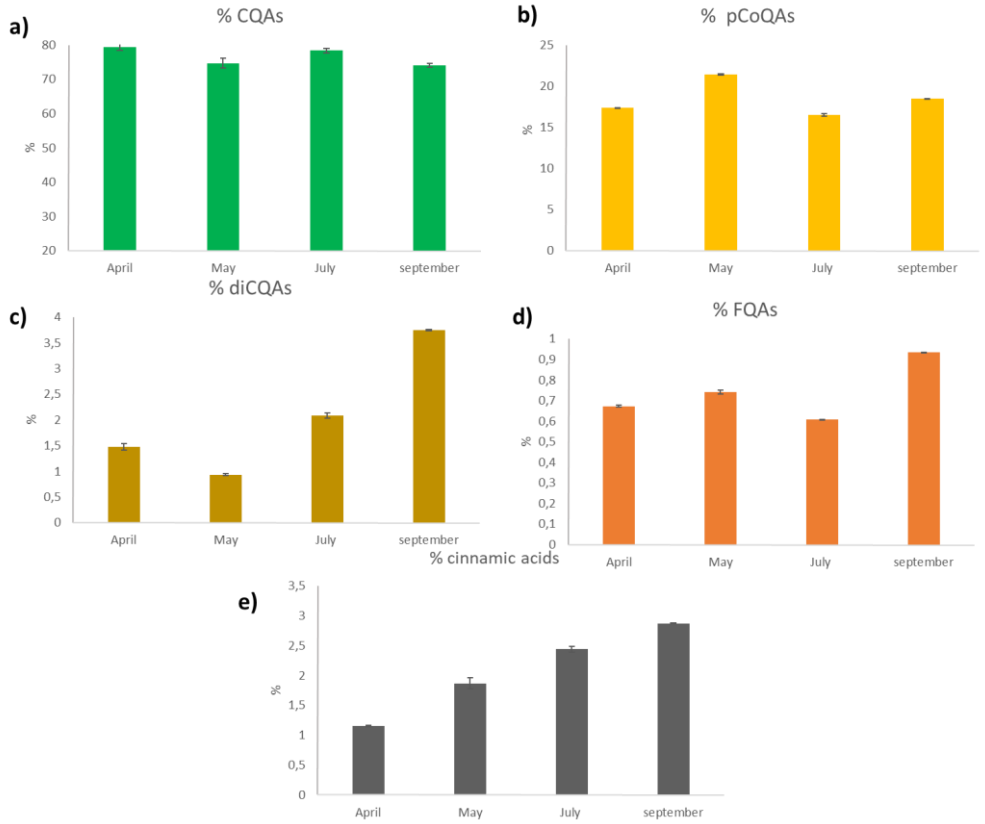

Figure 4.8. Percentages of the different hydroxycinnamic acid derivatives with respect to the quantified phenolic acid derivatives in walnut leaves, between April and September. **a)** % of caffeoylquinic acids (CQAs), **b)** % of *p*-coumaroylquinic acids (pCoQAs), **c)** % of dicaffeoylquinic acids (diCQAs), **d)** % of feruloylquinic acid (FQAs), **e)** % of cinnamic acids.

[1] Regueiro, J.; Sánchez-González, C.; Vallverdú-Queralt, A.; Simal-Gándara, J.; Lamuela-Raventós, R.; Izquierdo-Pulido, M. Comprehensive identification of walnut polyphenols by liquid chromatography coupled to linear ion trap-Orbitrap mass spectrometry. *Food Chem.*, **2014**, 152, 340-348.

[2] Solar, A.; Colarič, M.; Usenik, V.; Stampar, F. Seasonal variations of selected flavonoids, phenolic acids and quinones in annual shoots of common walnut (*Juglans regia* L.). *Plant Science*, **2006,** 170, 453-461.

[3] Nour, V.; Trandafir, I.; Cosmulescu, S. HPLC determination of phenolic acids, flavonoids and juglone in walnut leaves. *J. Chrom. Science*, **2013**, 51, 883-890.

[4] Kunhert, N.; Karaköse, H.; Jaiswal, R. Analysis of chlorogenic acids and other hydroxycinnamates in food, plants and pharmacokinetic studies; In Handbook of analysis of active compounds in functional foods. Nollet, L. M. L.; Toldra, F., Eds. CRC Press, **2012**, pp 461-512.

[5] Kusilic-Bilusic, T.; Katalinic, V.; Dragovic-Uzelac, V.; Ljubenkov, I.; Krisko, A.; Dejanovic, B.; Jukic, M.; Politeo, O.; Pifat, G.; Milos, M. Antioxidant and acetylcholinesterase inhibiting activity of several aqueous tea infusions in vitro. *Food Techn. Biotechn.*, **2008**, 46, 368-375.

[6] Gutiérrez Ortiz, A. L.; Colomban, S.; Berti, F.; Forzato, C.; Navarini, L. LC-MS identification of *cis*-isomers of caffeoylquinic acids and *p*-coumaroylquinic acids; poster presented at 5th MS Food Day, October 11-13, **2017**, Bologna; ISBN: 9788890738838.

[7] Dokli, I.; Navarini, L.; Hamersak, Z. Synthesis of 3,4-, and 5-*O*-feruloylquinic acids. *Tetrahedron: Asymmetry*, **2013**, 24, 785-790.

[8] Gutiérrez Ortiz, A. L.; Berti, F.; Navarini, L.; Monteiro, A.; Resmini, M.; Forzato, C. Synthesis of *p*-coumaroylquinic acids and analysis of their interconversion. *Tetrahedron: Asymmetry*, **2017**, 28, 419-427.

[9] Clifford, M. N.; Madala, N. E. Surrogate Standards: A cost-effective strategy for identification of phytochemicals. *J. Agric. Food Chemistry*, **2017**, 65, 3589-3590.
[10] Pereira, J. A.; Oliveira, I.; Sousa, A.; Valentão, P., Andrade, P. B.; Ferreira, I. C. F. R.; Ferreres, F.; Bento, A.; Seabra, R.; Estevinho, L.; Walnut (*Juglans regia* L.) leaves: phenolic compounds, antibacterial activity and antioxidant potential of different cultivars. *Food Chem. Toxic.*, **2007**, 45, 2287-2295.
[11] Santos, A.; Barros, L.; Calhelha, R. C.; Dueñas, M.; Carvalho, M.; Buelga, S. C.; Ferreira, I.; Leaves and decoction of *Junglans regia* L.: different performances regarding bioactive compounds in vitro antioxidant and antitumor effects. *Industrial Crops and Product*, **2013**, 51, 430-436.
[12] Clifford, N.; Kirkpatrick, J.; Kuhnert, N.; Roozendaal, H. LC-MS^n analysis of the *cis* isomers of chlorogenic acids. *Food Chem.*, **2008**, 106, 379-385.
[13] Clifford, M. N.; Johnston, K. L.; Knight, S.; Kuhnert, N. Hierarchical scheme for LC-MSn identification of chlorogenic acids. *J. Agric. Food Chem.,* **2003**, 51, 2900-11.
[14] Ncube, N.; Mhlongo, M.; Piater, L. A.; Steenkamp, P. A.; Dubery, I. A; Madala, N. E. Analyses of chlorogenic acids and related cinnamic acid derivates from *Nicotiana tabacum* tissues with the aid of UPLC-QTOF-MS/MS based on the in-source collision-induced dissociation method. *Chemistry Central Journal*, **2014**, 8:66, 1-10.
[15] Amaral, J. S.; Valentão, P.; Andrade, P. B.; Martins, R. C.; Seabra, R. M. Do cultivar, geographical location and crop season influence phenolic profile of walnut leaves.?. *Molecules*, **2008**, 13, 1321-1332.
[16] Karaköse, H.; Jaiswal, R.; Deshpande, S.; Kuhnert, N.; Investigation of the Photochemical Changes of Chlorogenic Acids Induced by Ultraviolet Light in Model Systems and in Agricultural Practice with Stevia rebaudiana Cultivation as an Example*, J. Agric. Food Chem*,**2015**, 63, 3338−3347.
[17] Kahnt, G.; Trans-cis equilibrium of hydroxycinnamic acids during irradiation of acqueous solutions at different pH. *Phytochemistry*, **1967**, 6, 755-758.
[18] Amaral, J. S.; Seabra, R. M.; Andrade, P. B.; Valentão, P; Pereira, J. A.; Ferreres, F. Phenolic profile in the quality control of walnut (Juglans regia L.) leaves.; *Food Chem*., **2004**, 88, 373-379
[19] Cosmulescu, S.; Trandafir, I.; Nour, V. Seasonal variation of the main individual phenolics and juglone in walnut (Juglans regia) leaves*, Pharm. Biol.,* **2014**, 52, 575-80.

RESULTS AND DISCUSSION

Chapter 5. Study of the Concentration of *p*CoQAs and CGAs profile in Coffee

5.1 Chlorogenic acids (CGAs) in coffee

As described before, green coffee beans are particularly rich of CGAs, especially of caffeoylquinic acids (CQAs), where 5-CQA is the most abundant one, accounting for 56-62% of the total CGAs content, but, although in lower amount, also dicaffeoylquinic acids (diCQAs), feruloylquinic acids (FQAs) and *p*-coumaroylquinic acids (*p*CoQAs) are present in green coffee beans.[1] Due to their potential beneficial effects, in recent years, pharmaceutical and nutrition industries have been focused special attention to the determination of CGAs content in green coffee extracts.

In literature there are several reports about the CGAs content and distribution in coffee, but these are mostly focused on the two most important species, from a commercial point of view, Arabica and Robusta.[2] Regarding other wild species, the CGAs profile has been reported only for a small number, including only CQAs, diCQAs and in few cases FQAs[3,4,5] while *p*-CoQAs profile has been determined only in *C. arabica* and *C. canephora* where all three isomers have been already quantified.[6] CGAs content depends on agriculture practices, geographical origin and soil composition, but genetic factors[1] are also very important, so the determination of the complete profile of CGAs in wild coffee species might provide useful data to establish a taxonomic classification based on the chemical patterns. This could contribute to open new worldwide trade markets as well as be useful for the pharmaceutical industry. As mentioned before, *p*CoQAs are the less studied since they are the less abundant ones in coffee and, due to the lack of disposable commercial standards [7] and to the complexity of the experimental procedures for the separation and quantification of chlorogenic acids in coffee, which comprise the extraction either with water or organic solvents, their identification is basically made by means of HPLC/MS analyses. [8,9,10,11] Although the HPLC/MS is generally accepted and it is considered a reliable technique, recent advances in UHPLC methods have made possible to develop reliable, fast and accurate methods for CGAs identification and quantification, without the need of a MS detector but using an UV detector for which it is useful to have authentic standards.[11]

Therefore, the previous synthetized feruloylquinic acids (FQAs)[12] and *p*-coumaroylquinic acids (*p*CoQAs)[7] have been used in this study to qualitative identify them in coffee while quantification was made using 5-CQA as the standard and expressing all results as 5-CQA equivalent, in order to have a reference of high purity and to avoid the possibility of artefacts during sample preparation. [13] This part of the project was carried out at the laboratory Aromalab of Illycaffè, where a UHPLC-DAD method was used for the qualitative and quantitative identification of the different CGAs in green coffee samples of *C. arabica* and *C. canephora* from different geographical origins and in eight wild species of the Eucoffea section: *C. liberica,* arabusta coffee (*C. arabica L.* x *C. canephora Pierre*), *C. eugenioides, C. sessiliflora, C. congensis, C. pseudozanguebarie, C. racemosa* and *C. brevipes*. It is important to mention that validation of the UHPLC-DAD method is not described in this project since an improvement and optimization of an analytical method already used by Illycaffè was performed and our results were fully in agreement with those previously reported by the

company .Moreover, since during roasting the CGAs content can vary due to the chemical transformations, which contribute to the bitterness of the final beverage,[14,15] the effect of the roasting conditions on the concentration of CGAs, specially on the concentrations of *p*CoQAs was also evaluated in the three main coffee species from the commercial and economical point of view.

5.2 Analyses of Chlorogenic Acids (CGAs) and hydroxycinnamic acids

Analyses were carried out using the following standards: 3-caffeoylquinic acid (3-CQA), 4-caffeoylquinic acid (4-CQA), 5-caffeoylquinic acid (5-CQA), 3-feruloylquinic acid (3-FQA), 4-feruloylquinic acid (4-FQA), 5-feruloylquinic acid (5-FQA), 3,4- dicaffeoylquinic acid (3,4-diCQA), 3,5-dicaffeoylquinic acid (3,5-diCQA), 4,5-dicaffeoylquinic acid (4,5-diCQA), 1-*p*-coumaroylquinic acid (1-*p*CoQA), 3-*p*-coumaroylquinic acid (3-*p*CoQA), 4-*p*-coumaroylquinic acid (4-*p*CoQA), 5-*p*-coumaroylquinic acid (5-*p*CoQA), caffeic acid (CA), *p*-coumaric acid (*p*-CoA), sinapic acid (SA) and ferulic acid (FA) (**Figure 5.1**). The total content of CGAs is expressed as the sum of all CGAs standard compounds used, i.e. the three isomers of CQAs, the three isomers of FQAs, the three isomers of *p*CoQAs and three diCQAs.

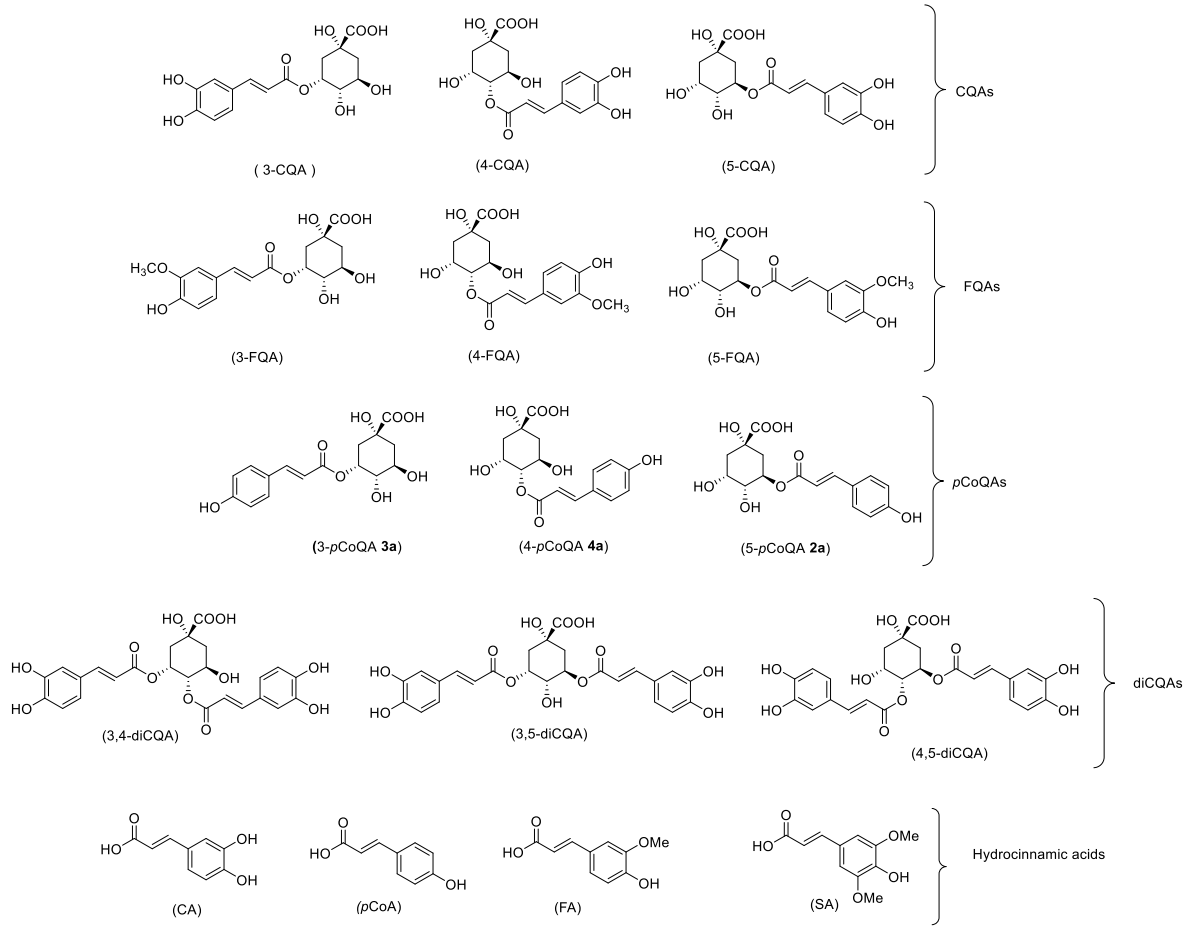

Figure 5.1. Chemical structures of the hydroxycinnamic acid derivatives identified in coffee beans. *p*CoQAs: 3-*p*-coumaroylquinic (3-*p*CoQA **3a**); 4-*p*-coumaroylquinic acid (4-*p*CoQA **4a**); 5-*p*-coumaroylquinic acid (5-*p*CoQA ***2a***); CQAs: 3-caffeoylquinic acid (3-CQA) ; 4-caffeoylquinic acid (4-CQA); 5-caffeoylquinic acid (5-CQA**)**; FQAs: 3-feruloylquinic acid (3-FQA); 4-feruloylquinic acid (4-FQA); 5-feruloylquinic acid (5-FQA) ; diCQAs: 3,4-dicaffeoylquinic acid (3,4-diCQA) ; 3,5-dicaffeoylquinic acid (3,5-diCQA) ; 4,5-dicaffeoylquinic acid (4,5-diCQA) **;** hydrocinnamic acids: *p*-coumaric acid (*p*-CoA); caffeic acid (CA); ferulic acid (FA); sinapic acid (SA).

Qualitatively identification of CGAs was achieved by comparison of specific retention times of standard solutions and by spiking samples with small amounts of each respective standard. Fragmentation of all pseudomolecular ions $[M-H]^-$ were in accordance with those reported in the literature[16]: m/z 353.6 were found for CQAs, 3-CQA and 5-CQA which showed a base peak at m/z 191, while 4-CQA showed the corresponding base peak at m/z 173. Fragmentations of pseudomolecular ion $[M-H]^-$ at m/z 337.1 were found for *p*CoQAs, yielding a base peak at m/z 163 for 3-*p*CoQA, 174 for 4-*p*CoQA and 191 for 5-*p*CoQA. FQAs with pseudomolecular ion $[M-H]^-$ at m/z 367 showed a base peak at m/z 193, 173 and 191 for 3-FQA, 4-FQA and 5-FQA, respectively. Pseudomolecular ion $[M-H]^-$ at m/z 515 corresponds to diCQAs, fragmentation of these ions yielded a characteristic m/z at 353 for all three isomers 3,4-diCQA, 3,5-diCQA and 4,5-diCQA.

Quantitative determination was performed by UHPLC based on the diode array value for peak areas, using calibration curve of 5-CQA. Furthermore, since some samples consisted of a few quantity of seeds, a 10% moisture content was assumed as have been done before by others authors.[17] Calibration curve of 5-CQA showed a good response linearity with a coefficient of correlation (r^2) of 0.999. Limit of quantification (LOQ) and limit of detection (LOD) were calculated as 3 times lower concentration of analyte on signal to noise ratio (LOD) or 10 times lowest concentration of analyte on signal to noise ratio (LOQ) resulting 0.88 µg/mL for LOQ and 0.26 µg/mL for LOD.

5.3 Total CGA content in Coffee Species

The distribution of the different monoesters, the dicaffeoyl esters as well as the total CGAs contents for each sample expressed in mg/g on dry matter bases are reported in table 5.1

Table 5.1 – Distribution of the different chlorogenic acids expressed as mg/g (dmb)

Sample	mg/g	CQAs (std)	FQAs (std)	*p*CoQAs (std)	diCQAs (std)	Total CGAs (std)
1	*C. arabica* Brazil	46.15 (0.14)	3.81 (0.09)	0.73 (0.01)	3.31 (0.05)	54.00 (0.28)

2	*C. arabica* Colombia	58.06 (4.81)	4.32 (0.31)	0.63 (0.00)	2.61 (0.39)	65.62 (5.51)
3	*C. arabica* Etiopia	47.58 (3.61)	2.69 (0.07)	0.55 (0.01)	1.07 (0.10)	51.92 (3.79)
4	*C. arabica* Etiopia-2	51.80 (0.19)	3.34 (0.16)	0.56 (0.01)	1.16 (0.12)	56.86 (0.47)
5	*C. arabica* Honduras	50.18 (0.66)	4.11 (0.56)	0.61 (0.01)	3.37 (0.37)	58.28 (1.61)
6	*C. arabica* India	52.82 (3.22)	4.53 (0.20)	0.70 (0.02)	2.87 (0.37)	60.91 (3.80)
7	*C. arabica* Yemen	57.60 (1.07)	5.51 (0.20)	0.86 (0.00)	0.80 (0.04)	64.77 (1.32)
8	*C. arabica* Yemen-2	56.52 (1.54)	4.14 (0.16)	0.73 (0.01)	1.95 (0.12)	63.35 (1.84)
9	*C. arabica var. laurina*	45.44 (4.19)	2.39 (0.09)	0.51 (0.00)	13.48 (0.63)	61.82 (4.92)
10	*C. canephora* Vietnam	41.70 (1.85)	7.69 (0.13)	0.37 (0.00)	8.20 (0.14)	57.97 (2.13)
11	*C. canephora* India	65.07 (3.40)	12.71 (0.40)	0.43 (0.00)	5.67 (0.26)	83.95 (4.07)
12	*C. liberica* -1	42.57 (1.36)	7.17 (0.09)	0.26 (0.01)	2.02 (0.02)	52.02 (1.47)
13	*C. liberica* -2	51.74 (2.01)	9.60 (0.47)	0.30 (0.01)	1.66 (0.01)	63.29 (2.49)
14	*C. liberica* -3	39.63 (0.88)	5.57 (0.08)	0.64 (0.00)	1.26 (0.02)	47.09 (0.98)
15	*C. liberica* -4	40.70 (2.16)	3.23 (0.03)	0.93 (0.00)	3.05 (0.04)	47.91 (2.24)
16	*C. liberica* -5	52.16 (5.47)	2.27 (0.17)	0.80 (0.01)	4.56 (0.13)	59.78 (5.77)
17	*C. liberica* -6	41,43 (0,23)	2.60 (0.04)	0.68 (0.00)	1.94 (0.33)	46.64 (0.61)
18	*C. arabica L. x C. canephora Pierre*	40.97 (2.83)	5.42 (0.13)	1.03 (0.01)	8.99 (0.30)	56.41 (3.27)
19	*C. arabica L. x C. canephora Pierre*	42.00 (0.94)	5.98 (0.10)	1.10 (0.00)	8.38 (0.15)	57.45 (1.19)
20	*C. eugenioides*	25.64 (0.02)	2.14 (0.00)	0.19 (0.00)	1.41 (0.00)	29.54 (0.06)
21	*C. eugenioides*-2	29.49 (2.85)	1.91 (0.02)	0.29 (0.00)	0.87 (0.02)	32.56 (2.89)
22	*C. sessiliflora*	41.77 (2.18)	1.37 (0.02)	2.12 (0.04)	0.12 (0.00)	45.38 (2.25)
23	*C. sessiliflora*-2	47.98 (1.46)	1.36 (0.02)	2.24 (0.04)	0.11 (0.00)	51.69 (1.52)
24	*C. congensis*	43.68 (0.70)	15.74 (0.15)	0.53 (0.01)	5.43 (0.89)	66.40 (1.81)
25	*C. pseudozanguebarie*	1.81 (0.03)	0.14 (0.00)	0.12 (0.00)	0.05 (0.00)	2.13 (0.03)
26	*C. racemosa*	60.31 (4.14)	0.67 (0.02)	0.37 (0.00)	0.79 (0.03)	62.14 (4.20)

27	*C. brevipes*	43.16 (3.03)	13.04 (0.31)	0.25 (0.00)	14.06 (1.81)	70.50 (5.15)

A total of seventeen compounds were qualitative identified from the aqueous extracts of green coffee samples and among these, twelve CGAs were clearly quantified, corresponding to all three isomers of the monoesters at positions 3,4 and 5 of caffeoylquinic acids (CQAs), *p*-coumaroylquinic acids (*p*CoQAs), feruloyquinic acids (FQAs) and dicaffeoylquinic acids (diCQAs). Four hydroxycinnamic acids (caffeic acid, *p*-coumaric acid, ferulic acid and sinapic acid) were only qualitatively identified because these were present as traces below the limit of quantification in all coffee species. We also tried to identify 1-*p*-coumaroylquinic acid (1-*p*CoQA **1a**) since we synthetized also this isomer but it was not found in any of the analyzed samples confirming that the ester at C-1 is not present in green coffee beans.

CGAs content is greatly dependent upon the coffee species, in *C. arabica* samples concentrations were between 52-66 mg/g dmb, while a higher content was found in *C. canephora* (58-84 mg/g dmb), in agreement with values extensively reported for the same species,[1,14,18,,19,20,21,22,23] confirming a significant difference between these two main species. As can be observed in **Figure 5.2a,** among all eight *C. arabica* samples, coffee from Colombia and Yemen showed higher concentrations (66 and 65mg/g dmb, respectively) than Brazil, Ethiopia, India and Honduras coffees, while coffee sample of *C. arabica* cv. blc Guatemala showed a total concentration of 62 mg/g, which is in accordance with data already reported in the literature for this variety.[5] Among the two *C. canephora* samples, India coffee showed a higher concentration (84 mg/g dmb) than Vietnam coffee (56 mg/g dmb). As can be noticed, a wide range was found in these two samples of *C. canephora*, while, in general, samples of *C. arabica* showed more similar concentrations between each other. This aspect has already been associated in literature with the low genetic diversity in Arabica, making this species more susceptible to aggression by external factors; furthermore, these variabilities inside the same specie depends on the geographical origin as well as on the agricultural and technological practices as has been extensively reported in the literature.[19,22,23] However, it is important to take into consideration that our small number of samples of *C. arabica* and *C. canephora* do not allow to stablish a defined pattern related to the geographical origin but gives information of how much the CGA content can vary within the species.

We observed that beside *C. canephora* (58 – 84 mg/g dmb), the highest concentrations 71 mg/g and 66 mg/g dmb belong to *C. brevipes and C. congensis,* respectively (**Figure 5.2b**). The same observation was done by Clifford et al.[5] who also reported similar total CGAs content for these three species and a lower concentration for *C. brevipes* than Campa et al.[3] Samples of *C. liberica* showed a lower content of CGAs than *C. arabica* while *C. canephora* had a wide range of total CGAs concentrations from 47-64 mg/g dmb, as previously described above, this could be due to the different geographic origins of the same specie; however, maximum concentrations found for *C. liberica* are slightly lower than the literature data.[3,5,17]

On the other hand, as far as we know this is the first time that the CGA content for arabusta coffee is reported. These samples of arabusta (*C. arabica L. x C. canephora Pierre*) showed a total CGAs content lower than *C.*

arabica and *C. canephora* (57 mg/g dmb), these concentrations are in agreement with data reported by Gimase et al.[24] while Clifford et al.[5] reported higher and similar concentration to *C. arabica* and *C. canephora* for this specie. Data found for *C. racemosa* (62 mg/g dmb) are in agreement with the literature, while our total content of *C. sissiliflora* is slightly lower than the reported values.[3,5,17] A discrepancy was noted for *C. eugenoides* (30-33 mg/g dmb) for which we have registered significant lower concentrations than Clifford et al.[5] and Campa et al.[3] Moreover, *C. pseoudozanguebarie* showed the lowest CGAs content as have been extensively reported[3,5,17,25] (Table 5.2).

In our study it was possible to identify three groups by means of their CGAs content, the first one comprises those species with high CGA content, more than 59mg/g dmb (*C. canephora*, *C. arabica*, *C. congensis, C. racemosa* and C. *brevipes*), a second group that includes species with a relative intermediate CGA content (*C. liberica,* C. *eugenioides,* arabusta *coffee (C. arabica L. x C. canephora Pierre*) and *C. sissiliflora* and finally the last group which includes species with the lower CGA content (*C. pseoudozanguebarie*) (**Figure 5.2.b**)

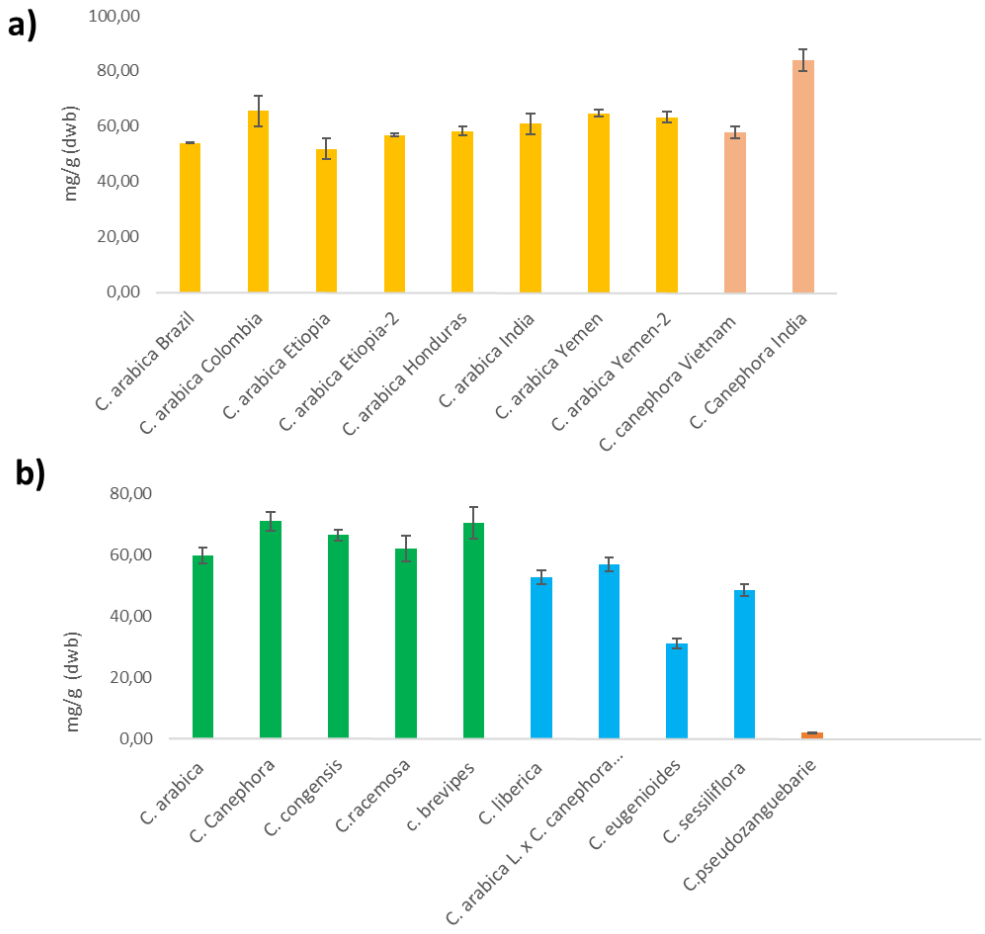

Figure 5.2. a) Total CGAs content in samples of *C. arabica* and *C. canephora* from our different geographical origins. **b)** Averages of the total CGAs content for each coffee species (first group in green, second group in blue, third group in orange). Values are expressed as mg/g of dry weight.

It is important to mention that the discrepancies between the concentrations can be due to many variables such as different number of samples considered, geographical origins and agricultural practices among others that could influence the CGAs content. As reported in Table 5.2, for example, data obtained from Campa et al[3]. in 2005 are different from data reported by other authors, in particular, the total CGA content in *C. canephora* and in *C. brevipes* was significantly higher with respect to the values reported by Anthony et al[17] in 1993. In general, our values are quite in line with the data obtained by Anthony and Clifford except for arabusta coffee (*C. arabica L. x C. canephora Pierre*), *C. eugeniodes* and *C. sessiliflora* which are lower. Moreover, it must be also to consider that moisture values, which are not reported for all literature data, could also influence the differences between reported concentrations.

Table 5.2 - Current data and literature values for total CGAs on % dry matter basis

Coffea species	Total CGAs Current data % dry matter	Total CGAs % dry matter [Campa et al.[3]]	Total CGAs % dry matter [Anthony et al.[17]]	Total CGAs % dry matter [Clifford et al.[5]]	Total CGAs % dry matter [Narita[4]][a]
C. arabica	5.20 – 6.60	-	5.17-7.49 (n.s. 21)	5.17-7.49 (n.s. 21)[d]	4.05-7.26 (n.s. 27[b])
C. canephora	5.80 – 8.40	9.76-14.4 (n.s. unknown)	6.57-9.21 (n.s. 6)	7.25-9.63 (n.s. 5)	5.19-9.77
C. liberica	4.66 – 6.33	6.22-10.7 (n.s. unknown)	7.48-7.69 (n.s. 3)	7.48-10.63 (n.s. 2)	7.45-7.98 (n.s. 2)
C. arabica L. x C. canephora PierreC	5.64 – 5.75	-	-	8.04 (n.s. 1)	8.24 (n.s. 1)
C. eugenioides	2.95 – 3.26	4.55-6.08 (n.s. unknown)	4.53-6.27 (n.s. 4)	4.53-6.27 (n.s. 4)[d]	5.12[c]
C. sessiliflora	4.54 – 5.17	-	5.61-9.93 (n.s. 4)	5.68-6.99 (n.s. 2)	8.69[c]
C. congensis	6.64	8.15-8.77 (n.s. unknown)	7.66 (n.s. 1)	7.76-7.98 (n.s. 2)	7.66 (n.s. 1)
C. pseudozanguebarie	0.21	1.30-1.61 (n.s. unknown)	0.87-1.75 (n.s. 2)	0.93-1.79 (n.s. 2)	0.87-1.75 (n.s. 2)
C. racemosa	6.21	4.78-5.57 (n.s. unknown)	4.91-5.93 (n.s. 3)	4.97-6.03 (n.s. 3)	5.33-5.93 [d] (n.s. 2)
C. brevipes	7.05	10.4-12.3 (n.s. unknown)	6.41 (n.s. 2)	6.74 (n.s. 1)	6.41[d]

[a]and references cited within; [b]the data reported in the book are referred to already reported data so some samples are average of other samples; [c]average value of three samples; [d]see ref Anthony et al.; n.s. = number of samples

5.4 Classes of CGAs present in Coffee.

The total content of CGAs discussed above is derived from the sum of all isomers of monoesters of caffeoyl, feruloyl and *p*-coumaroylquinic acids and the dicaffeoylquinic acid while in literature *p*-coumaroylquinic acids

are not considered. Moreover, if we observe the content of the dicaffeoylquinic acid, our results are lower with respect to the one reported in the literature. This minor value is due to the type of filter used in the extraction process and in the preparation of the samples as will be explained later on. All these factors determine the total value of CGAs that could be different from the one reported in the literature. Mean values of different groups of CGA for each species are reported in table 5.3 while in table 5.4 are reported the relative percentages of the different classes of chlorogenic acids. As far as we know this is the first time that all three isomers of *p*CoQAs were clearly identified and quantified by using their authentic standards previously synthesized.

Table 5.3 – Range of different CGAs content expressed as mg/g (dmb)

mg/g	**CQAs**		**FQAs**		**pCoQAs**		**diCQAs**		**Total CGAs**	
	Mean	range	Mean	range	Mean	range	Mean	range	Mean	Range
C. arabica	52.59	46.15–58.06	4.06	2.69 – 5.51	0.67	0.55 – 0.86	2.14	0.81 – 3.37	59.46	52.00 – 65.62
C. arabica var. laurina	45.44	---	2.39	---	0.51	---	13.48	---	61.82	---
C. canephora	53.39	41.70 – 65.07	10.20	7.69 – 12.71	0.40	0.37 – 0.43	6.94	5.67 – 8.20	70.96	58.00 – 83.95
C. liberica	45.67	40.70 – 51.74	4.16	2.27 – 9.60	0.63	0.26 – 0.80	2.46	1.26 – 4.56	52.92	46.64 – 63.29
C. arabica L. x C. canephora Pierre	41.49	40.97 – 42.00	5.70	5.42 – 5.98	1.06	1.03 – 1.10	8.68	8.38 – 8.99	56.93	56.41 – 57.45
C. eugenioides	27.56	25.64 – 29.49	2.03	1.91 – 2.14	0.24	0.19 – 0.29	1.14	0.87 – 1.41	31.05	29.54 – 32.56
C. sessiliflora	44.88	41.77 – 47.98	1.37	1.36 – 1.37	2.18	2.12 – 2.24	0.12	0.11 – 0.12	48.54	45.38 – 51.69
C. congensis	43.68	---	15.74	---	0.53	---	5.43	---	66.40	---
C. pseudozanguebarie	1.80	---	0.14	---	0.12	---	0.05	---	2.13	---
C. racemosa	60.31	---	0.67	---	0.37	---	0.79	---	62.14	---
C. brevipes	43.16	---	13.04	---	0.25	---	14.06	---	70.50	---

Table 5.4 - Relative percentages of the different classes of chlorogenic acids

Sample		**%CQAs**	**%FQAs**	**%pCoQA**	**%diCQAs**
1	***C. arabica* Brazil**	85.46	7.06	1.35	6.12
2	***C. arabica* Colombia**	88.48	6.58	0.96	3.98
3	***C. arabica* Etiopia**	91.66	5.19	1.06	2.06
4	***C. arabica* Etiopia-2**	91.10	5.88	0.99	2.04
5	***C. arabica* Honduras**	86.10	7.05	1.05	5.79
6	***C. arabica* India**	86.71	7.43	1.15	4.71
7	***C. arabica* Yemen**	88.93	8.51	1.32	1.24
8	***C. arabica* Yemen-2**	89.22	6.54	1.16	3.08
9	***C. Arabica var. laurina* Guatemala**	73.50	3.86	0.82	21.80

10	***C. canephora* Vietnam**	71.94	13.27	0.64	14.15
11	***C. canephora* India**	77.51	15.14	0.51	6.75
12	***C. liberica* -1**	81.82	13.78	0.51	3.89
13	***C. liberica* -2**	81.74	6.47	0.47	3.09
14	***C. liberica* -3**	84.16	11.82	1.36	2.67
15	***C. liberica* -4**	84.94	6.75	1.94	6.37
16	***C. liberica* -5**	87.25	3.79	1.34	7.63
17	***C. liberica* -6**	88.82	5.57	1.45	4.16
18	***C. arabica L. x C. canephora Pierre*-1**	72.63	9.61	1.83	15.93
19	***C. arabica L. x C. canephora Pierre*-2**	73.10	10.41	1.91	14.58
20	***C. eugenioides***	86.81	7.25	0.64	4.78
21	***C. eugeniodes*-2**	90.57	5.87	0.89	2.67
22	***C. sessiliflora* -1**	92.05	3.01	4.67	0.27
23	***C. sessiliflora* -2**	92.82	2.63	4.34	0.22
24	***C. congensis***	65.78	23.70	0.80	8.18
25	***C. pseudozanguebarie***	85.15	6.73	5.65	2.42
26	***C. racemosa***	97.05	1.08	0.60	1.27
27	***C. brevipes***	61.22	18.49	0.35	19.94

5.4.1 Concentrations of CQAs

As we expected all three isomers of CQAs were present in all coffee species and they represent the main group of CGAs.[26] In terms of percentages (**Figure 5.3**) CQAs vary in a range from 61% (*C. brevipes*) up to 97% (*C. racemosa*) of total CGAs. In particular, we have found that *C. arabica*, *C. canephora* and *C. racemosa* represent the species with the highest CQAs concentration (53- 60 mg/g dmb). CQAs in different samples of *C. arabica* were found in range from 46 to 58 mg/g dmb, with the highest concentration found in *C. arabica* from Colombia, while in C. *canephora* were present from 42 up to 65 mg/g dmb, accounting for 85-91% and 72-78% respectively, in accordance with literature data.[5,6,14] Among all six samples of *C. liberica* it was found a wide range of CQAs concentration (from 41 to 58 mg/g dmb) representing 81- 89% of the total content. CQAs concentrations of *C. sessiliflora, C. racemosa and C. brevipes* (42-48 mg/g, 60 mg/g, 43 mg/g dmb, respectively) were in accordance with literature data reported by Anthony et al. and Clifford et al. On the contrary, CQAs content in arabusta coffee, *C. congensis and C. eugenioides* (42*,* 44 and 26-29 mg/g dmb, respectively) was lower with respect to the one reported by Anthony et al. and Clifford et al.[5,17] However, if we consider data reported by Rakotomala et al.[27,28], concentration of *C. eugenioides* is quite in agreement while the current concentration of C. *congensis* is considerable higher. The lowest concentration of CQAs was found in *C. pseoudozanguebarie,* [5,17,25,27] with 2 mg/g dmb, which represents around 85% of the total CGAs content for this specie. As already reported,[22, 28] among all three isomers of CQAs, 5-CQA represents the major chlorogenic acid in all analyzed coffee species, followed by 4-CQA and 3-CQA.[6]

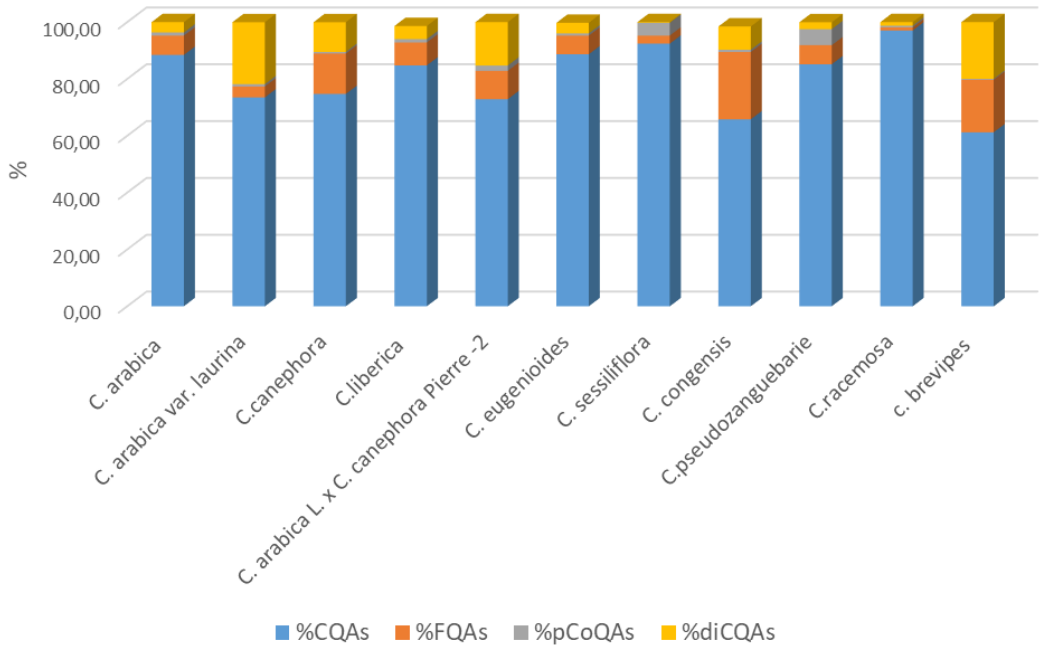

Figure 5.3. Averages of the percentages of the different classes of CGAs with respect to the total quantified CGAs content for each coffee specie.

5.4.2 Concentrations of *p*CoQAs

p-Coumaroylquinic acids (*p*CoQAs) represent the minor class of CGAs identified in this study. Several authors identified *p*CoQAs in Arabica and Robusta but only Perrone et al.[6] quantified all three isomers in both *C. arabica* and *C. canephora* while Salces et al.[22] identified and quantified the only isomer 5-*p*CoQA in coffee brews, with a higher concentration in Arabica coffees. As expected, similar to CQAs distribution, 5-*p*CoQA is the major compound of the three isomers of *p*CoQAs, except in *C. canephora* from India (sample 11, table 5.5) where isomer 3-*p*CoQA was slightly higher and in *C. liberica* (samples 16 and 17, table 5.5) were the concentration of 3-*p*CoQA was more than twice the concentration of isomer 5. It is interesting to note that although *C. canephora* is well known to have a higher chlorogenic acid content, the *p*CoQAs content can be twice higher in *C. arabica* than in *C. canephora*. The concentration of *p*CoQAs in *C. arabica* was between 0.5-0.9mg/g dwb while in *C. canephora* it was 0.40 mg/g dwb, accounting for an average of 1.13% and 0.57 % respectively of the total CGAs content and this observation is in agreement with data published by Perrone

et al.[6] who also observed a higher percentage of *p*CoQAs in *C. arabica*. To our knowledge, no data were found in the literature regarding to the concentration of *p*CoQAs in other wild coffee species.

C. liberica samples showed a great variability in the *p*CoQAs concentration with a range from 0.3 to 0.9 mg/g dwb. *C. eugenioides, C. racemosa, C. brevipes* and *C. congensis* had a lower content than *C. canephora* (0.2-0.3; 0.4; 0.30 and 0.5 mg/g dwb, respectively) but the lowest one was found in *C. pseudozanguebarie (*0.12 mg/g dwb); however, this concentration is similar to the FQAs concentration in this specie and it accounts for around 5.7% of the total content. On the contrary, concentrations in arabusta coffee (1 mg/g dwb) were higher than in *C. arabica* but particularly attention was focused on *C. sissiliflora* (**Figure 5.4**), which showed the highest concentration of *p*CoQAs, between 2.12-2.24 mg/g dwb, representing 4.5% of the total CGAs content and being in fact higher than the concentration of FQAs found for this specie.

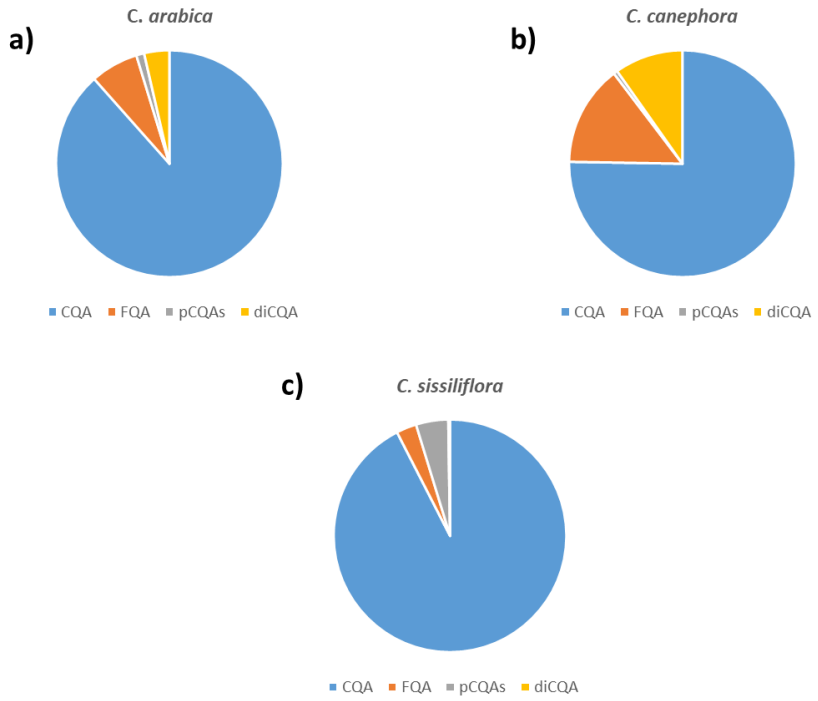

Figure 5.4 Distribution of different classes of CGAs in mg/g dmb found for *C. arabica, C. canephora* and *C. sissiliflora.*

In general, (Table 5.5) isomer at position five (5-*p*CoQA) was the major *p*CoQA in all coffee species, accounting for about 70% of the total *p*CoQAs content. The highest concentrations were found in *C. sissiliflora, C. arabica* and arabusta coffee while the lowest were registered in *C. racemosa, C. brevipes,* and *C. pseudozanguebarie.* It is worth noting that significant differences were not observed between 3-*p*CoQA and 4-*p*CoQA in *C. congensis, pseudozanguebarie, racemosa, brevipes* and *arabica,* where concentrations of both isomers were ranged from 0.01 up to 0.1 mg/g dwb while for others species, such as *C. sissiliflora*, concentrations of 4-*p*CoQA were almost twice higher than 3-*p*CoQA. On the other hand, a quantitative pattern could not be identified for *C. canephora*, *C. arabica L. x C. canephora Pierre and C. eugenioides as well as* for all six samples of *C. liberica* since for three of them we have found relative higher concentrations of isomer 3-*pCoQA (*0.01-0.6mg/g dwb) than 4*pCoQA (*0.03-0.2 mg/g dwb).

Table 5.5 – Distribution of *p*CoQAs in our commercial and wild coffee species.

Sample	mg/g	3*p*CoQA	4*p*CoQA	5*p*CoQA
1	*C. arabica* Brazil	0.08	0.12	0.54
2	*C. arabica* Colombia	0.07	0.06	0.50
3	*C. arabica* Etiopia	0.03	0.04	0.47
4	*C. arabica* Etiopia-2	0.04	0.05	0.48
5	*C. arabica* Honduras	0.08	0.09	0.45
6	*C. arabica* India	0.09	0.10	0.52
7	*C. arabica* Yemen	0.09	0.09	0.58
8	*C. arabica* Yemen-2	0.08	0.07	0.79
9	*C. arabica var. laurina*	0.05	0.07	0.39
10	*C. canephora* Vietnam	0.04	0.06	0.27
11	*C. canephora* India	0.20	0.06	0.17
12	*C. liberica* -1	0.10	0.03	0.14
13	*C. liberica* -2	0.05	0.03	0.21
14	*C. liberica* -3	0.15	0.18	0.31
15	*C. liberica* -4	0.09	0.18	0.66
16	*C. liberica* -5	0.55	0.03	0.21
17	*C. liberica* -6	0.48	0.03	0.17
18	*C. arabica L. x C. canephora Pierre*	0.18	0.18	0.67
19	*C. arabica L. x C. canephora Pierre* -2	0.19	0.02	0.72
20	*C. eugenioides*	0.02	0.03	0.14
21	*C. eugenioides*-2	0.07	0.02	0.20
22	C. sessiliflora	0.12	0.23	1.76
23	*C. sessiliflora*-2	0.14	0.26	1.84
24	*C. congensis*	0.10	0.09	0.34
25	*C. pseudozanguebarie*	0.01	0.01	0.10
26	*C. racemosa*	0.09	0.10	0.19

27	*C. brevipes*	0.04	0.03	0.18

5.4.3 Concentrations of FQAs

A clear distinction was also found in FQAs concentrations of Arabica and Robusta.FQAs in *C. arabica* were found between a range of 2-6mg/g (7% of the total CGA content), among which *C. arabica* from Yemen and Colombia showed the highest values, while concentrations in *C. canephora* were more than twice higher (8-13mg/g), representing 14% of the total CGA content, in accordance with data already reported.[3,5,17] The lowest concentration of FQAs was found in *C. racemosa* and C. *pseudozanguebarie* (0.7 and 0.1 mg/g dmb, respectively). On the contrary with values already reported by Clifford et al.[5] and Anthony et al.[17], our samples of *C. congensis* (16 mg/g dmb) and *C. brevipes* (13mg/g dmb) were particularly rich of FQAs **(Figure 5.5).** In general isomer 5-FQA was the most abundant one of this class of CGAs followed by 4-FQA and 3-FQA, except for samples of *C. liberica-3, C. liberica-4* and *C. pseudozanguebarie* where the concentrations of 3-FQA were higher than 4-FQA.

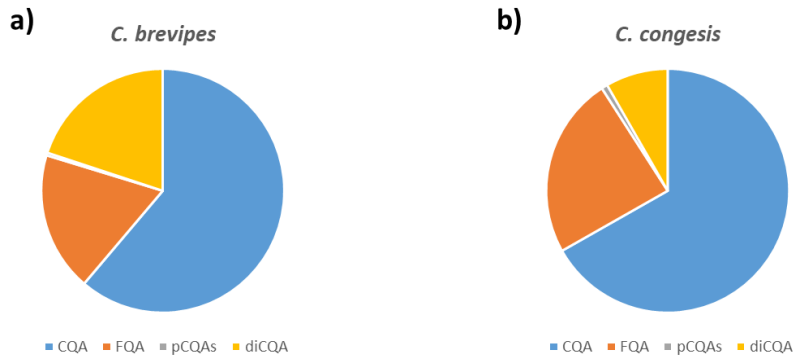

Figure 5.5. Distribution of different classes of CGAs in mg/g dmb found for a) *C. brevipes* and b) *C. congensis*

5.4.4 Concentrations of diCQAs

All three isomers of diCQAs (3,4-diCQA, 3,5-diCQA and 4,5-diCQA) were also present in all coffee species. As reported in the literature,[5] *C. brevipes* is particularly rich of diCQAs (14.06mg/g dmb), while concentrations of dicaffeoylquinic acids were clearly different between *C. arabica* and *C. canephora* (0.8-3 mg/g and 6-8 mg/g, respectively). Although *C. canephora* is richer in diCQAs, these concentrations are significantly lower than diCQAs content already reported by Perrone[6] and Farah et al[14]. Since the content of diCQAs was

observed to be dependent on the level of maturation we thought at the beginning that the lower content found of diCQAs could be attributed to different levels of maturation of the samples analyzed but calculating the ratio between CQAs and diCQAs, as reported in the literature, our results were significantly different. Therefore, in order to clarify our lower content in diCQAs we checked carefully all the steps performed in the extraction process and we found that the nylon filters used for purification, prior to UHPLC analyses, could alter the results. Different tests were performed using standard solutions of the different class of CGAs to evaluate the effect of the filters. Characteristics of the filters are reported in Table 5.6.

Table 5.6. Different types of filters.

Filter type	Characteristics
RC (regenerated cellulose)	Very low non-specific protein binding membrane Ok with acetonitrile, methanol, formic acid. Compatible with water and organic solvents
PTFE (Polytetrafluoroethylene)	Hydrophobic Good for aggressive/corrosive samples Generally good chemical compatibility Compatible with acetonitrile, methanol, formic acid.
PVDF (polyvinylidene fluoride)	hydrophilic low binding properties broad chemical and temperature resistance
NY (nylon)	Good for acqueos and organic samples within pH 3-10 Compatible with acetonitrile and methanol

As an afterthought we evaluated recoveries and possible compounds adsorption for each type of filter (Nylon, Polyvinylidene Fluoride, Polytetrafluoroethylene and regenerated cellulose). Actually, we found that for dichlorogenic acids class the nylon membrane has a slight impact on total recovery (Table 5.7), as already mentioned in the literature for other polyphenolic compounds.[29,30]

Table 5.7 Recoveries of standards solutions of CGAs using different types of filters.

Filter type	Without Filtration	RC*	PVDF*	PTFE*	NY*
	%	%	%	%	%
3CQA	100	99	123	123	97
3CQA	100	99	123	123	98
5CQA	100	100	123	123	97
caffeic	100	99	123	122	98
4CQA	100	99	123	122	96

cumarico	100	100	124	123	97
5FQA	100	100	124	124	101
4FQA	100	100	125	124	100
ferulic	100	100	123	123	99
sinapic	100	99	123	123	100
3,4diCQA	100	100	126	125	84
3,5diCQA	100	100	125	124	88
4,5diCQA	100	100	125	125	89

*RC (regenerated cellulose), PVDF (polyvinylidene fluoride), PTFE (Polytetrafluoroethylene), NY (nylon).

As can be observed in **Figure 5.6**, when a diluted sample solution of *C. arabica* from Colombia was analyzed without any filtration and using the nylon filter a great difference in the peaks areas of all three isomers of diCQAs was observed, while the others CGAs were not affected. Furthermore, some tests were carried out using standards solutions of isomers of diCQAs by passing different volumes of these standard solutions through the filters and we have found that the hold-up volume is a very important factor when nylon filters are used, since with nylon filters of 25 mm if a volume of at least 5 mL is not discarded, in some cases more than 50% of the concentration of diCQAs can be retained by the filters. Unfortunately, the scarce quantity of samples was not sufficient to reply all the extraction and purification steps with a more appropriate filter membrane.

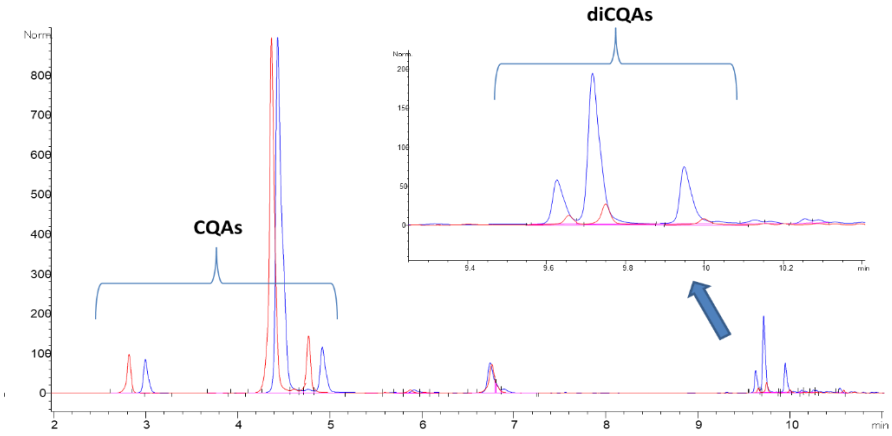

Figure 5.6. Chromatogram of *C. arabica* from Colombia diluted 1:10. Without any filtration (blue) and filtered with nylon membrane (red).

5.5 Evaluation of CGAs concentrations during roasting

The three most important species from a commercial point of view (*C. arabica, C. canephora and C. liberica*) were analyzed under roasting conditions and the variation of the single chlorogenic acid classes were analyzed during time of roasting. At industrial level, depending on the desired degree of roasting, the process is performed between the range 175-235 C and lasts between 8-25 min. During our studies we performed

the roasting in duplicate at a constant temperature of 211°C and the CGAs content was determined at different times in the roasting process (for 3 to 45min).

The percentage of weight loss (%WL) of coffee beans after roasting are reported in table 5.8 and were calculated, according with the literature[6,14] using the following equation:

$$\%WL = \frac{WBR - WAR}{WBR} * 100$$

where WBR is the weight before roasting and WAR is the weight after roasting.

Table 5.8 Percentages of WL of coffee beans after roasting.

min	*C. arabica*	*C.canephora*	*C. liberica*
	%WL	**%WL**	**%WL**
3	2.22	1.06	1.72
5	3.95	2.61	3.72
7	5.70	4.64	5. 49
10	8.00	6.69	7.79
12	9.63	7.92	10.21
15	11.12	9.59	13.41
20	13.23	11.08	15.50
25	14.06	12.55	17.06
30	15.33	13.48	18.29
35	15.52	14.52	18.99
40	16.57	15.40	19.65
45	16.28	18.53	20.37

As can be observed in table 5.8, the %WL were very similar among the three species, registering values between 10 and 13% after 15 min of roasting and reaching a maximum of about 20% after 45min. The results obtained for the total CGAs content according to the roasting time are reported in Table 5.9. As has been already reported,[14,18,31] due to their thermal instability, the CGAs can be transformed in other compounds, like the formation of the corresponding lactones, which contribute to the bitterness of the final beverage. Moreover, other reactions can occur, such as degradation or decomposition reactions, which contribute to decrease their content inside the beans.

Table 5.9. Total CGAs content in roasted samples of *C. arabica, C. canephora* and *C. liberica*

	Total CGAs content mg/g dmb (std)		
Time (min)	**Arabica**	**Canephora**	**Liberica**
green coffee	54.00 (0.28)	57.97 (2.13)	63.29 (2.49)
3	54.03 (0.47)	66.23 (0.84)	52.14 (1.50)
5	48.83 (0.50)	72.18 (5.72)	53.60 (0.28)
7	45.55 (2.64)	78.67 (4.96)	52.91 (2.89)
10	48.36 (0.73)	68.73 (3.36)	43.50 (0.98)
12	29.13 (0.38)	66.36 (3.77)	37.66 (0.55)
15	26.91 (0.43)	59.27 (3.28)	30.46 (2.36)
20	16.03 (0.15)	52.06 (1.17)	23.61 (1.03)
25	12.30 (0.62)	41.54 (0.72)	20.41 (0.10)
30	7.72 (0.12)	36.11 (0.52)	15.65 (0.38)
35	5.05 (0.07)	25.02 (0.08)	12.01 (0.47)
40	4.26 (0.06)	26.03 (1.04)	11.27 (0.38)
45	4.46 (0.03)	24.03 (0.19)	11.56 (0.21)

Although it is important to consider that the final chemical composition of roasted coffees depends not only on the raw material but also on roasting conditions such as roaster type, time of roasting, temperature, and air-flow speed in the roasting chamber, in our studies the variation of CGAs content during roasting time of *C. arabica* and *C. liberica* were slightly similar and a content of 4,5 and 11,6mg/g of CGA was observed after 45min for Arabica and Liberica respectively (~20% weight loss). The behavior of *C. canephora* was different, showing an enhancement of the CGAs content at the beginning and a smaller degradation content at the end of roasting (45 min), where the total CGAs were quite half of the initial concentration. In fact, the total content of CGAs in very light roasted coffee (5-7min) was 35% higher than the concentration in green coffee for *C. canephora*. While for the other two species a gradual decrease of the total content was observed. *C. arabica* and *C. liberica* lost approximately half of the initial concentration of CGAs after 15 minutes of roasting. Therefore, the CGAs content could be used as an index of roasting degree for each specie.

Each class of CGAs (**Figure 5.7**) was also analyzed during roasting time and it was observed that the behavior of CQAs was very similar between Arabica and Liberica while Robusta showed a gradual increase of CQAs up to 10 min of roasting achieving values of 45mg/g dmb (~7% weight loss). This is in line with what observed for the total content of CCGAs. Also FQAs were degraded during roasting but in this case there was an enhancement at the beginning in both *C. canephora* and *C. liberica* while in *C. arabica* the degradation process started immediately.in *C. canephora*, diCQAs enhanced their value until twice in the first 7min and then a decrease started but they do not disappear at the end of roasting as it happened in the other two species. *p*CoQAs showed a completely different behavior in the three species, during the first minutes of roasting, levels of *p*CoQAs increased from 0.37 mg/g in green coffee to 0.44 mg/g at 5 min (~3% weight loss) in Robusta. In Liberica, total pCoQAs concentration remains quite constant during the first 7min of roasting (~5% weight loss), while in Arabica, concentration of *p*CoQAs immediately starts to decrease.

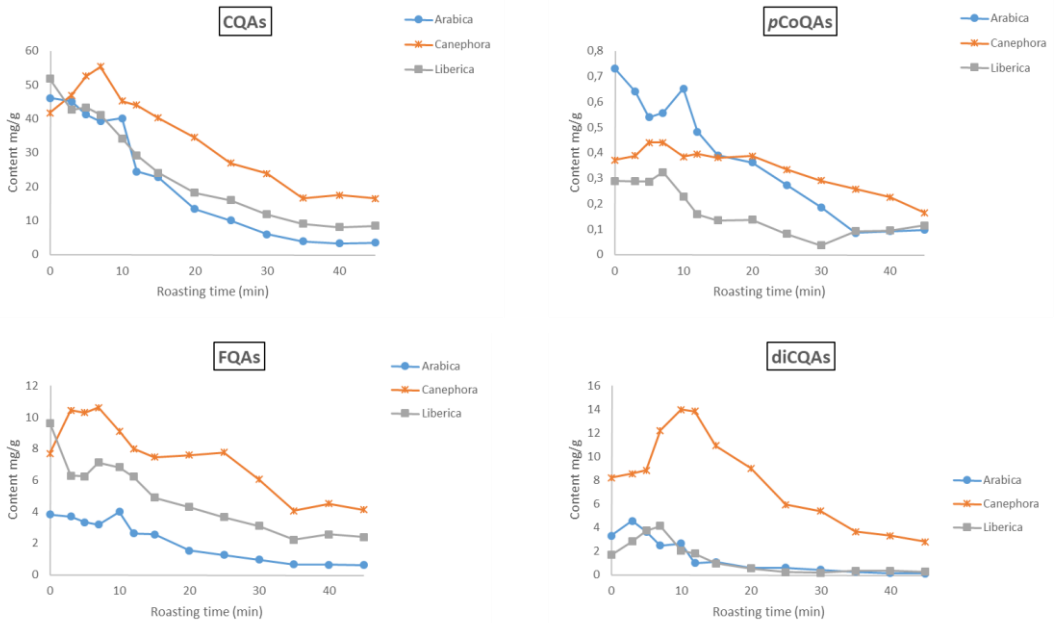

Figure 5.7. CQAs, FQAs, pCoQAs and diCQAs content during roasting.

In **Figure 5.8**, **a**,**c** and **5.8e** are reported the behavior of the different isomers of *p*CoQA during time of roasting in the three commercial species. 5-*p*CoQA starts to decrease immediately in Arabica and Liberica, while in Robusta a slightly increase of this isomer during the first 7min of roasting was registered to continue with a significantly decrease over the time and at the end of roasting, all three isomers are present in a very similar amount in each specie, since the concentrations of 3-*p*CoQA and 4-*p*CoQA are quite constant during roasting. This is in accordance with literature data although roasting conditions are different.[6] As can be observed, the behavior between the different CQAs and *p*CoQAs isomers during roasting is very similar in the three

commercial species, also in this case the 5-CQA, present in major amount in the green coffee bean, decreases rapidly during roasting in Arabica and Liberica and increase in Robusta during the first minutes of roasting. (**Figure 5.8 b**, **d** and **f**). Also these data are in accordance with the literature,[14] although only *C. arabica* and *C. canephora* are reported. It can be noted that *C. canephora* seems to be more resistant to degradation of CGAs during roasting as has been already reported in literature [14] since the content, at the end of roasting, of the different chlorogenic acids is higher than in the other two species. As far as we know this is the first time that chlorogenic acids in *C. liberica* roasted coffee beans were analyzed.

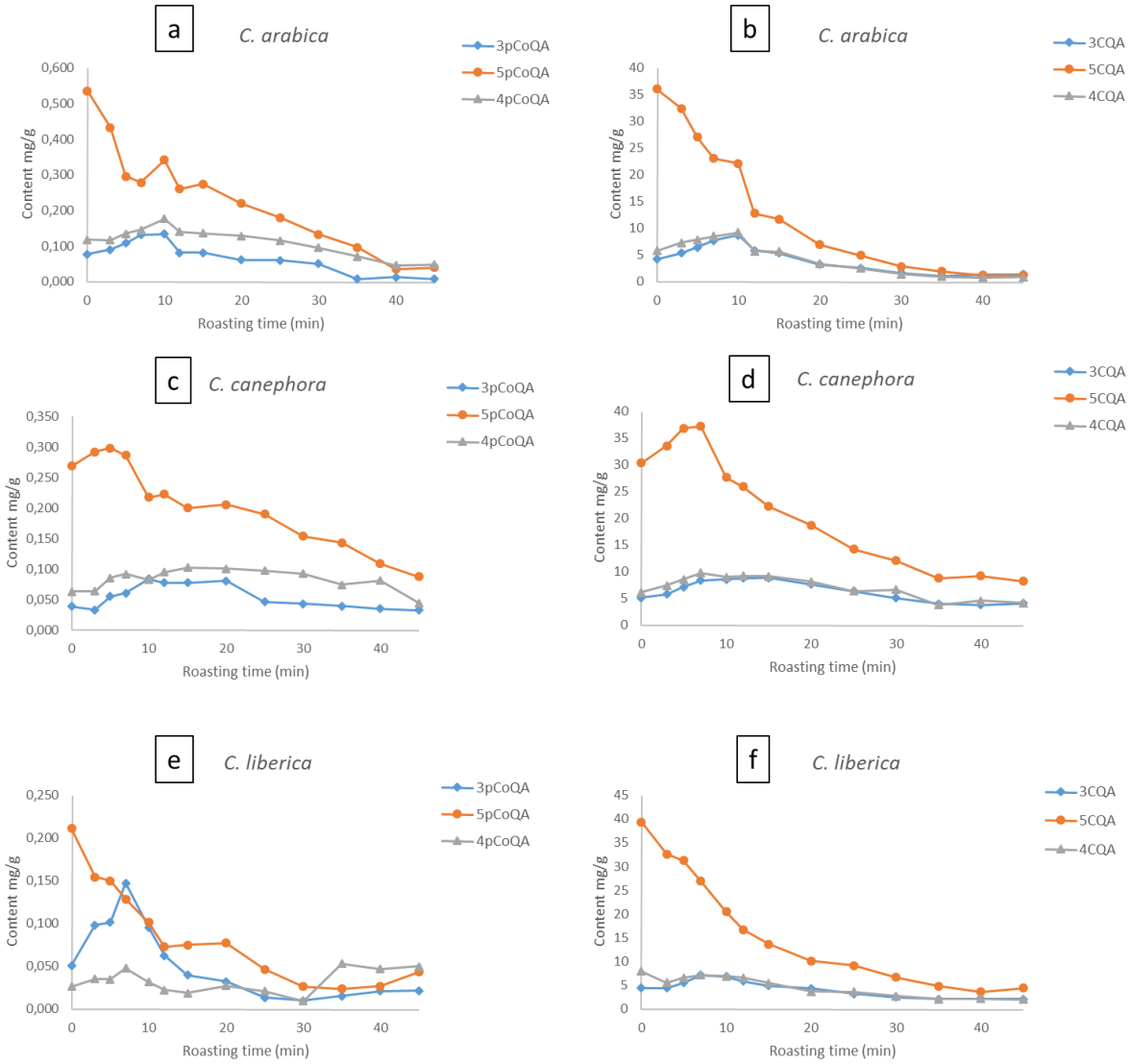

Figure 5.8 – Different isomers of *p*CQAs and CQAs content during roasting

[1] Farah, A.; Donangelo, C. M. Phenolic compounds in coffee. *Br. J. Plant Physiol*., **2006**, 18, 23–36.

[2] Rodrigues, N. P.; Bragagnolo, N. Identification and quantification of bioactive compounds in coffee brews by HPLC-DAD-MSn. *J. Food Composition and Analysis*, **2013**, 32, 105-115.
[3] Campa, C.; Doulbeau, S.; Dussert, S.; Hamon, S.; Noirot, M. Qualitative relationship between caffeine and chlorogenic acid contents among wild coffea species. *Food Chem*., **2005**, 93, 135-139.
[4] Narita, Y.; Inouye, K. Chlorogenic acids from Coffee in Coffee in Health and Disease Prevention. Ed by Preedy, V. R. Elsevier, **2015**, ISBN 9780124095175, Chapter 21.
[5] Clifford, M. N.; Williams, T.; Bridson, D. Chlorogenic acids and Caffeine as possible taxonomic criteria in Coffea and Psilanthus. *Phytochemistry*, **1989**, 28, 829-838.
[6] Perrone, D.; Farah, A.; Donangelo; C. M., De Paulis, T., Martin, P.R. Comprehensive analysis of major and minor chlorogenic acids and lactones in economically relevant Brazilian coffee cultivars. *Food Chem*., **2008**, 16, 859-867.
[7] Gutiérrez Ortiz, A. L.; Berti, F.; Navarini, L.; Monteiro, A.; Resmini, M.; Forzato, C. Synthesis of p-coumaroylquinic acids and analysis of their interconversion. *Tetrahedron: Asymmetry*, **2017**, 419-427.
[8] Jeszka-Skowron, M.; Zgola-Grzeskowiak, A.; Grzeskowiak, T. Analytical methods applied for the characterization and determination of bioactive compounds in coffee. *Eur. Food Technol*., **2015**, 240, 19-31.
[9] Ky, C.; Noirot, M.; Hammon, S. Comparison of five purification methods for chlorogenic acids in green coffee beans (coffea sp). *J. Agric. Food Chem*., **1997**, 45, 786-790.
[10] Clifford, M. N.; Knight, S.; Surucu, B.; Kuhnert, N. Characterization by LC-MS(n) of four new classes of chlorogenic acids in green coffee beans: dimethoxycinnamoylquinic acids, diferuloylquinic acids, caffeoyl-dimethoxycinnamoylquinic acids, and feruloyl-dimethoxycinnamoylquinic acids. *J. Agric. Food Chem*., **2006**, 54, 1957-69.
[11] Craig, A. P.; Fields, C.; Liang, N.; Kitts, D.; Erickson, A. Performance review of a fast HPLC-UV method for the quantification of chlorogenic acids in green coffee bean extracts. *Talanta*, **2016**, 54, 481-485.
[12] Dokli, I.; Navarini, L.; Hamersak, Z. Synthesis of 3,4- and 5-O-feruloylquinic acids. *Tetrahedron: Asymmetry*, **2013**, 24, 785-790.
[13] Clifford M. N., Madala, N. E. Surrogate standards: A Cost-Effective Strategy for Identification of Phytochemicals. *J. Agric. Food Chem*., **2017**, 65, 3589−3590.
[14] Farah, A.; De Paulis, T.; Trugo, L. C.; Martin, P. R. Effect of Roasting on the Formation of Chlorogenic Acid Lactones in Coffee. *J. Agric. Food Chem*. **2005**, 53, 1505−1513.
[15] Frank, O.; Zehentbauer, G.; Hofmman, T. Bioresponse-guided decomposition of roast coffee beverage and identification of key bitter taste compounds. *Eur. Food Res. Technol.,* **2006**, 222, 492–508.
[16] Clifford, M. N.; Johnston, K. L.; Knight, S.; Kuhnert, N. Hierarchical scheme for LC-MSn identification acids. *J. Agric. Food Chem*., **2003**, 51, 290-2911.
[17] Anthony, F.; Noirot, M.; Clifford, M. N. Biochemical diversity in the genus Coffea L.: chlorogenic acids, caffeine and mozambioside contents. *Genet. Resour. Crop Evol.*, **1993**, 40, 61-70.
[18] Trugo, L. C.; Macrae, R. A study of the effect of roasting on the chlorogenic acid composition of coffee using HPLC. *Food Chem*., **1984**, 15, 219-227.
[19] Gema, B.; Sarrià, B.; Bravo, L.; Mateos, R. Exhaustive qualitative LC-DAD-MSn analysis of arabica green coffee beans: cinnamoyl-glycosides and cinnamoylshikimic acids as new polyphenols in green coffee. *J. Agric. Food Chem*., **2016**, 64, 9663-9674.
[20] Monteiro, M. C.; Farah, A. Chlorogenic acids in Brazilian Coffea arabica cultivars from various consecutive crops. *Food Chem*., **2012**, 134, 611–614.
[21] Jaiswal, R.; Patras, M. A.; Eravuchira, P. J.; Kuhnert, N. Profile and Characterization of the Chlorogenic Acids in Green Robusta Coffee Beans by LC-MSn: Identification of Seven New Classes of Compounds. *J. Agric. Food Chem.*, **2010**, 58, 8722–8737.
[22] Alonso-Salces, R. M.; Serra, F.; Reniero, F.; Hèberger, K. Botanical and Geographical Characterization of Green coffee (coffea arabica and coffea canephora): Chemometric evaluation of phenolic and methylxanthine contents. *J. Agric. Food Chem*., **2009**, 57, 4224-4235.
[23] Babova, O.; Occhipinti, A.; Maffei, M. E. Chemical Partitioning and antioxidant capacity of green coffee (coffea arabica and coffea canephora) of different geographical origin. *Phytochemistry*, **2016**, 123, 33-39.

[24] Gimase, J. M.; Thagana, W. M.; Kirubi, D. T.; Gichuru, E. K.; Kathurima, C. W. Beverage quality and biochemical attributes of arabusta coffee (C. arabica L. x C. canephora Pierre) and their parental genotypes. *Afr. J. Food science*, **2014**, 8, 456-464.

[25] Bertrand, C.; Noirot, M.; Doulbeau, S.; de Kochko, A.; Hamon, S.; Campa, C. Chlorogenic acid content swap during fruit maturation in Coffea pseudozanguebariae Qualitative comparison with leaves. *Plant Science*, **2003**, 165, 1355–1361.

[26] Koshiro, Y.; Jackson, M. C.; Katahira, R.; Wang, M. L.; Nagai, C.; Ashihara, H. Biosynthesis of chlorogenic acids in growing and ripening fruits of coffea arabica and coffea canephora plants. Z. *Naturforsch*, **2007**, 62c, 731-742.

[27] Rakotomalala, J. J. Diversité biochimique des caféiers: Analyse des acides hydroxycinnamiques, bases puriques et diterpènes glycosidiques. Particularités des caféiers sauvages de la région malgache (Mascarocoffea Chev.), Travaux et Documents 3Microédités**. 1993**, ORSTOM. Paris.

[28] Campa, C.; Rakotomalala, J .J.; de Kochko, A.; Serge, H. Chlorogenic acids: diversity in green beans of wild coffee species. *Adv. Plant Physiol.*, **2008**, 10, 421-437.

[29] Sapozhnikova, Y. Development of liquid chromatography–tandem mass spectrometry method for analysis of polyphenolic compounds in liquid samples of grape juice, green tea and coffee, *Food Chem.*, **2014**, 150, 87–93.

[30] Lee, S. The Liquid Chromatographic Determination of Chlorogenic and Caffeic Acids in Xu Duan (Dipsacus asperoides) Raw Herb, ISRN *Analytical Chemistry*, Volume 2014, Article ID 968314.

[31] Schrader, K.; Kiehne, A.; Engelhardt, U. H.; Maier, H. G. Determination of chlorogenic acids with lactones in roasted coffee. *J. Sci. Food Agric*. **1996**, 71, 392-398.

RESULTS AND DISCUSSION

Recognition Elements for 5-CQA

Chapter 6. Fluorescent Molecularly Imprinted Polymers (fMIPs)

In this part of the project fluorescent polymeric imprinted nanoparticles (fMIPs) with 5-caffeoylquinic acid (5-CQA) were synthesized following the non-covalent approach since this is a simple method where only a few synthetic steps are required and a great variety of functional monomers can be used. The synthesis of a MIP involves the participation of a suitable functional monomer and sometimes a co-monomer, crosslinker, radical initiator and the template molecule. Therefore, in order to obtain a polymer with high specificity and selectivity, it is necessary to select good functional monomers able to interact with the analyte. In the non-covalent approach formation of relatively weak non-covalent interactions like π-staking, hydrogen bonding, hydrophobic interactions or van der Waals forces and ion interactions between template and functional monomer(s) occur before polymerization and their strength will depend on the environment that surrounds the polymer and on the solvent polarity.[1] The synthesis of the fMIPs was carried out at the University of Trieste, while the study of the fluorescent properties as well as the immobilization of the polymer were carried out at COBIK.

6.1 Functional Monomers.

Functional monomers must have a polymerizable acryoyl or vinyl groups in their structures in order to allow their incorporation in the polymeric matrix. Since in the template molecule are present polar groups, two functional monomers, 4-vinyl-pyridine (**4VPy**) and a naphthalimide derivate (**16b**) containing a polymerizable vinyl group and others functions capable of interacting with the template (**Figure 6.1**), were chosen to carry out the synthesis of a fluorescent molecularly imprinted polymer. The choice of these monomers was based on the interactions that 5-CQA is able to establish and which could be exploited in specific binding sites. The aromatic ring may be involved in π-π interactions with other aromatic functions or unsaturated systems, while the hydroxyl groups may act both as donors or receptors for hydrogen bonds or they can be involved in other interactions with dipoles, dipole-induced or ionic bonds if deprotonated.

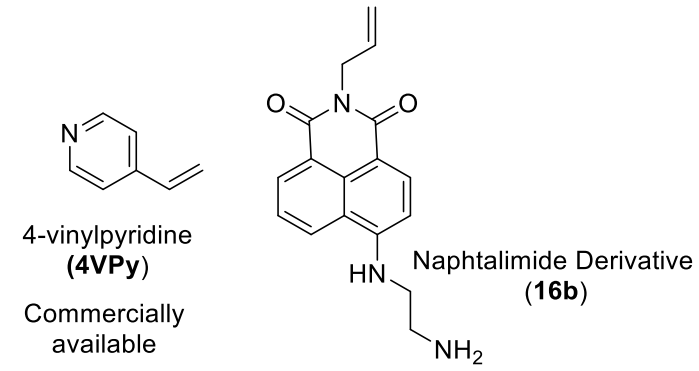

Figure 6.1. Structure of functional monomers.

4-vinyl-pyridine (**4VPy**) has already been used as a functional monomer for interactions with 5CQA[2] and is one of the most common functional monomer used for the preparation of MIPs due to its commercial availability and low cost.[3,4]

4-[(2-ethylenediamine)]N-allyl-1,8-naphthalimide (**16b**) is a fluorescent molecule synthesized from 4-chloro-1,8-naphthalic anhydride, following the synthesis procedure described by Konstantinova and al.[5] (scheme 6.1). Analogues of this functional monomer have been widely used in literature to obtain fluorescent polymers to be used in sensor development.[6] Naphthalimide fluorophores have been widely used as recognition probes, due to their visible emission wavelength and high photostability. Substituted naphthalimides have shown strong intramolecular charge transfer (ICT) in solution state as a consequence of their planar architecture combined with the electron-withdrawing ability of the imide core.[7,8,9] Some MIPs have been designed using this fluorophore as a functional monomer, for instance a MIP based on **16b** was developed for detecting caffeine.[10]

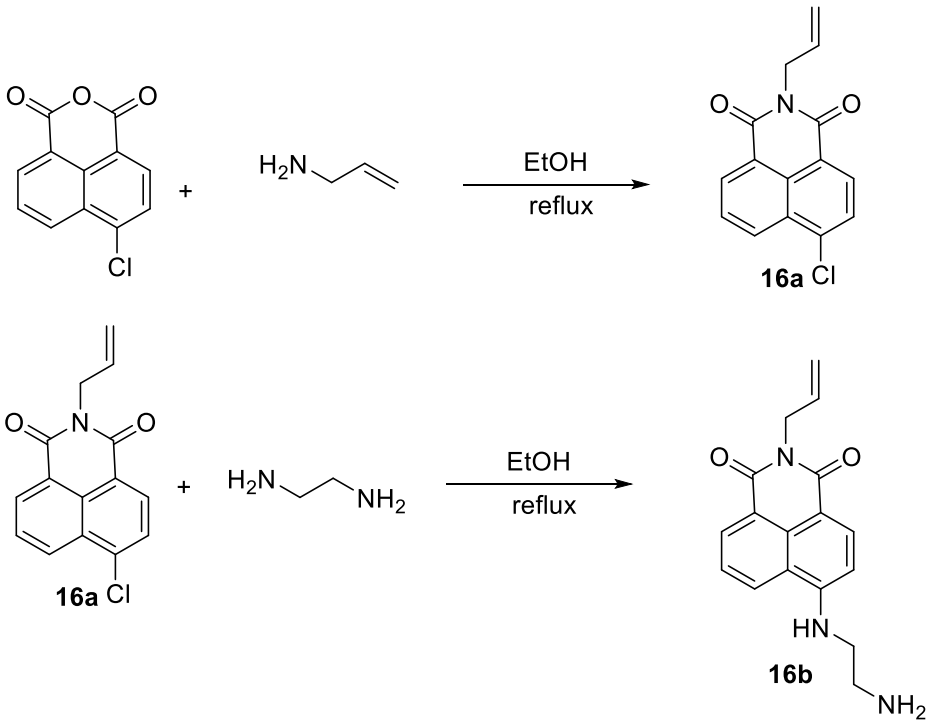

Scheme 6.1. Synthesis of functional monomer **16b**.

6.2 Study of the interactions between the two different monomers and the analyte: ^{1}H NMR Titrations.

^{1}H NMR titrations were carried out in order to identify the specific functionalities that are involved in the formation of the functional monomer-template complex before polymerization, as the degree of template–monomer complexation is directly dependent upon the type of interactions employed and the chemical composition of the polymerization reaction mixture.[11] ^{1}H NMR titrations consist on the addition of increasing equivalents of template (5-CQA) to a fixed concentration of functional monomer.

Analyses were performed in deuterated DMSO since the synthesis of the polymers was carried out in the same solvent. First, the respective proton spectra were recorded for each monomer and spectra were recorded after addition of increasing amounts of the analyte, comprised between 0.5 and 10 equivalents. In this way, depending on the downfield or upfield chemical shift it is possible to identify protons involved in the interactions and the type of the interaction.[12]

NMR allows to distinguish between three possible situations (**Figure 6.2**) during the complex formation, known as slow, intermediate and fast exchange regimen. These have been identified considering that the complex formation (LR) between two molecules named ligand (L) and receptor (R) is a dynamic process where the free molecules are in equilibrium with the bond counterpart. Therefore, the free receptor and the ligand-bond state have two different frequencies (ν_R and ν_{RL}) and the appearance of the characteristic signal of the two species will depend on three factors: the population of each state (P_R and P_{LR}), the chemical shift difference between the two frequencies ($\Delta\nu = \nu_{RL} - \nu_R$) and the relative values of the exchange rate: $k_{ex} = k_R + k_{RL}$. In the first regimen mentioned above, the ligand binding equilibrium has a very slow exchange rate compared to the NMR time scale ($k_{ex} << |\Delta\nu|$) and therefore, signals from both the free ligand and the bond ligand are observed in the spectrum with different chemical shifts. On the other hand, when the exchange regimen is fast, the ligand binding equilibrium has a very fast exchange rate compared to the NMR time scale ($k_{ex} >> |\Delta\nu|$, a very fast interconversion between L and LR occurs during the detection period of the NMR experiment and only one signal is observed with a population-weighted chemical shift ($\delta_{obs} = P_R\delta_R + P_{LR}\delta_{LR}$). A different signal is observed in the intermediate exchange regimen where $K_{ex} \approx |\Delta\nu|$. In this case one signal is observed, at a chemical shift between δ_R and δ_{LR}, with a linewidth that is "exchange broadened" due to interference from the interconversion between L and LR during the detection period.[13,14]

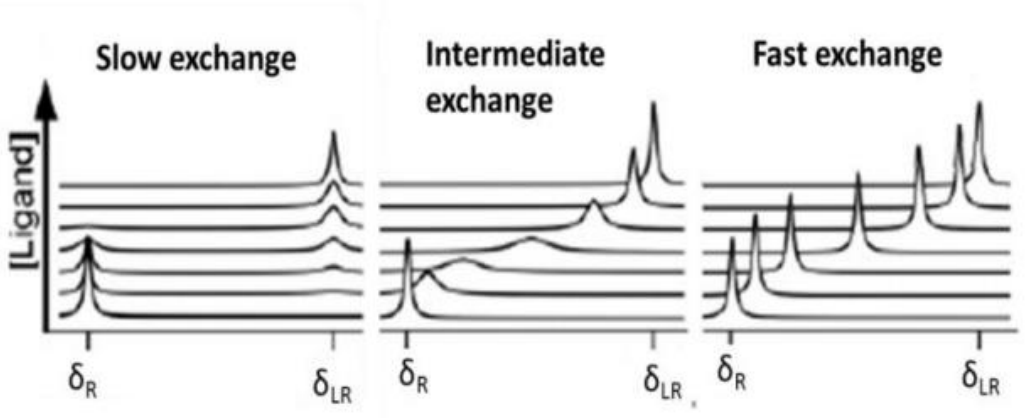

Figure 6.2 Different regimens during ^{1}H NMR titrations [14]

6.2.1 Titration of 4-Vinylpyridine (4VPy) with 5-caffeoylquinic acid (5CQA).

The addition of the template to the functional monomer solution causes a progressive shift of all signals. The variation of the proton chemical shift (δ_{final}-$\delta_{initial}$) of the 4Vpy after addition of 10 equivalents of template is shown in **Figure 6.3**. Signals of vinyl protons of the monomer were overlap by signals of the one proton of the hydroxyl groups the quinic acid core and vinyl protons of the template molecule (**Figure 6.3a**), but slightly variations of the aromatic protons of the monomer towards downfield are evident (**Figure 6.3b**).

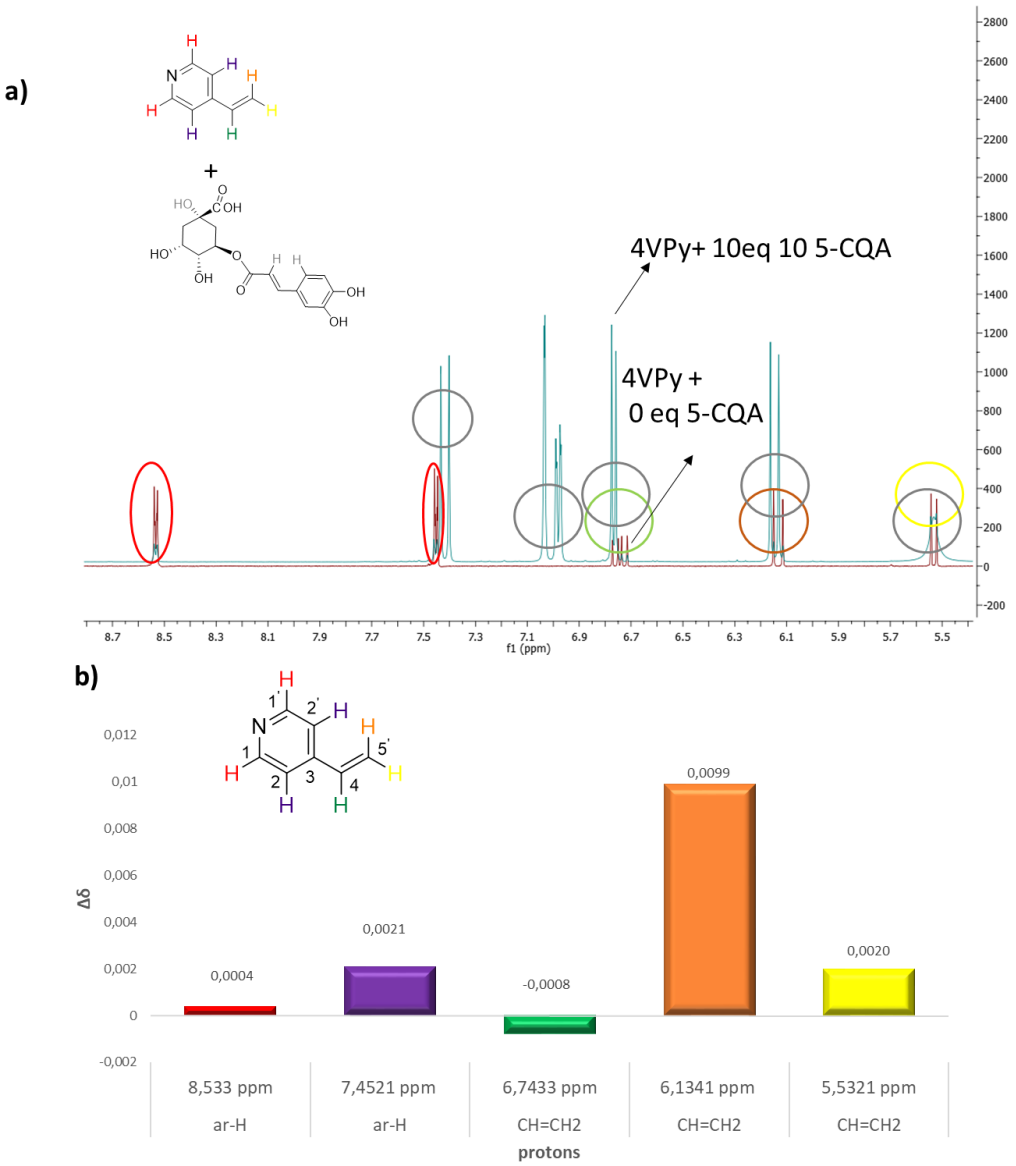

Figure 6.3. a) Overlapping of the vinyl protons of the monomer (4VPy) after addition of 5-CQA (red 4Vpy + 0eq 5-CQA; blue 4Vpy+ 10eq 5-CQA). **b)** Histogram of the chemical shift variations in the ^{1}H-NMR spectrum of 4-Vinylpyridine upon progressive additions of 10 equivalents of 5-caffeoylquinic acid

Comparing the shifts of both the functional monomer and the template we can deduce that the interaction could take place through the formation of hydrogen bonds between the nitrogen atom of the pyridine moiety and the hydrogen atom of the carboxyl group present in the template molecule resulting in a deshielded effect[15,16] and a downfield shift; however, this interactions cannot be confirmed since the small variations in the chemical shift of the aromatic proton of the functional monomer could also indicate another type of phenomena such as the formation of aggregates. Vinyl hydrogen at C4 was the only signal with a slight upfield shift, in accordance with a characteristic variation of Π- Π stacking interactions.[17] However, interactions between the two aromatic rings cannot be confirmed since the signal of C4 is overlapped with the signal of aromatic protons of 5-CQA. Moreover, in all registered spectra upon addition of the template, only one set of signals were visible indicating probably that complexation equilibrium is close to a *fast exchange* regime described above. In **Figure 6.4a** it is possible to observe the trend of titration curve for only the aromatic protons. The plateau is reached after 1,5 equivalents added, thus corresponding to the saturation point. while in **6.4b** it can be notice that with the increase of the template concentration, the signal has changed shape and lost resolution, which could be a possible indication of the presence of a molecule population bonded in different ways that are free to exchange.

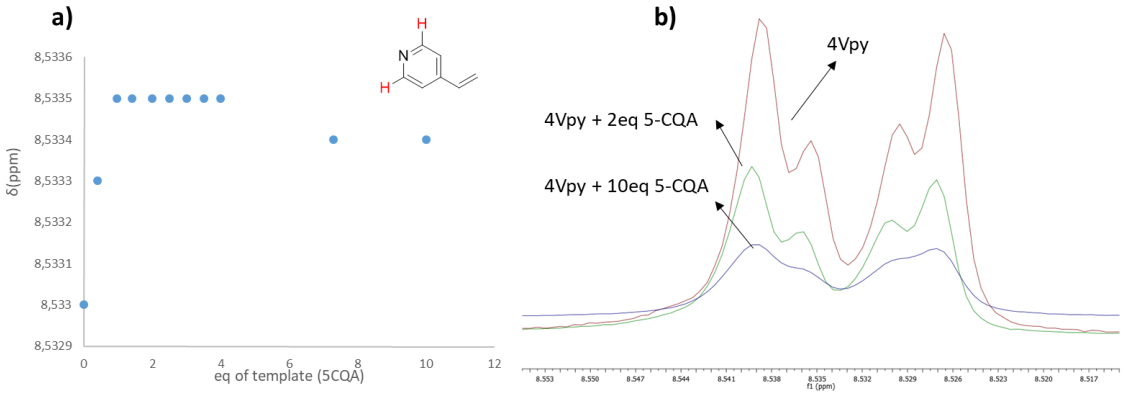

Figure 6.4: **a)** Chemical shift variation of aromatic proton of 4-vinypiridine (4Vpy) upon interaction with template molecule (5-CQA). **b)** progressive shift of the proton aromatic protons adjacent to the nitrogen atom of the pyridine ring in the ^{1}H-NMR spectra. Pure 4VPy (red), addition of 2eq of 5-CQA (green) and 10eq (blue).

6.2.2 Titration of 4-[(2-ethylenediamine)-N-allyl-1,8-naphthalimide (16b) with 5-caffeoylquinic acid (5-CQA).

The variation of the proton chemical shift (δ_{final}-$\delta_{initial}$) of **16b** after addition of 10 equivalents of template is shown in **Figure 6.5**. As can be noticed, protons CH_2NH_2 showed a greater shift towards downfield than the

others and this is possibly the result of the proton exchange due to the acid-base reaction between the amino group of the monomer and the carboxyl group of the template.

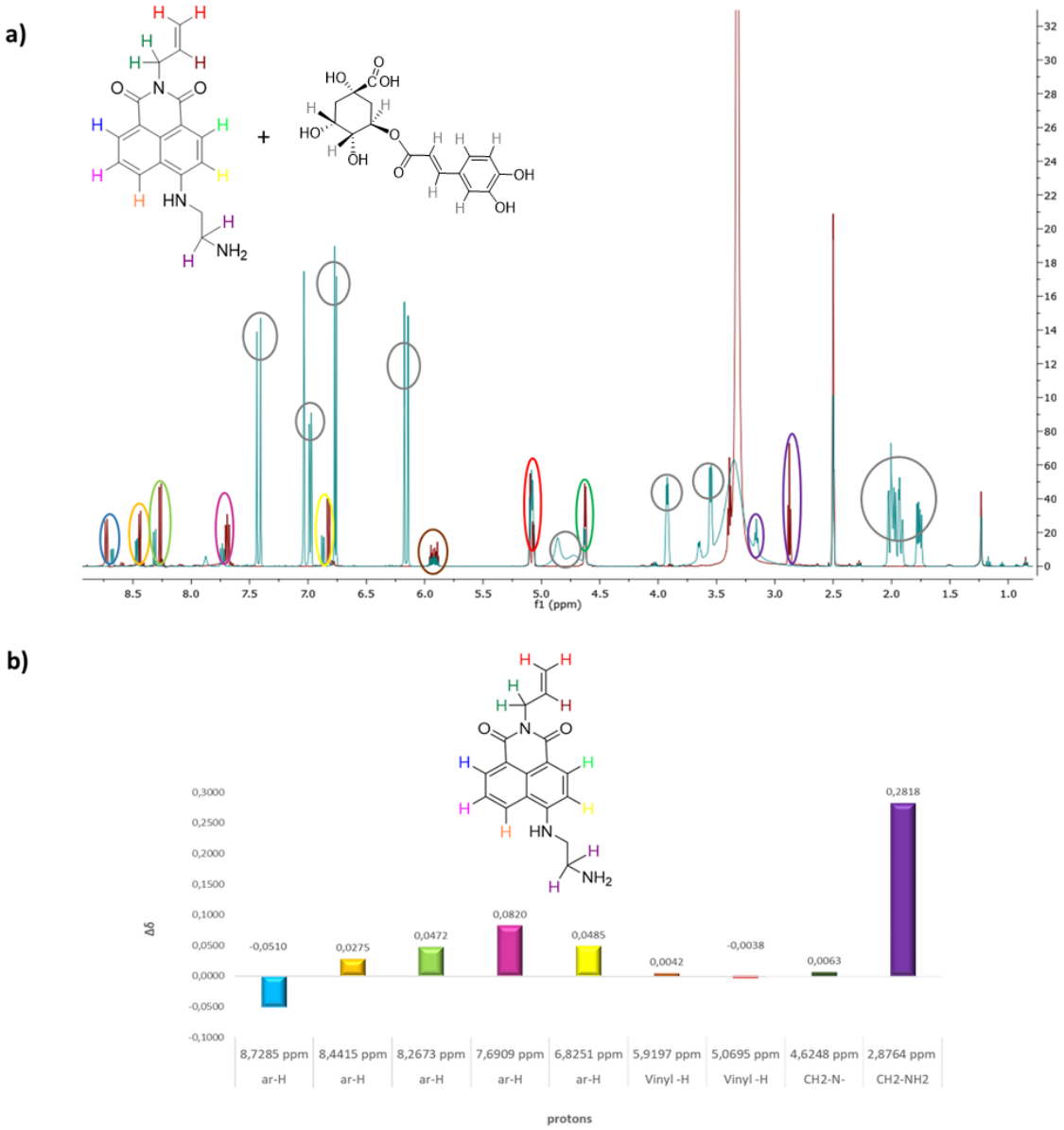

Figure 6.5. a) ^{1}H-NMR spectra of monomer **16b** + 0 eq of 5-CQA (red) and monomer **16b** + 10 eq of 5-CQA (blue) **b)** Histogram of the chemical shift variations in the ^{1}H-NMR spectrum of 4-[(2-ethylenediamine) N-allyl-1,8-naphthalimide (**1b**) upon progressive additions of 10 equivalents of 5-caffeoylquinic acid

In **Figure 6.6** it is possible to observe the trend of titration curve of the protons adjacent to the amino group. The plateau is reached after approximately 2 equivalents added which represents the saturation point.

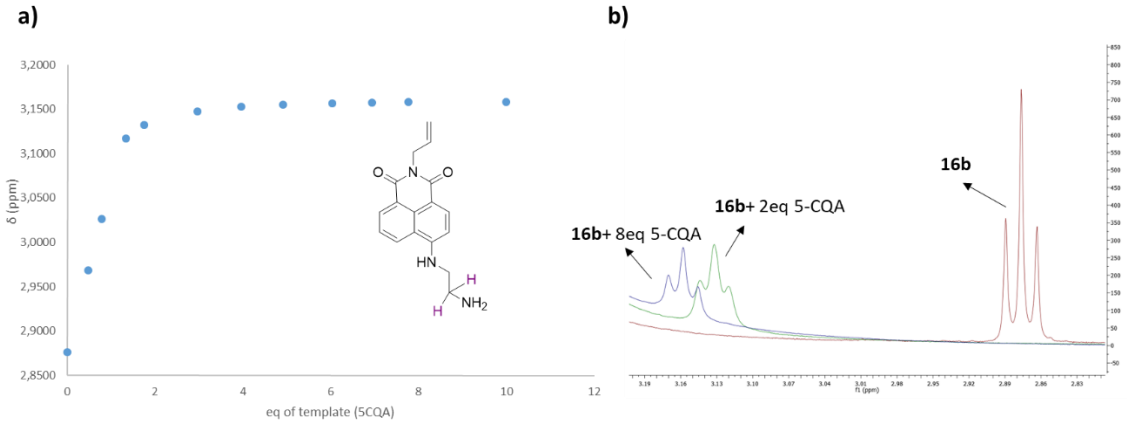

Figure 6.6: **a)** Chemical shift variation of C**H**$_2$NH$_2$ protons of monomer **16b** upon interaction of template molecule (5-CQA). **b)** progressive shift of protons C**H**$_2$NH$_2$ in the ^{1}H-NMR spectra. Pure **16b** (red), addition of 2eq of 5-CQA (green) and 8eq (blue).

The trend of the titration curves is variable between the two monomers, it seems that **4-VPy** react faster with 5-CQA than monomer **16b**, however the chemical shift of monomer **16b** towards downfield is significantly higher and this behavior suggest the formation of a stronger complex between the template 5-CQA and monomer **16b** due to the acid-base reaction**.** In order to evaluate the behavior of the template in presence of both monomers, a ^{1}H NMR titration was carried out by adding increasing amounts of template to a mix of monomer **4VPy** and **16b.** As can be observed in **Figure 6.7b** a first plateau is reached by the aromatic proton of **4VPy** after 0.5eq added, but increasing the template concentration, the chemical shift linearly increases to reach a second plateau after 8 equivalents, in accordance with hydrogen bond formation between the nitrogen atom of the pyridine and the hydroxyl groups of the phenol ring. Alternatively, a Π- Π stacking interaction between aromatic rings could explain an upfield shift of the aromatic protons. Anyway, the main interaction of 5-CQA occurs with monomer **16b** (**Figure 6.7a**)**.** The downfield shift of the protons CH_2NH_2 indicates a deshielding effect due to the positive charged NH_2 due the hydrogen transfer from the carboxylic group.

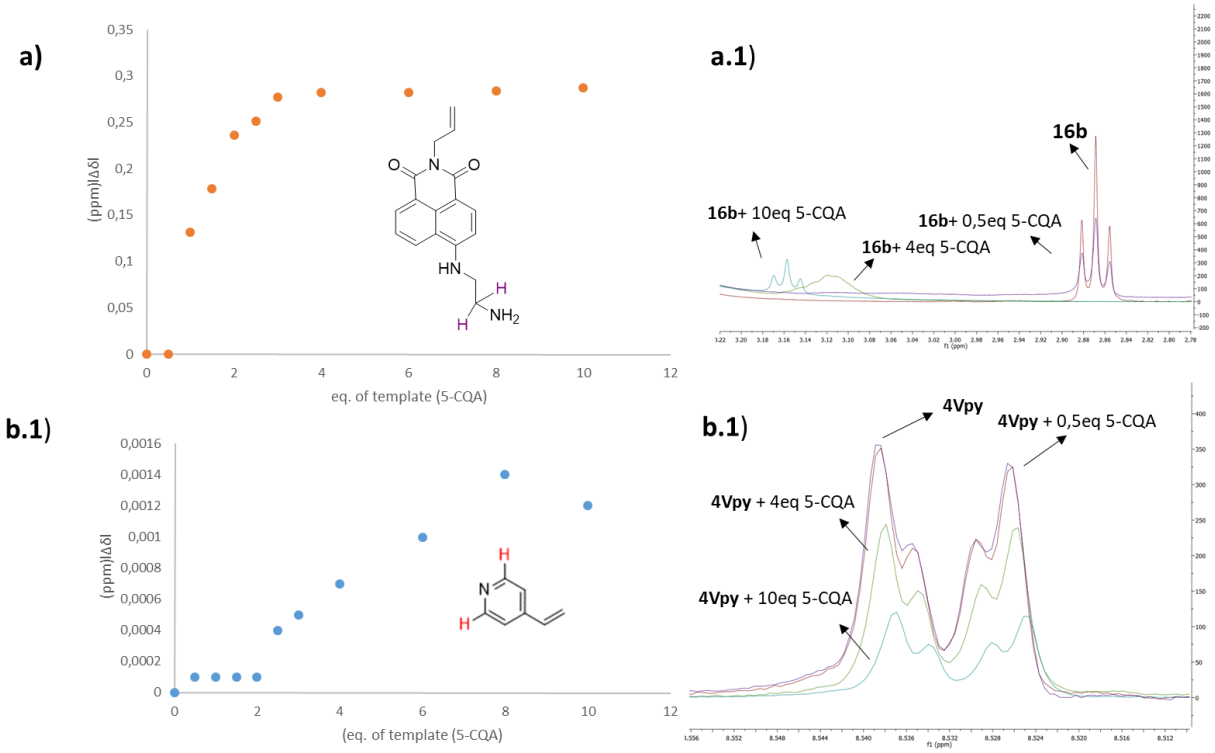

Figure 6.7: **a)** Chemical shift variation of C**H**$_2$NH$_2$ protons of monomer **16b** upon interaction of a monomers mix with template molecule (5-CQA). **a.1)** progressive shift of the protons C**H**$_2$NH$_2$ in the ^{1}H-NMR spectra: **16b** (red), addition of 0.5eq of 5-CQA (purple), 4eq (green) and 10q (blue). **b)** Chemical shift variation of aromatic proton of 4-vinypiridine (4Vpy) upon interaction of a mixture of monomers and the template molecule (5-CQA). **b.1)** progressive shift of the proton Ar-**H** in the ^{1}H-NMR spectra. 4VPy (red), addition of 0.5eq of 5-CQA (purple), 4eq (green) and 10q (blue).

6.3 Synthesis of Fluorescent Molecularly Imprinted Polymers (fMIPs)

The polymers were imprinted with a mimic compound of 5-caffeoylquinic acid (5-CQA) prepared in order to avoid polymerization of the double bond present in the real analyte. Hydrogenated 5-CQA (H-5CQA) was prepared following a literature procedure[2] as shown in **scheme 6.2.** The product was obtained in 90% of yield.

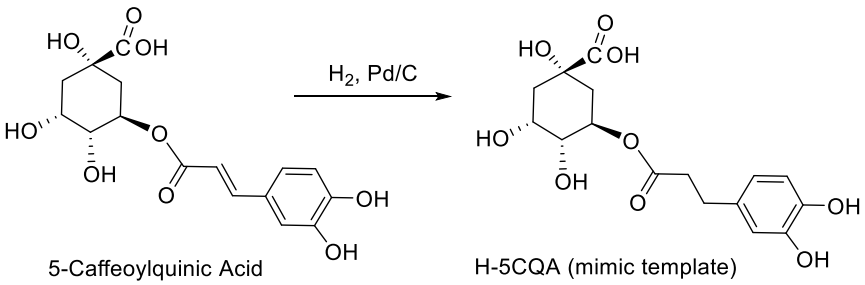

Scheme 6.2. Synthesis of Hydrogenated 5-caffeoylquinic acid (H-5CQA).

fMIPs were synthesized under high dilution radical polymerization conditions following a standard protocol.[18] By optimization of solvent and monomers concentrations it was possible to obtain polymer particles of micro or nanometric dimensions. In this way, interactions between the template and functional monomers are favored thanks to high surface area of the particles, allowing the formation of more accessible binding sites in a short diffusion time.[19] The choice of a suitable solvent allows the formation of highly stable micro or nano gels due to the high viscosity of the colloidal solutions. The solvating power of the solvent prevents macrogelation via osmotic repulsion forces and steric hindrance, without adding surfactants, and furthermore, under diluted conditions in a suitable solvent, each polymeric particle is stabilized avoiding intermolecular crosslinking.[20]

To avoid aggregation and macrogelation of the polymer, it is important to keep the concentration of all monomers under a critical value, called critical monomer concentration (C_M). The C_M is defined as the percentage by weight of all monomers used for the polymerization as compared to the percentage of the overall mass of monomers and solvent used for a polymer preparation[21]. For our purposes, DMSO was chosen as the solvent for polymer preparation due to its ability of dissolve all reagents involved in the synthesis. fMIPs were prepared following the non-covalent approach in three steps:

I. pre-polymerization

II. Radical polymerization

III. Removal of the template.

In **Figure 6.8** it can be observed a representation of the synthesis of a fMIP for the mimic template H-5CQA.

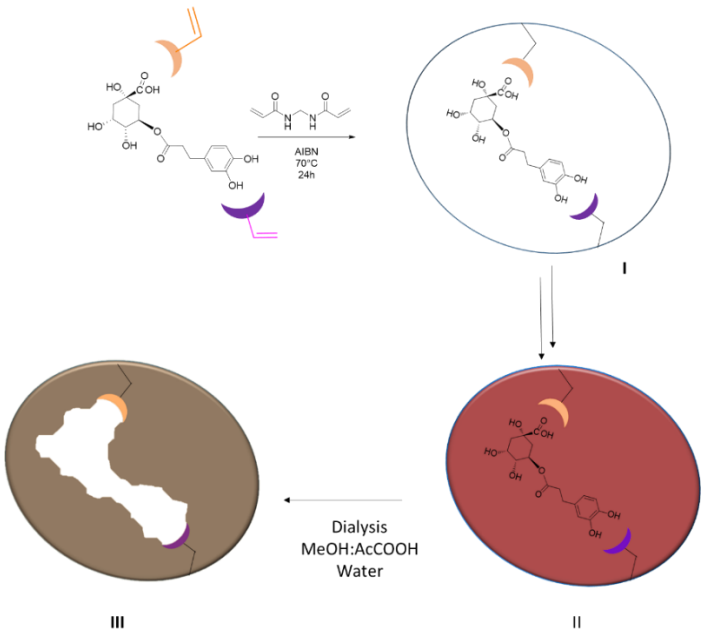

Figure 6.8 The three steps synthesis of fMIPs for H-5CQA. I. pre-polymerization, II. Radical polymerization and III. Removal of the template.

Two fMIPs were prepared using a C_M of 0.5% w/w and the following functional monomers:

- **16b** and **4VPy** as functional monomers for the synthesis of MIP01
- **16b** as the functional monomer and NIPAM (N-Isopropylacrylamide) as the co-monomer for the synthesis of MIP02.

In the synthesis of MIP02, NIPAM was chosen since it is capable of modulating the solubility of the polymer in water. As it has been reported in the literature, it does not interact with the template agent in polar solvents like water or DMSO, but limits itself to acting as an inert and stabilizing component of the polymeric structure.[22]

In table 6.1 are reported the percentage composition of each component in the synthesized polymers. For each polymer also a non-imprinted polymer (fNIP) was prepared as control polymer using the same polymerization procedure and the same concentrations of monomers but without the presence of H-5CQA as the mimic template molecule.

Table 6.1 Composition of fMIPs imprinted with H-5CQA for 5-*O*-caffeoylquinic acid recognition.

		MIP01	**MIP02**
Functional Monomers	4-Vinylpiridine (**4VPy**)	20%	-
	4-[(2-ethylenediamine)-N-allyl-1,8-naphthalimide (**16b**)	20%	10%
Co-monomer	N-Isopropylacrylamide (NIPAM)	-	30%
Crosslinker	N,N'-methylenebisacrylamide (MBA)	60%	60%
Initiator	Azobisisobutyronitrile (AIBN)	5%	5%

The amount of solvent necessary to obtain polymeric nanoparticles was calculated by the following equation:

$$m(S)\frac{[m(fm)+m(bm)+m(cl)]*\%solvent\ in\ mixture}{\%monomer\ in\ mixture\ (C_M)}$$

Where m(fm), m(bm) and m(cl) are the mass of the functional monomer, the co-monomer and the crosslinker respectively.[23]

I. Pre-polymerization. A mixture of the functional monomers and the template in DMSO was kept under stirring for 1h at room temperature in order to favor the formation a complex functional monomer-template. The ratio used between functional monomer and the template was fixed at 1:1.2 (fm:t). A little excess of the template was used in order to obtain a high number of specific binding sites, assuming a 1:1 monomer: template interaction. The aim of this step is to favor the formation of monomer-template complexes through non-covalent bonds, allowing the pre-formation of the binding sites that will then be incorporated in the polymeric matrix.

II. Radical Polymerization. After the formation of the complex, the co-monomer, the crosslinker MBA (N,N'-methylenebisacrylamide) and the radical initiator AIBN were added to the solution. The concentration of the crosslinker was fixed to 60%. The use of high percentages of crosslinker is essential to impart the necessary rigidity to preserve the shape and stability of the binding sites formed inside the polymeric matrix. However, polymers with a crosslinker content above 90% lead to too rigid and less flexible polymers[24]. The amount of radical initiator was fixed at 5% of the amount of the available double bonds in the pre-polymerization mixture. The polymerization was carried out at 70°C for 24h and the concentration of initiator and crosslinker were calculated using the following equations:

$$n(I) = [n(fm)+n(bn)+2n(cl)]*\%initiator$$

$$n(cl) = \frac{n(fm) + n(bn)}{\%(fm) + \%(bn)} * \%\ (cl)$$

Where n(I), n(fm), n(bm) and n(cl) are respectively the number of moles of the initiator, the functional monomer, the co-monomer and the crosslinker.

III. Removal of the template. After polymerization yellow and orange solutions were obtained. Removal of the template was carried out by dialyzing the polymers first in water and then in methanol and methanol:acetic acid (8:2). The use of methanol increases the solubility of template molecules and leads to a polymer shrinkage that force the dissociation of the MIP-template complex, while water allows to remove the unreacted functional monomers or by-products and to resume the better polymer conformation.[25]

In table 6.2 are reported the yield of polymerization calculated following the equation:

$$\%yield = \frac{polymer\ weight}{\sum monomer\ weights}$$

Table 6.2. Yield of fMIPs for 5-*O*-caffeoylquinic acid recognition.

Polymer	Template	Functional Monomers	Yield %
MIP01	H-5CQA	4-Vinylpiridine (**4VPy**) 4-[(2-ethylenediamine)N-allyl-1,8-naphthalimide (**16b**)	40
NIP01	-	4-Vinylpiridine (**4VPy**) 4-[(2-ethylenediamine)N-allyl-1,8-naphthalimide (**16b**)	23
MIP02	H-5CQA	4-[(2-ethylenediamine)N-allyl-1,8-naphthalimide (**16b**)	12
NIP02		4-[(2-ethylenediamine)N-allyl-1,8-naphthalimide (**16b**)	4

6.4 .^{1}H-NMR Characterization of fMIPs.

Polymerization was verified by ^{1}H-NMR spectroscopy. For this purpose, 2mg of the polymers were dissolved in 750 µL of DMSO-d_6. The resulting spectra did not show any signals corresponding to the H-5CQA, indicating the complete removal of the template from the polymer binding sites during the dialysis process. In **Figure 6.9** the ^{1}H NMR for **MIP01** is reported where it can be observed the set of signals in the range between 6 and 8 ppm corresponding to the amide groups and to the aromatic protons of monomers **16b** and **4VPy,** which when incorporated into the polymeric matrix generate a broad signal. Other signals can be observed in the

range 1 -4 ppm, which are generated by the aliphatic protons of the polymer. Signals between 3 and 4 ppm are due to the CH_2-N protons while signals between 1.5 and 2.5 ppm can be associated to α and β protons to amide groups.

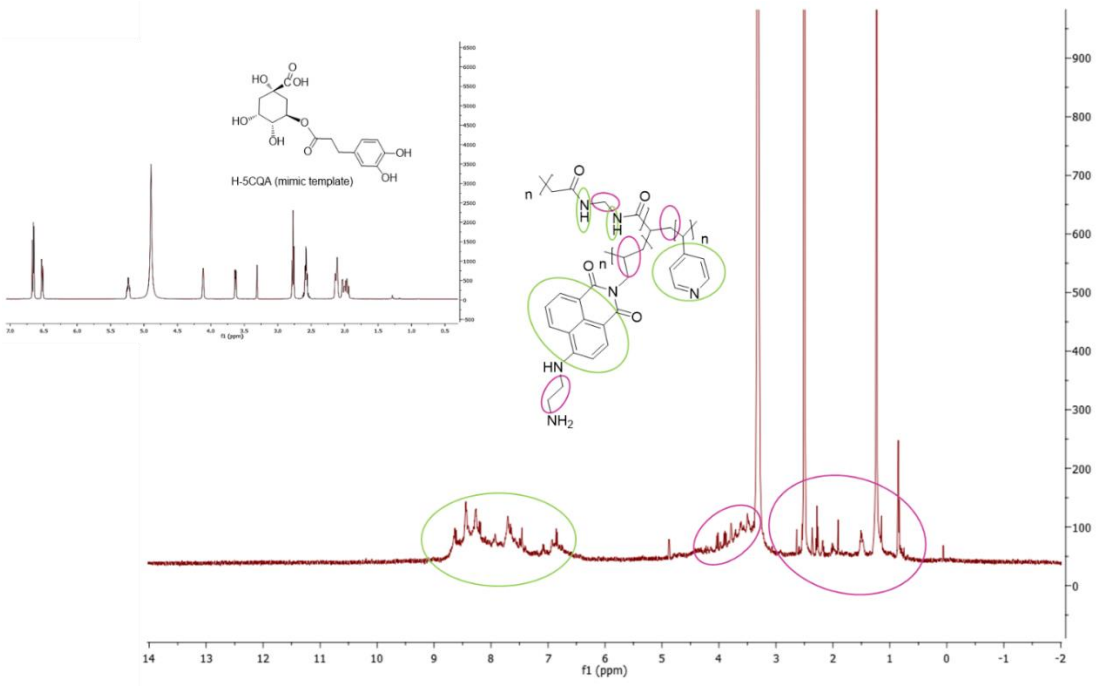

Figure 6.9. ^{1}H-NMR spectrum of MIP01. Insert: ^{1}H-NMR spectrum of H-5CQA.

6.5. Monomer Dye content

The amount of the monomer dye **16b** incorporated into the polymers MIP01 and MIP02 was determined by UV-visible spectroscopy. UV-visible absorption of the polymers and the free dye in DMSO did not show any significant change at λ_{max} (440nm), this is an evidence that there were no changes in the basic chromophore dye structure as a result of its bonding to the polymer chain, making possible the construction of a calibration curve in DMSO of free dye **16b** (**Figure 6.10**). [26]

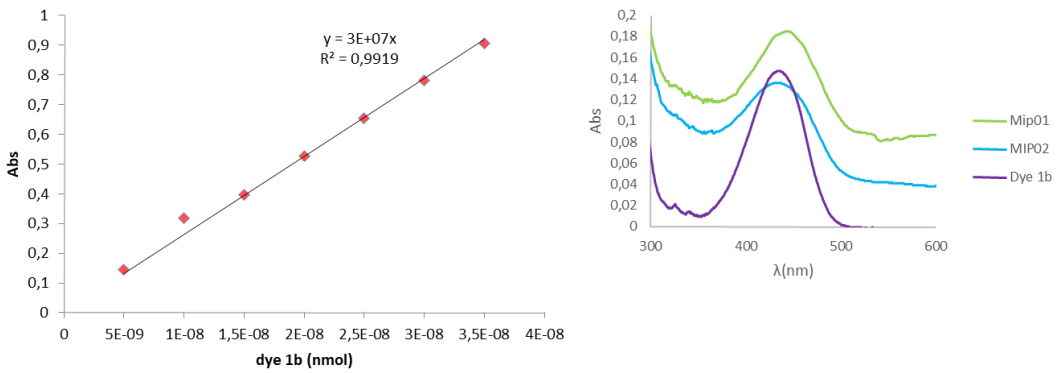

Figure 6.10. Calibration curve of Dye **16b** and UV spectra of dye **16b** (purple), **MIP01** (green) and **MIP02** (blue).

UV spectrum of polymers solutions in DMSO were recorded. For polymers MIP01 and NIP01 stock solutions at concentration 630 µg/mL and 473 µg/mL were prepared and then spectrum of 500 µL of 1:2 diluted solutions were recorded, while for polymers MIP02 and NIP02 solutions at 200 and 193 µg/mL were prepared and directly analyzed**.** The maxima of the absorbance were corrected considering the perturbation in the baseline observed for the solutions of the polymers (**Figure 6.10**) and not in the spectra of the free monomer, which is a characteristic behavior of the scattering in colloidal solutions.[27] Corrected values of absorbance intensity at 440nm were used to quantify the functional monomer covalently bonded into the polymer. Concentration values are reported in table 6.3

Table 6.3. Amount of monomer **16b** in the polymers.

Polymer	Polymer Concentration (µg/mL)	Mean Intensity (Abs)	Mean Intensity Corrected (Abs)	16b (nmol/mg polymer)
MIP01	630	0.185	0.098	20.60
NIP01	473	0.141	0.091	19.20
MIP02	200	0.136	0.098	32.6
NIP02	193	0.13	0.090	30

As can be noticed in table 6.3, there are not significant differences between the **16b** content between MIP and the corresponding NIP in both polymers. Monomer content in MIP02 was higher than in MIP01 and this could be due to the presence of 4VPy in MIP01 which could have a higher polymerization rate and compete for the binding sites in the polymer. Furthermore, as already reported in the literature for other polymers containing 1,8-naphtalimides moieties,[28] less than 5% of the free dye was incorporated into the polymers indicating that not all the monomers polymerized. This could be explained if side reactions between the monomer **16b** and other components of the polymers are taking place which could interfere with the polymerization process.

6.6 Recognition of the Target: Rebinding tests by UHPLC.

Polymers absorption capacity was calculated by performing rebinding tests: a mixture of 80 µM of 5-CQA and 1mg/mL of the prepared fMIP in water was prepared and left under stirring. At fixed intervals, an aliquot of the mixture was centrifuged and the supernatant was analyzed to quantify the concentration of free analyte (5-CQA). Quantification was performed by means of UHPLC method already developed for the analyses of CGAs (see chapter 4).[29] The absorption capacity, which mean the amount of analyte captured by MIP and NIP for mg of polymer was calculated following the equation:

$$Q = \frac{(Co - Cs)V}{W}$$

Where:

Q is the absorption capacity in moles of captured analyte/mg of polymer; C_o and Cs are the initial and the equilibrium concentrations of the target molecule in solution, respectively; V is the volume of the solution and W is the weight (mg) of the polymer.

Fluorescent molecularly imprinted polymer MIP01 showed a good affinity for 5-CQA, binding 48nmol after few minutes of incubation and achieving the saturation point after 90min. However, NIP01 did not show any significant differences with respect to the binding affinity of MIP01. This tendency could probably indicate that the interactions between functional monomers and template occur in a very similar way between both imprinted and non-imprinted polymers with a prevalence for the non-specific interactions. Other molecularly imprinted polymers reported in the literature, using a mimic template, have shown similarly favorable performances between MIPs and NIPs indicating that the imprinting binding sites play a minor role in selective target detection.[30] On the other hand, MIP02 showed a very low affinity for 5-CQA with respect to MIP01, recovering only 8nmol after 60 min, which could demonstrate the key role of the **4VPy** in establishing the right interactions with the template within the polymeric matrix (**Figure 6.11**).

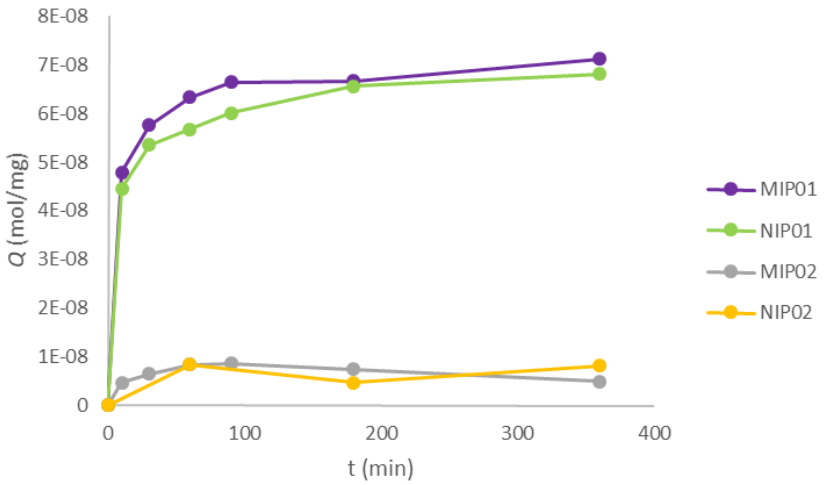

Figure 6.11. Rebinding kinetics of 5-CQA with MIP01 and MIP02 and NIP01 and NIP02

- **Imprinting Factor**

The normalization of the imprinting process removes non-specific binding interactions between monomers and the template[31] and the efficiency of this process can be evaluated by calculating the imprinting factor (*IF*), which is defined as the ratio between the binding capacity of the fMIPs and that of the corresponding fNIPs. Since the same formulation was used for preparing MIPs and NIPs we can assume that the number of functional monomers incorporated into the fMIPs and fNIPs are the same:

$$IF = \frac{Q_{fMIP}}{Q_{fNIP}}$$

Where Q_{MIP} and Q_{NIP} are the absorption capability of the imprinted and non-imprinted polymers.

The values of IF and the binding capacities of the polymers studied in this project are summarized in table 6.4. From the values obtained it is evident the increase of non-specific interactions within a time of 180 min (IF= 1.02), when the binding capacity between MIPs and NIPs are the same. MIP02 showed the highest binding capacity after 180 minutes, however, after this period it starts releasing the template with a higher rate than the non-imprinted polymer.

Table 6.4 Rebinding capabilities and selectivity of fMIPs synthesized for 5-CQA

Polymer	**Functional Monomer**	**Rebinding (QMIP) [nmol mg^{-1}]**			**IF**		
		60 min	**90 min**	**180min**	**60min**	**90 min**	**180min**
MIP01	(**4VPy**) (**16b**)	63.3	66	74.3	1.1	1.10	1.02
MIP02	(**16b**)	7.9	/	7.8	1.00	/	1.6

6.7 Cross Reactivity: Analysis by UHPLC

The selectivity of MIP01 and NIP01 for the analyte 5-CQA were analyzed by carrying out rebinding tests with a mixture of free hydroxycinnamic acids such as caffeic and coumaric acid as well as with caffeine. As it was described in the previous section, the tests were carried out treating a solution of 1mg/mL of polymer with a mixture of 80µM of each pure standard of 5-CQA, caffeic acid (CA), *p*-coumaric acid (*p*CoQA) and caffeine (CAF). The remaining standard concentrations in solution were measured by UHPLC after different incubation times.

MIP01 was able to capture 5-CQA, CA and *p*-CoQA and unable to bind caffeine. The cinnamic part of the 5-CQA is formed by CA, which only differs from *p*-CoQA structure by the presence of two phenolic hydroxyl groups instead of one, so these molecules could have access to the binding sites of the polymeric matrix and can be recognized by the polymer. However, as it can be observed from **Figure 6.12**, during the first minutes of incubation, MIP01 showed a higher affinity towards 5-CQA. After 60 min of incubation MIP01 was able to capture 69nmol/mg of target molecule 5-CQA, 20% more than caffeic acid and 37% more than *p*-coumaric acid. Moreover, no release of the target molecule was observed after 24 hours.

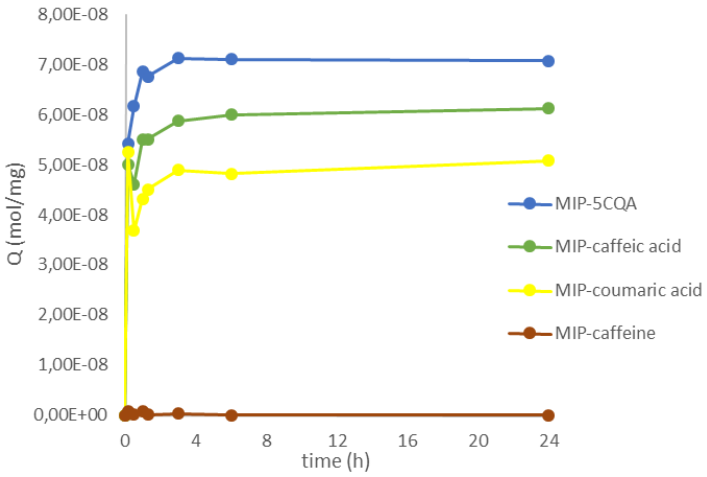

Figure 6.12 Rebinding kinetics of 5-CQA, CA, *p*CoQA and CAF with MIP01.

When comparing the binding capacity of MIP01 and NIP01 (**Figure 6.13**), it is evident that although the non-imprinted polymer shows the same high binding capacity towards the target molecule during the first minutes of incubation as the imprinted polymer, NIP01 is also capable of capturing higher concentrations of caffeic and *p*-coumaric acid with increasing the incubation time. In fact, after 60min, the non-imprinted polymer was able to capture 1.5% more caffeic acid and 14% more *p*-coumaric acid than the imprinted polymer. But, the most significant difference between the two polymers can be observed after 24 hours, when the NIP01 shows the same affinity for both chlorogenic acid and caffeic acid, capturing 120nmol of each secondary metabolite. Moreover, the non-imprinted polymer was able to capture a maximum of 95 nmol of *p*-coumaric acid while MIP01 captured 76nmoles after 24 hours. As can be noticed, despite the low value recorded for the imprinting factor (IF), the imprinted polymer shows a good selectivity for the analyte, this better performance of polymer MIP01 is due to the presence of specific binding sites capable of recognizing the analyte that are absent in NIP01. For this reason, the fluorescence changes of the imprinted polymer when interacting with the template was evaluated and the results will be discus below.

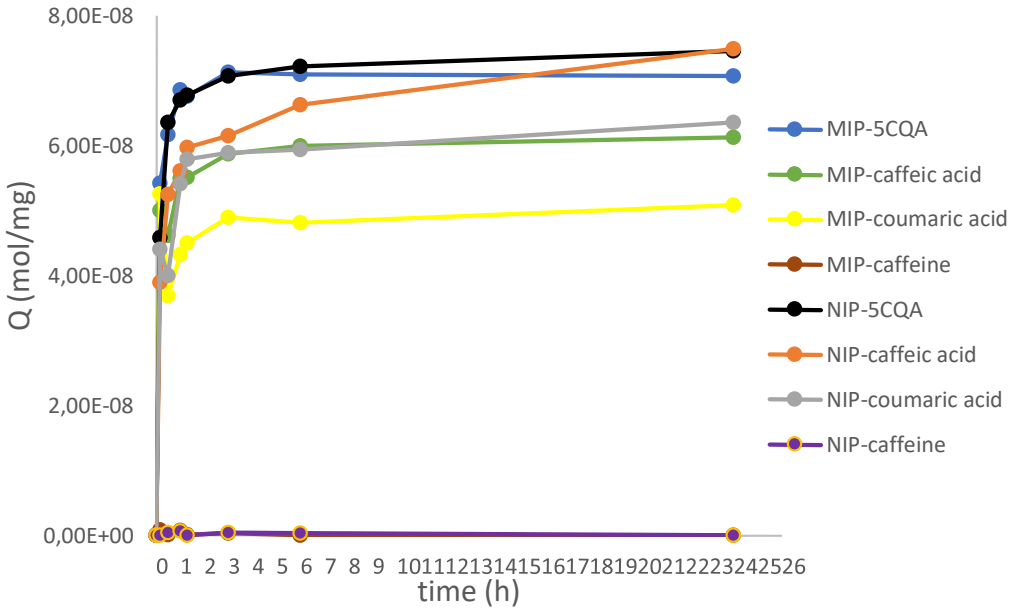

Figure 6.13. Rebinding kinetics of 5-CQA, CA, *p*CoQA and CAF with MIP01 and NIP01

6.8. Fluorescent Properties of MIPs.

1,8-napahtalimides have been designed based on the model "fluorophore-spacer-receptor"[32] (**Figure 6.14**) and in monomer **16b,** the primary amino group at the end of the spacer chain, with its lone pair of electrons, acts as the receptor, while the N-allylic group acts as the linker with the polymeric matrix. Fluorescent properties of naphtalimide derivatives are very sensitive to the environment and depend on the medium and polarization of the naphtalimide molecules.[10]

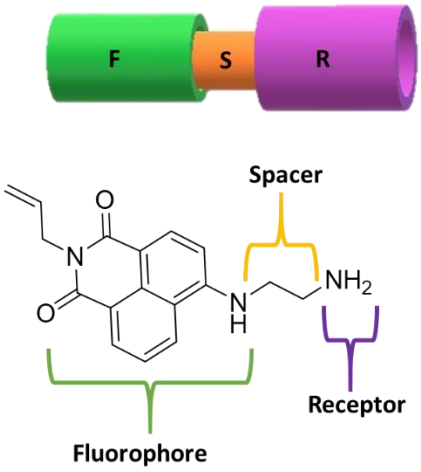

Figure 6.14. Model representation of the "fluorophore-spacer-receptor" of 1,8-napahtalimides dyes.

These dyes are known as "off-on" or "on-off" fluorescent switches and they have been widely used in the development of PET (photoinduced electron transfer) sensors in which the electron transfer goes from the receptor to the excited state of the fluorophore.[33] Several reports have demonstrated how fluorescence of

these type of dyes is quenched and quickly switched ″on″or ″off″by recognition of protons or different metal ions. Therefore, the spacer must be short enough to allow fast PET rates between the two states of the sensor. In the "on" state enhancement of the fluorescent due to the excitation of the fluorophore occurs because the PET process is arrested by the recognition of the analyte for the receptor while, in the ″off″state PET process takes places quenching the fluorescent[32,34,35,36.] (**Figure 6.15**). It is important to consider that in PET ideal system the quenching of the fluorescent must not cause any change or at least not any significant change in the absorption spectra with respect to the free monomer under the same conditions,[37] which was previously demonstrated (**Figure 6.10**)

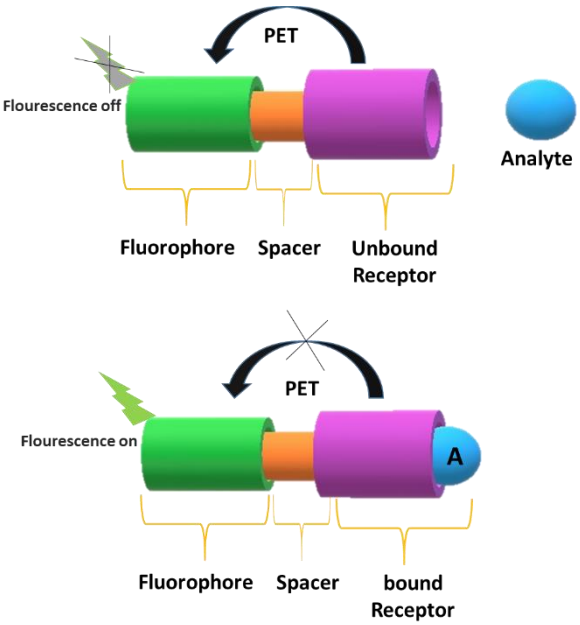

Figure 6.15 Representation of a switch “on” and switch “off” system.

Fluorescent properties of polymers MIP01 and MIP02 were evaluated by studying the interactions between the fMIPs and the target molecule (5-CQA). Changes in the polymer fluorescence at low concentrations were registered by fluorescence titration of the polymers with increasing amounts of the analyte in two different solvents: DMSO and water:DMSO (9:1).

As a first choice, titrations were carried out by adding increasing amounts of the analyte 5-CQA from micromolar to milimolar concentrations to a solution of 30 µg/mL in DMSO of the polymer. **Figure 6.16** shows the emission spectra of polymer MIP01 at increasing concentrations of 5-CQA. A 3-fold increase in fluorescent intensity at the emission maximum of 530 nm was observed with the addition of the analyte. The mechanism for the fluorescence enhancement is probably the hydrogen transfert between the carboxilic gruop of the analyte and the amino group of the monomer **16b,** so PET communication between the receptor and the fluorophore is not thermodinamically favored and gets cuttoff since the lone pair of electrons of the receptor are not longer available after recognition of the analyte. As it has been reported in the literature, in these

type of "off-on" systems, protons from the analyte electrostatically attracts the electrons increasing the oxidation potential of the analyte-bound receptor.[32,38]

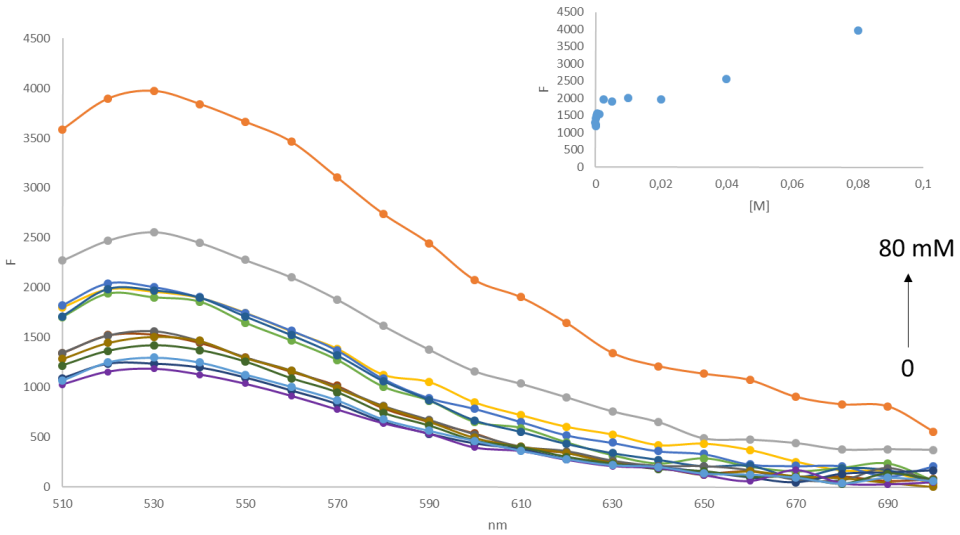

Figure 6.16 Fluorescent emission titration spectra of MIP01 in DMSO after addition of 5-CQA.

Following the same approach, titrations were carried out using the same concentration of polymers (30 µg/mL) in water:DMSO (9:1) and a quenching of the fluorescence was observed in both cases MIP01 and MIP02 (**Figure 6.17**). As expected, the intensity of the fluorescence is greater for the polymer MIP02 since, according to the results shown above, this polymer has a higher concentration of fluorescent monomer. MIP01 and MIP02 showed a decrease in fluorescence of 58% and 6% respectively, by adding a 39µM solution of the analyte, while both polymer achieve a total quenching of 92% at a final concentration of 80 mM of the target molecule.

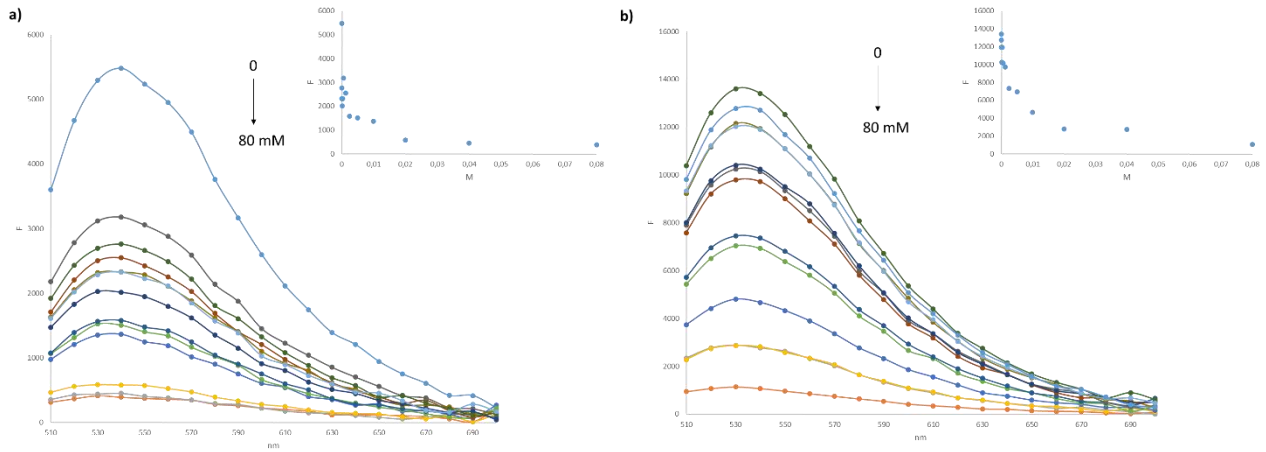

Figure 6.17. Fluorescent emission titration spectra of: **a)** MIP01 and **b)** MIP02 in water:DMSO (9:1) after addition of 5-CQA.

As can be observed in **Figure 6.17** the emission maxima were registered at 540 nm and the bathochromic shift with respect to the system in DMSO is a consequence of the $\pi \rightarrow \pi^*$ internal electron transfer transitions (ITC) that has been already observed for these type of dyes when the polarity of the solvent increases.[5] A possible explanation for the quenching is that, in presence of water, the receptor of the dye (amino group) can be protonated, cutting off the PET process, which means that the system has been switched "on" prior to the recognition event. Therefore, considering the molecular orbital energy diagram (**Figure 6.18**), PET mechanism takes place when the free electron pair of the receptor (amino group) are transfer to the partially unoccupied HOMO orbital of the photoexcited fluorophore. Then, Back-electron transfer occurs from the excited state of the fuorophore to the HOMO of the receptor, which generate a deactivation of the excited state, and fluorescence is quenched ("off" state). when, the analyte binds to the receptor, the PET is interrupted and fluorescence is turned "on" due to the stabilization of the orbital HOMO of the analyte bound receptor, which lies below the HOMO of the fluorophore.[10,37,39]

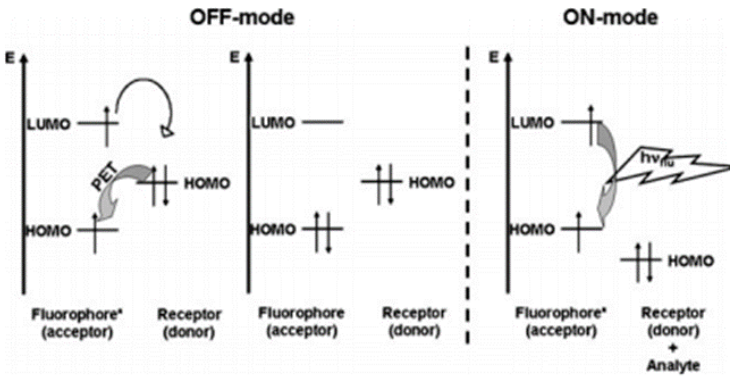

Figure 6.18. Molecular orbital energy diagrams for relative energetic dispositions of HOMO/LUMO of the fluorophore and HOMO of the donor involved in PET. The asterisk (*) symbolizes the excited fluorophore [39]

The decrease in fluorescence can be a consequence of two possible mechanisms known as dynamic or static quenching.

Dynamic quenching or collisional quenching takes place when the fluorophore in its excited state is deactivated by contact with the quencher that diffuses in solution. This process is described by the widely known Stern Volmer equation[40]:

$$\frac{F_0}{F} = 1 + k_q \tau_0 [Q] = 1 + K_D [Q]$$

Where:

F_0 is the fluorescence emission intensity in absence of the quencher [Q]

F is the emission intensity in presence of the quencher.

K_q is the bimolecular quenching constant. K_D is used to indicated a dynamic quenching.

τ_0 is the lifetime of the fluorophore in absence of the quencher. The lifetime (τ_0) is defined as the average time between excitation and return to the ground state, considering that the fluorescent molecule after excitation in absence of the quencher will rapidly return to the ground state by emission of a photon. According to the literature, the emission rates of fluorescence are typically in the order of 10^8 s^{-1}, therefore; a typical lifetime is in the order of ns.

Static quenching occurs when the interaction between the fluorescent molecule and the quencher can lead to non-fluorescent ground state complex. In this mechanism the dependence of fluorescence intensity from the quencher concentration can be calculated considering the association constant of a typical complex formation:

$$F + Q \rightleftharpoons FQ \qquad K_S = \frac{[FQ]}{[F][Q]} \qquad F_0 = [F] + [FQ]$$

$$K_S = \frac{[F_0] - [F]}{[F][Q]} = \frac{[F_0]}{[F][Q]} - \frac{1}{[Q]}$$

Where:

[*F*] is the concentration of the free fluorophore.

[*Q*] is the concentration of the free quencher.

[*FQ*] is the concentration of the complex.

K_S is the association constant and the Stern Volmer constant

Therefore, the Stern Volmer equation for static quenching is described by the following equation[40]:

$$\frac{F_0}{F} = 1 + K_S[Q]$$

The quenching phenomenon observed in water:DMSO for polymer MIP01 and MIP02 were studied by the Stern-Volmer equation, plotting the ratio of the fluorescence emission before and after addition of the quencher (analyte) in function of the quencher concentration. In **Figure 6.19** it can be noticed a bimodal quenching behavior that can be an indication of the presence of non-homogeneous binding sites inside the polymers with different affinity for the chlorogenic acid.

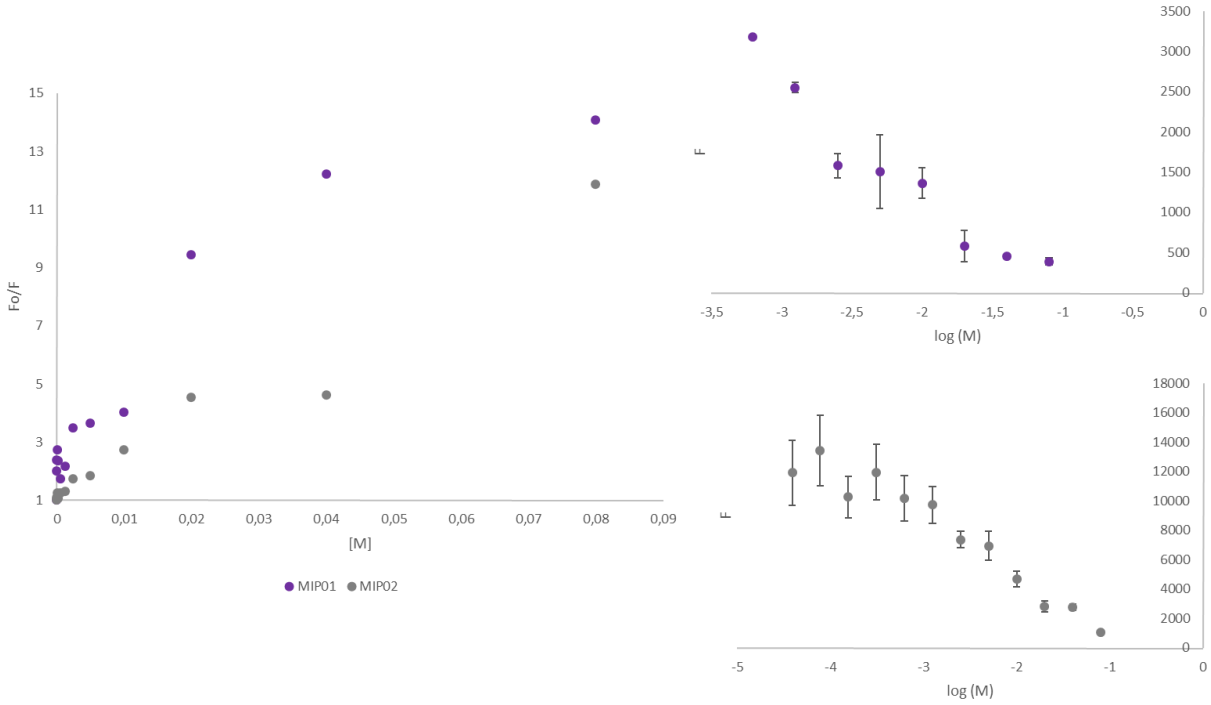

Figure 6.19 Stern-volmer plots of fMIPs for 5-CQA. MIP01 (purple) MIP02 (grey).

The Stern-Volmer equation was applied to the linear region of the plots and the apparent Stern Volmer constant (K^{app}_{sv}) for the non-homogeneous MIP was obtained from the slope of the equation (**Figure 6.20**)

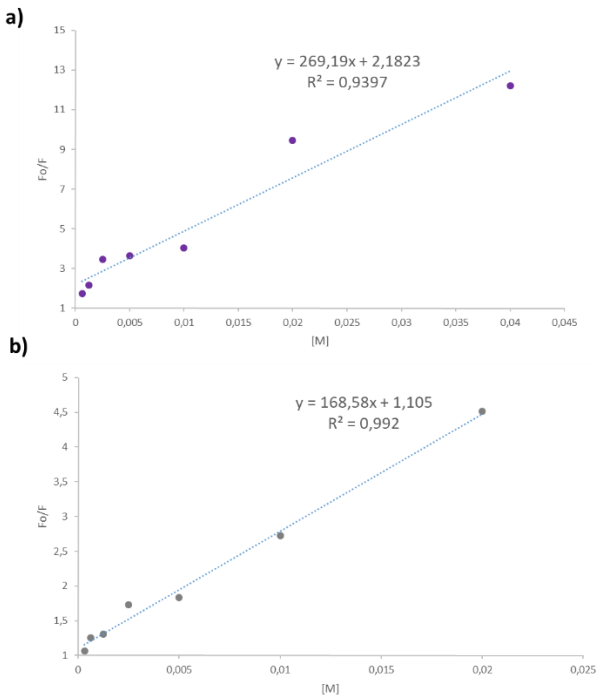

Figure 6.20 Linear regression of Stern-Volmer plots of a) MIP01 and b) MIP02

The bimolecular quenching constant K_q^{app} can be calculated by the equation [34]:

$$k_q^{app} = \frac{K_{SV}^{app}}{\tau_0}$$

K_q^{app} was calculated using the lifetime (τ_0) of an analogue 4-amino substituted naphtalimide monomer used to develop fMIPs to respond to carboxylate-containing guests. The reported τ_0 of this molecule in DMSO corresponds to 0.11ns.[41] Values of K^{app}_{sv} and K_q^{app} are reported in table 6.5.

Table 6.5 Apparent Stern-Volmer and quenching constants of MIP01 and MIP02

Polymer	K_{sv}^{app} [10^2 L·mol^{-1}]	K_q^{app} [10^{12} L·mol^{-1}s^{-1}]
MIP01	2.7	2.4
MIP02	1.7	1.5

According to the literature, quenching constants (K_q) with values below $1{\cdot}10^{-10}$ L·mol^{-1}s^{-1} are found for dynamic interaction mechanisms, while higher values of K_q suggest that a static mechanism is taking place.[34,40,42] In our case, since K_q^{app} for both fMIPs are higher than the limit value for the diffusion controlled quenching ($1{\cdot}10^{-10}$ mol^{-1}L^{-1}s^{-1}), the observed quenching of the polymer fluorescence with the presence of the analyte can be considered as the result of a static interaction and K^{app}_{sv} can be considered as an apparent association constant between the population of fluorophores in the MIP and the quencher. It is worth noting, that even though a slightly higher quenching constant (K_q^{app}) was found for MIP01, MIP02 showed a wider linear region at lower concentrations, 78µM compared to 625µM for MIP01, which could be the result of the presence of more homogeneous binding sites since the incorporation of 4-vinylpyridine in MIP01, which is able to interact with the analyte and could generate non-homogenous sites with different affinities for the analyte.

6.9 Determination of Particles Size: Dynamic Laser Light Scattering (DLLS) Measurements.

DLLS is a technique used to measure the particle size from 0.3 nm to 10 microns. The instrument consists of a laser beam that illuminates a particle suspension and measures their size by analyzing the fluctuations intensity in the light scattered during their Brownian motion. The Brownian motion consists in the movement of particles due to the random collision with the molecules of the liquid that surrounds the particles. Therefore, small particles will move quickly, while large particles will move slowly. The speed of the motion is defined by the translational diffusion coefficient (D) from the Stokes-Einstein equation:

$$d(H) = \frac{KT}{3\pi\eta D}$$

Where: d (H) is the hydrodynamic diameter, D is the translational diffusion coefficient, k is the Boltzmann constant, T is the temperature in Kelvin and η is the viscosity of the fluid. The diameter measured by the DLS technique is known as hydrodynamic diameter because the value refers to the way in which particles move in the fluid. There are several factors that can influence the Brownian motion such as the ionic strength of the medium, the surface structure and the shape of the particles. Moreover, conformational changes of polymeric macromolecules can determine a variation in Brownian motion that also affects the value of the hydrodynamic diameter.

If a small particle is illuminated by a light source such as a laser, the particle will scatter the light in all directions (isotopic dispersion of Rayleigh). In a sample containing thousands of particles, the incident laser beam produces the light scattering of particles leading to a speckle pattern in the screen. The speckle pattern will show some bright and dark areas, created by constructive or destructive interactions between different waves propagated from the particles.[43] Constructive interference occurs when the waves arrive to the screen with the same phase, leading to bright patch, while if the waves have different phases, dark areas are observed in the speckle due to a destructive interaction. When the particles move around the sample, the constructive and destructive phase addition of the scattered light will cause the bright and dark areas to grow and diminish in intensity leading to a fluctuating speckle. The instrument measures the rate of this fluctuation intensity allowing the determination of the particles size. A digital correlator is able to measure the degree of similarity between two signals over a very short period of time (from 1 to 10 milliseconds). The intensity of the light scattered from different particles becomes even more different during the time, leading to an exponential decrease of the correlation in function of the time.[44]

The DLS analyses provides the dynamic information obtained by recording the scattering intensity evaluated through an autocorrelation function of the speed which records data varies over time. The size distribution by intensity shows the relative intensity of the scattered light in function of the particles size in nanometers. This size distribution by intensity could also be converted in distribution by volume using Mie theory.[45] Algorithms are used by the instrument software to obtain a particle size distribution from the decay rates of the correlation function measured from the sample.[46]

The particle size of MIP01 and NIP01 were determined using particles suspensions of 0.25 mg/mL for MIP01 and 0.5 mg/mL for NIP01 in DMSO. Measurements were performed after sonication for 30min and filtration on 0.45µm filter.

As can be observed in **Figure 6.21**, the size distribution by intensity show the presence of two populations of particles of 1 nm and 100 nm and 10 nm and 100nm for the imprinted and non-imprinted polymer, respectively, while in the size distribution by volume only one peak corresponding to particles of around 1 nm size is visible for MIP01 and 10 nm for NIP01. This tendency could be explained if we consider that large

particles scattered the light more intensely than small particles, as explained by Rayleigh scattering equation where the intensity of a particle is related to the 6th power of the diameter[47]:

$$I = I_o \frac{1 + cos^2\theta}{2R^2}\left(\frac{2\pi}{\lambda}\right)^4 \left(\frac{(n^2-1)}{(n^2+2)}\right)^2 \left(\frac{d}{2}\right)^6$$

Where:

λ is wavelength of the light

I_o is the intensity of the beam of light

Θ is the scattering angle

R is the distance between the particle and the detector

n is the refractive index of the particle and d is the diameter of the particle

For instance, a sample containing an equal number of particles of 5 nm and 50 nm, in the size distribution by intensity graph, the peak corresponding to 50 nm size population will be 10^6 higher than the one with5 nm size. On the contrary, in the size distribution by volume, the peak corresponding to 50 nm size will be 10^3 higher than the one with 5 nm size because the distribution by volume is obtained from the distribution by intensity considering the volume of one sphere (V):

$$V = \frac{4}{3}\pi r^3$$

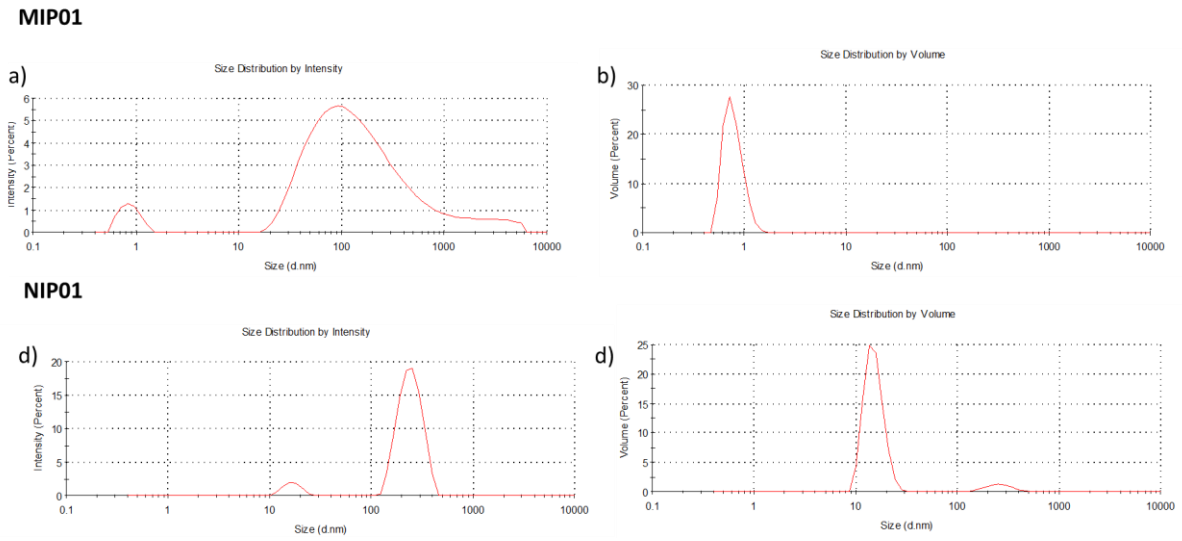

Figure 6.21 Measurements by DLLS: **a)** size distribution by intensity of MIP01, **b)** size distribution by volume of MIP01, c) size distribution by intensity of NIP01 and d) size distribution by volume of NIP01.

The results obtained indicated the presence of a large population of 1nm size for MIP01 and 10nm size for NIP01. The presence of a very intense signal at 100 and 200 nm for MIP and NIP respectively, in the size

distribution by intensity, suggests the presence also of a few particles that could correspond to aggregates. This tendency of the polymer to aggregate can be due to the presence of 4-Vpy as well as to other polar groups in the polymeric matrix, since the formation of aggregates in polymers in which 4-Vpy is present has been already reported in the literature[48]. Table 6.6 shows the particle size of MIP01 and NIP01.

Table 6.6 Particle sized of MIP01 and NIP01 measured by DLLS.

Polymer	Concentration	Solvent	Particle size (nm)
MIP01	0.25mg/mL	DMSO	0.82
NIP01	0.5mg/mL	DMSO	18.85

6.10 Towards the development of an optical sensor: Immobilization of the fMIP

In the previous section it was demonstrated that fluorescence emissions of the fMIPs can be deactivated (switched "off") or activated (switched "on") depending on the environment thanks to the PET mechanism which occurs in the presence of the isomer 5-CQA. These fluorescence properties can be exploited for developing an optical sensor; therefore, MIP01 was chosen as the potential fluorescent recognition element and an immobilization test was performed in order to evaluate the response of the polymer towards the analyte. Although one of the main issues in using MIPs for sensor development is the lack of chemical methods that allow MIPs to be fixed on transducer surface they can be temporally or permanently immobilized on insoluble supports.[49,50] This means that their mobility can be restricted either by covalent bonding or adsorption to the support.[51,52] Since physical entrapment of MIPs into gels or membranes has been previously reported in the literature for their use as electrochemical transducer,[53] the fluorescent polymer MIP01 has been physical entrapped into a gelatin gel covalently bonded to a functionalized support.

The entrapment has been carried out using a suspension of 100 µg/mL of the MIP01 in water:DMSO (9:1) and a solution of 20mg/mL of gelatin which were mixed together in a ratio 1:1 and immobilized on a poly-lysine glass support using glutaraldehyde (GA) as a bifunctional crosslinking agent. (**Figure 6.22**)

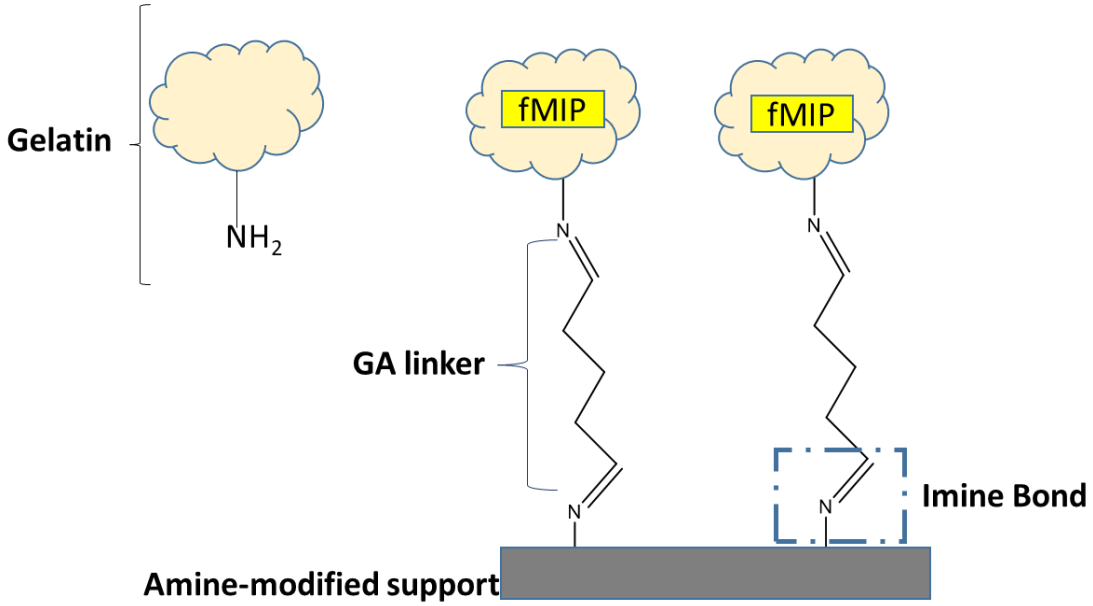

Figure 6.22. Schematic representation of fMIP immobilization

Gelatin is a bio-macromolecule obtained by the hydrolysis of collagen mostly from skin and connective tissue of animals. Because of the gel-forming property at around 35°C of gelatin and its versatility in the amino acid composition it has been widely used not only as a stabilizer, emulsifier and clarifying agent but also as a protective coating material.[54,55] Moreover, due to its low cost and efficiency in the stabilization of collagenous materials, GA is the most widely used cross-linking molecule. The mechanism of the covalent bond formation between the gelatin and the GA is greatly depending upon pH conditions and it has been extensively reported in the literature[54] (**Figure 6.23**). The reaction takes place through a nucleophilic addition of the non-protonated amino groups (-NH_2) of lysine to the carbonyl groups (C=0) of the aldehyde to allow the formation of a tetrahedral unstable carbinolamine intermediate. Then, conjugated Schiff bases are formed by protonation of the -OH groups and the loss of a water molecule. The new covalent bonds can be either intramolecular (short-range) or intramolecular (long-range) which are the result of the polymerization of glutaraldehyde or aldol condensation reaction.

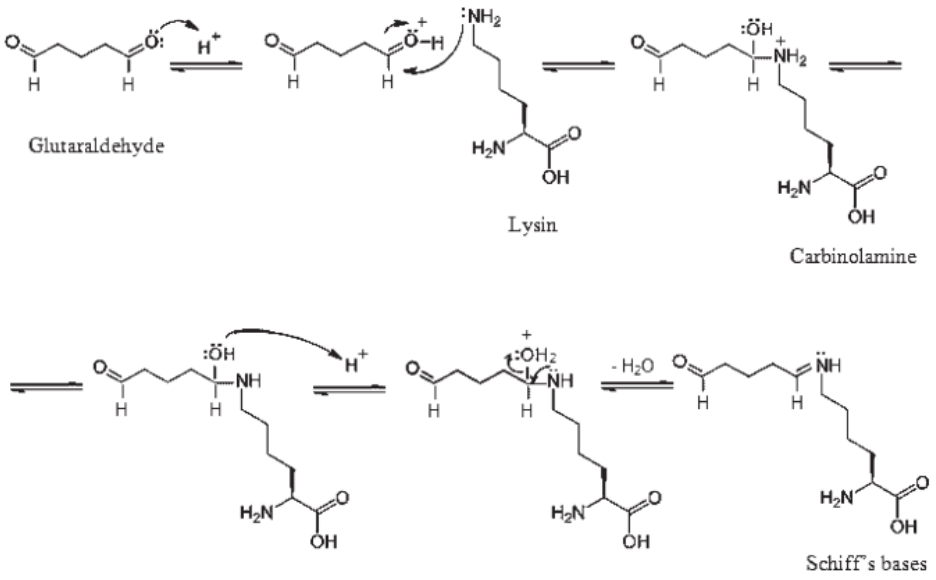

Figure 6.23 Reaction mechanism between amino groups of lysine and carbonyl groups of glutaraldehyde[54].

The residual immobilized concentration of the fluorescent polymer was estimated by calculating the ratio between the initial fluorescent intensity and the intensity after washing the glass plates with water at 540nm of different polymers solutions immobilized on fifteen different poly-lysine plates in different times. Mean values are reported in table 6.7 and as can be noticed about 70% of the initial polymer concentration remains on the plates.

Table 6.7 Fluorescent intensities of immobilized MIP01.

Initial MIP concentration (µg/mL)	F intensity before washing (STD)	F intensity after washing (STD)	Immobilized MIP concentration (µg/mL)
100	39453.17 (6437.04)	27941(5766)	71

Once the polymer was immobilized, the fluorescence properties of the polymer were evaluated by carrying out titrations, in duplicate, with increasing concentrations between 78 µM and 80mM of a standard solution of 5-CQA. The fluorescence emission of the fMIP was measured at 540nm when excited at 480nm before and after incubation for 90min. The fMIP fluorescence resulted in a correlated quenching in a range from 156 µM to 40mM of the analyte. (**Figure 6.24**).

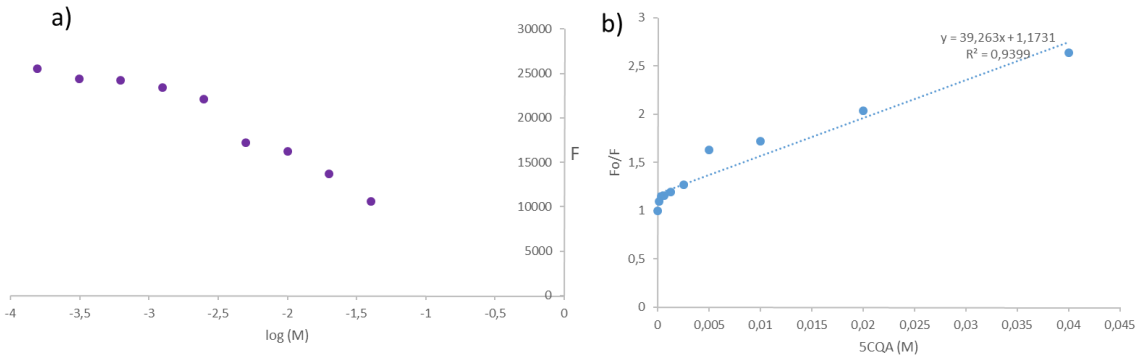

Figure 6.24. **a)** Preliminary calibration curve of immobilized MIP01 with 5-CQA. **b)** Stern-volmer plots of immobilized fMIP01 for 5-CQA.

From the slope of the equation in the Stern-Volmer plot the apparent quenching constant was calculated as described in the previous section and the obtained value is $3.5 \cdot 10^{11}$ $L \cdot mol^{-1}s^{-1}$. Although this value indicates that a static quenching is taking place, the significantly lower value of the apparent Stern Volmer constant (39 $L \cdot mol^{-1}$), with respect to the one obtained carrying out the titrations in solution (270 $L \cdot mol^{-1}$), could indicate a lower or non-specific binding affinity of the polymer for 5-CQA. This result could be a consequence of some diffusion kinetic problems due to the difficulty of depositing a uniform layer of polymer on the glass surface.[56] For this reason, it is important that parameters such as the concentration of gelatin and crosslinker as well as the ratio gelatin: polymer must be carefully optimized in order to improve the fMIP affinity toward the target molecule to afford a better sensitivity. However, although these first attempts could not be optimized at the moment, the results obtained open the possibility to use MIP01 as a recognition element in an optical sensor for determining the CGA concentration.

[1]Hu, Y.; Pan, J.; Zhang, K.; Lian, H.; Li, G. Novel applications of molecularly-imprinted polymers in sample preparation. *Trends Anal. Chem*., **2013**, 43, 37-52.
[2] Ji, W.; Zhang, M.; Yan, H.; Zhao, H.; Mu, Y.; Guo, L.; Wang, X. Selective extraction and determination of chlorogenic acids as combined quality markers in herbal medicines using molecularly imprinted polymers based on a mimic template. *Anal. Bioanal. Chem.*, **2017**, 409, 7087-7096.
[3] Scorrano, S.; Mergola, L.; Del Sole, R.; Vasapollo, G. Synthesis of molecularly imprinted polymers for amino acid derivates by using different functional monomers. *Int. J. Mol. Sci.*, **2011**, 12, 1735-1743.
[4] Puoci, F.; Gereffa, C.; Iemma, F.; Muzzalupo, R.; Spizzirri, U. G.; Picci N. Molecularly imprinted solid phase extraction for detection of sudan I in food matrices. *Food Chem.*, **2005**, 93, 349-35.
[5] Konstantinova, T. N.; Miladinova, P. M. Synthesis and properties of some fluorescent 1,8-naphthalimide derivatives and their copolymer with methyl methacrylate. *J. Appli. Polym Sci.,* **2008,** 111, 1991-1998.
[6] Syu, M. J.; Hsu, T. J.; Lin, Z. K. Synthesis of recognition matrix from 4 -Methylamino-N-Allylnaphthal-Imide with fluorescent effect for the imprinting of creatinine. *Anal. Chem*., **2010**, 82, 8821–8829.
[7] Qu, Y.; Wang, L.; Wu, J.; Rui, Y.; Cao, J.; Xu, J. 4-Phenyl-1,8-naphthalimides: Brightness and tuning emission over widely visible gamut in different aggregated states. *Dyes and Pigments*, **2018**, 148, 99-107.
[8] Shi, J.; Wang, Y.; Tang, X.; Liu, W.; Jiang, H.; Dou, W.; Liu, W. A colorimetric and fluorescent probe for thiols based on 1, 8-naphthalimide and its application for bioimaging. *Dyes and Pigments*, **2014,** 100, 255-260.

[9] Choi, S. A.; Park, C. S.; Kwon, O. S.; Giong, H.K.; Lee, J.S.; Ha T.H.; Lee, C.S. Structural effects of naphthalimide based fluorescent sensor for hydrogen sulfide and imaging in live zebrafish. *Scientific Reports*, **2016**, 6,1-10
[10] Rouhani, S.; Nahavandifard, F. Molecular imprinting-based fluorescent optosensor using a polymerizable 1,8-naphthalimide dye as a florescence functional monomer. *Sensors and Actuators B*, **2014**, 197, 185–192.
[11] Svenson, J.; Karlsson, J. G.; Nicholls, I. A. ^{1}H Nuclear magnetic resonance study of the molecular imprinting of (-)-nicotine: template self-association, a molecular basis for cooperative ligand binding. *J. Chromatogr. A*, **2004**, 1024, 39-44.
[12] Athikomrattanakul, U.; Katterle, M.; Gajovic-Eichelmann, N.; Scheller, F. W. Development of molecularly imprinted polymers for the binding of nitrofurantoin. *Biosens. Bioelectron*., **2009**, 25, 82-87.
[13] Hirose K. A pratical guide for the determination of binding constants. *J. Incl. Phenom. Macroc. Chem.*, **2001**, 39, 193-209.
[14] Kleckner, I. R.; Foster, M. P. An introduction to NMR-based approaches for measuring protein dynamics. *Biochim. Biophys. Acta,* **2011**, 1814, 942-968.
[15] Quaglia, M.; Chenon, K; Hall, A. J.; De Lorenzi, E.; Sellergren, B. Target analogue imprinted polymers with affinity for folic acid and related compounds. *J. Am. Chem. Soc*., **2001**, 123, 2146-2154.
[16] Dai, Z.; Liu, J.; Tang, S.; Wang, Y.; Wang, Y.; Jin, R. Optimization of Enrofloxacin-Imprinted Polymers by Computer-Aided Design. *J. Mol. Model*., **2015**, 21, 1-9
[17] Powell, E.; Lee, Y.-H.; Partch, R.; Dennis, D.; Morey, T.; Varshney, M. Pi-Pi Complexation of Bupivacaine and Analogues with Aromatic Receptors: Implications for Overdose Remediation. *Int. J. Nanomedicine,* **2007**, 2, 449–459.
[18] Carboni, D.; Flavin, K.; Servant, A.; Gouverneur, V.; Resmini, M. The first example of molecularly imprinted nanogels with aldolase type I activity. *Chem. Eur. J*, **2008**, 14, 7059-7065.
[19] Flavin, K.; Resmini, M. Imprinted Nanomaterials: A New Class of Synthetic Receptors. *Anal. Bioanal. Chem*. **2009**, 393, 437–444.
[20] Graham, N. B.; Cameron, A. Nanogels and microgels: The new polymeric materials playground. *Pure. App. Chem.*, **1998**, 70, 1271-127.
[21] Pasetto, P.; Maddock, S. C.; Resmini, M. Synthesis and characterisation of molecularly imprinted catalytic microgels for carbonate hydrolysis. *Anal. Chim. Acta*, **2005**, 542, 66-75.
[22] Hien Nguyen, T.; Ansell, R. J. N-Isopropylacrylamide as a Functional Monomer for Noncovalent Molecular Imprinting: NIPAM, a Monomer for Noncovalent Molecular Imprinting. *J. Mol. Recognit*., **2012**, 25, 1–10.
[23] Wulff, G.; Chong, B. O.; Kolb, U. Soluble single-molecule nanogels of controlled structure as a matrix for efficient artificial enzymes. *Angew. Chem. Int. Ed*., **2006**, 45, 2955- 2958.
[24] Yan, H.; Row, K. H. Characteristic and synthetic approach of molecularly imprinted polymer. *Int. J. Mol. Sci*., **2006**, 7, 155-17.
[25] Lorenzo, R. A.; Carro, A. M.; Alvarez-Lorenzo, C.; Concheiro, A. To remove or not to remove? The challenge of extracting the template to make the cavities available in molecularly imprinted polymers (MIPs). *Int. J. Mol. Sci.,* **2011**, 12, 4327-434.
[26] Sali, S.; Guittonneau, S.; Grabchev, I. A novel blue fluorescent chemosensor for metal cations and protons, based on 1,8-naphthalimide and its copolymer with styrene. *Polym. Adv. Technol*., **2006**, 17, 180-185.
[27] Heirwegh, K.P.M.; Meuwissen, J. A.T.P.; Lontie, R. Selective absorption and scattering of light by solutions of macromolecules and by particulate suspensions. *J Biochem Biophys Methods*, **1987**,14,303-322
[28] Mei, C.; Tu, G.; Zhou, Q.; Cheng, Y.; Xie, Z.; Ma, D.; Geng, Y.; Wang, L. Green electroluminescent polyfluorenes containing 1,8-naphthalimide moieties as color tuner. *Polymer*, **2006**, 27, 4976-4984.
[29] Pellizzoni, E.; Tommasini, M.; Maragon, E.; Rizzolio, F.; Saito, G.; Benedetti, F.; Toffoli, G.; Resmini, M.; Berti, F. Fluorescent molecularly imprinted nanogel for the detection of anticancer drugs in human plasma. *Bios. Bioelectr.,* **2016***,* 86, 913-919.
[30] Maier, N. M.; Buttinger, G.; Welhartizki, S.; Gavioli, E.; Lindner, W. Molecularly imprinted polymer-assisted sample clean-up of ochratoxin A from red wine: merits and limitations. *J. Chromatogr. B,* **2004***,* 804, 103-111.
[31] Cela-Pérez, M. C.; Lasagabáster-Latorre, A.; Abad-López, M. J.; López-Vilariño, J. M.; Gónzalez Rodríguez, M. V. A study of competitive molecular interaction effects on imprinting of molecularly imprinted polymers. *Vibr. Spectrosc.*, **2013**, 65, 74– 83.

[32] Prasanna de Silva, A.; Moody, T. S.; Wright, G. D. Fluorescent PET (Photoinduced Electron Transfer) sensors as potent analytical tools. *Analysts*, **2009**, 134, 2385-2385.
[33] Prasanna de Silva, A.; Nimal Gunaratne, H. Q.; Gunnlaugsson, T.; Huxley, A. J. M.; McCoy, C. P.; Rademacher, J. T.; Rice, T. E. Signaling Recognition Events with Fluorescents sensors and switches. *Chem. Rev.*, **1997**, 97, 1515-1566.
[34] Ramachandram, B.; Saroja, G.; Sankaran, B.; Samanta, A. Unusually High Fluorescence Enhancement of Some 1,8-Naphthalimide Derivatives Induced by Transition Metal Salts. *J. Phys. Chem. B*, **2000**, 104, 11824-11832.
[35] Gunnlaugsson, T.; Kruger, P. E.; Jensen, P.; Pfeffer, F. M.; Hussey, G. M. Simple naphthalimide based anion sensors: deprotonation induced colour changes and CO_2 fixation. *Tetrahedron Lett*., **2003**, 44, 8909-8913.
[36] Alaei, P.; Rouhani, S.; Gharanjig, K.; Ghasemi, J. A new polymerizable fluorescent PET chemosensor of fluoride (F^-) based on naphthalimide–thiourea dye. *Spectrochimica Acta Part A,* **2012**, 85-92.
[37] Veale, E. B.; Tocci, G. M.; Pfeffer, F. M.; Kruger, P. E.; Gunnlaugsson, T. Demonstration of bidirectional photoinduced electron transfer (PET) sensing in 4-amino-1,8-naphthalimide based thiourea anion sensors. *Org. Biomol. Chem*.**, 2009**, 7, 3447-3454.
[38] Rèmy, C.; Allain, C.; Leray, I. Synthesis and photophysical properties of extended π conjugated naphtalimides. *Photochem. Photobiol. Sci.*, **2017**, 16, 539-546.
[39] Schäferling, M.; Gröge, D. B. M.; Schreml, S. Luminescent probes for detection and imaging of hydrogen peroxide. *Microchimica Acta*,**2011**, 174,1-18.
[40] Lakowicz, J. R. Principles of Fluorescence Spectroscopy. Springer, Third Edition. **2006**. ISBN 978-0-387-46312-4.
[41] Wagner, R.; Wan, W.; Biyikal, M.; Benito-Peña, E.; Moreno-Bondi, M. C.; Lazraq, I.; Rurack, K.; Sellergren, B. Synthesis, Spectroscopic, and Analyte-Responsive Behavior of a Polymerizable Naphthalimide-Based Carboxylate Probe and Molecularly Imprinted Polymers Prepared Thereof. *J. Org. Chem.*, **2013**, 78, 1377-1389.
[42] Yu, X.; Yang, Y.; Lu, S.; Yao, Q.; Liu, H.; Li, X.; Yi, P. The fluorescence spectroscopic study on the interaction between imidazo[2,1-b] thiazole analogues and bovine serum albumin. *Spectrochim. Acta A*, **2011**, 83, 322-32.
[43] Mishchenko, M. I.; Travis, L. D.; Lacis, A. A. Scattering, absorption and emission of light by small particles. Cambridge 2002, ISBN 0 521 78252.
[44] Long, Y.; Philip, J. Y. N.; Schllen, K.; Liu, F.; Ye, L. Insight into molecular imprinting in precipitation polymerization systems using solution NMR and dynamic light scattering. *J. Mol. Recognit*., **2010**, 24, 619-63.
[45] Zetasizer nano series-user manual Malvern mano0485. **2013**, issue 1.
[46] Malvern Instruments. Dynamic Light Scattering: An Introduction in 30 Minutes - DLS Technical Note.
[47] Atkins, P.; De Paula, J. Physical Chemistry Oxford ISBN 978 0 19 96740 3, **2014**, p. 725.
[48] Tommasini, M. Sviluppo Di Polimeri Ad Imprinting Molecolare per Il Therapeutic Drug Monitoring. Master Degree Thesis. University of Trieste, Italy, **2013.**
[49] Mazzotta, E.; Picca, R. A.; Malitesta, C.; Piletsky, S. A.; Piletska, E. V. Development of a sensor prepared by entrapment of MIP particles in electrosynthesised polymer films for electrochemical detection of ephedrine. *Biosensors and Bioelectronics*, **2008**, 23, 1152–1156.
[50] Kamra, T.; Chaudhary, S.; Xu, C.; Johansson, N.; Montelius, L.; Schnadt, J.; Ye, L. Covalent immobilization of molecularly imprinted polymer nanoparticles using an epoxy silane. *J. Colloid Interface Sci.,* **2015**, 445, 277–284.
[51] Marques, M. E.; Mansur, A. A. P.; Mansur, H. S. Chemical functionalization of surfaces for building three-dimensional engineered biosensors. *Applied Surface Science*, **2013**, 275, 347-360.
[52] Tischer, W; Wedekind, F. Immobilized enzymes: methods and applications, biocatalysis: from discovery to application, *Topics in Current Chemistry*, **1999**, 200, 95–126.
[53] Kriz, D.; Ramstrum, O.; Svensron, A.; Mosbach, K. introducing Biomimetic Sensors Based on Molecularly Imprinted Polymers as Recognition Elements. *Anal. Chem*. **1995**, 67, 2142-2144.
[54] Farris, S.; Song, J.; Huang, Q. Alternative Reaction Mechanism for the Cross-Linking of Gelatin with Glutaraldehyde. *J. Agric. Food Chem*., **2010**, 58, 998–100.

[55] Mahmood, K.; Muhammad, L.; Ariffin, F.; Kamilah, H.; Razak, A.; Sulaiman, S. Review of Fish Gelatin Extraction, Properties and Packaging Applications. *Food Science and Quality Management*, **2016**, 56, 47-59.
[56] Blanco-López, M. C.; Gutiérrez-Fernández, S.; Lobo-Castañón, M. J.; Miranda-Ordieres, A. J.; Tuñón-Blanco, P. Electrochemical sensing with electrodes modified with molecularly imprinted polymer films. *Anal. Bioanal. Chem.*, **2004**, 378, 1922–1928.

RESULTS AND DISCUSSION

Recognition Systems for 5-CQA

Chapter 7. Molecularly Imprinted polymers (MIPs)

As demonstrated in the previous chapter, sensors based on molecularly imprinted polymers (MIPs) can be developed taking advantage of the fluorescent properties of some of its components. Fluorescence spectroscopy offers a high sensitivity in comparison to other spectroscopic techniques, allowing the detection and quantification of the desired analyte in low concentrations. However, in cases where neither the polymer or template are fluorescent a different approach can be followed. Fluorescent properties can be exploited by synthesizing a fluorescent analogue of the analyte that can compete for the binding sites in the polymer or displace the analyte in the matrix polymer. According to this approach two different fluorescent dyes were chosen for the synthesis of the fluorescent 5-CQA derivative, such as: 5-[(2-Aminoethyl) amino] naphthalene-1-sulfonyl (EDANS), which shows an excitation wavelength at 320 nm and an emission wavelength at 490nm and Fluorescein Isothiocyanate (FITC), with excitation and emission wavelength at 490 nm 520 nm respectively. To synthetize the desired 5-CQA derivative, a diamino linker was attached at the carboxylic group of the quinic acid core in order to have a disposable amino group for the derivatization with the fluorescent compound. These fluorescent derivatives were used to carry out rebinding tests with a molecularly imprinted polymer prepared to recognize 5-CQA following the non-covalent approach.

7.1. Synthesis of mono 5-caffeoylquinic acid fluorescent derivatives.

7.1.1. 5-caffeoylquinic acid with Fluorescein Isothiocyanate (FITC)

In order to label 5-CQA with FITC it was necessary to active the carboxylic group by preparing the corresponding amide derivatives,[1,2] therefore two different intermediates were prepared using diamino compounds with different numbers of carbon atoms in the alkyl chain. Intermediates **17a** and **17b** were identified by ^{1}H NMR and were used without further purification in the next step. Coupling with FITC (scheme 7.1) was carried out under standard conditions using TBTU and DIPEA as the coupling agents[3]. ^{1}H NMR analysis of the crude confirmed the presence of the products, which were subsequently purified by column chromatography to afford compounds **19a** and **19b** as orange solids in 40% yield.

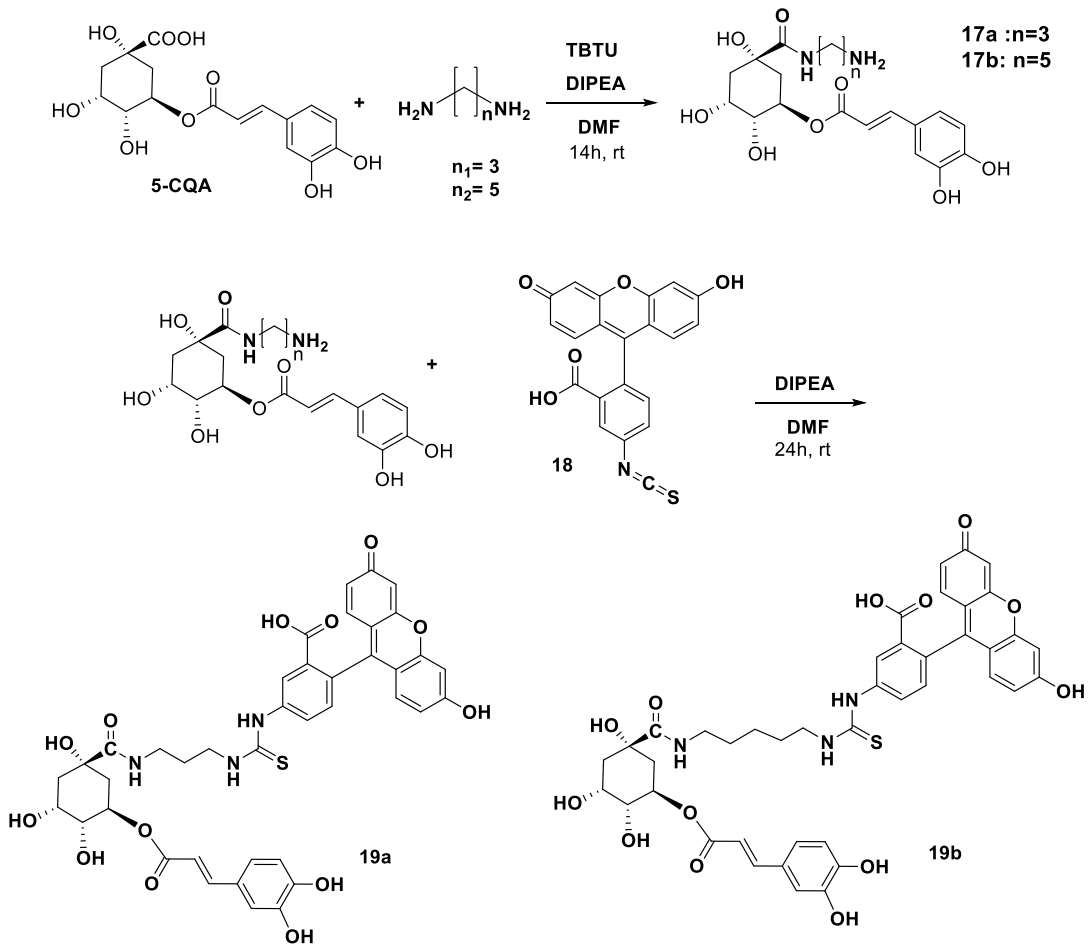

Scheme 7.1. Synthesis of 5-CQA derivatives with FITC.

Fluorescent spectra of compounds **19a** and **19b** did not show significant differences in the intensity with respect to that of the free fluorophore as can be observed in **Figure7.1.**

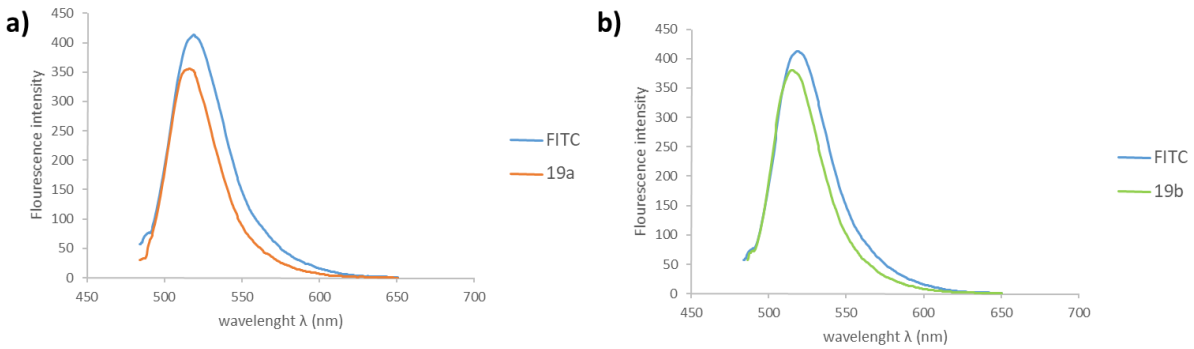

Figure 7.1. Fluorescent spectra of: **a)** FITC (blue) and **19a** (orange). **b)** FITC (blue) and **19b** (green) in H_2O, slit 5-5, 1µM.

7.1.2. 5-caffeoylquinic acid with 5-[(2-Aminoethyl) amino] naphthalene-1-sulfonyl (EDANS)

Compound **20a** was prepared following scheme 7.2 under standard reaction conditions described above.[3] ^{1}H NMR of the crude revealed the presence of the desired compound, which was purified by column chromatography to give compound **20a** as a green solid in 30% yield.

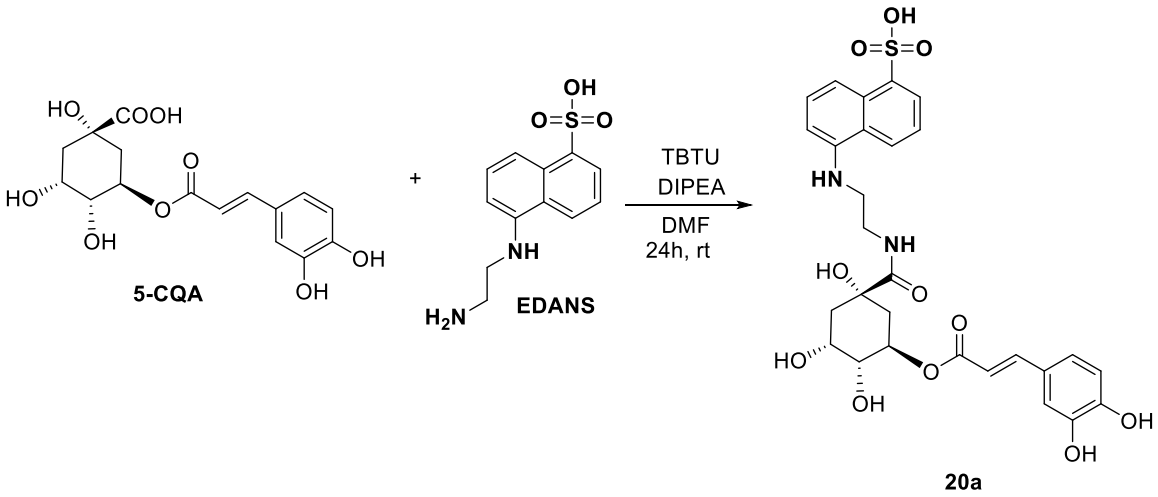

Scheme 7.2 Coupling between 5-CQA and EDANS.

However, as can be seen in the fluorescent spectrum (**Figure 7.2**) there is a considerable decrease in the intensity of the fluorescence of the labeled compound with respect to the one of the free fluorophore that can be caused by the inner filter effect[4], since 5-CQA could act as a quencher reabsorbing the emitted light. The ability of the quencher of absorbing the emitted light will increase with increasing its concentration, interfering with fluorescent Stern-Volmer analysis and with the development of an optical assay. Therefore, compound **20a** was not taken in consideration during the performance of the rebinding tests with the MIP.

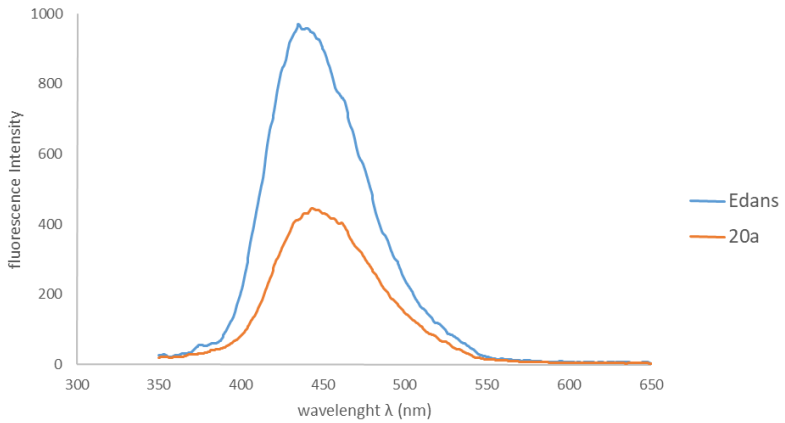

Figure 7.2. Fluorescent spectra of EDANS (blue) and **20a** (orange) in DMSO, slit 5-5, 1µM.

7.2 Functional Monomer

MIP to recognize 5-CQA was prepared using a N-acryoyl-L-histidine (**21a**) which was prepared from histidine as the functional monomer (**Figure 7.3**). Monomer **21a** was prepared by the research group of Prof. Resmini at the Queen Mary University of London and was obtained by methyl esterification of the respective amino acid, followed by C-terminal amidation and acylation with acryloyl chloride.[5] The selection of monomer was based taking in consideration existing biological interactions with chlorogenic acids[6]. Computational analyses were carried out in order to understand the complex formation between the monomer and the 5-CQA at a 1:1 molar ratio, allowing the calculation of the biding energy -25,2Kcal/mol.

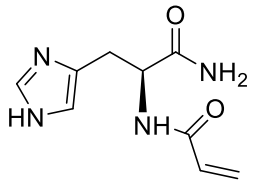

Figure 7.3 Structure of Functional Monomer N-acryoyl-L-histidine (**21a**).

7.3 Study of the interactions between functional monomer and analyte: ^{1}H NMR Titrations.

As previously described in section 6.2, from analysis of the chemical shift in ^{1}H NMR spectrum of the monomer-template complex formed before polymerization it is possible to identify the protons involved in the formation of the functional complex.[7,8] ^{1}H NMR titration was carried out adding between 0 and 8 equivalents of template (5-CQA) to a fixed concentration of functional monomer in deuterated DMSO.

Variations of the proton chemical shift (δ_{finall}-$\delta_{initial}$) of the monomer **21a** after addition of 8 equivalents of target molecule can be observed in **Figure 7.4**.

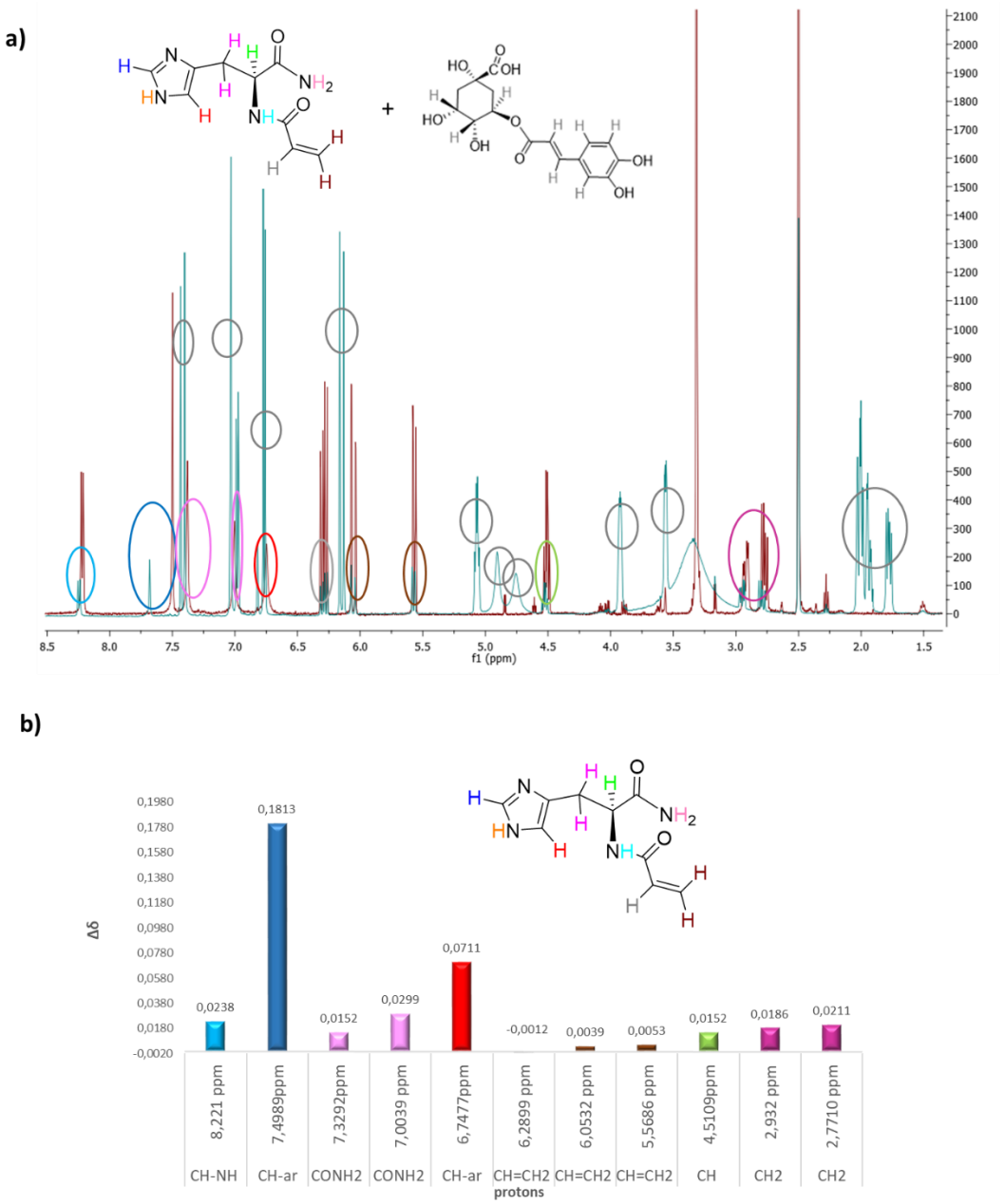

Figure 7.4 a) ^{1}H-NMR spectra of monomer 1c + 0 eq of 5-CQA (red) and monomer 1b + 8 eq of 5-CQA (blue) **b)** Histogram of the chemical shift variations in the ^{1}H-NMR spectrum of N-acryoyl-L-histidine (**21a**) upon progressive additions of 8 equivalents of 5-caffeoylquinic acid.

The addition of 5-CQA causes a downfield shift of all signals according to the literature,this tendency suggests that the interaction takes place through the formation of hydrogen bonds.[9,10] Moreover, comparing the chemical shift of the functional monomer and template it was observed that the signal corresponding to the N-H of the imidazole ring completely disappeared after the addition of 1,5 equivalents of 5-CQA, confirming the hydrogen bond formation between the sp^2 nitrogen atom of imidazole ring and the hydroxyl groups of the phenol ring in the 5-CQA. The highest variations correspond to the aromatic protons in the functional monomer as a consequence of the deshielded effect. As can be noticed in **Figure 7.5a**, which reports the trend of titration curve of aromatic proton, the plateau is not reached even after addition of 8 equivalents.

Nevertheless, in all registered spectra after addition of the template, only one set of signals were visible, indicating probably that complexation equilibrium is close to a *fast exchange* regime.[11]

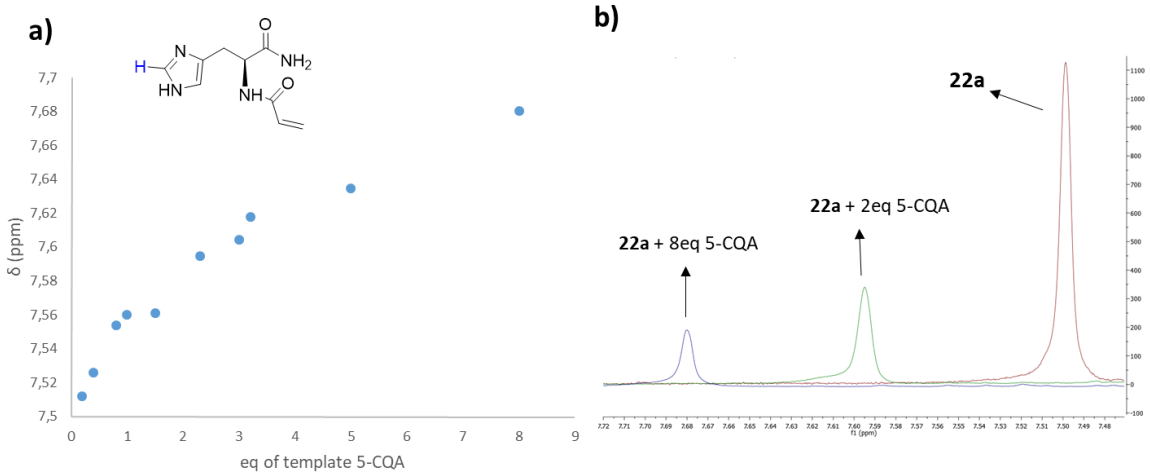

Figure 7.5: a) Chemical shift variation of Ar protons of monomer **21a** upon interaction with the template molecule (5-CQA). b) progressive shift of Ar proton in the ^{1}H-NMR spectra. Pure **21a** (red), addition of 2eq of 5-CQA (green) and 8eq (blue).

7.4 Synthesis of the molecularly imprinted polymer (MIP) for 5-CQA

As for the previous preparation of fluorescent polymers (fMIPs), the polymer was imprinted with the hydrogenated product (H-5CQA) in order to avoid undesired polymerization of the real target molecule.

The MIP was synthetized under the same high dilution radical polymerization conditions following the non-covalent approach described in the previous section[12], which consists in three preparation steps: **I**. pre-polymerization **II**. Radical polymerization and **III**. Removal of the template. The C_M was fixed to 0.5% w/w and the polymer (MIP03) was prepared using **21a** as the functional monomer and assuming a 1:1 interaction between the functional monomer and the template. NIPAM (N-Isopropylacrylamide) was used as the co-monomer to improve the solubility of the polymer in water[13] and MBA (N,N'-methylenebisacrylamide) as the crosslinker. MIP03 and NIP03 were obtained in 71% and 41% yield, respectively. In table 7.1 are reported the percentage composition of each component in the polymer. In the same way, the non-imprinted polymer (NIP03) was prepared as the control polymer using the same polymerization procedure and the same component concentrations but without the presence of H-5CQA as the template molecule.

Table 7.1 Composition of MIP03 imprinted with H-5CQA for 5-caffeoylquinic acid recognition.

		MIP03
Functional Monomers	N-acryoyl-L-histidine (**21a**).	10%
Co-monomer	N-Isopropylacrylamide. (NIPAM)	30%
Crosslinker	N,N'-methylenebisacrylamide (MBA)	60%

Initiator	Azobisisobutyronitrile (AIBN)	5%

7.5 .^{1}H-NMR Characterization of MIP03.

Formation of the polymer was verified by ^{1}H-NMR spectroscopy. For this purpose, 3mg of the polymer were dissolved in 750 µL of DMSO-d_6. As can be observed in **Figure 7.6**, the resulting spectra did not show any signals corresponding to the H-5CQA, indicating the completely removal of the template from the polymer binding sites during the dialysis process. Signals at upfield correspond to the aliphatic protons of the polymer. The ones between 3.5 and 5 ppm correspond to the CH_2-N protons while signals between 1.0 and 2.6 ppm can be associated to α and β protons of the amide groups as well as to the co-monomer methyl groups. The downfield set of signals between 6.5 and 7.3 ppm correspond to the amide groups of the polymeric matrix and to the imidazole protons of monomer **21a**.

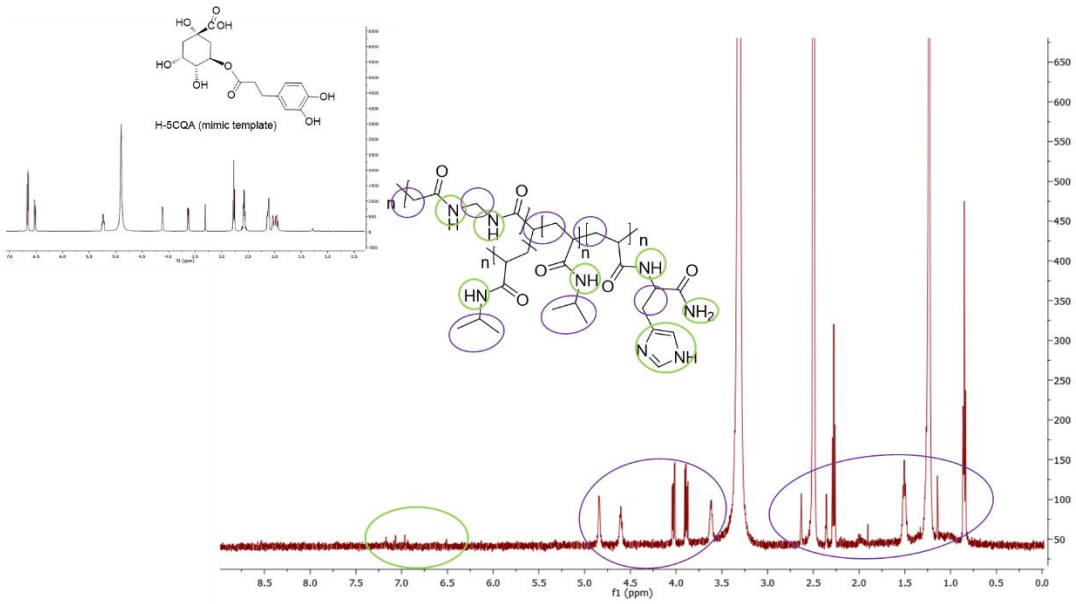

Figure 7.6 ^{1}H-NMR spectrum of MIP03. Insert ^{1}H-NMR spectrum of H-5CQA.

7.6. Recognition of the Target: Rebinding tests by UHPLC.

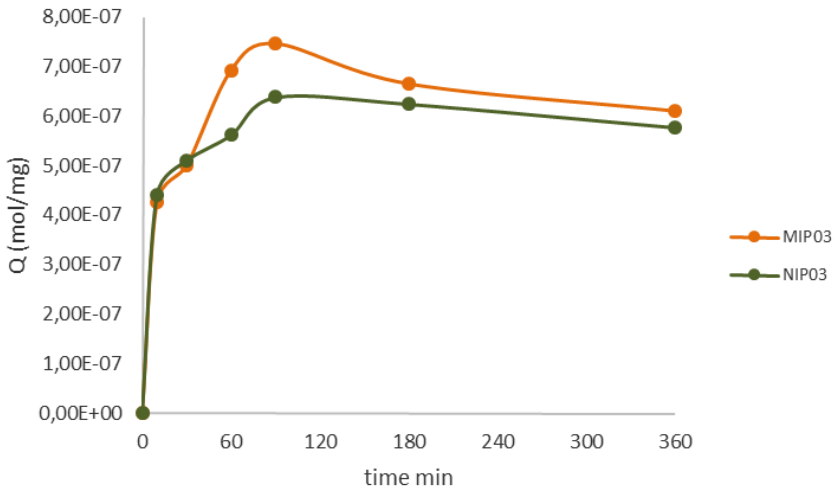

Figure 7.7. Rebinding kinetics of 5-CQA with MIP03 and NIP03.

MIP03 absorption capacity was calculated by performing rebinding tests by UHPLC as already performed for fluorescent polymers. A solution of 1mg/mL of polymer was prepared in water solution at an initial concentration of 2mM of 5-CQA and after certain periods of time, the solution was centrifuged and the concentration of the free analyte was quantified by UHPLC method already developed for the analyses of CGAs (see chapter 4).[14] The absorption was calculated following the equation previously described.

MIP03 was able to bind 426 nmol after few minutes of incubation. However, during the first minutes of incubation no significant difference was observed between NIP03 and MIP03. The imprinting efficiency is observed after 60 min of incubation where the polymer reaches its saturation point capturing 692nmol. However, after 180min of incubation the polymer tends to slightly release the chlorogenic acid reducing the binding capacity between both the MIP and NIP, which suggests that with the increase of the incubation time there is also an increase in non-specific interactions between the target molecule and the polymer MIP03. **(Figure 7.7**).

Following the same approach, evaluation of the binding capacity of the polymers with labeled compounds **19a** and **19b** were carried out separately and it was observed that MIP03 apparently shows a good affinity for the fluorescent derivatives of the chlorogenic acid, in particularly, a higher affinity for compound **19b** was observe and a saturation point was afforded within 60min when the polymer was able to capture 850nmol of the labelled target. This observation could indicate that the dimension of the alkyl chain used to connect the fluorophore with the chlorogenic acid moieties influences the recognition of the analyte by the polymeric matrix. A longer chain, as in the case of **19b**, could keep away the fluorophore from the binding cavities, allowing the chlorogenic acid to be recognized by the specific sites of interaction created by the imprinting process, which would result in a greater affinity. After 90min of incubation there is a release of both

molecules but afterwards, the ratio between the quantity of both analytes captured by the MIP remains fairly constant up to six hours. (**Figure 7.8**)

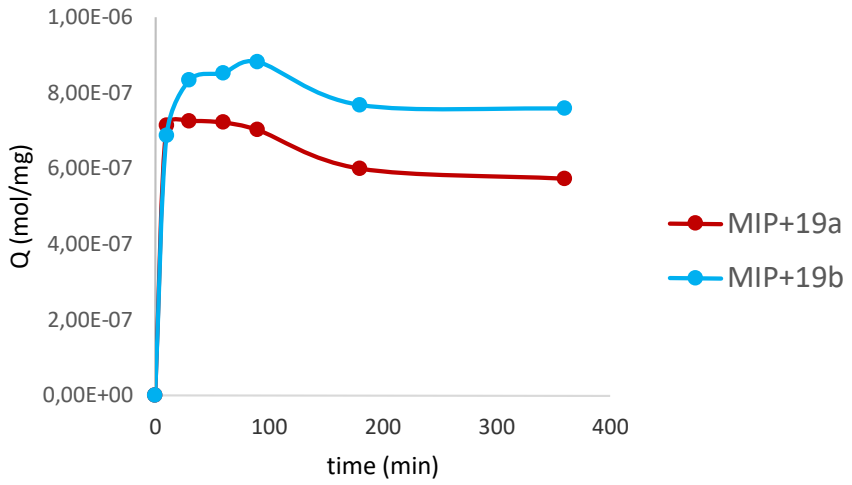

Figure 7.8. Rebinding kinetics of MIP031 with 5-CQACADPFITC **19a** (red) and 5-CQADAPFITC **19b** (blue).

- **Imprinting Factor**

The efficiency of the imprinting process was calculated by the imprinting factor,[15] assuming that the number of functional monomers incorporated into the MIPs and NIPs are the same. The values of IF and the binding capacities of the polymer MIP03 are summarized in table 7.2 and it can be noticed a decrease of the imprinting factor from 1.23 at 60min to 1.05 at 180min as a result of an increase of non-specific interactions, equaling the binding capacity between the imprinted and non-imprinted polymer.

Table 7.2 Rebinding capability and selectivity of MIP03 synthesized for 5-CQA

Polymer	**Functional Monomer**	**Rebinding (QMIP) [nmol mg^{-1}]**			**IF**		
		60 min	90 min	360min	60min	90 min	180min
MIP03	1c	692	746	610	1.23	1.17	1.05

7.7 Cross Reactivity: Analysis by UHPLC

Rebinding test of a 1mg/mL solution of MIP03 in a 2mM mixture water solution of 5-CQA and free hydrocinnamic acids such as caffeic acid (CA), *p*-coumaric acid (*p*CoQA) and caffeine (CAF) was carried out in order to evaluate the selectivity of MIP03. Also in this case, the un-bounded standards concentration in solution were determined by UHPLC after different incubation times. The bounded standards concentrations after 24h are reported in table 7.3

Table 7.3 Concentrations of different standards captured by MIP03 and NIP03 after 24h.

	5-CQA	**CA**	***p*CoA**	**CAF**
24h	mol/mg polymer	mol/mg polymer	mol/mg polymer	mol/mg polymer
MIP03	2,13E-07	3,53E-08	1,34E-07	2,69E-09
NIP03	2,00E-07	6,98E-08	1,52E-07	3,57E-08

Although in the mixture considered the binding capacity of MIP03 towards the target molecule was lower with respect to the previous test performed with a pure solution of the analyte, the polymer showed a good selectivity towards 5-CQA with an increasing affinity up to 3 hours (binding capacity 253 nmol/mg). This binding capacity is around 80% higher than the captured concentration of caffeic and *p*-coumaric acid for the same period. After 3 hours there is a slightly release of the target molecule, which reached a concentration of 210nmol/mg after 6 hours and then it remained constant even after 24 h of incubation. Also concentrations of caffeic acid changed during time with achieving concentrations of 172nmol/mg after 10min and 35nmol/mg after 24 hours. Concentrations of *p*-coumaric acid changed in the first 3 hours when the values started to increase with increasing of incubation time until a concentration of 134nmol after 24hours. Values of hydrocinnamic acids after 24h are 30% less than the captured concentration of analyte (5-CQA) for the same period, but the increase of captured concentration of hydrocinnamic acids with the incubation time could suggest also in this case an enhancement of non-specific interactions inside the polymeric matrix. Furthermore, MIP03 did not show any significant affinity for caffeine.

Comparing the binding capacity of the non-imprinted polymer with that of the imprinted polymer (table 7.3) it can be noticed that they have the same ability to bind the chlorogenic acid, but, a considerable higher capacity to capture the hydrocinnamic acids *p*-coumaric acid and caffeic acid was observed for NIP03 affording concentrations of 152 and 70nmol/mg after 24 hours respectively. Concentrations of *p*-coumaric acid remained constant from 10 min up to 24 hours, without any release, while the captured concentrations of caffeic acid gradually decreased over time, but always remained higher than the concentrations bound by the imprinted polymer. NIP03 also showed some affinity for caffeine, capturing 36nmol after 24 hours, and this tendency is an evidence of the non-specific binding sites present in the polymeric matrix of the non-imprinted polymer. These results are an evidence of the higher selectivity of MIP03 towards the target molecule 5-CQA.

7.8 Determination of Particles Size: Dynamic Laser Light Scattering (DLLS) Measurements.

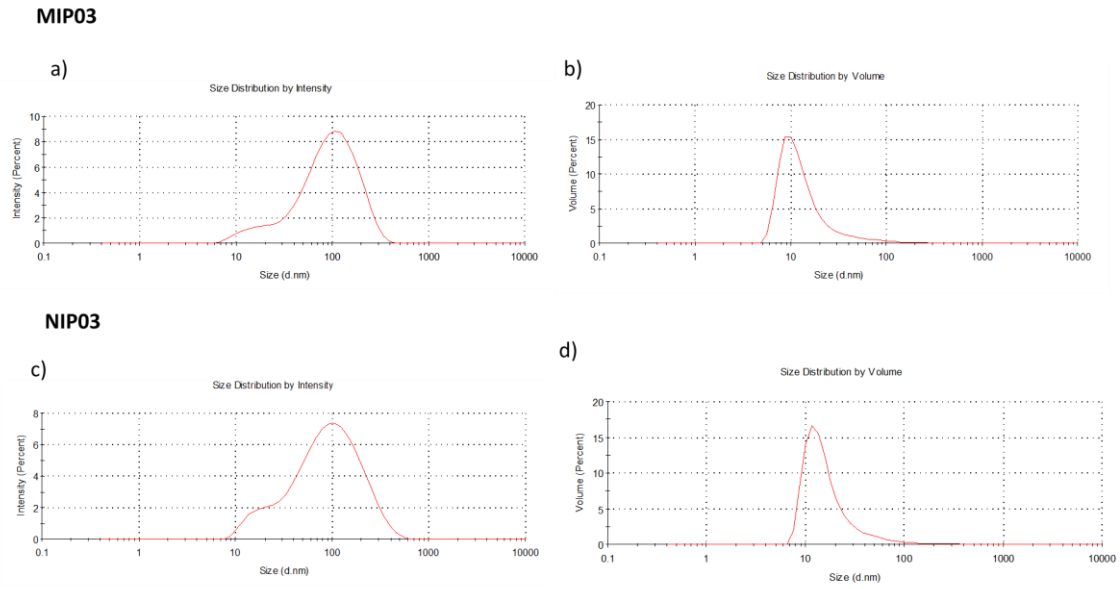

Figure 7.9 Measurements by DLLS: **a)** size distribution by intensity of MIP03, **b)** size distribution by volume of MIP03, **c)** size distribution by intensity of NIP03 and **d)** size distribution by volume of NIP03.

Particle size of both imprinted and non-imprinted polymers (MIP03 and NIP03) were determined by DLLS. Measurements were performed using 1.0mg/mL and 0.5 mg/mL particles suspensions in DMSO of MIP03 and NIP03, respectively, after sonication for 30min and filtration on 0.45 µm filter. The size distribution by intensity of both MIP03 and NIP03 (**Figure 7.9**) showed the presence of two population of particles around 15 nm and 100nm. The size distribution by volume showed only one peak indicating the presence of only one pure family of smaller particles. As explained before, the intense peak for particles of 100nm in the size distribution by intensity could be due by the tendency of polymers to form aggregates, which can be formed due to the presence of polar groups in the polymeric matrix, that in this case is made of methylenbiscrylamide and N-Isopropylacrylamide. The particle size of the imprinted polymer was smaller than the corresponding NIP, indicating that probably the creation of specific biding cavities can affect the particle size. Table 7.4 shows the particle size of MIP03 and NIP03.

Table 7.4 Particle sized of MIP03 and NIP03 measured by DLLS.

Polymer	Concentration	Solvent	Particle size (nm)
MIP03	1mg/mL	DMSO	16.36
NIP03	0.5mg/mL	DMSO	20.12

7.9 Competitive Test with MIP03

The previous rebinding experiments showed the capability of MIP03 to capture both molecules, the isomer 5-CQA as well as its corresponding fluorescent derivatives. Therefore, taking advantage of this property MIP03 can be used as recognition element through a competitive test for CGA quantification as has been already reported in the literature for other types of molecules, where the concentrations of the analyte have been calculated measuring the emission signal of the fluorescent competitor.[16] This first approach consisted on the evaluation of the capability of the fluorescent derivative **19b** to displace the analyte 5-CQA from the polymer binding sites.

For this purpose, suspensions of 100 µg/mL in water of MIP03 were first immobilized in a functionalized glass surfaces by physical entrapment in gelatin, following the same approach described in the previous chapter for the fluorescent polymer. Then, solutions of different concentrations of 5-CQA in a range between 100nM and 1mM were added to the different plates containing the immobilized polymer and were incubated for 90min to allow the total incorporation of the target molecule into the polymer. After this period, a solution of 50 µM of the fluorescent derivative **19b** was added to all plates, the intensities of fluorescence emission were measured after 90 min of incubation to allow the system to reach the equilibrium. The addition of the labelled compound should displace the target molecule from the polymer cavities leading to a decrease of the fluorescence intensity.

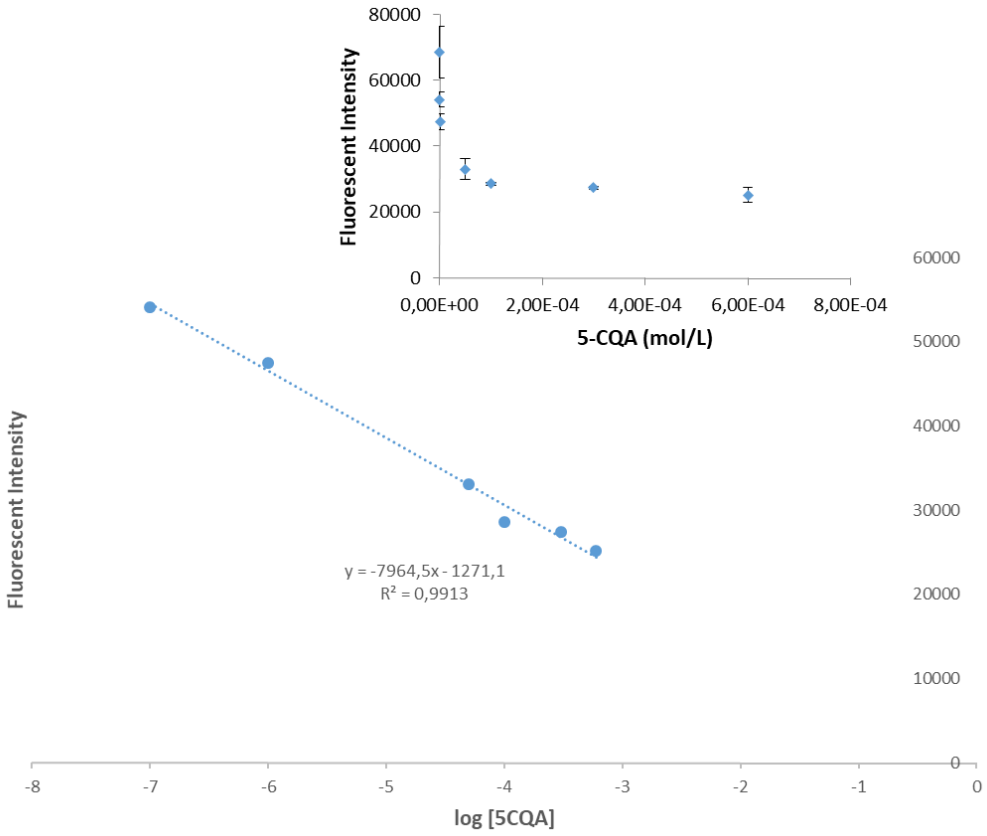

Figure 7.10. First attempt to set up a competition test of MIP03 with 5-CQA and **19b**: Calibration curve of 5-CQA. Insert: fluorescent intensity of 5-CQACADFITC in function of the concentration of 5-CQA.

In **Figure 7.10** it can be observed a proportional relationship between the quenching of the fluorescence and the concentration of the real target 5-CQA. Experiments were performed in duplicate and a possible calibration curve could be designed in a linear range between 100nM and 600µM. With this proof of concept on MIP03 it is opened the possibility to use this type of polymers in sensor for monitoring CGA concentration through a competitive assay in aqueous media. However, the system will require a further optimization to reach a better sensitivity in real coffee samples.

[1] Montalbetti, C. A.G.N.; Falque, V. Amide bond formation and peptide coupling. *Tetrahedron*, **2005**, 61, 10827–10852.
[2] Valeur, E.; Bradley, M. Amide bond formation: beyond the myth of coupling reagents. *Chem. Soc. Rev*., **2009**, 38, 606–631.
[3] Maggiora, L. L.; Smith, C. W.; Zhang, Z. Y. A general method for the preparation of internally quenched fluorogenic protease substrates using solid-phase peptide synthesis. *J. Med. Chem*, **1992**, 35, 3727-3730.
[4] Kubista, M.; Sjoback, R.; Eriksson, S.; Albinsson, B. Experimental Correction for the Inner-filter Effect in Fluorescence Spectra. *Analyst*, **1994**, 119, 417-419.
[5] Pasetto, P.; Maddock, S. C.; Resmini, M. Synthesis and characterisation of molecularly imprinted catalytic microgels for carbonate hydrolysis. *Anal. Chim. Acta*, **2005**, 542, 66–75.
[6] Otani, P.; Stogios, P. J.; Xu, X.; Nocek, B.; Li, S. N.; Savchenko, A.; Eltis, L. D. The activity of CouR, a MarR family transcriptional regulator, is modulated through a novel molecular mechanism. *Nucleic Acids Res*., **2015**, 1–13.

[7] Athikomrattanakul, U.; Katterle, M.; Gajovic-Eichelmann, N.; Scheller, F. W. Development of molecularly imprinted polymers for the binding of nitrofurantoin. *Biosens. Bioelectron*., **2009**, 25, 82-87.
[8] Svenson, J.; Karlsson, J. G.; Nicholls, I. A. 1H Nuclear magnetic resonance study of the molecular imprinting of (-)-nicotine: template self-association, a molecular basis for cooperative ligand binding. *J. Chromatogr. A*, **2004**, 1024, 39-44.
[9] Quaglia, M.; Chenon, K; Hall, A. J.; De Lorenzi, E.; Sellergren, B. Target analogue imprinted polymers with affinity for folic acid and related compounds. *J. Am. Chem. Soc*., **2001**, 123, 2146-2154.
[10] Dai, Z.; Liu, J.; Tang, S.; Wang, Y.; Wang, Y.; Jin, R. Optimization of Enrofloxacin-Imprinted Polymers by Computer-Aided Design. *J. Mol. Model*., **2015**, 21, 1-9
[11] Svenson, J.; Karlsson, J. G.; Nicholls, I. A. ^{1}H Nuclear magnetic resonance study of the molecular imprinting of (-)-nicotine: template self-association, a molecular basis for cooperative ligand binding. *J. Chromatogr. A*, **2004**, 1024, 39-44.
[12] Carboni, D.; Flavin, K.; Servant, A.; Gouverneur, V.; Resmini, M. The first example of molecularly imprinted nanogels with aldolase type I activity. *Chem. Eur. J.*, **2008**, 14, 7059-7065.
[13] Hien Nguyen, T.; Ansell, R. J. N-Isopropylacrylamide as a Functional Monomer for Noncovalent Molecular Imprinting: NIPAM, a Monomer for Noncovalent Molecular Imprinting. *J. Mol. Recognit*., **2012**, 25, 1–10.
[14] Pellizzoni, E.; Tommasini, M.; Maragon, E.; Rizzolio, F.; Saito, G.; Benedetti, F.; Toffoli, G.; Resmini, M.; Berti, F: Fluorescent molecularly imprinted nanogel for the detection of anticancer drugs in human plasma. *Bios. Bioelectr.,* **2016** ,86, 913-919.
[15] Cela-Pérez, M. C.; Lasagabáster-Latorre, A.; Abad-López, M. J.; López-Vilariño, J. M.; Gónzalez Rodríguez, M. V. A study of competitive molecular interaction effects on imprinting of molecularly imprinted polymers. *Vibr. Spectrosc.*, **2013**, 65, 74– 83.
[16] Urraca, J.L.; Moreno-Bondi, M. C.; Orellana, G.; Sellergren, B.; Hall, A. J. Molecularly Imprinted Polymers as Antibody mimics in Automated On-Line Fluorescent Competitive Assays. *Anal. Chem***., 2007**, 79, 4915-4923.

Chapter 8

EXPERIMENTAL PART

8.1 Synthesis of *p*-Coumaroylquinic Acids (*p*CoQAs)

Instrumentation

- **Thin layer chromatography (TLC)** was performed on Merck silica gel 60 F_{254} silica gel plates. TLC Plates were examined under UV light or were stained with aqueous permanganate solution or iodine vapors.
- **Flash chromatography purifications** were carry out with Merck silica gel 60 (230-240 Mesh).
- **Nuclear magnetic resonance (NMR)**: 400 MHz, 500 MHz ^{1}H-NMR and 125 MHz ^{13}C-NMR spectra were obtained on a Varian 400 and 500 spectrometers (residual solvent peaks were used as the internal standard, δ= 7.26 ppm for $CDCl_3$ and 3.31 ppm for CD_3OD). The resonances multiplicity is described as s (singlet), d (doublet), t (triplet), q (quartet), m (multiplet), dd (doublet of doublets), br (broad signal).
- **Electrospray Ionization (ESI) mass spectrometry** measurements were performed with an Esquire 400 (Bruker-Daltonics) spectrometer.
- **Infrared spectra (IR**) were recorded with an Avatar 320-IR FTIR (ThermoNicolet).
- **Optical rotations** were recorded on a Jasco P2000 polarimeter at the wavelength of sodium D band (λ =589) using a quartz cell of 1dm path length.
- **Circular dichroism** spectra were recorded on a Jasco J-710 spectropolarimeter with a 0.1cm path length cell.
- **Melting points** were measured with a Sanyo Gallenkamp apparatus and were uncorrected.
- **Reverse Phase high-performance liquid chromatography analyses (RP-HPLC)** were run on an Amersham Pharmacia Biotech liquid chromatograph equipped with an UV Amersham detector, using a Gemini C18 3 µm 2x150 mm column for the analytical runs and a Gemini C18 5 µm 10x250 mm column for the semi-preparative ones.

Materials

All reagents and solvents were purchased from Sigma-Aldrich and were used without further purification. Dichloromethane was dried over $CaCl_2$. Esterification reactions were performed under argon atmosphere.

Experimental procedures

- ***p*-acetylcoumaroylchloride**

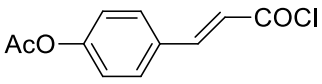

Acetic anhydride was added (4.66g, 45.69mmol) at 0°C to a suspension of *p*-coumaric acid (5g, 30.46mmol) and DMAP (93mg, 0.76 mmol) in pyridine (10mL). The reaction mixture was stirred for 3h at room temperature and then poured onto crushed ice. After acidification with aq. HCl (pH<2), acetyl *p*-coumaric acid was obtained as a white solid which was filtered and washed with water (93% yield). Oxalyl chloride was added at -5 ° C to a suspension of acetyl *p*-coumaric acid (1g, 4.85mmol) in toluene (17mL) containing two drops of DMF and the reaction mixture was stirred at -5 ° C for 2h and then overnight at room temperature. Solvent was removed under reduced pressure to afford *p*-acetylcoumaroylchloride as a yellow solid in 95% yield. NMR data were in accordance with the literature.[1]

- **3,4-*O*-Isopropylidine -1,5-quinic lactone 5**

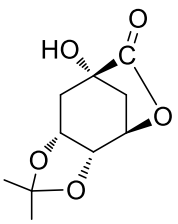

2,2-dimethoxypropane (4.87g, 46.83 mmol) was added to a suspension of quinic acid (3g, 15.61 mmol) and *p*-toluenesulfonic acid (216 mg, 1.15 mmol) in acetone (60mL) and the mixture was heated under reflux for 2 h. After cooling, neutralization with $NaHCO_3$ (5%) was performed and the mixture was stirred for 1h at room temperature. The reaction mixture was subsequently extracted with CH_2Cl_2 (three times, 20 mL at time) and washed with water (two times, 20 mL at time). The organic layer was dried with Na_2SO_4 and the solvent was removed under reduced pressure. Lactone **5** was obtained as a white solid in 72% yield and was used in the next step without further purification. NMR data were in accordance with the literature.[2]

- **1-acetyl p-coumaroyl-3,4-*O*-Isopropylidene quinide 6**

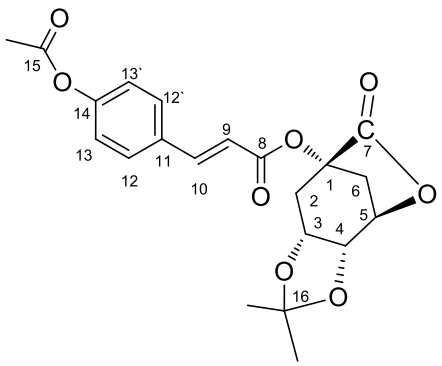

To a suspension of 3,4-O-isopropylidene-1,5-quinic lactone **5** (500 mg, 2.33mmol) in CH_2Cl_2 (20 mL), DMAP (86 mg, 0.7 mmol), pyridine (0.47 mL, 4.66mmol) and *p*-acetylcoumaroylchloride (783 mg, 3. 49mmol) were added. The mixture was stirred 24h at room temperature. The reaction mixture was diluted with CH_2Cl_2 and subsequently extracted with 1 M aqueous HCl solution (three times, 10 mL at time), $NaHCO_3$ (5%) (10 mL) and brine (10mL). The organic layer was dried over Na_2SO_4, filtered and the solvent was removed under reduced pressure. The residue was purified by column chromatography on silica gel (diethyl ether/CH_2Cl_2 50:50) to afford ester **6** (57%) as a colorless solid.

^{1}H NMR (500 MHz, $CDCl_3$), δ: 7.72 (1H, d, *J* = 16.0 Hz, H-10), 7.55 (2H, d, *J* = 8.6 Hz, H-12+H-12'), 7.14 (2H, d, *J* = 8.6 Hz, H-13+H-13'), 6.41 (1H, d, *J* = 16.0 Hz, H-9), 4.82 (1H, dd, *J* = 6.5, 2.5 Hz, H-4), 4.59 (1H, dt, *J* = 2.19, 6.9 Hz, H-5), 4.36 (1H, m, H-3), 3.11 (1H, m, H-6), 2.65 (1H, apparent d, H-6), 2.53 (1H, ddd, *J* = 14.0, 6.5, 2.3 Hz, H-2ax), 2.45 (1H, dd, *J* = 14.5, 3.2 Hz, H-2eq), 2.31 (3H, s, CH_3CO), 1.54 (3H, s, CH_3), 1.35 (3H, s, CH_3);

^{13}C NMR (500 MHz, $CDCl_3$), δ: 173.65 (s, C-7), 169.21 (s, C-15), 164.99 (s, C-8), 152.59 (s, C-14), 145.71 (d, C-10), 131.86 (s, C-11), 129.59 (d, C-12+C-12'), 122.37 (d, C-13+C-13'), 117.09 (d, C-9), 110.14 (s, C-16), 76.39 (s, C-1), 75.57 (d, C-5), 72.64 (d, C-4), 71.33 (d, C-3), 35.82 (t, C-2), 30.87 (t, C-6), 27.15 (q, C(CH_3)$_2$), 24.50 (q, C(CH_3)$_2$), 21.29 (q, CH_3CO).

- **1-*p*-coumaroylquinic acid 1a**

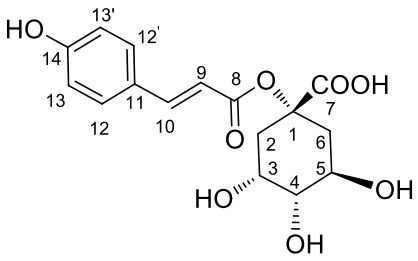

Ester **6** (500mg, 1.24mmol) was dissolved in a mixture of THF (10 mL) and aq. 2M HCl (40mL) and the yellowish solution formed was stirred for 11 days at room temperature. The solution was saturated with solid NaCl and then extracted with EtOAc (3*20 mL). The organic layer was dried over Na_2SO_4, filtered and the solvent was removed under reduced pressure. 1-*p*-coumaroylquinic acid **1a** was obtained as a colorless solid in 84% from the corresponding protected ester **6.**

M.p. 130-135°C.

^{1}H NMR (500 MHz, CD_3OD), δ: 7.61 (1H, d, *J* = 15.9 Hz, H-10), 7.45 (2H, d, *J* = 8.6 Hz, H-12+H-12'), 6.81 (2H, d, *J* = 8.6 Hz, H-13+H-13'), 6.35 (1H, d, *J* =15.9 Hz, H-9), 4.15 (1H, q, *J* = 4.3, Hz, H-5), 4.06 (1H, dt, *J* = 9.1, 3.6 Hz, H-3), 3.48 (1H, dd, *J* = 8.3, 3.3 Hz, H-4), 2.57 (1H, m, H-6), 2.44 (1H, m, H-2), 2.21 (dd, *J* = 14.9, 3.5 Hz, H-6), 1.91 (1H, dd, *J* = 13.8, 8.5 Hz, H-2).

^{13}C NMR (500 MHz, CD_3OD), δ: 174.91 (s, C-7), 167.55 (s, C-8), 160.79 (s, C-14), 146.40 (d, C-10), 130.67 (d, C-12+C-12'), 126.73 (s, C-11), 116.30 (d, C-13+C-13'), 114.97 (d, C-9), 80.95 (s, C-1), 75.77 (d, C-4), 69.13 (d, C-5), 67.40 (d, C-3), 39.40 (t, C-2), 35.38 (t, C-6);

IR (nujol): ν̃ =3582.61, 3358.97, 2950, 1693.99, 1631.07, 1170.67, 1113.35, 831.61 cm^{-1}.

MS (ESI^+): *m/z* [M+Na]: 361.0.

$[\alpha]^{20}_D$=+5.11 (*c* 1.10, MeOH) (lit.[3] $[\alpha]^{22}_D$=-5.0 (*c* 2, MeOH)); UV (MeOH): ε_{314} = 84200.

- **Ethyl 3,4-*O*-Isopropylidene-1,5-quinate 7**

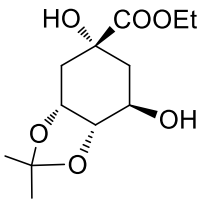

A suspension of crude lactone **5** (1 g, 4.67mmol) in absolute EtOH (30 mL) was treated with NaOEt (12.71mg, 0.19 mmol) dissolved in EtOH (160 µL). The brownish solution was stirred at room temperature for 2 h and then stored at -20^{0}C for 24h. The unreacted NaOEt was quenched by addition of acetic acid (13 µL) and the solvent was removed under reduced pressure at 30 ^{0}C. The residue obtained showed to be a mixture of lactone **5** and ester **7** in ratio 13:1 determined by ^{1}H NMR analysis. The crude mixture was used without further purification in the next step.[4]

- **Ethyl-5-*O*-acetyl-*p*-coumaroyl-3,4-*O*-Isopropylidenquinate 8**

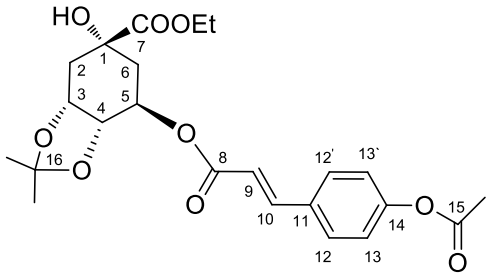

To a solution of ethyl-3,4-*O*-isopropylidenquinate **7** (500 mg,1.92mmol)**,** DMAP (35mg, 0,15mmol) and pyridine (6 mL) in CH_2Cl_2 (25mL), *p*-acetylcoumaroylchloride (645.18 mg, 2.88mmol) was added. The mixture was stirred 24h at room temperature and acidified with aq. HCl 1M (pH 2-3) and then extracted with CH_2Cl_2 (three times, 50 mL at time). The organic layer was dried over Na_2SO_4, filtered and the solvent was removed under reduced pressure. The brownish residue was purified by column chromatography on silica gel (diethyl ether/CH_2Cl_2 50:50) to afford ester **8** in 34% yield as a colorless solid.

^{1}H NMR (500 MHz, $CDCl_3$), δ: 7.69 (1H, d, *J* = 15.9 Hz, H-10), 7.53 (2H, d, *J* = 8.6 Hz, H-12+H-12'), 7.13 (2H, d, *J* = 8.6 Hz, H-13+H-13'), 6.40 (1H, d, *J* = 15.9 Hz, H-9), 5.49 (1H, dt, *J* = 11.7, 4.5 Hz, H-5), 4.55 (1H, dt, J=3.7, 5.6, H-3), 4.28 – 4.20 (3H, m, OCH_2 + H-4), 2.31 (3H, CH_3CO), 2.32 – 2.28 (2H, m, H-2), 2.25 (1H, dd, *J* = 13.2, 4.4 Hz, H-6_{eq}), 1.94 (1H, dd, *J* = 13.3, 11.3 Hz, H-6_{ax}), 1.60 (s, $C(CH_3)_2$), 1.38 (s, $C(CH_3)_2$), 1.30 (3H, t, *J* = 7.2 Hz, CH_3CH_2).

^{13}C NMR (500 MHz, $CDCl_3$), δ: 174.48 (s, C-7), 169.27 (s, C-15), 166.03 (s, C-8), 152.27 (s, C-14), 144.19 (d, C-10), 132.24 (s, C-11), 129.37 (d, C-12+C-12'), 122.30 (d, C-13+C-13'), 118.29 (d, C-9), 109.76 (s, C-16), 77.05 (d, C-3), 75.65 (s, C-1), 73.81(d, C-4), 71.11 (d, C-5), 62.36 (t, CH_2CH_3), 37.13 (t, C-6), 34.56 (t, C-2), 28.17 (q, $C(CH_3)_2$), 26.01 (q, $C(CH_3)_2$), 21.30 (q, CH_3CO), 14.28 (q, CH_3CH_2).

- **5-*O*-*p*-coumaroylquinic acid 2a**

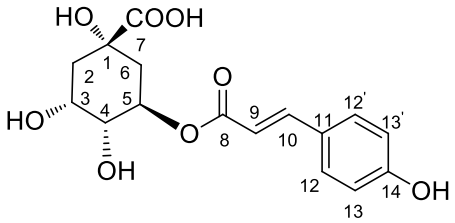

Ethyl 1-acetyl *p*-coumaroyl-3,4-*O*-isopropylidenquinate **12** (290mg, 0.65mmol) was dissolved in a mixture of THF (10 mL) and aq. 2M HCl (40mL) and the solution was stirred for 6 days at room temperature. After

saturation with solid NaCl the mixture was extracted with EtOAc (3*30 mL) and the organic phase was dried over anhydrous Na_2SO_4. Evaporation of the solvent gave 5-*O*-*p*-coumaroylquinic acid as a colorless solid in 77% yield from the corresponding protected ester **12.**

M.p. 215-218°C (lit.[5] 247-248°C); IR (nujol): ν̃ =3582.67, 3302.38, 2917.48, 1687.13, 1633.37, 1170.30, 1080.85, 825.27 cm^{-1}; ^1H NMR is in accordance with literature data.[6]

^{13}C NMR (126 MHz, CD_3OD), δ: 177.02 (s, C-7), 168.61 (s, C-8), 161.28 (s, C-14), 146.68 (d, C-10), 131.18 (d, C-12+C-12'), 127.23 (s, C-11), 116.80 (d, C-13+C-13'), 115.33 (d, C-9), 76.15 (s, C-1), 73.41 (d, C-4), 72.00 (d, C-5), 71.15 (d, C-3), 38.77 (t, C-2), 38.22 (t, C-6).

MS (ESI^+): *m/z* [M+Na]: 361.4.

$[\alpha]_D^{20}$ = -39.5 (*c* 0.79, MeOH) [lit.[5] $[\alpha]_D^{20}$ = -53.6 (*c* 1.04, MeOH)]. UV (MeOH): ε_{314} =70000.

- **4,5-*O*-(2',3'-Dimethoxybutane-2',3'-diyl)-1,3-dihydroxycyclohexanecarboxylic acid methyl ester 10**

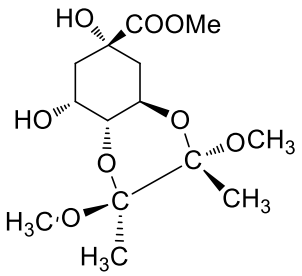

To a suspension of quinic acid (1g, 5.20mmol) in MeOH (30mL), (-)-10-camphorsulfonic acid (15 mg, 0.065mmol) was added and the mixture was refluxed for 15 h under Ar atmosphere. Subsequently, to the methyl quinate **9** so obtained, 2,2,3,3-tetramethoxybutane (1.01 g, 5,7mmol), trimethylorthoformate (2.6mL, 0.024mmol) and (-)-10-camphorsulfonic acid (12 mg, 0.052mmol) were added and the mixture was refluxed again. After 15 h the mixture was cooled and $NaHCO_3$ (0.1 g) was added. Solution was concentrated under reduced pressure and the orange suspension was partitioned between EtOAc (30mL) and saturated aqueous $NaHCO_3$ (30mL). The aqueous layer was extracted with EtOAc (30mL) and the organic layer was dried over Na_2SO_4, filtered and the solvent was removed under reduced pressure. Recrystallization of the brownish residue from EtOAc and hexane (1:5, v/v) afforded **10** in 15% yield as an orange oil. NMR data were in accordance with the literature.[7,8]

- **3-Acetyl-*p*-coumaroyl-4,5-*O*-(2',3'-Dimethoxybutane-2',3'-diyl)-1-hydroxycyclohexanecarboxylic acid methyl ester 11**

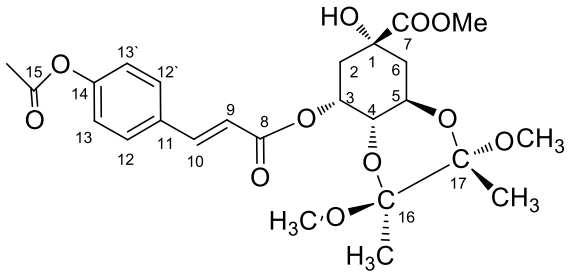

4,5-*O*-(2',3'-dimethoxybutane-2',3'-diyl)-1,3-dihydroxycyclohexanecarboxylic acid methyl ester **10** (122 mg, 0.38mmol) was suspended in CH_2Cl_2 (20 mL) and DMAP (4,17 mg, 0.034 mmol), pyridine (320 µL, 4.03mmol) and *p*-acetylcoumaroylchloride (128mg, 0.57mmol) were added. The mixture was stirred 24h at room temperature and then acidified with aq. HCl 1M (pH 2-3). After extraction with CH_2Cl_2 (three times, 30 mL at time) the organic layer was dried over Na_2SO_4, filtered and the solvent was removed under reduced pressure. The brownish residue was purified by column chromatography on silica gel (diethyl ether/CH_2Cl_2 50:50) to afford ester **11** in 20% yield as a colorless solid.

^{1}H NMR (500 MHz, $CDCl_3$), δ: 7.71 (1H, d, *J* = 15.8 Hz, H-10), 7.57 (2H, d, *J* = 8.6 Hz, H-12+H-12'), 7.14 (2H, d, *J* = 8.6 Hz, H-13+H-13'), 6.47 (1H, d, *J* = 15.9 Hz, H-9), 5.38 (1H, q, *J* = 9.1 Hz, H-3), 4.45 (1H, dt, *J* = 10.2, 5.6 Hz, H-5), 3.79 (3H, s, $COOCH_3$), 3.71 (1H, dd, *J* = 9.9, 3.2 Hz, H-4), 3.31 (3H, s, OCH_3), 3.27 (3H, s, OCH_3), 2.29 (3H, s, CH_3CO), 2.28 (2H, m, H-2 + H-6), 2.14 (1H, dd, *J* = 15.7, 3.2 Hz, H-2), 2.04 (1H, m, H-6).

^{13}C NMR (500 MHz, $CDCl_3$), δ: 175.62 (s, C-7), 169.26 (s, C-15), 166.61 (s, C-8), 152.19 (s, C-14), 144.19 (d, C-10), 132.45 (s, C-11), 129.47 (d, C-12+C-12'), 122.21 (d, C-13+C-13'), 118.79 (d, C-9), 100.29 (s, C-16), 99.73 (s, C-17), 74.78 (s, C-1), 71.38 (d, C-4), 70.02 (d, C-3), 62.94 (d, C-5), 53.39 (q, *C*H_3COO), 48.3 (q, OCH_3), 48.14 (q, OCH_3), 38.91 (t, C-6), 36.81 (t, C-2), 21.3 (q, *C*H_3CO), 18.03 (q, *C*$H_3C(OCH_3)$), 17.81 (q, *C*$H_3C(OCH_3)$).

- **3-*O*-*p*-coumaroylquinic acid 3a**

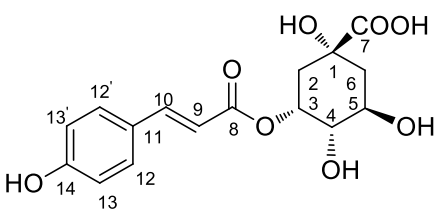

3-Acetyl-*p*-coumaroyl-4,5-*O*-(2',3'-dimethoxybutane-2',3'-diyl)-1-hydroxycyclohexanecarboxylic acid methyl ester **11** (35mg, 0.069mmol) was dissolved in a mixture of THF (0.5 mL) and aq. 2M HCl (1.5mL) and the solution was stirred for 6 days at room temperature. After saturation with solid NaCl the mixture was extracted with EtOAc (3*20 mL) and the organic phase was dried over anhydrous Na_2SO_4. Evaporation of the solvent gave a yellowish solid with 62% yield, which was defined to be a mixture of 3-*p*-coumaroylquinic acid **3a** and 4-*p*-coumaroylquinic acid **4a** in a ratio 8:2 as determined from ^{1}H-NMR. The crude mixture was purified by semi-preparative RP-HPLC on a Phenomenex Gemini C18 5 µm 10 x 250 mm column, using a gradient of H_2O+0.1% formic (A) acid and MeOH+0.1% (B), (20 min A 80% and B 20%, from 20 to 90 min increase of B until A 40% and B 60%, from 90 to 110 min A 5% and B 95%, from 110 to 125 min A 95% and B 5%) at a flow rate of 2 mL/min. The elution was monitored with an UV/vis detector λ 325nm and the fractions corresponding to each peak were collected and keep at -80^{o}C and then freeze dried and analyzed by ^{1}H NMR. 3-*O*-*p*-coumaroylquinic acid **3a** (3mg) was obtained as a white solid.

M.p. 192-194^{o}C [lit.[5] 194°C].

IR (nujol): ν̃ =3582.64, 3381.37, 2921.16, 1694.22, 1631.26, 1171.87, 1019.74, 831.37 cm^{-1}.

^{1}H NMR (500 MHz, CD_3OD), δ: 7.67 (1H, d, *J* = 15.9 Hz, H-10), 7.47 (2H, d, *J* = 8.5 Hz, H-12+H-12'), 6.81 (2H, d, *J* = 8.3 Hz, H-13+H-13'), 6.39 (1H, d, *J* = 15.9 Hz, H-9), 5.39 (1H, m, W_H 13.7, H-3), 4.10 (1H, m, W_H 17.8, H-5), 3.71 (1H, dd, *J* = 7.6, 2.7 Hz, H-4), 2.20 – 1.93 (4H, m, H-2+H-6).

^{13}C NMR (500 MHz, CD_3OD), δ: 177.59 (s, C-7), 168.91(s, C-8), 161.15 (s, C-14), 146.43 (d, H-10), 131.09 (d, C-12+C-12'), 127.39 (s, C-11), 116.79 (d, C-13+C-13'), 115.85 (d, H-9), 76.42 (s, C-1), 74.22 (d, C-4), 72.61 (d, C-3), 68.93 (d, C-5), 36.93 (t, C-2), 36.22 (t, C-6).

MS (ESI$^+$): *m/z* [M+Na]: 361.0.

$[\alpha]^{20}_D$ = 2.23 (*c* 0.12 MeOH) [lit[5]. $[\alpha]_D^{19}$ = -5.6 (*c* 0.6, MeOH); UV (MeOH): ε_{314} =73000.

- **1,5-γ-Quinide 12**

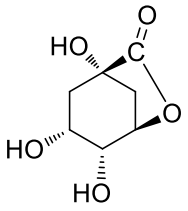

Quinic acid (3g, 15.61mmol) was heated in an open flask at 220^{0}C for 90 min. The brown sticky residue was refluxed with EtOAc (60 mL) for 4h and then the solution was cooled to room temperature. The solvent was removed under pressure to give 1,5-γ-quinide as a colorless solid in 85% yield. NMR data were in accordance with the literature.[9,10]

- **3-*tert*-Butyldimethylsiloxy-1,4-dihydroxy-cyclohexane-1,5-carbolactone and 4-*tert*-Butyldimethylsiloxy-1,3-dihydroxy-cyclohexane-1,5-carbolactone 13 and 14**

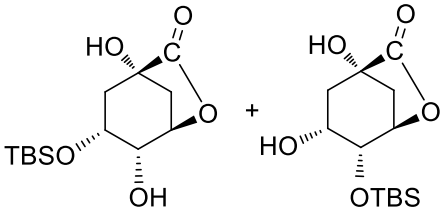

TBSi-Cl (1.31 g, 8.68 mmol) was added to a stirred solution of 1,5-γ-quinide (1.31 g, 7.55 mmol) and imidazole (1.9 g, 28 mmol) in anhydrous DMF (14 mL) at 0 °C. The mixture was stirred at 0 °C for 30 min followed by 1 h at room temperature and then poured into water (50 mL) and extracted with EtOAc (50 ml) and diethyl ether (40 mL). The organic layer was washed with water (3 × 100 mL), dried over Na_2SO_4 and concentrated under reduced pressure to give a white solid in 57% yield containing esters **13** and **14** in ratio 7:3. The crude mixture was used in the next step without further purification. NMR data were in accordance with the literature.[11,12]

- **4-Acetyl-*p*-coumaroyl-3-tert-butyldimethylsiloxy-1-hydroxycyclohexane-1,5-carbolactone 15**

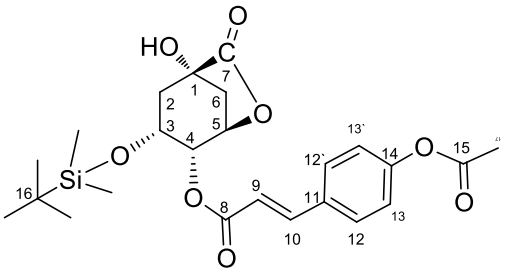

To a solution of 3-*tert*-Butyldimethylsiloxy-1,4-dihydroxy-cyclohexane-1,5-carbolactone, as a mixture of **13** and **14**, (500 mg, 1.74mmol) and DMAP (32 mg, 0.26 mmol) in pyridine (15 mL), *p*-acetylcoumarylchloride (700mg, 3.12mmol) was added. The mixture was stirred 24h at room temperature and then poured onto crushed ice and successively, CH_2Cl_2 (20mL) was added. The mixture was acidified with aq. HCl 1M (pH 2-3) and then extracted with CH_2Cl_2 (three times, 30 mL at time). The organic layer was dried over Na_2SO_4, filtered and the solvent was removed under reduced pressure. The brownish residue was purified by column

chromatography on silica gel (diethyl ether/CH_2Cl_2 50:50) to afford the only ester **15**, in 20% yield, as a colorless solid.

^{1}H NMR (500 MHz, $CDCl_3$), δ: 7.72 (1H, d, *J* = 15.9 Hz, H-10), 7.57 (2H, d, *J* = 8.6 Hz, H-12+H-12'), 7.15 (2H, d, *J* = 8.6 Hz, H-13+H-13'), 6.46 (1H, d, *J* = 15.9 Hz, H-9), 5.43 (1H, t, *J* = 4.8 Hz, H-4), 4.88 (1H, dt, *J* = 12.6, 5.3 Hz, H-5), 4.03 (1H, dt, *J* = 10.7, 4.6 Hz, H-3), 2.55 (1H, d, *J* = 11.8 Hz, H-6), 2.43 (1H, dd, *J* = 11.8, 5.8 Hz, H-6), 2.32 (3H, s, CH_3CO), 2.11 (2H, apparent d, H-2), 0.81 (9H, s, $C(CH_3)_3$), 0.06 (3H, s, CH_3Si), 0.03 (3H, s, CH_3Si).

^{13}C NMR (500 MHz, $CDCl_3$), δ: 177.48 (s, C-7), 169.27 (s, C-15), 165.61 (s, C-8), 152.50 (s, C-14), 145.15 (d, C-10), 131.98 (s, C-11), 129.53 (d, C-12+C-12'), 122.38 (d, C-13+C-13'), 117.40 (d, C-9), 74.42 (d, C-5), 72.15 (s, C-1), 66.68 (d, C-4), 66.06 (d, C-3), 41.14 (t, C-2), 37.64 (t, C-6), 25.71 (q, $C(CH_3)_3$), 21.28 (q, CH_3CO), 18.05 (s, C-16), -4.92 (q, $(CH_3)_2Si$).

- **4-*p*-coumaroylquinic acid 4a**

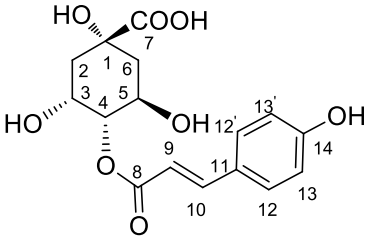

4-*O*-acetyl-*p*-coumaroyl-3-*tert*-butyldimethylsiloxy-1-hydroxycyclohexane-1,5-carbolactone **15** (332mg, 0.7mmol) was dissolved in a mixture of THF (5 mL) and aq. 2M HCl (15mL) and the solution was stirred for 6 days at room temperature. After saturation with solid NaCl the mixture was extracted with EtOAc (3*50 mL) and the organic phase was dried over Na_2SO_4. Evaporation of the solvent gave a yellowish solid in 43% yield which was a mixture of 3-*p*-coumaroylquinic acid **3a** and 4-*p*-coumaroylquinic acid **4a** as determined by ^{1}H-NMR. The crude was purified by semi-preparative RP-HPLC on a Phenomenex Gemini C18 5 µm 10 x 250 mm column, using a gradient of H_2O+0.1% formic (A) acid and MeOH+0.1% (B) (20 min A 80% and B 20%, from 20 to 90 min increase of B until A 40% and B 60%, from 90 to 110 min A 5% and B 95%, from 110 to 125 min A 95% and B 5%) at a flow rate of 2 mL/min. A total of 4 runs were performed, each one injecting 15 mg of the crude mixture. The elution was monitored with UV/vis detector at λ 325nm and the fractions corresponding to each peak were collected and kept at -80°C and then freeze dried and analyzed by ^{1}H NMR. 4-*p*-coumaroylquinic acid **4a** (5mg) was obtained as a white solid. M.p. 179-182°C [lit.[3] 192-193°C]

IR (nujol): ṽ =3580, 3382.60, 2952.03, 1689.11, 1604.93, 1172.21, 1024.40.85, 830.63 cm^{-1}.

^{1}H NMR (500 MHz, CD_3OD), δ: 7.73 (1H, d, *J* = 15.9 Hz, H-10), 7.49 (2H, d, *J* = 8.6 Hz, H-12+H-12'), 6.82 (2H, d, *J* = 8.6 Hz, H-13+H-13'), 6.45 (1H, d, *J* = 15.9 Hz, H-9), 4.81 (1H, dd, *J* = 10.0, 2.8 Hz, H-4), 4.32 (2H, m, H-3 + H-5), 2.22 (4H, m, H-2 + H-6).

^{13}C NMR (126 MHz, CD_3OD), δ: 177.97 (s, C-7), 168.97 (s, C-8), 161.25 (s, C-14), 146.73 (d, C-10), 131.16 (d, C-12+C-12'), 127.31 (s, C-11), 116.82 (d, C-13+C-13'), 115.44 (d, C-9), 79.26 (d, C-4), 76.95 (s, C-1), 69.65 (d, C-5), 65.69 (d, C-3), 42.64 (t, C-6), 38.49 (t, C-2).

MS (ESI^+): *m/z* [M+Na]: 361.0 $[\alpha]^{20}_D$=-28.26 (*c* 0.3, MeOH) [lit[3] $[\alpha]^{20}_D$ = -47.3 (*c* 1.4, MeOH)];

UV (MeOH): ε_{316} =63200.

Computational Calculations

Preliminary Molecular Mechanics calculations and HF optimizations were performed using the Spartan 14 package (ref: Hehre, W. J. *A Guide to Molecular Mechanics and Quantum Chemical Calculations*; Wavefunction, Inc., 2003.), which was installed on an Antec P193 V3, with two six core AMD opteron Processor 2427 2.20GHz, 4 GB RAM, 1 TB physical memory, and 64-bit Windows 7 Enterprise as operating system. Convergence criteria for geometry optimization were set as follow: energy $1.0x10^{-6}$ hartrees, gradient tolerance $3x10^{-4}$ hartrees, distance tolerance $1.2x10^{-3}$ Å. The DFT simulations were performed on the same machine with the Schrodinger suite of programmes using the B3LYP functional[13] and a localized 6-31G* basis set.

8.2. Study of the Concentration profile of CGAs in Walnut (Juglans regia L.) leaves.

Instrumentation

Analysis of *trans* and *cis* caffeoylquinic acids (CQAs), dicaffeoylquinic acids (diCQAs), feruloylquinic acids (FQAs) and *p*-coumaroylquinic acids (*p*CoQAs) along with the hydroxycinnamic acids (caffeic acid, *p*-coumaric acid, ferulic acid and sinapic acid) were performed using a 1290 UHPLC system (Agilent, Germany), consisting of a degasser, a quaternary pump, a column thermostated comparment and a diode array detector (DAD) operating at 305 nm (specific for *p*CoQAs and *p*-coumaric acid) and 324 nm. A Kinetex XB-C18 column 2.6 µm 100 x 2.1 mm (Phenomenex, USA) was used at 25°C. Solvents were used at a total flow rate of 0.5 mL/min and the volume of injection was 2.0 mL. Solvent A was water/formic acid (1000:1 v/v) and solvent B acetonitrile. The gradient profile was from initial 97% of solvent A to 85% of A in 8 min, then 60% of A at 11min, and a return to 97% A at 12 min to re-equilibrate.

Qualitatively identification of CGAs was achieved by comparison of specific retention times of diluted standard solutions and by spiking samples with small amounts of each respective standard. Stereoisomers *cis* 3-caffeoylquinic acid (*cis* 3-CQA), *cis* 4-caffeoylquinic acid (*cis* 4-CQA), *cis* 5-caffeoylquinic acid (*cis* 5-CQA), *cis* 3-*p*-coumaroylquinic acid (*cis* 3-*p*CoQA), *cis* 4-*p*-coumaroylquinic acid (*cis* 4-*p*CoQA) and *cis* 5-*p*-

coumaroylquinic acid (*cis* 5-*p*CoQA) were clearly identified using a 1290 UHPLC system (Agilent Technologies) equipped with a Triple Quad 4500 (Sciex) with an electrospray ionization source. In order to discriminate the isomers a Monitoring Reaction Mode (MRM) acquisition method was used in negative ionization, as previously reported[14].

Quantitative determination was performed by UHPLC using calibration curve of *trans* 5-CQA. Standard stock solution was prepared in MeOH:H_2O (1:1) at appropriate concentration and different diluted solutions were prepared from stock solution.

Chemicals

3-Caffeoylquinic acid (3-CQA), 4-caffeoylquinic acid (4-CQA), 5-caffeoylquinic acid (5-CQA), 3,4 dicaffeoylquinic acid (3,4-diCQA), 3,5-dicaffeoylquinic acid (3,5-diCQA) and 4,5-dicaffeoylquinic acid (4,5-diCQA) were purchased from Phytolab. Hydroxycinnamic acids standards and acetonitrile (HPLC grade) were purchased from Sigma –Aldrich while formic acid was obtained from CARLO ERBA Reagents S.r.l. (Cornaredo, Italy). Not commercially available standards such as feruloylquinic acids (FQAs) and *p*-coumaroylquinic acids (*p*-CoQAs) were obtained by carrying out their chemical synthesis[15,16]. Water was treated in a Milli-Q water purification system (Millipore Academic).

Samples

Fresh leaves from different branches were collected from a single *Juglans regia* L. tree, in an urban context (Trieste, Italy), in four different period of growth, from spring to late summer 2016 (April 21th, May 3rd, July 21th and September 9th). After sampling, leaves were cleaned and dried on an absorbent paper and the ones with similar size were chosen and weighed. Then, they were immediately put in plastic bags and stored in a freezer at -20 °C. In a second time, samples were freeze dried (lyophilizer Christ Alpha 1-2) for subsequent analysis.

Extraction of Phenolic Compounds and Sample preparation

Extractions were performed in duplicate by decoction preparation, in order to simulate home preparation for medicinal uses. For this purpose, 1g of lyophilized leaves for each collection time was added to 200 mL of boiling water[17]. The mixture was stirred for 5 min at 200 rpm on a heated plate (Arex Velp Scientifica) and filtered through qualitative filter paper n. 302 (VWR Europe). The aqueous extract was frozen with liquid nitrogen and freeze dried for 3 days.

For quantification purposes, lyophilized decoction material, around 235 mg/g of dry material, was dissolved in water to afford concentrations of 30 mg/mL. In order to analyze each compound accurately, diluted

solutions in ratios of 1:2, 1:4 and 1:10 were prepared in water and filtered across a nylon filter (pore size 0.2 μm), transferred to a vial and immediately analyzed by Ultra High Pressure Liquid Chromatography (UHPLC).

8.3 Study of Chlorogenic acids in coffee

Instrumentation

Green coffee and roasted coffee beans were ground to a powder in a mixer mill (Restsch, model MM400). Green coffee beans were roasted in a thermoblock Thermostatic Dry Bath (Fratelli Galli G-Block) at 211°C at different times (3, 5, 7, 10, 12, 15, 20, 25, 30, 35, 40 and 45min).

Analysis of caffeoylquinic acids (CQAs), dicaffeoylquinic acids (diCQAs), feruloylquinic acids (FQAs) and *p*-coumaroylquinic acids (*p*CoQAs), along with the hydroxycinnamic acids: caffeic acid, coumaric acid, ferulic acid and sinapic acid, were performed using a 1290 UHPLC system (Agilent, Germany), consisting of a degasser, a quaternary pump, a thermostated column compartment and a diode array detector (DAD) operating at 305 nm (specific for *p*CoQA) and 324 nm. A Kinetex XB-C18 column 2.6 μm 100 x 2.1 mm (Phenomenex, USA) was used at 25°C. Solvents were used at a total flow rate of 0.5 mL/min and the volume of injection was 2.0 μl. Solvent A was water/formic acid (1000:0.001 v/v) and solvent B acetonitrile. The gradient profile was from initial 97% of solvent A to 85% of A in 8 min, then 60% of A at 11min, and a return to 97% A at 12 min to re-equilibrate.

Identity of each CGA was confirmed by comparison of the fragment ions already reported by Clifford et al.[18] as well as those observed from diluted pure standard solutions in an ABSciex Triple Quad 4500 coupled with a 1290 UHPLC system from Agilent. LC separation was performed using the same method described above and MS was operating in negative mode, ionization voltage of 4500, desolvation temperature of 350°C and gas flows of GS1 30 and GS2 40.

Qualitatively identification of CGAs was achieved by comparison of specific retention times of diluted standard solutions and by spiking samples with small amounts of each respective standard. Quantitative determination was performed by UHPLC using calibration curve 5-CQA. Standard stock solution was prepared in MeOH:H_2O (1:1) at appropriate concentration and different diluted solutions were prepared from stock solution.

Chemicals

3-Caffeoylquinic acid (3-CQA), 4-caffeoylquinic acid (4-CQA), 5-caffeoylquinic acid (5-CQA), 3,4 dicaffeoylquinic acid (3,4-diCQA), 3,5-dicaffeoylquinic acid (3,5-diCQA) and 4,5-dicaffeoylquinic acid (4,5-diCQA) were purchased from Phytolab (Vestenbergsgreuth, Germany). Caffeine, magnesium oxide, hydroxycinnamic acids standards, acetonitrile and methanol (HPLC grade) were purchased from Sigma – Aldrich S.r.l. (Milano, Italy) while formic acid was obtained from CARLO ERBA Reagents S.r.l. (Cornaredo, Italy). Standards not commercially available such as feruloylquinic acids (FQAs) and *p*-coumaroylquinic acids (pCoQA) [16] were obtained by carrying out their chemical synthesis described before. Feruloylquinic acids (FQAs) [15] were provided by Aromalab laboratory of Illycaffè. Water was treated in a Milli-Q water purification system (Millipore Academic).

Samples

A total of twentyseven fresh green coffee samples from different geographical origins and different species were analyzed. (Table 8.1) Samples were provided by Illycaffè S.p.A, Trieste- Italy in collaboration with CATIE, Costa Rica.

Table 8.1 – Samples of green coffee beans

Sample	Coffee species	Origin	Identification Code	Geographical Origin
1	*C. arabica*	Commercial Lot		Brazil
2	*C. arabica*	Commercial Lot		Colombia
3	*C. arabica*	Commercial Lot		Ethiopia
4	*C. arabica*	Commercial Lot		Ethiopia
5	*C. arabica*	Commercial Lot		Honduras
6	*C. arabica*	Commercial Lot		India
7	*C. arabica*	Commercial Lot		Yemen (Harazi)
8	*C. arabica*	Commercial Lot		Yemen (Matari)
9	*C. arabica var. laurina*	Commercial Lot		Guatemala
10	*C. canephora*	Commercial Lot		Vietnam
11	*C. canephora*	Commercial Lot		India
12	*C. liberica*	Commercial Lot		Indonesia
13	*C. liberica*	CATIE	T.03447	Costa Rica
14	*C. liberica*	CATIE	T.03475	Costa Rica
15	*C. liberica*	CATIE	T.03476	Costa Rica
16	*C. liberica*	Commercial Lot		Indonesia
17	*C. liberica*	Commercial Lot		Indonesia
18	*C. arabica L.* x *C. canephora Pierre*	CIRAD	15	France
19	*C. arabica L.* x *C. canephora Pierre*	CIRAD	24	France
20	*C. eugenioides*	CATIE	T.21387	Costa Rica
21	*C. eugenioides*	CATIE	T.02725	Costa Rica
22	*C. sessiliflora*	CATIE	T.21348	Costa Rica

23	*C. sessiliflora*	CATIE	T.21345	Costa Rica
24	*C. congensis*	CATIE	005241	Costa Rica
25	*C. pseudozanguebariae*	CATIE	T.21352	Costa Rica
26	*C. racemosa*	Commercial Lot		Mozambique
27	*C. brevipes*	CATIE	T.21372	Costa Rica

Extraction of Chlorogenic acids and Sample preparation

Green and roasted coffee beans were ground to a powder and extractions were performed in duplicate by decoction preparation, for this purpose, 1g of powdered green coffee beans for each species was added to 100 mL of boiling water[17]. The mixture was stirred for 10 min at 200 rpm on a heated plate (Arex Velp Scientifica) and filtered through qualitative filter paper n.302 (VWR International Srl, Milano, Italy). The aqueous extract was frozen with liquid nitrogen and freeze dried for 3 days.

For quantification purposes, lyophilized decoction material was redissolved in water to afford concentrations of 30 mg/mL. In order to analyze each compound accurately every class of compounds was quantified on a specific diluted solution, because concentration of caffeoylquinic acids is appreciably higher than other minor compounds, so dilution of 1:2, 1:4 1:10 and 1:20 were prepared in water and filtered across a nylon filter (pore size 0.2 µm), transferred to a vial and immediately analyzed by Ultra High Pressure Liquid Chromatography (UHPLC).

8.4 Recognition Systems for 5-CQA

Materials

Chemicals and solvents were purchased from Sigma Aldrich, deuterated solvents from Aldrich and Cambridge Isotope Laboratories. When anhydrous conditions were required, reaction flasks were flame-dried and placed under a flux of argon. Crimp cap Weaton vials used for the polymer synthesis were purchased from Sigma Aldrich. Dialysis membrane MWCO 3500 Da was purchased from Spectrumlabs. For immobilization of polymers, polysine^{R} slides were purchased from Thermo Scientific.

Instrumentation

- **Nuclear magnetic resonance (NMR):** 500 MHz ^{1}H-NMR and 125 MHz ^{13}C-NMR spectra were obtained on a Varian 500 spectrometer. ^{1}H-NMR titrations were performed on a Varian 500

spectrometer. The resonances multiplicity is described as s (singlet), d (doublet), t (triplet), q (quartet), m (multiplet), dd (doublet of doublets), br (broad signal).

- **Fluorescence measurements** were performed on a Synergy H1 hybrid reader (Biotek) spectrophotometer.
- **UV-visible spectra** were recorded on a UV-1800 spectrophotometer (Shimadzu) and on a CARY-100 UV-visible spectrophotometer (Varian).
- **Particles size** were measured by a Dynamic Laser Light Scattering (DLLS) on Zetasizer nano-S (Malvern) instrument .
- **Rebinding tests** were performed on a 1290 UHPLC system (Agilent, Germany), consisting of a degasser, a quaternary pump, a thermostated column compartment and a diode array detector (DAD) operating at 305 nm (specific for *p*-coumaric acid), 324 nm (for 5-CQA and caffeic acid) and 273nm (for caffeine). A Kinetex XB-C18 column 2.6 µm 100 x 2.1 mm (Phenomenex, USA) was used at 25°C. Solvents were used at a total flow rate of 0.5 mL/min and the volume of injection was 2.0 mL.

Synthesis of mimic template H-5CQA

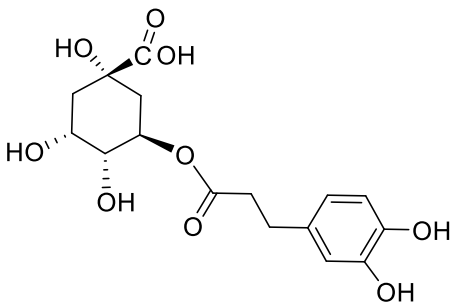

5-caffeoylquinic acid (200 mg, 0.56 mmol) was dissolved in EtOH (30 ml) under argon atmosphere and 40 mg of Pd/C 10% were added. The reaction mixture was stirred at room temperature under H_2 atmosphere for 6h. Pd/C was removed by filtering the solution over celite. EtOH was removed under pressure and the resulting oil was redissolved in water and freeze-dried to afford reduced H-5CQA as a white solid (181mg, 95%). NMR data were in accordance with the literature.[19]

Recrystallization of AIBN

2.0 g of AIBN were placed in a round-bottomed flask equipped with a stirring bar and a condenser. The vacuum and a flow of argon was alternated in the system for 3 times, to avoid any trace of oxygen. AIBN was dissolved in 5mL of ethanol and the temperature was increased to 50-55 °C. At this temperature, 2 mL of

ethanol were added to solubilize the product and the flask was then left to reach room temperature to allow the crystallization.

8.4.1 Fluorescent Molecularly Imprinted Polymers (fMIPs) for 5-CQA: MIP01 and MIP02

Synthesis of Functional monomer 16b

- **Synthesis of 4-chloro N-allyl-1,8-naphthalimide (16a)**

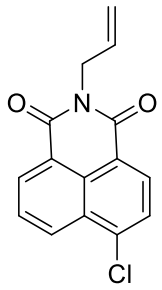

1.0065g (1 eq) of 4-chloro-1,8-naphthalic anhydride were dissolved in 45 mL of ethanol and the resulting solution was heated up to 55 °C under continuous stirring; at this temperature 330µL of allyl amine (1 eq) and 5mL of ethanol were added. The mixture was refluxed for four hours. After cooling at room temperature, the solid was filtered, washed with ethanol and dried under vacuum to give 652 mg (yield 55%) of a light brown powder. NMR data were in accordance with the literature.[20]

- **Synthesis of 4-[(2-ethylenediamine)] N-allyl-1,8-naphthalimide (16b)**

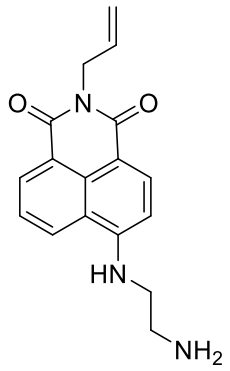

A mixture of 645 mg of **16a** (2.04 mmol, 1 eq), 1.9 mL of ethylene diamine (1.7 g, d=0.90 g/mL, 24.5 mmol, 12 eq) and 40 mL of ethanol was heated under reflux. After 20, 23, 42 and 46 hours, further three equivalents of ethylene diamine were added. 66 hours were required to complete the reaction. At the end of the reaction, solvent was removed under reduced pressure to obtain a red oil. Subsequently, 60 mL of water were added to the oil and the mixture was cooled overnight at 4 °C. The solid obtained was filtered, washed with cool water and dried at 60 °C for two days. 553 mg of pure **16b** were obtained as a red solid (yield 92%). NMR data were in accordance with the literature.[20]

^{1}H NMR Titrations

Interactions between the functional monomers and the template molecule were investigated by titrating each functional monomer **4VPy** and **16b** with 5-caffeoylquinic acid. In general, 4 mM solutions of monomers in DMSO-d_6 were titrated with increasing amounts of chlorogenic acid (5-CQA) to obtain final concentrations ranging from 2 mM to 40 mM.

Synthesis of fluorescent molecularly imprinted polymers (fMIPs):

- **Synthesis of MIP01 and NIP01**

1 eq of functional monomers **4VPy** and **16b** and 1 eq of the mimic template (H-5CQA) were dissolved in a total amount of DMSO corresponding to the 99% in weight of total functional monomers and crosslinker. After stirring for 60 minutes, the solution was transferred in a crimp cap Wheaton vial and 60% (in mol) of N,N'-methylenebisacrylamide (MBA), 5% (in mol, calculated on the amount of the available double bonds) of recrystallized azobisisobutyronitrile (AIBN) were added. The vial was left first under vacuum and then was flushed with argon (3 times for 5 minutes). Radical polymerization was achieved heating the vial up to 70°C for 24 hours. Each polymer was synthesized either in presence of the template molecule (to obtain fMIP) and without the template (to obtain fNIP). The resulting orange solutions were dialyzed against water for 2 days, a mixture of acetic acid and methanol 2:8 for two days, methanol (10%) for 2 days, and against water for one day changing the solvent 3 times a day. Finally, the solutions were freeze-dried leading to a fluffy orange polymer for fMIP and a yellow polymer for fNIP.

- **Synthesis of MIP02 and NIP02**

1 eq of functional monomer **16b** and 1 eq of the mimic template (H-5CQA) were dissolved in a total amount of DMSO corresponding to the 99% in weight of total functional monomers and crosslinker. After stirring for 60 minutes, the solution was transferred in a crimp cap Wheaton vial and 60% (in mol) of MBA, 5% (in mol, calculated on the amount of the available double bonds) of recrystallized AIBN and 30% (in mol, 3eq) of N-isopropylacrilamide (NIPAM) were added. The vial was left first under vacuum and then was flushed with argon (3 times for 5 minutes). Radical polymerization was achieved heating the vial up to 70°C for 24 hours. Each polymer was synthesized either in presence of the template molecule (to obtain fMIP) and without the template (to obtain fNIP). The resulting orange solutions were dialyzed against water for 2 days, a mix of acetic acid and methanol 2:8 for two days, methanol (10%) for 2 days, and against water for one day changing the solvent 3 times a day. Finally, the solutions were freeze-dried leading to a fluffy orange polymer for fMIP and a yellow polymer for fNIP.
The composition of the polymerization mixtures for each polymer is reported in table 8.2.

Table 8.2 – Composition of polymerization mixtures

Component (mg)	fMIP01	fNIP01	fMIP02	fNIP02
Template (H-5CQA)	16.0	-	8.0	-
Functional monomer (16b)	13.3	13.3	6.6	6.6
Functional monomer (4Vpy)	4.7	4.7	-	-
Co-monomer (NIPAM)	-	-	7.6	7.6
Crosslinker (MBA)	20.8	20.8	20.8	20.8
Initiator (AIBN)	3.0	3,0	3.0	3.0
Porogen solvent (DMSO)	7761	7761	6965	6965

4-[(2-ethylenediamine)] N-allyl-1,8-naphthalimide (16b) content in fMIPs and fNIPs 01 and 02

The concentration of monomer **16b** in the corresponding fluorescent polymers was calculated by UV-visible spectroscopy. The absorbance intensities at 44 nm in the UV-visible spectrum of DMSO solutions in a quartz cuvette of 500µL of 630 µg/mL for fMIP01 and 200µg/mL for fMIP02, after sonication for 20 min, were measured. Solutions of 473 µg/mL and 193µg/mL were used to measure the absorbance of fNIP01 and fNIP02 respectively. The obtained values were used to calculate the monomer concentration from a calibration

curve of free 4-[(2-ethylenediamine)]-N-allyl-1,8-naphthalimide (**16b)** in DMSO. Calibration was carried out measuring the absorbance intensity at 440 nm of increasing solutions of free dye from 10 µM to 70 µM.

Rebinding Tests

The rebinding kinetics of 5-CQA with fluorescent polymers were investigated dissolving 1.5 mg of fMIP01 and 2mg of fMIP02 in 1.5 mL and 2mL respectively of an 80 µM of 5-CQA solution in water. The mixtures were incubated at 25°C under continuous stirring and 200 µL aliquots of the solution were taken at different times (from 10 min to 6 h). Each aliquot was centrifuged (12000 rpm for 10 min) to remove the polymer and the supernatants containing an unknown amount of the analyte were analyzed by the same UHPLC method developed for the quantification of chlorogenic acids in coffee to quantify the free 5-CQA concentration. The ratio between the area of the reference peak of the analyte and the peak in the chromatogram of the sample treated with the polymer were calculated to obtain the amount of 5-CQA captured by the polymers[21].

Cross-reactivity Studies

The polymer selectivity was investigated following the same approach of the rebinding test by UHPLC. The fMIP01 and fNIP01 were treated with an 80 µM solution of a mixture of pure standards of 5-CQA, caffeic acid, *p*-coumaric acid and caffeine. The mixtures were incubated at 25°C under continuous stirring and 200 µL aliquots of the solution were taken after different times (from 10 min to 24 h). Each aliquot was centrifuged (12000 rpm for 10 min) to remove the polymer and the supernatants containing an unknown amount of the standards were analyzed by the same UHPLC method developed for the quantification of chlorogenic acids in coffee.

Fluorescence Titration of MIP01 and MIP02

The fluorescent properties of MIP01 and MIP02 were analyzed by fluorescence titrations of a 30 µg/mL solution of the polymers obtained by dilution of the 1 mg/mL solution in DMSO and water:DMSO (9:1) ,with increasing concentrations of the target molecule 5-CQA from micromolar to millimolars concentrations. The fluorescence emission of the polymers was analyzed at 530 nm, when the titrations were carried out in DMSO, and 540 nm when titrations were carried out in water: DMSO. Both polymers were excited at 440 nm.

Dynamic Laser Light Scattering

Solutions of 1mg/mL MIP01 and fNIP01 were prepared in DMSO and diluted to obtain a concentration of 0.25 and 0.5 $mg \cdot mL^{-1,}$ respectively. The solutions were placed into an ultrasonic bath for 1 h. After filtration

on 0.45 µm filter, the size distribution by intensity and by volume was recorded in triplicate on a Malvern Zetasizer instrument using a 1 mL quartz cuvette with light path of 1 cm.

Immobilization Test

80µL of 10% solution of glutaraldehyde in PBS were added to different commercial polysine^{R} slides and left at room temperature for one hour. Subsequently, the glass plates were washed with 3 mL of water (1mL at a time). A mixture was prepared by mixing a 20mg/mL gelatin solution in water and 100µg/mL suspension of fluorescent polymer MIP01 in water in a ratio 1: 1 and 80µL of the mixture were added to different polysine^{R} slides. These glass plates were kept in the dark at room temperature for 24 hours. Then, the fluorescence of the immobilized polymer on the plates was measured before and after washing with 3mL of water (1 mL at a time) to determine the residual concentration of the immobilized polymer. Soon after, 40µL of solutions of a range of concentrations between 78µM and 40mM of a 5-CQA pure standard solution were added to the different plates in duplicate and the samples were incubated for 90 min in the dark at room temperature. Finally, the fluorescence intensity of the polymer in each plate was measured before and after washing them with 2 mL of water (500µL at a time).

8.4.2 Molecularly Imprinted Polymers (MIP) for 5-CQA: MIP03

Synthesis of mono 5-caffeoylquinic acid fluorescent derivatives

- **Intermediates (17a) and (17b): Amidation of 5-CQA**

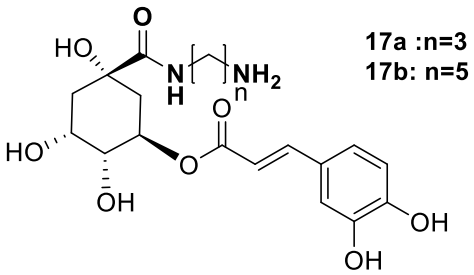

To a solution of 5-CQA (300 mg, 0.85 mmol) and TBTU (1.3mmol) in DMF, DIPEA (1.70mmol) was added, under argon atmosphere. The reaction was stirred at 25°C for 40 minutes, and then, the appropriate amine (diaminopropane or cadaverine) (1,3mmol) was added followed by a second amount of DIPEA (1.70 mmol). The reaction was monitored by TLC ($CHCl_3$: MeOH 9:1) until disappearance of the starting material. After 14 hours the solvent was removed under pressure to obtain an oil that was redissolved in water (20mL and freeze-dried to afford the corresponding amides as a yellowish solid. The formation of the products was confirmed by ^{1}H NMR and they were used in the next step without further purification.

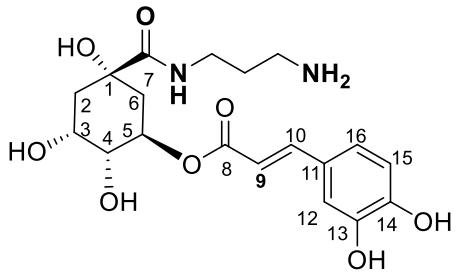

Yield: 56%, yellowish solid. (**17a**)

^{1}H NMR (500 MHz, CD_3OD), δ: 7.97 (3H, br, Ar-OH+CONH), 7.57 (1H, d, *J* = 15.9 Hz, H-10), 7.05 (1H, d, *J* = 1.84 Hz, H-12), 6.95 (1H,d d, *J*= 8.2; 1.9 Hz, H-16), 6.78 (1H, *J* = 8.2 Hz, H-15), 6.26 (1H, d, *J* = 15.9 Hz, H-9), 5.40 (1H, dt, *J*=11.42, 5.0, 21.2 Hz, H-5), 4.24 (1H, m, W_H 13.8, H-3), 3.72 (1H, m, W_H =18.46 Hz, H-4), 3.60 (1H, m, NH-CH_2-), 3.25 (1H,m, NH-CH_2-), 3.08 (1H, t, *J* = 7.63 Hz, CH_2-NH_2), 2.92 (1H, t, *J* = 7,3 Hz, CH_2-NH_2), 2.81 (1H, br, NH_2), 2.16 – 1.80 (6H, m, H-2+H-6+ CH_2-).

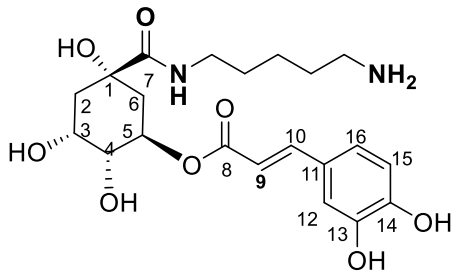

Yield: 47%, yellowish solid. (**17b**)

^{1}H NMR (500 MHz, CD_3OD), δ: 7.97 (3H, br, Ar-OH+ CONH), 7.57 (1H, d, *J* = 15.8 Hz, H-10), 7.05 (1H, d, *J* = 1.1 Hz, H-12), 6.95 (1H, dd, *J*= 8.2, 1.5 Hz, H-16), 6.78 (1H, *J* = 8.2 Hz, H-15), 6.30 (1H, d, *J* = 15.8 Hz, H-9), 5.40 (1H, dt, *J*=11.33, 5.1, 26.1 Hz, H-5), 4.24 (1H, m, W_H 10.5, H-3), 3.72 (1H, m, W_H=19.46 Hz, H-4), 3.20 (4H, m, NH-CH_2+CH_2-NH_2), 2.81 (1H, br, NH_2) 2.12 – 1.92 (4H, m, H-2+H-6), 1.51-1.73 (6H, m, CH_2-CH_2-CH_2).

- **Synthesis of Fluorescein derivative 19a**

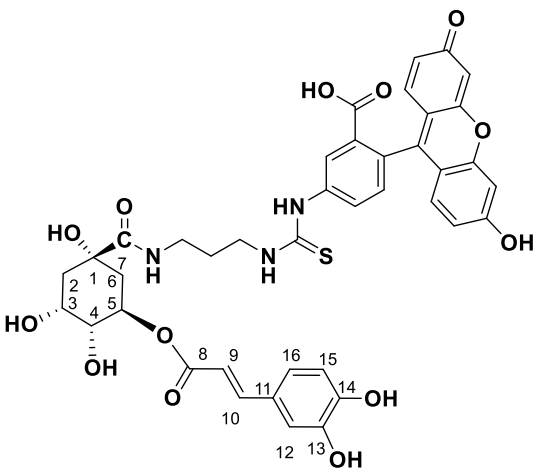

To a solution of the intermediate **17a** (133mg, 0.32 mmol) and DIPEA (0.75mmol) in DMF, FITC (0.48mmol) was added under argon atmosphere. The mixture was stirred 24h at room temperature. Subsequently, 40mL of water were added and extraction with EtOAc was performed (three times, 30 mL at time). The organic layer was dried over Na_2SO_4, filtered and the solvent was removed under reduced pressure. The orange residue was purified by column chromatography on silica gel (gradient CH_2Cl_2/MeOH) to afford the product in 41% yield as an orange solid.

^{1}H NMR (500 MHz, DMSO-d_6), δ: 8.10 (1H, br, Ar-H_{FITC}), 7.89 (1H, m, Ar-H_{FITC}), 7.64 (1H, d, *J* = 8.2, Ar-H_{FITC}), 7.40 (1H, d, *J* = 15.6 Hz, H-10), 7.05 (3H, m, Ar-H_{FITC}+H-12), 6.90 (1H, d, *J*= 7.11, H-16), 6.64 (4H, br,Ar-H_{FITC}), 6.61 (1H, m, H-15), 6.13 (1H, d, *J* = 16.0 Hz, H-9), 5.20 (1H, dt, *J*=9.9, 5.3, 25.7 Hz, H-5), 4.03 (1H, m, H-3), 3.48 (5H, m, partially overlapped with water peak), 1.94 – 1.61 (6H, m, H-2+H-6+ CH_2-).

MS (ESI$^+$): *m/z* [M-H]: 798.2

^{13}C NMR (500 MHz, DMSO-d_6), δ: 177.33 (s, CSNH), 176.47 (s, COOH), 174.27 (s, C-7), 173.91 (C-8), 166.31 (s, C-Ar), 160.83 (s, C-Ar), 156.56 (s, C-Ar), 156.52 (s, C-Ar), 146.99 (s, C-14), 145.66 (s, C-13), 145.26 (d, C-10), 135.85 (s, C-11), 135.65 (s, C-Ar), 132.99 (s, C-Ar), 132.69 (s, C-Ar), 130.73 (d, C-Ar), 130.31 (d, C-Ar), 129.74 (d, C-Ar), 128.38 (s, C-Ar), 127.56 (d, C-Ar), 127.05 (d, C-Ar), 122.16 (d, C-12), 116.81 (d, C-15), 115.70 (s, C-Ar), 115.68 (s, C-Ar), 115.60 (d, C-9), 113.03 (d, C-16), 109.53 (d, C-Ar), 102.40 (d, C-Ar), 81.08 (s, C-1), 72.23 (d, C-5), 72.87 (d, C-4), 70.83 (d, C-3), 45.23 (d, CH_2NH), 39.93 (t, CH_2NH), 38.22 (t, C-2), 37.84 (t, C-6), 28.72 (t, CH_2).

MS (ESI$^+$): *m/z* [M-H]: 798.2

- **Synthesis of Fluorescein derivative 19b**

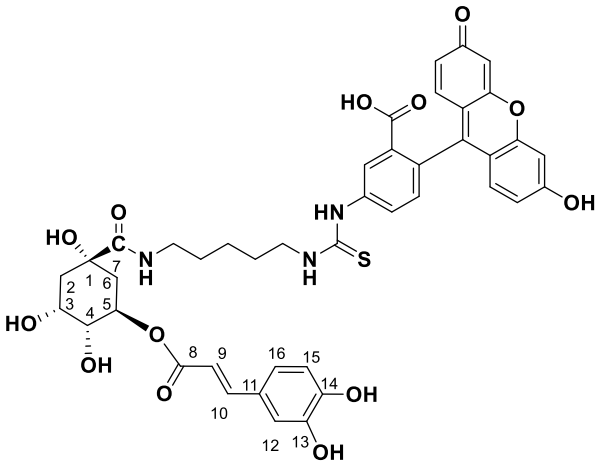

To a solution of the intermediate **17b** (71mg, 0.16 mmol) and DIPEA (0,65mmol) in DMF, FITC (0.24mmol) was added under argon atmosphere. The mixture was stirred 24h at room temperature. Subsequently, 40mL of water were added and extraction with EtOAc was performed (three times, 30 mL at time). The organic

layer was dried over Na_2SO_4, filtered and the solvent was removed under reduced pressure. The orange residue was purified by column chromatography on silica gel (gradient CH_2Cl_2/MeOH) to afford the product in 40% yield as an orange solid.

^{1}H NMR (500 MHz, CD_3OD), δ: 8.11 (1H, br, Ar-H_{FITC}), 8.05 (1H, d, J=1,7Hz, Ar-H_{FITC}), 8.0 (1H, dd, *J*= 2.02, 9.5 Hz, Ar-H_{FITC}), 7.74 (1H, m, Ar-H_{FITC}), 7.57 (1H, d, *J* = 15.9 Hz, H-10) ,7.17 (2H, m, Ar-H_{FITC}), 7.05 (1H, d, *J* = 2.01 Hz, H-12), 6.93 (1H, dd, *J*= 8.2, 2.0 Hz, H-16), 6.77 (1H, d, *J*= 8.1, H-15), 6.68 (2H, br, Ar-H_{FITC}), 6.61 (1H, m, Ar-H_{FITC}), 6.30 (1H, d, *J* = 15.9 Hz, H-9), 5.20 (1H, dt, *J*=10.04, 5.2, 26.1 Hz, H-5), 4.22 (1H, m, W_H=9.0, H-3), 3.72 (5H, m, H4+NH-CH_2+CH_2NH_2), 2.1– 1.61 (6H, m, H-2+H-6), 1.71 (6H, m, CH_2-CH_2-CH_2).

MS (ESI$^+$): *m/z* [M-H]: 826.2

^{13}C NMR (500 MHz, CD_3OD), δ: 177.70 (s, CSNH), 177.54 (s, COOH), 176.34 (s, C-7), 173.73 (C-8), 169.61 (s, C-Ar), 167.85 (s, C-Ar), 157.65 (s, C-Ar), 157.40 (s, C-Ar), 146.72 (s, C-14), 145.59 (s, C-13), 145.42 (d, C-10), 135.28 (s, C-11), 133.82 (s, C-Ar), 133.05 (s, C-Ar), 132.79 (s, C-Ar), 131.99 (d, C-Ar), 130.1 (d, C-Ar), 129.42 (d, C-Ar), 128.64 (s, C-Ar), 127.36 (d, C-Ar), 127.29 (d, C-Ar), 121.79 (d, C-12), 117.74 (d, C-15), 117.66 (s, C-Ar), 115.48 (s, C-Ar), 117.24 (d, C-9), 112.00 (d, C-16), 109.53 (d, C-Ar), 102.40 (d, C-Ar), 81.60 (s, C-1), 72.22 (d, C-5), 72.87 (d, C-4), 70.24 (d, C-3), 44.80 (d, CH_2NH), 44.57 (t, CH_2NH), 38.29 (t, C-2), 37.72 (t, C-6), 29.00 (t, CH_2), 28.92 (t, CH_2), 28.68 (t, CH_2).

- **Synthesis of EDANS derivative 20a**

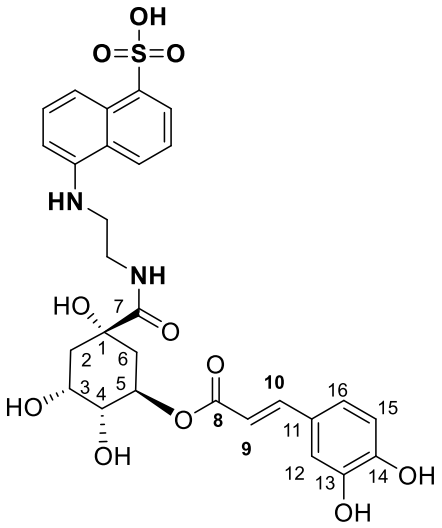

To a solution of 5-CQA (300 mg, 0.85 mmol) and TBTU (1.3mmol) in DMF, DIPEA (1.70mmol) was added under argon atmosphere. The reaction was stirred at 25°C for 40 minutes and then EDANS (1.3mmol) was added followed by a second amount of DIPEA (1.70 mmol). The reaction was monitored by TLC (CH_2 Cl_2: MeOH 4:1) until disappearance of the starting material. After 24 hours the solvent was removed under pressure. The

sticky brown product was purified by column chromatography on silica gel (gradient CH_2Cl_2/MeOH) to afford the product in 50% yield as a green solid.

^{1}H NMR (500 MHz, CD_3OD), δ: 8.17 (1H, dd, *J*=2.80, 8.7 Hz, Ar-H_{EDANS}), 8.12 (2H, d, J=7.7 Hz, Ar-H_{EDANS}), 7.57 (1H, d, *J* = 15.8 Hz, H-10), 7.40 (2H, t, *J*=7.8 Hz, Ar-H_{EDANS}), 7.05 (1H, d, *J* = 2.0 Hz, H-12), 6.94 (1H, dd, *J*= 8.2, 2.0 Hz, H-16), 6.80 (1H, d, *J*= 8.2, H-15), 6.64 (1H, d, *J*=7.7, Ar-H_{EDANS}), 6.30 (1H, d, *J* = 15.8 Hz, H-9), 5.20 (1H, dt, *J*=11,3, 5.0, 26.2 Hz, H-5), 4.22 (1H, m, W_H=9.0 Hz, H-3), 3.72 (1H, m, H-4), 3.42 (2H, t, J=6 Hz, NH-CH_2-), 3.49 (2H, m, CH_2-NH), 2.1– 1.9 (4H, m, H-2+H-6).

^{13}C NMR (500 MHz, CD_3OD), δ: 177.39 (s, C-7), 168.52 (s, C-8), 149.69 (s, C-14), 145.28 (s, C-13), 146.90 (d, C-10), 137.72 (s, C-Ar), 131.43 (s, C-Ar), 128.97 (s, C-11), 128.53 (d, C-Ar), 126.40 (d, C-Ar), 125.65 (s, C-Ar), 125.20 (d, C-Ar), 123.40 (d, C-Ar), 122.61 (d, C-12), 116.53 (d, C-15), 115.43 (d, C-Ar), 115.19 (d, C-9), 114.89 (d, C-16), 104.76 (d, C-Ar), 77.71 (s, C-1), 71.84 (d, C-5), 72.34 (d, C-3), 74.26 (d, C-4), 44.79 (d, CH_2), 39.51 (t, CH_2), 39.40 (t, C-2), 38.46 (t, C-6).

MS (ESI^+): *m/z* [M-H]: 601.3.

^{1}H NMR Titrations

Interactions between the functional monomer and the template molecule were investigated by titrating the functional monomer **21a** with 5-caffeoylquinic acid. In general, a 4 mM solution of monomer was prepared in DMSO-d_6 and increasing amounts of chlorogenic acid (5-CQA) were added to obtain final concentrations ranging from 2 mM to 32 mM. ^{1}H NMR were recorded after each addition of 5-CQA.

Synthesis of Molecularly imprinted polymer MIP03 and NIP03

1 eq of functional monomer **21a** and 1 eq of the mimic template (H-5CQA) were dissolved in a total amount of DMSO corresponding to the 99% in weight of total functional monomers and crosslinker. After stirring for 60 minutes, the solution was transferred in a crimp cap Wheaton vial and 60% (in mol) of MBA, 5% (in mol, calculated on the amount of the available double bonds) of recrystallized AIBN and 30% (in mol, 3eq) of N-isopropylacrilamide (NIPAM) were added. The vial was left first under vacuum and then was flushed with argon (3 times for 5 minutes). Radical polymerization was achieved heating the vial up to 70°C for 24 hours. The polymer was synthesized either in presence of the template molecule (to obtain MIP03) and without the template (to obtain NIP03). The resulting solutions were dialyzed against water for 2 days, a mixture of acetic acid and methanol 2:8 for two days, methanol (10%) for other 2 days, and against water for one day, changing the solvent 3 times a day. Finally, the solutions were freeze-dried leading to a fluffy white polymer.

The composition of the polymerization mixtures is reported in the table 8.3.

Table 8.3 – Composition of the polymerization mixtures for MIP03 and NIP03

Component (mg)	MIP03	NIP03
Template (H-5CQA)	8	-
Functional monomer (21a)	4.7	4.7
Co-monomer (NIPAM)	7.6	7.6
Crosslinker (MBA)	21	21
Initiator (AIBN)	3.0	3.0
Porogen solvent (DMSO)	6626	6626

Rebinding Tests

The rebinding kinetics of 5-CQA with polymer MIP03 was investigated dissolving 1.5 mg of polymer in 1.5mL of a 2mM water solution of 5-CQA. The mixture was incubated at 25°C under continuous stirring and 200 µL aliquots of the solution were taken at different times (from 10 min to 6 h). Each aliquot was centrifuged (12000 rpm for 10 min) to remove the polymer and the supernatants, containing an unknown amount of the analyte, were analyzed by the same UHPLC method developed for the quantification of chlorogenic acids in coffee, to quantify the free 5-CQA concentration. The ratio between the area of the reference peak of the analyte and the peak in the chromatogram of the sample treated with the polymer were calculated to obtain the amount of 5-CQA captured by the polymers[21]. The same procedure was followed using the non-imprinted polymer NIP03.

Cross-reactivity Studies

MIP03 selectivity was investigated following the same approach of the rebinding test by UHPLC. The polymer was treated with a 2 mM solution of a mixture of pure standards of 5-CQA, caffeic acid, *p*-coumaric acid and caffeine. The mixtures were incubated at 25°C under continuous stirring and 200 µL aliquots of the solution were taken at different times (from 10 min to 24 h). Each aliquot was centrifuged (12000 rpm for 10 min) to remove the polymer and the concentrations of the supernatants containing the unbounded standards were determined by UHPLC.

Dynamic Laser Light Scattering

Solutions of 1mg/mL for MIP03 and 0.5 mg/mL NIP03 were prepared in DMSO and placed into an ultrasonic bath for 1 h. After filtration on 0.45 µm filter, the size distribution by intensity and by volume was recorded in triplicate on a Malvern Zetasizer instrument using a 1 mL quartz cuvette with light path of 1 cm.

Competitive Test with MIP03

80µL of 10% solution of glutaraldehyde in PBS were added to different commercial polysine^{R} slides and left to stand at room temperature for one hour. Subsequently, the glass plates were washed with 3 mL of water (1mL at a time). A mixture was prepared by mixing a 20mg/mL gelatin solution in water and 100ug/mL suspension of the imprinted polymer MIP03 in water in ratio 1:1. 80µL of the mixture were added to different polysine^{R} slides and these glass plates were kept in the dark at room temperature for 24 hours. Subsequently, 80µL of solutions of a range of concentrations between 100nM and 1mM of a pure standard of isomer 5-CQA were added to the different plates in duplicate and the samples were incubated for 90 min in the dark at room temperature. After the incubation time all slides were washed with 2 mL of water (500µL at a time) and immediately 80µL of 50µM solution of fluorescent derivative 5-CQACADFITC in water was added to all plates. The fluorescence intensity of the fluorescent derivative in each plate was measured before and after washing them with 2 mL of water (500µL at a time).

---

[1] Criton, M.; Le Mellay-Hamon. Dimeric Cinnamoylamide Derivatives as Inhibitors of Melanogenesis. V. *Biol. Pharm. Bull*., **2011**, 34, 420-425.

[2] Rohloff, J.; Kent, K.; Postich, M.; Becker, M.; Chapman, H.; Kelly, D.; Lew, W.; Louie, M.; McGee, L.; Prisbe, E.; Schultze, L.; Yu, R.; Zhang, L. Practical Total Synthesis of the Anti-Influenza Drug GS-4104. *J. Org. Chem*., **1998**, 63, 4545-4550.

[3] Haslam, E.; Makinson, G.; Naumann, G.; Cunningham, J. Synthesis and Properties of Some Hydroxycinnamoyl Esters of Quinic Acid. *J. Chem. Soc*., **1964**, 2137-2146.

[4] Federspiel, M.; Fisher, R.; Hennig, M. et al. Industrial Synthesis of the Key Precursor in the Synthesis of the Anti-Influenza Drug Oseltamivir Phosphate (Ro 64-0796/002, GS-4104-02): Ethyl(3R,4S,5S)-4,5-epoxy-3-(1-ethyl-propoxy)-cyclohex-1-ene-1-carboxylate. *Org. Process Res. & Dev*., **1999**, 3, 266-274.

[5] Haslam, E.; Haworth, R.; Makinson, G. Synthesis of 3-0-p-Coumaroylquinic Acid. *J. Chem. Soc*., **1961**, 5153-5156.

[6] Ma, C.; Kully, M.; Khan, J.; Hattori, M.; Daneshtalab, M. Synthesis of chlorogenic acid derivatives with promising antifungal activity. *Bioorg. Med. Chem.*, **2007**, 15, 6830-6833.

[7] Dokli, I.; Navarini, L.; Hamerŝak, Z. Syntheses of 3-, 4-, and 5-O-feruloylquinic acids, *Tetrahedron: Asymmetry***, 2013**, 24, 785-790.

[8] De Pooter, H.; De Brucker, J.; van Sumere, C. F. Synthesis of 3-O-coumaryl-, 4-O-coumaryl- and 3-O-ferulyl-D-(-)-quinic acid. Improved Synthesis of 3-O-sinapyl-D-(-)-quinic acid. *Bull. Soc. Chim. Belge*, **1976**, 85, 663-671.

[9] Choi, Y. H.; Kim, H. K.; Linthorst, H. J. M.; Hollander, J. G.; Lefeber, A. W. M.; Erkelens, C.; Nuzillard, J.-M.; Verpoorte, R. NMR metabolomics to revisit the tobacco mosaic virus infection in Nicotiana tabacum leaves. *J. Nat. Prod.*, **2006**, 69 (5), 742-748.

[10] Montchamp, J.; Tian, F.; Hart, M.; Frost, J. Butane 2,3-Bisacetal Protection of Vicinal Diequatorial D. *J. Org. Chem.*, **1996**, 61, 3897-3899.

[11] Glebocka, A.; Sicinski, R.; Plum, L.; Clagett-Dame, M.; De Luca, H. New 2-Alkylidene 1,25-Dihydroxy-19-norvitamin D3. Analogues of High Intestinal Activity: Synthesis and Biological Evaluation of 2-(3'-Alkoxypropylidene) and 2-(3'-Hydroxypropylidene) Derivatives. *J. Med. Chem.*, **2006**, 49, 2009-2020.

[12] Raheem, K.; Botting, N.; Williamson, G.; Barron, D. Total synthesis of 3,5-O-dicaffeoylquinic acid and its derivatives. *Tetrahedron Lett*., **2011**, 52, 7175-7177.

[13] Becke, A. D. Density-Functional Thermochemistry. III. The Role of Exact Exchange. *J. Chem. Phys***. 1993**, 98, 5648–5652.

[14] Clifford, M. N.; Johnston, K. L.; Knight, S.; Kuhnert, N.; Hierarchical scheme for LC-MSn identification of chlorogenic acids. *J. Agric. Food Chem.,* **2003**, 51, 2900-11.

[15] Dokli, I., Navarini, L., Hamersak, Z.; Synthesis of 3,4- and 5-O-feruloylquinic acids; *Tetrahedron: Asymmetry*, **2013,** 24, 785-790.

[16] Gutiérrez Ortiz, A. L.; Berti, F.; Navarini, L., Monteiro, A., Resmini, M., Forzato, C.; Synthesis of *p*-coumaroylquinic acids and analysis of their interconversion. *Tetrahedron: Asymmetry*, **2017**, 28, 419-427.

[17] Santos, A., Barros, L., Calhelha, R. C., Dueñas, M., Carvalho, M., Buelga, S. C., Ferreira, I. Leaves and decoction of *Junglans regia* L.: different performances regarding bioactive compounds in vitro antioxidant and antitumor effects. *Industrial Crops and Product*, **2013**, 51, 430-436.

[18] Clifford, M. N.; Johnston, K. L.; Knight, S.; Kuhnert, N. Hierarchical scheme for LC-MS^n identification acids. *J. Agric. Food Chem*., **2003**, 51, 290-2911.

[19] Ji, W.; Zhang, M.; Yan, H.; Zhao, H.; Mu, Y.; Guo, L.; Wang, X. Selective extraction and determination of chlorogenic acids as combined quality markers in herbal medicines using molecularly imprinted polymers based on a mimic template. *Anal. Bioanal. Chem*., **2017**, 409, 7087-7096.

[20] Konstantinova, T. N., Miladinova, P. M. Synthesis and properties of some fluorescent 1,8-naphthalimide derivatives and their copolymer with methyl methacrylate. *J. Appl. Polym. Sci.,* **2008,** 111, 1991-1998.

[21] Pellizzoni, E.; Tommasini, M.; Maragon, E.; Rizzolio, F.; Saito, G.; Benedetti, F.; Toffoli, G.; Resmini, M.; Berti, F. Fluorescent molecularly imprinted nanogel for the detection of anticancer drugs in human plasma. *Bios. Bioelectr.,* **2016***,* 86, 913-919.

Chapter 9

Conclusions

In this research project, a detailed study about *p*-coumaroylquinic acids synthesis and their analysis in coffee beans of different species as well as in roasted coffee beans were performed. The development of a sensing element for recognition of the most abundant chlorogenic acid in coffee 5-*O*-caffeoylquinic acid was also proposed and preliminary studies for the development of a sensor device were also performed.

All four isomers of *p*-coumaroylquinic acids (5-*p*CoQA, 3-*p*CoQA, 4-*p*CoQA and 1-*p*CoQA) were synthetized by condensation of an acyl chloride with differently protected quinic acid which was prepared in order to selectively protect the hydroxyl groups present in the cyclohexane ring of the quinic acid core. However, during the synthesis process, acyl migrations at C-4 and C-3 of the cyclohexane ring were observed and mixtures of 3-*p*CoQA and 4-*p*CoQA were obtained. 3-*p*CoQA and 4-*p*CoQA could be separated by semi-preparative RP-HPLC and all isomers were fully characterized, while the interconversion occurring between the isomers during their synthesis has been explained by a computational study on the basis of the relative stability of the isomers and of the intermediates leading to them.

A UHPLC method for the identification of all isomers of *p*-coumaroylquinic acid in vegetable matrix was developed and the synthesized compounds were used as standards to identify them. The complete chlorogenic acids profile was also established using original standards of caffeoylquinic acids (CQAs), feruloylquinic acids (FQAs) and dicaffeoylquinic acids (FQAs) and hydrocinnamic acids were quantified as well, using standards of caffeic acid (CA), *p*-coumaric acid (*p*CoQA), ferulic acid (FA) and sinapic acid (SA). Several qualitative analyses were performed to ensure the development of a correct protocol for the identification of these compounds in coffee. However, since *p*CoQAs are present only in low concentrations in coffee, in order to facilitate their identification and to improve the analytical analyses, extractions of phenolic compounds from other sources richer in *p*CoQAs, like walnut leaves, were performed and a rapid and reliable method for quantification of chlorogenic acids by means of UHPLC analysis employed at Illycaffè was optimized.

Since chlorogenic acids biosynthesis can change due to climatic conditions or seasonal variations, the CGAs content in walnut leaves was analyzed from May to September and fifteen different chlorogenic acids, including *cis* isomers of CGAs, were identified and quantified in walnut leaves samples. Dicaffeoylquinic acids were for the first time identified in *Juglans regia* L. The extraction method, in comparison with other proposed in the literature (e.g. methanol extraction), revealed to be very successful since comparable amounts of chlorogenic acids derivatives could be obtained and results confirmed that walnut leaves infusion could be considered as an interesting source of polyphenolic compounds and could contribute to antioxidants intake to the human diet. Furthermore, the obtained results considering seasonal variations in Italy for the year 2016 could be helpful to choose spring or early summer as the best period for walnut leaves (*Juglans regia* L) harvesting in order to maximize antioxidants content of the infusion preparation. When quantitative data are discussed, geographical location, cultivar and crop season could influence remarkably

the concentration of this class of polyphenols, moreover environmental pollution is something to take into consideration and needs to be deeply investigated to elucidate the role of stress induction of urban plants with subsequent possible production of higher amount of CGAs, as data collected in our study seem to suggest. Since our method allowed the identification also of the *cis* isomers, this could be applied in the analyses of other chlorogenic acids rich matrices exposed to UV radiations, such as coffee leaves, in order to determine the exact amount of minor compounds such as *p*CoQAs as *cis* and *trans* isomers. Determination of a suitable isomers profile could give important information to elucidate seasonal variation on the biosynthetic pathway of formation of CGAs and genetic variations that can be involved in the defense mechanism of the plant.

The developed UHPLC method was applied in the determination of CGA profiles of twenty-seven fresh green coffee samples from different geographical origins and different wild species belonging to the *Eucoffea* section, where the concentration of *p*CoQAs have not been reported yet. As far as we know, this is the first time that all three isomers of *p*CoQAs were clearly identified by using authentic standards previously synthesized. Twelve CGAs were quantified, corresponding to all three *trans* isomers of the monoesters at positions 3,4 and 5 of the different classes of CGAs, i.e. CQAs, *p*CoQAs, FQAs and diCQA. Our results confirm the data already reported in the literature that clearly show a distinction in chlorogenic acids composition between Arabica and Robusta. *C. canephora* is, in fact, well known for having higher concentrations of FQAs and diCQAs; on the contrary, concentrations of *p*CoQAs were twice higher in *C. arabica*. The concentration of *p*CoQAs was found to be the lowest one among all CGAs in all the evaluated coffee species, accounting for no more than 1.94% of the total CGA content. Only *C. sessiliflora* showed considerably higher concentrations (2.12-2.24 mg/g) in comparison with the other species, being in fact the second most abundant class of CGAs in this specie, accounting for ~5% of the total CGA content. Considering that the finest coffee market is based on cultivation of *C. arabica*, which is highly susceptible to climate changes and external threats, the determination of an adequate CGAs profile could be very useful to characterize single species and to define its fingerprint as well as might provide useful data to establish a taxonomic classification that could help to understand the specific functions of each isomer in the plants and to create new markets of trades. However, it is important to take in consideration that the geographical origin, as well as the degree of maturation and the extraction method, can influence the CGAs content.

The effect of roasting conditions in CGAs content was also evaluated in the most important species from an economical point of view. As it has been already reported in the literature, the CGAs composition considerably decreased according to the roasting degree. However, the changes for each isomer during roasting were greatly depended not only to the chlorogenic acid class but also upon the coffee specie. Important differences were found in *Coffea canephora,* which seems to be more resistant to roasting

treatment and showed a smaller degradation content at the end of roasting. This important aspect can influence not only the aroma and taste of the final beverage but also the antioxidant activities.

Finally, two different systems for the recognition of CGA were developed by using the molecularly imprinting technology (MIT). As a first approach, fluorescent molecularly imprinted polymers (fMIPs), based on a naphtalimide derivative monomer, have been developed to selectively recognize 5-*O*-caffeoylquinic acid. Fluorescence emissions of the fMIPs were evaluated and it was observed that they can be "switched on" or "switched off "depending on the environment, due to the presence of the isomer 5-CQA. The switched on/off mechanism depends on the PET mechanism of the fluorophore. Polymer MIP01, containing 4VPy and the naphtalimide derivative as monomers, showed a good response of the fluorescence quenching in the range between 625µM and 40mM, while polymer MIP02, containing only the fluorophore as the functional monomer, showed a linear response between 78µM and 20mM. To demonstrate this is a promising system that can be exploited in the design of an optical sensor for CGAs detection, polymer MIP01 was immobilized by physical entrapment in a functionalized glass surface, showing a quenching of the fluorescence with an increase of the CGA concentration between 78µM and 40mM.

As a second approach, a molecularly imprinted polymer, based on a histidine derivative as functional monomer, was prepared to recognize CGA. Since no fluorescent groups are present in the polymer, fluorescent chlorogenic acid derivatives were prepared and the synthetized polymer was tested in a competition system. The polymer showed a good affinity towards both the simple 5-CQA as well as towards the fluorescent chlorogenic acid derivatives, which was prepared by coupling between the isomer 5-CQA and fluorescein isothiocyanate in order to set up a competition or displacement test in aqueous media. As a proof of concept, a calibration curve for 5-CQA quantification was created through a fluorescent competitive assay. This assay is based on the measurement of fluorescence emissions of the derivative 5-CQACADFITC after displacement of chlorogenic acid. The system showed a good linear response in the range 100nM-600µM.

As future perspective, optimization of the polymer preparation will be carried out such as functional monomer/template ratios and crosslinker concentrations in order to improve the selectivity towards the target molecule. Moreover, in collaboration with Center of excellence for Biosensors, instrumentation and process control (COBIK), the conditions for the immobilization of the sensing element will be further optimized in order to setup an optical sensor for CGA detection. On the other hand, it is important to mention that the synthesis of non-commercially available CGA, such as *p*CoQAs, could be useful for carrying out in vitro and animal studies to understand the pharmacological effects of each isomer.

Acknowledgements

Thanks to:

The IPCOS project for this great opportunity.

Dr. Luciano Navarini and all members of Aromalab lab at Illycaffè, specially to Silvia Colomban and Paola Crisafulli for their kindness, supervisions, advices and teachings.

Dr. Matjaz Perterka and all members of COBIK for their supervision.

Prof. Dr. Marina Resmini (School of Biological and Chemical Sciences at Queen Mary University of London) for her suggestions during these three years.

Dr. Federico Berti and Dr. Cristina Forzato for believing in me and giving me the opportunity to be part of this project, for all your teaching, advices and patience, also for the corrections and the encouragements.

Dr. Fabio Benedetti for having me in his research group

Dr. Sara Drioli for her kindness and collaboration during all these three years

Dr. Milena Guida for her collaboration with the HPLC.

My *alma mater*, the University of Los Andes in Mérida-Venezuela and to all my professors, specially Prof. Ricardo Contreras, Prof. Fernando Bellandi for giving me the tools that three years ago allowed me to start this professional challenge.

Martina Tommasini, Giorgia Regini, Luca Redivo, Elena Guercia, Elisabetta Deangelis, persons that more than colleagues became friends, thank you not only for sharing your knowledge and academic advices with me but also for all the laughs and the good moments.

All my old friends, Germán Paparoni, Alejandra Jimenez, Stefanie Landaeta, Brian Leon, Oscar Viloria, Luisanna Lobo, Leopoldo Gómez., Moira Castañeda and so many others, for your unconditional support

All people that have kindly contributed to my personal and professional formation.

And finally I would like to give special thanks to: My grandma, Brisaida Fernandez for teaching me that there are no limits when you believe in yourself, my parents Brisa Ortiz and José Gutiérrez, my big family, all my aunts and my cousins, even when the distance separates us, I know you have been always with me and your unconditional love is the force that continuously drives me to improve myself and Renato D'Angelo for standing by me, thank you for supporting me in the good and not so good moments and for all your love.